

AD-A198 305



A TOPICAL WORKSHOP



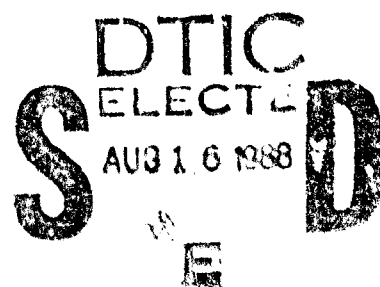
ORGANIC AND POLYMERIC NONLINEAR OPTICAL MATERIALS

sponsored by

THE DIVISION OF POLYMER CHEMISTRY
AMERICAN CHEMICAL SOCIETY

MAY 16 - 19, 1988

VIRGINIA BEACH, VIRGINIA



AD A198305

REPORT DOCUMENTATION PAGE

1a. REPORT SECURITY CLASSIFICATION Unclassified		1b. RESTRICTIVE MARKINGS	
2a. SECURITY CLASSIFICATION AUTHORITY		3. DISTRIBUTION / AVAILABILITY OF REPORT Approved for public release; Distribution unlimited	
2b. DECLASSIFICATION / DOWNGRADING SCHEDULE			
4. PERFORMING ORGANIZATION REPORT NUMBER(S)		5. MONITORING ORGANIZATION REPORT NUMBER(S) AFOSR-TR- 88-0718	
6a. NAME OF PERFORMING ORGANIZATION American Chemical Society Division of Polymer Chemistry	6b. OFFICE SYMBOL (If applicable)	7a. NAME OF MONITORING ORGANIZATION AFOSR/NC	
6c. ADDRESS (City, State, and ZIP Code) Polytechnic University Brooklyn, N.Y. 11201		7b. ADDRESS (City, State, and ZIP Code) Bldg. 410 Bolling AFB, D.C. 20332-6448	
8a. NAME OF FUNDING / SPONSORING ORGANIZATION AFOSR	8b. OFFICE SYMBOL (If applicable) NC	9. PROCUREMENT INSTRUMENT IDENTIFICATION NUMBER AFOSR-88-0221	
8c. ADDRESS (City, State, and ZIP Code) AFOSR/NC Bolling AFB, Washington, DC 20332-6448		10. SOURCE OF FUNDING NUMBERS	
		PROGRAM ELEMENT NO. 61102F	PROJECT NO. 2303
		TASK NO. A3	WORK UNIT ACCESSION NO.
11. TITLE (Include Security Classification) Organic and Polymeric Nonlinear Optical Materials			
12. PERSONAL AUTHOR(S) Gerbi, D. J. and Tripathy, S. K.			
13a. TYPE OF REPORT Final	13b. TIME COVERED FROM 5-16-88 TO 5-19-88	14. DATE OF REPORT (Year, Month, Day) 88/7/8	15. PAGE COUNT 6
16. SUPPLEMENTARY NOTATION Workshop on Organic and Polymeric Nonlinear Optical Materials, May 16-19, 1988 at Virginia Beach, VA.			
17. COSATI CODES		18. SUBJECT TERMS (Continue on reverse if necessary and identify by block number) nonlinear optical materials, second order nonlinear optical susceptibility, third order nonlinear optical susceptibility, electro-optic, nonlinear optical devices	
FIELD	GROUP		
19. ABSTRACT (Continue on reverse if necessary and identify by block number) At this Workshop on Organic and Polymeric Nonlinear Optical Materials, the latest developments in the areas of theory, characterization, synthesis, molecular assemblies, and potential device applications for organic and polymeric materials exhibiting nonlinear optical behavior are discussed. <i>to present discussion</i>			
20. DISTRIBUTION / AVAILABILITY OF ABSTRACT <input checked="" type="checkbox"/> UNCLASSIFIED/UNLIMITED <input checked="" type="checkbox"/> SAME AS RPT. <input type="checkbox"/> DTIC USERS		21. ABSTRACT SECURITY CLASSIFICATION Unclassified	
22a. NAME OF RESPONSIBLE INDIVIDUAL Dr. Donald Ulrich		22b. TELEPHONE (Include Area Code) (202) 767-4960	22c. OFFICE SYMBOL NC

INTRODUCTION

The objective of the workshop was to provide a forum for the sharing of information and the discussion of device applications in the area of organic and polymeric nonlinear optical materials. The workshop addressed the issues of theory, characterization, synthesis, molecular assemblies, and potential device applications. Multidisciplinary interactions are vital to the advancement of research in this field, and the seventy-six participants included scientists from the USA, Japan, UK, France, Germany, and Canada and represented academic, industrial and government laboratories.

WORKSHOP FOCUS

The workshop focus was divided into five half-day sessions and addressed the following topics.

Theory: Current theoretical work on nonlinear optical interactions in organic and polymeric materials was reviewed, with a focus on understanding the microscopic properties of these systems and their correspondence to the macroscopic properties. The value of modelling these systems and the usefulness of the theoretical projections for determining structural requirements for enhanced nonlinear optical activity was discussed.

Characterization: Experimental studies to determine the second and third order nonlinear optical susceptibilities of organic and polymeric systems was discussed. Limiting values

for device applications derived from characterization studies were presented.

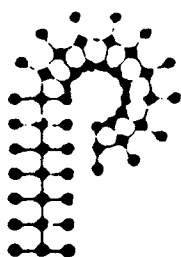
Molecular Assemblies: Characterization measurements have been carried out on many materials in a variety of forms to provide information on structure-property relationships. Molecular order is essential for second order nonlinear optical effects and may enhance third order effects. Therefore, control of molecular orientation in these systems is important. Useful molecular assemblies, including Langmuir-Blodgett films and electrically poled polymer systems were discussed.

Synthesis: The synthesis of organic and polymeric systems is most effective when carried out in conjunction with theoretical development and characterization efforts. Examples of how synthetic efforts can be used to enhance nonlinear optical activity and to improve the physical properties of materials under consideration for use in devices were presented.

Device Applications: Discussions addressed the current status and the future potential of devices utilizing organic and polymeric nonlinear optical materials.

SUMMARY

The Workshop on Organic and Polymeric Nonlinear Optical Materials was very successful. The informal atmosphere encouraged informal discussions, of particular importance in this interdisciplinary field.



A Topical Workshop
**ORGANIC AND POLYMERIC
NONLINEAR OPTICAL MATERIALS**

sponsored by

**The Division of Polymer Chemistry
AMERICAN CHEMICAL SOCIETY**

May 16-19, 1988
Virginia Beach, VA

Co-Chairmen

Diana Gerbi

Sukant Tripathy

The generous support of the contributors is gratefully acknowledged: Air Force Office of Scientific Research, Office of Naval Research, Du Pont Company, Hoechst-Celanese and 3M Company.

Monday Evening, May 16, 1988

3:00-9:00 p.m.

REGISTRATION

6:30-9:30 p.m.

WELCOMING RECEPTION

PROGRAM:

Tuesday Morning, May 17, 1988

8:15 A.M.

Opening Remarks

8:20-9:10

A. *"An Overview on Nonlinear Optical Polymer Systems and Devices"* by D.R. Ulrich (Air Force Office of Scientific Research)

9:10-10:00

B. *"Nonlinear Optical Effects in Polymeric Films"* by P.N. Prasad (State University of New York at Buffalo)

10:00-10:30

Break

10:30-11:20

C. *"Recent Advances in Nonlinear Optical Properties of Organic and Polymer Systems"* by A.F. Garito (University of Pennsylvania)

11:20-12:10

D. *"Conjugated Polymers and Nonlinear Optics"* by S. Etemad (Bell Communications)

Lunch

Tuesday Afternoon, May 17, 1988

1:30-2:20

E. *"Anisotropy of the Third Order Nonlinear Optical Susceptibility in Conjugated Polymers"* by A.J. Heeger (University of California at Santa Barbara)

2:20-3:10

F. *"Nonlinear Optics in Ordered Molecular Systems"* by K.D. Singer (AT&T)

3:10-3:40

Break

- 3:40-4:30 G. *"Several Series of Novel Polydiacetylenes for Nonlinear Optics"* by H. Nakanishi (Research Institute for Polymers and Textiles, Japan)
- 4:30-5:20 H. *"Resonance Effects in Cubic Hyperpolarisabilities of Conjugated Polymers,"* by F. Kajzar (CEN Saclay, France)

Wednesday Morning, May 18, 1988

- 8:30-9:20 I. *"Nonlinear Optical Measurements on Liquid Crystals and Quasi-Liquid Crystals"* by Y.R. Shen (University of California at Berkeley)
- 9:20-10:10 J. *"Nonlinear Optical Effects in Conjugated Systems"* by D. J. Gerbi (3M Co.)
- 10:10-10:40 **Break**
- 10:40-11:30 K. *"Optical Nonlinearity: Molecules, Assemblies and Wave Phenomena"* by G. R. Meredith (E.I. DuPont DeNemours and Co.)
- 10:30-12:20 L. *"Characterization of Polymeric Nonlinear Optical Materials"* by G. Khanarian (Hoechst-Celanese)

LUNCH

Wednesday Afternoon, May 18, 1988

- 1:30-2:20 M. *"Preparation and Characterization of Organo-Transition Metal Langmuir-Blodgett Films"* by T. Richardson (University of Oxford, U.K.)
- 2:20-3:10 N. *"Optical Properties of Organized Assemblies"* by S.K. Tripathy (University of Lowell)
- 3:10-3:40 **Break**
- 3:40-4:30 O. *"The Nonlinear Optics of Langmuir-Blodgett Films"* by I. Peterson (GEC Research, Ltd., Great Britain)

Wednesday Evening, May 18, 1988

6:00 p.m. POSTER SESSION
Wine & Cheese

8:00 p.m. BANQUET

Thursday Morning, May 19, 1988

8:30-9:20 P. *"Advances in Organic Electro-Optic Devices"* by
R.S. Lytel (Lockheed Research and Develop-
ment)

9:20-10:10 Q. *"Organic Nonlinear Optical Devices and Mater-
ial Considerations"* by B.K. Nayar (British Tele-
com Research Laboratories, U.K.)

10:10-10:40 **Break**

10:40-11:30 R. *"Towards Nonlinear Optical Applications of
Polydiacetylenes"* by M. Thakur (AT&T)

11:30-12:20 S. *"High Resolution Laser Spectroscopy in Poly-
mers"* by D. Haarer (Universitat Bayreuth,
West Germany)

12:20 *"Closing Remarks"* by K.J. Wynne (Office of Naval
Research)

List of Registrants

"ORGANIC AND POLYMERIC NONLINEAR OPTICAL MATERIALS"

MAY 16 - 19, 1988
Virginia Beach, VA

Gregory L. Baker
Bellcore
331 Newman Springs Road
3X-275
Red Bank, NJ 07701-7020
(201) 756-2932

David N. Beratan
Jet Propulsion Laboratory
4800 Oak Grove Drive
M.S. 67-201
Pasadena, CA 91109
(818) 354-6548

Murrae J. Bowden
Bellcore
331 Newman Springs Rd.
Red Bank, NJ 07701
(201) 758-3360

Michael E. Boyle
Naval Research Laboratory
Polymeric Materials
NRL Code 6123
Washington, D. C. 20375-5000
(202) 767-2472

Eve Chauchard
Dept. of Electrical Engineering
University of Maryland
College Park, MD 20742
(301) 454-6834

Paula Cockerham
Martin Marietta Labs
1450 S. Rolling Rd.
Baltimore, MD 21227
(301) 247-0700

David B. Cotts
KRI International
Advanced Materials Lab.
19-9 Torishima 6-Chome
Konohana-ku
Osaka 554, Japan
(06) 466-2531

Daniel R. Coulter
Jet Propulsion Laboratory
4800 Oak Grove Drive
M.S. 67/201
Pasadena, CA 91109
(818) 354-3638

William Daly
Department of Chemistry
Louisiana State University
Baton Rouge, LA 70803
(504) 388-3237

John Eichelberger
Pennwalt Corporation
900 First Avenue
P.O. Box C
King of Prussia, PA 19406
(215) 337-6729

Susan Erner
Lockheed
0/93-50 B/204
3251 Hanover St.
Palo Alto, CA 94304
(415) 424-3131

Shahab Etemad
Bellcore
Room 3X-291
Red Bank, NJ 07701
(201) 758-2942

Warren T. Ford
Dept. of Chemistry
Oklahoma State University
Stillwater, OK 74078
(405) 624-5946

Robert P. Foss
E.I. du Pont de Nemours & Co.
CR&D
Experimental Station E328/215
Wilmington, DE 19898
(302) 695-4367

Anthony Garito
Dept. of Physics
University of Pennsylvania
Philadelphia, PA 19104

Diana J. Gerbi
3M Company
3M Center Bldg. 201-2E-08
St. Paul, MN 55144
(612) 736-2557

Frederick J. Goetz
Pennwalt Corporation
900 First Avenue
P.O. Box C
King of Prussia, PA 19406
(215) 337-6758

Robert Gulotty
Dow Chemical Co.
CRIMCL Bldg. 1776
Midland, MI 48674
(517) 636-2861

Dietrich Haarer
Experimentalphysik IV
Postfach 101251
University of Bayreuth
Bayreuth D-8580
Federal Republic of Germany
(0921)55-3240

Michael Hayden
Unisys Corp.
P.O. Box 64525
M.S. U1L14
St. Paul, MN 55164
(612) 456-3669

Alan J. Heeger
Polymer Institute
University of California
Santa Barbara, CA 93106
(805) 961-2001

Keith A. Horn
Allied-Signal Co.
Engineered Materials Sector
Box 1087R
Columbia Tpke & Park Ave.
Morristown, NJ 07960
(201) 455-3022

Phelps Johnson
Rohm & Haas
P.O.Box 219
Bristol, PA 19007
(215) 785-8552

Francois Kajzar
CEA IRDI D. LETI
Dept. d'Electronique et
d'Instrumentation Nucleaire -CENIS
91191 Gif Sur Yvette Cedex
France
(33)1-69-08-6810

G. Khanarian
Hoechst-Celanese
86 Morris Ave.
Summit, NJ 07901
(201) 522-7918

Peter Leung
3M
St. Paul, MN 55144

Richard Lytel
Lockheed
R-202 D-9720
3251 Hanover St.
Palo Alto, CA 94304
(415) 424-2363

Robert J. McMahon
Dept. of Chemistry 6-427
M.I.T.
Cambridge, MA 02139
(617) 253-4546

Michael A. Meador
NASA Lewis Research Center
21000 Brookpark Road
M.S. 49-1
Cleveland, OH 44136
(216) 433-3228

Gerald Meredith
E.I. du Pont de Nemours & Co.
Experimental Station
CR&D 356
Wilmington, DE 19898
(302) 695-4984

Joann Milliken
Office of Naval Research
800 N. Quincy St.
Arlington, VA 22217
(202) 696-4409

Jovan Moacanin
Jet Propulsion Laboratory
4800 Oak Grove Drive
M.S. 122-123
Pasadena, CA 91109
(818) 354-3178

Machiro Nakanishi
Research Inst. for Polymers & Textiles
1-1-4 Yatabe-Higashi
Tsukuba 305, Japan
(0298) 54-6310

Piero Nannelli
Pennwalt Corporation
900 First Avenue
P.O. Box C
King of Prussia, PA 19406
(215) 337-6367

B. K. Nayar
British Telecom
R2121
British Telecom Research Labs.
Martlesham Heath
Suffolk IPS TRE, U.K.

Moris K. Niknam
Chemical Abstracts Service
2540 Olentangy River Rd.
P.O. Box 3012
Columbus, OH 43210
(614) 421-3600

Raphael Ottenbrite
Dept. of Chemistry
Virginia Commonwealth University
Richmond, VA 23284
(804) 367-1298

Joseph W. Perry
Jet Propulsion Laboratory
4800 Oak Grove Drive
M.S. 67-201
Pasadena, CA 91109
(818) 354-5794

Ian Peterson
GEC Research Ltd.
Hirst Research Center
Wembley, U.K.

Juergen L. W. Pohlmann
Dept. of the Army, USACECOM
Center for Night Vision
& Electro-Optics
AMSEL-RD-NV-L, Bldg. #317
Fort Belvoir, VA 22060-5677
(703) 664-1432

Pamela Porter
Martin Marietta Labs
1450 S. Rolling Rd.
Baltimore, MD 21227
(301) 247-0700

Richard S. Potember
JHU/Applied Physics Lab.
Johns Hopkins Rd.
Laurel, MD 20707-6099
(310) 953-6251

Paras Prasad
Dept. of Chemistry
SUNY at Buffalo
52 Acheson Hall
Buffalo, NY 14214
(716) 831-3026

Tim Richardson
Oxford University
Dept. of Engineering Science
Parks Road, Oxford OX1 3PJ
England, U.K.
(0865) 273092

Gareth Roberts
Dept. of Engineering Science
University of Oxford
Parks Road
Oxford, OXI 3PJ
England, U.K.

Guerino Sacripante
Xerox Research Center of Canada
2660 Speakman Drive
Mississauga, Ontario
Canada L5K 2L1
(416) 823-7031

Marcia L. Schilling
AT&T Bell Laboratories
600 Mountain Ave.
Rm. 1A-234
Murray Hill, NJ 07974
(201) 582-6434

Paul J. Shannon
Hercules Inc.
Rt 48 & Hercules Rd.
Wilmington, DE 19894
(302) 995-3854

Y. R. Shen
Physics Dept.
University of California, Berkeley
Berkeley, CA 94720
(415) 602-4856

Kenneth Singer
AT&T Engineering Research Center
P.O. Box 900
Princeton, NJ 08540

Karen Stetyick
Johns Hopkins University
Applied Physics Lab.
Johns Hopkins Road
Bldg. 2, Rm. 252
Laurel, MD 20707
(301) 953-6242

Albert E. Stiegman
Jet Propulsion Laboratory
4800 Oak Grove Drive
M.S. 67/201
Pasadena, CA 91109
(818) 354-4857

Shao-Tang Sun
Hercules Inc.
Rt. 48 & Hercules Road
Wilmington, DE 19894
(302) 995-3112

Murial Thakur
AT&T Bell Laboratories
600 Mountain Ave.
Rm. #6C-312
Murray Hill, NJ 07974
(201) 582-2522

John M. Torkelson
Dept. of Chemical Engineering
Northwestern University
Evanston, IL 60208
(312) 491-7449

Donald R. Ulrich
Air Force Office of
Scientific Research
Bolling AFB
Washington, D.C. 20332
(202) 767-4963

Maria M. Vida
Chemical Abstracts Service
2540 Olentangy River Rd.
Columbus, OH 43210
(614) 421-3600

Jane C. Vogl
Division of Polymer Chemistry
Polytechnic University
333 Jay St.
Brooklyn, NY 11201
(718) 260-3125

Otto Vogl
Herman F. Mark Prof. of Poly. Sci.
Polytechnic University
333 Jay St.
Brooklyn, NY 11201
(718) 260-3180

Bruce D. Webber
Amoco Technology Co.
P.O. Box 400, F-4
Naperville, IL 60566
(312) 420-4670

James K. Whitesell
Dept. of Chemistry
University of Texas at Austin
Austin, TX 78712
(512) 471-1094

C.C. Winter
British Telecom Research Labs
Rt 2333
Martlesham Heath, Ipswich
England, IP5 7RE, U.K.

Kenneth Wynne
National Science Foundation
Materials Research
1800 G Street N.W.
Washington, D.C. 20550
(202) 696-4410

Frederick C. Zumsteg
E.I. du Pont de Nemours & Co.
Experimental Station
CR&D E356-213
Wilmington, DE 19898
(302) 695-1485

Accompanying Guests

Mrs. G. Khanarian
Mrs. G. Meredith (Leslie)
Mrs. S. Thakur

"ORGANIC AND POLYMERIC NONLINEAR OPTICAL MATERIALS"

May 16 - 19, 1988
Virginia Beach, VA

List of Registrants: Addendum

Jan Bartus
H.F. Mark Dept.
Polytechnic University
333 Jay Street
Brooklyn, NY 11201
(718) 260-3403

Francis Wang
Lawrence Livermore National Lab.
L-250, P.O. Box 808
Livermore, CA 94550
(415) 422-7305

Michael A. Lee
Dept. of Physics
Kent State University
Kent, OH 44242

T. Mookherji
Teledyne Brown Engineering
M.S. 52
300 Sparkman Dr.
Huntsville, AL 35807
(205) 532-2875

Peter Palffy-Muhoray
Liquid Crystals Institute
Kent State University
Kent, OH 44242

Wei-Fang Su
Westinghouse R&D
Pittsburgh, PA 15235
(412) 256-2096

Laren Tolbert
Georgia Institute of Technology
School of Chemistry
Atlanta, GA 30332
(404) 894-4043

Eric Van Styland
CREOL
University of Central Florida
12424 Research Parkway
Suite 600
Orlando, FL 32826
(407) 558-6814

"ORGANIC AND POLYMERIC NONLINEAR OPTICAL MATERIALS"

May 16 - 19, 1988
Virginia Beach, VA

List of Registrants: Addendum #2

William Krug
Boeing Electronics High Tech Center
P.O. Box 24969
M.S. 7J-27
Seattle, WA
(206) 865-3033

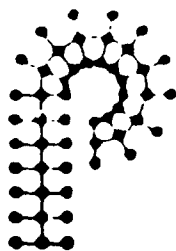
James Le May
Lawrence Livermore National Lab.
P.O. Box 808
Livermore, CA 94550
(415) 422-7305

Edward Miao
Boeing Electronics High Tech Center
P.O. Box 24969
M.S. 7J-27
Seattle, WA 98124
(206) 865-3027

George Rayfield
University of Oregon
Eugene, OR 97403
(503) 382-4100

Nan-Loh Yang
Chemistry Dept.
St. George Campus
CCNY
50 Bay St.
Staten Island, NY 10301
(718) 390-7994

Stanley C. Israel
Dept. of Chemistry
University of Lowell
Lowell, MA 01854
(617) 452-5000



A Topical Workshop
**ORGANIC AND POLYMERIC
NONLINEAR OPTICAL MATERIALS**

sponsored by

**The Division of Polymer Chemistry
AMERICAN CHEMICAL SOCIETY**

May 16-19, 1988
Virginia Beach, VA

Co-Chairmen

Diana Gerbi

Sukant Tripathy

The generous support of the contributors is gratefully acknowledged: Air Force Office of Scientific Research, Office of Naval Research, Du Pont Company, Hoechst-Celanese and 3M Company.

Monday Evening, May 16, 1988

3:00-9:00 p.m.

REGISTRATION

6:30-9:30 p.m.

WELCOMING RECEPTION

PROGRAM:

Tuesday Morning, May 17, 1988

8:15 A.M.

cont'd
Opening Remarks

8:20-9:10

A. *"An Overview on Nonlinear Optical Polymer Systems and Devices"* by D.R. Ulrich (Air Force Office of Scientific Research)

9:10-10:00

B. *"Nonlinear Optical Effects in Polymeric Films"* by P.N. Prasad (State University of New York at Buffalo)

10:00-10:30

Break

10:30-11:20

C. *"Recent Advances in Nonlinear Optical Properties of Organic and Polymer Systems"* by A.F. Garito (University of Pennsylvania)

11:20-12:10

D. *"Conjugated Polymers and Nonlinear Optics"* by S. Etemad (Bell Communications)

Lunch

Tuesday Afternoon, May 17, 1988

1:30-2:20

E. *"Anisotropy of the Third Order Nonlinear Optical Susceptibility in Conjugated Polymers"* by A.J. Heeger (University of California at Santa Barbara)

2:20-3:10

F. *"Nonlinear Optics in Ordered Molecular Systems"* by K.D. Singer (AT&T)

3:10-3:40

Break

3:40-4:30

- G. *Several Series of Novel Polydiacetylenes for Nonlinear Optics*, by H. Nakanishi (Research Institute for Polymers and Textiles, Japan)

4:30-5:20

- H. *Resonance Effects in Cubic Hyperpolarisabilities of Conjugated Polymers*, by F. Kajzar (CEN Saclay, France)

Wednesday Morning, May 18, 1988

8:30-9:20

- I. *Nonlinear Optical Measurements on Liquid Crystals and Quasi-Liquid Crystals*, by Y.R. Shen (University of California at Berkeley)

9:20-10:10

- J. *Nonlinear Optical Effects in Conjugated Systems* by D. J. Gerbi (3M Co.)

10:10-10:40

Break

10:40-11:30

- K. *Optical Nonlinearity: Molecules, Assemblies and Wave Phenomena* by G. R. Meredith (E.I. DuPont DeNemours and Co.)

10:30-12:20

- L. *Characterization of Polymeric Nonlinear Optical Materials* by G. Khanarian (Hoechst-Cel-anese)

LUNCH

Wednesday Afternoon, May 18, 1988

1:30-2:20

- M. *Preparation and Characterization of Organo-Transition Metal Langmuir-Blodgett Films*, by T. Richardson (University of Oxford, U.K.)

2:20-3:10

- N. *Optical Properties of Organized Assemblies* by S.K. Tripathy (University of Lowell)

3:10-3:40

Break

3:40-4:30

- O. *The Nonlinear Optics of Langmuir-Blodgett Films* by I. Peterson (GEC Research, Ltd., Great Britain)

Wednesday Evening, May 18, 1988

6:00 p.m. POSTER SESSION
Wine & Cheese

8:00 p.m. BANQUET

Thursday Morning, May 19, 1988

8:30-9:20 P. *"Advances in Organic Electro-Optic Devices"* by
R.S. Lytel (Lockheed Research and Develop-
ment)

9:20-10:10 Q. *"Organic Nonlinear Optical Devices and Mater-
ial Considerations"* by B.K. Nayar (British Tele-
com Research Laboratories, U.K.)

10:10-10:40 **Break**

10:40-11:30 R. *"Towards Nonlinear Optical Applications of
Polydiacetylenes"* by M. Thakur (AT&T)

11:30-12:20 S. *"High Resolution Laser Spectroscopy in Poly-
mers"* by D. Haarer (Universitat Bayreuth,
West Germany)

12:20 *"Closing Remarks"* by K.J. Wynne (Office of Naval
Research)

✓ 10:10

A-1

D. R. Ulrich
Air Force Office of Scientific Research

AN OVERVIEW ON NONLINEAR OPTICAL POLYMER SYSTEMS AND DEVICES

Accession For	
NTIS GRA&I	<input checked="" type="checkbox"/>
DTIC TAB	<input checked="" type="checkbox"/>
Unannounced	<input type="checkbox"/>
Justification	
By	
Distribution/	
Availability Codes	
Avail and/or	
Dist	Special
A-1	





BRIEFER:

Dr. Donald R. Ulrich

Directorate of Chemical &
Atmospheric Sciences
AFOSR

NLO Response in Polymers

Molecular Level — Microscopic Polarization Related to Applied Electric Field

$$P(E) = \alpha E + \beta E^2 + \gamma E^3 \dots$$

Macroscopic NLO — Originates From Polarization Response of Molecular Electrons

$$P(E) = \chi^{(1)}E + \chi^{(2)}E^2 + \chi^{(3)}E^3 + \dots$$

- $\chi^{(1)}$ — Represents Linear Optics
- $\chi^{(2)}$ — Represents Third Order Nonlinear Process i.e., Third Harmonic Generation, Self-Focusing

First and Third Order Terms of Odd Power of E Common to All Materials — Centrosymmetric

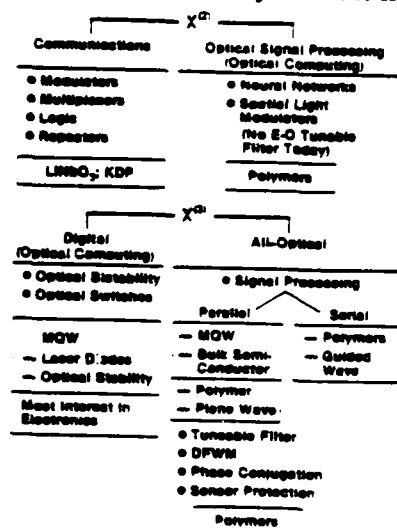
- $\chi^{(2)}$ — Second Order Response i.e., Second Harmonic Generation, Optical Rectification

Only in Noncentrosymmetric Medium — Lacks Center of Inversion Symmetry

Why NLO Polymers?

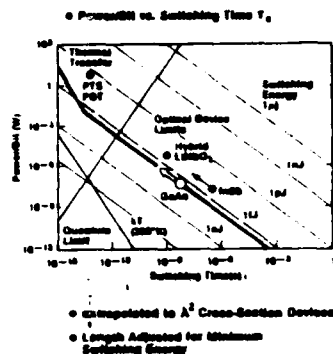
- Subpicosecond Response Times
- Large, Nonresonant Nonlinearities
- Low DC Dielectric Constants
- Low Switching Energy
- Broadband
- Low Absorption
- Absence of Diffusion Problems
- Potential for Resonant Enhancement
- Ease of Processing and Synthesis Modification
- Room Temperature Operation
- Environmental Stability
- Mechanical and Structural Integrity

Where Will NLO Polymers Fit In?



Comparison of Optical Switching Technologies

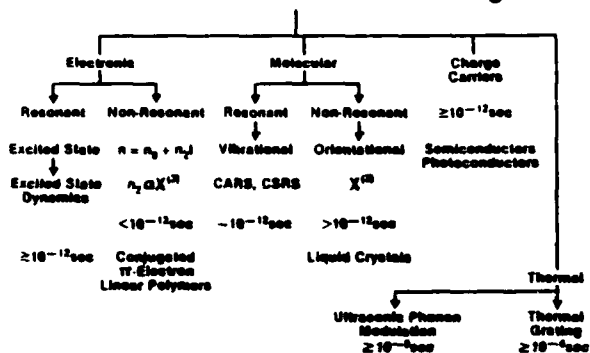
- Fastest Switches Based on Nonresonant Modulation
- Power Requirements Inversely Proportional to Nonlinearity
- New Organic Polymers May Exceed Optical Switch Limits of Resonant Materials
 - Requires Larger n_2 Without Introducing Significant New Absorption
- For $\lambda \geq 0.85 \mu\text{m}$, There are No Alternatives to Organics for Fast Optical Switching



Optical Performance Comparison

	Polymers	GaAs/GnAlAs
Switch On/ Switch Off, T (Recovery Period)	• Femtoseconds	• Nanoseconds
Energy Required to Induce Switching	• Moderate N_2 • Nonresonant • Not Defined by λ • Broad Band of Response and Light Sources • Shows all NLO Processes	• High N_2 • Resonance Enhanced • Limited by λ • Close to Bandgap
Absorption Coefficient, α Associated With Switching	• $\frac{1}{10^4}$ GaAs	• Large
Figure of Merit $FOM = \frac{n_2}{\alpha T}$	• High (1×10^7)	• Moderate (1.5×10^5 on Resonance)

Mechanisms of Four Wave Mixing



Research Directions NLO Polymer Requirements

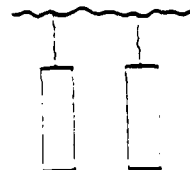
- Nonlinear Susceptibilities $\geq 10^{-3}$ esu
 - Resonant vs Nonresonant
- Ease of Processing
 - Solubility
- Thin Films of Reasonable Optical Quality
 - Transparency
 - Surface Smoothness
- Environmental Stability
- Low Switching Energy (P.J. Diode Lasers)
- Characterization and Separation of Electronic, Molecular, Thermal and Charge Carrier Contribution Mechanisms to Response Time

Status NLO Polymer Classes

Class	Examples	NLO Function
ISO Tropic	Glasses Alloys Composites	$\chi^{(2)}$, $\chi^{(3)}$
Bond Alternation	Ladder Polymers PTL, PQL Polyacetylene Polythiophene	$\chi^{(2)}$
Liquid Crystalline Polymers (LCP)	Side Chain LCPs	$\chi^{(2)}$
Rigid Rod Aromatic Heterocyclics	PBT LCPs PBO SBL	$\chi^{(2)}$
Polydiacetylenes		Mostly $\chi^{(2)}$ Some $\chi^{(3)}$

Second Order Polymers for Electrooptical Devices

• Pendant Side Chain Structure



• High Activity

	Polymer	LiNbO ₃
For SHG	$\chi^{(2)} = 120 \text{ pm/V}$	10 pm/V
For Electrooptics	$r = 35 \text{ pm/V}$	30 pm/V
FOM = $\frac{r}{\epsilon}$	10	1

• Excellent Secondary Properties

Spin Coatable for Thin Film Waveguides,
2-4 Micron

Low Dielectric Constant ($\epsilon_{\text{polymer}} = 3$;
 $\epsilon_{\text{LiNbO}_3} = 30$)

Low Loss ($< 1 \text{ dB/cm}$ at 830 nm)

Melt Processable for Optics

$T_g \sim 120^\circ\text{C}$

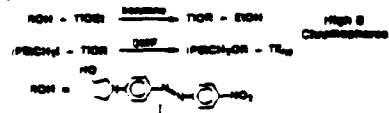
Nonlinear Chromophores Covalently
Linked to Glassy Polymer Constructs
Noncentrosymmetric Assembly

Synthesis and Poling of Covalently-Functionalized
Polymers for Frequency Doubling

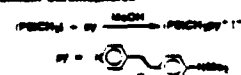
I. Functionalization



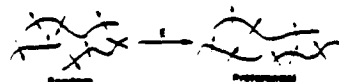
A. Alcohol Chromophores



B. Pyridinium Chromophores

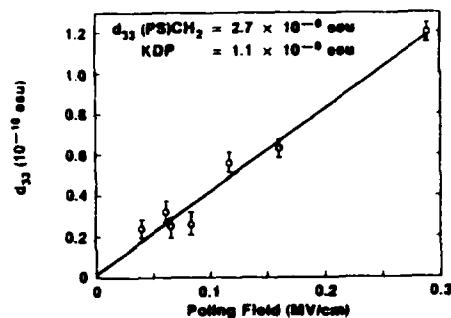


II. Alignment

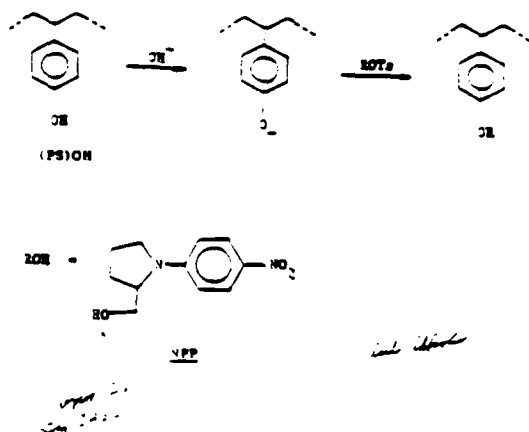


Dependence of SHG On Poling Field

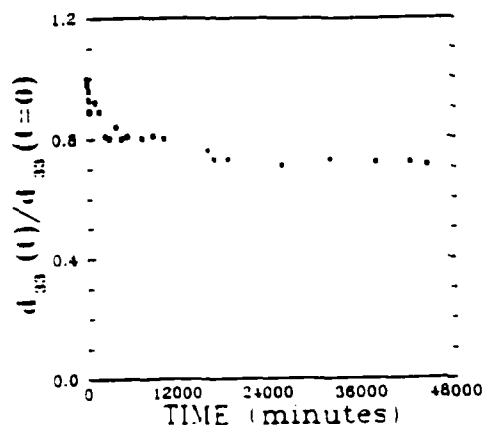
• Significant Non-Random Chromophore Alignment



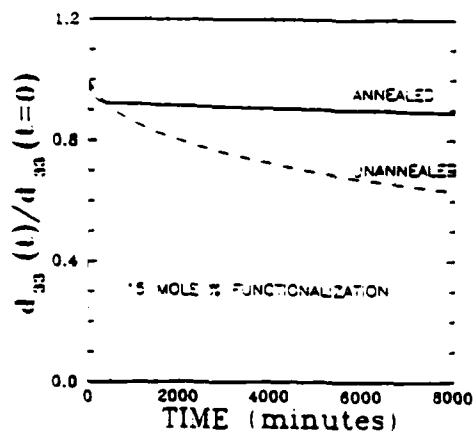
FUNCTIONALIZATION OF POLY(p-HYDROXY- STYRENE) WITH NLO CHROMOPHORES



PSIO-NPP FILMS
TIME DEPENDENCE OF d_{33}



(PS)O-NPP FILMS
EFFECTS OF ANNEALING



Values for $\chi^{(3)}$, Eg. W From Semiempirical
Calculations and Experimentally Determined
 $\gamma(\text{HOMO})^2$ Delocalization Length for Prototype
Ladder Polymers and Polyacetylene

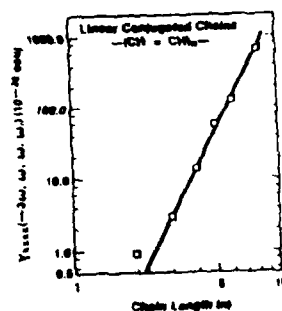
Polymer	Band Gap Eg(eV)	Band Width W(eV)	$\chi^{(3)}$ (esu)	N_d
Pristine Trans-PA	1.8	10	6.5×10^{-10}	20
Pristine PXL X = CH Ladder (Chance)	0.7	1.5	5×10^{-10}	20-28
Bipolaron State of PXL X = CH Ladder (DeHorn)	0.3	2	10^{-7}	
Protonated PXL	3.0	3	2×10^{-10}	

Implications of $\gamma(\text{HOMO})^2$ Delocalization Experiments For NLO Polymer Synthesis

- Negative Spin Density Confirms Electronic Excitation (Electron Correlation)
- Delocalization Length in Ladder Polymers and Polystyrene the Same — 26 to 28 Atoms
- Indicates $X^{(2)}$ Wm Not Increase Beyond 25 Repeat Units (66 Å)
- Ladder Polymers May be Superior to Open Chain Polyenes Because Improved π -Orbital Overlap Wm Lead to Enhanced Delocalization and Reduced Optical Gap

Dependence of $\gamma(-3\omega, \omega, \omega, \omega)$ On Chain Length

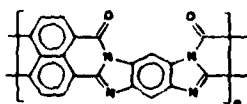
- Finite Chain Limit: $\gamma \propto n^{1.5}$
 - Decreasing Excitation Energy
 - Increasing Number of Spin Correlated States
- Polymer Chains: $X^{(2)} \sim 10^{-9}$ esu
 - 25 Repeat Units (66 Å)



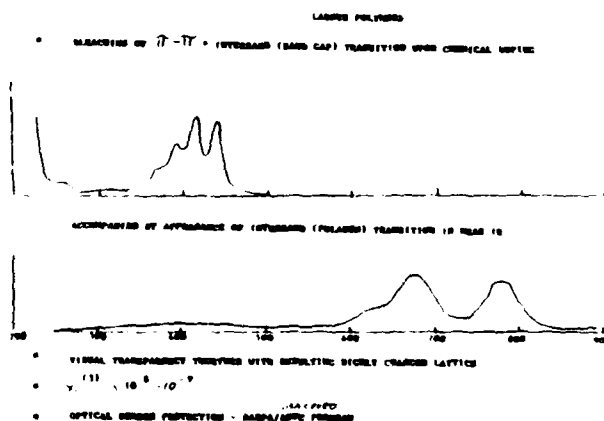
Application of Dalton's Results

- Solubilized Ladder Polymers by Lewis Acid Charge Transfer Complex Forming Agents

Soluble Benzimidazophenanthroline (BBL)



- Soluble in Organic Acids
- Reduces Intermolecular Attractive Forces and Allows Solubilization of Rigid Macromolecules



NONLINEAR OPTICAL AND PHOTOCHROMIC POLYMERS

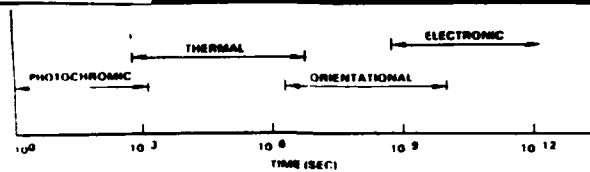
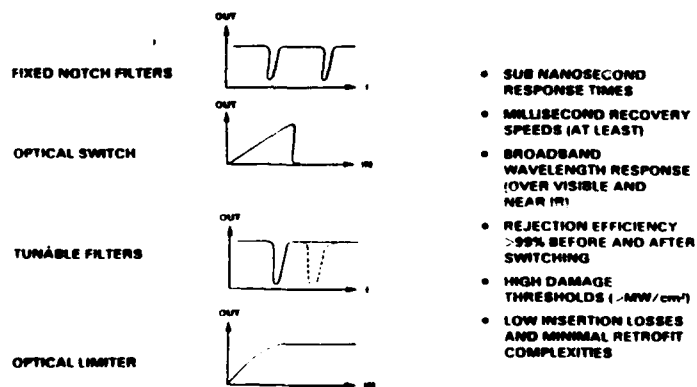
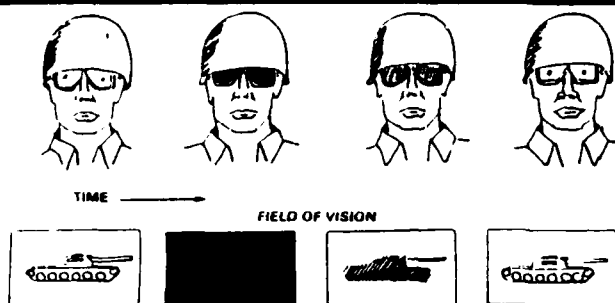


PHOTO-CHROMIC	THERMAL NONLINEARITY	ORIENTATIONAL KERR NONLINEARITY	ELECTRONIC KERR NONLINEARITY
- OPTICAL FUSE	- DYE SENSITIZED THERMAL EFFECT	- LIQUID CRYSTAL POLYMERS	- ELECTRONIC K(3) POLYMERS
- 10^{-3} D.C.	- $10^{-3} - 10^{-7}$ SEC	- $10^{-7} - 10^{-10}$ SEC	- $10^{-9} - 10^{-12}$ SEC
THREAT	THREAT	THREAT	THREAT
- GAS LASERS	- PULSED FLASH LAMP PUMPED LASERS	- Q-SWITCHED SOLID STATE LASERS	- Q-SWITCHED SOLID STATE LASERS
- CW SOLID STATE LASERS	- GAS LASERS	- PULSED FLASH LAMP PUMPED LASERS	- MODE LOCKED LASERS
	- CW SOLID STATE LASERS		

HARDENING TECHNIQUES



SENSOR PROTECTION



FOCUS IS ON CONCEPTS WHICH CAN:

- PROTECT AGAINST RAPIDLY TUNABLE, PULSED, VISIBLE AND NEAR IR LASER THREATS TO HIGH GAIN OPTICAL SYSTEMS
- USEFUL FOR RANGEFINDERS, VISUAL SENSORS, CAMERAS, AND MOST IMPORTANTLY, THE EYE

Third Order Polymers for Optical Devices

- Planar Structure With Extended π Orbitals

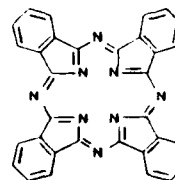


M = Metal Atom

- Shift in Focus From Conjugated Off-Resonance to Systems on Resonance With Narrow Molecular Extinction Coefficients
- High Activity Through Saturable Absorption
 - Effective N_2 Equivalents AlGaAs MQW Structures
- Excellent Secondary Properties
 - Spin Coatable For Thin Film Structure Applications

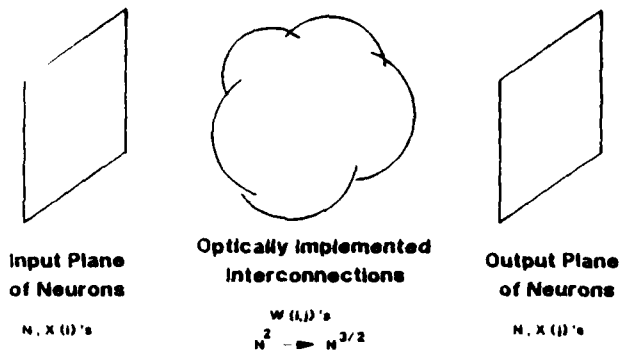
Optical Stability
Parallel Processing

Phthalocyanines

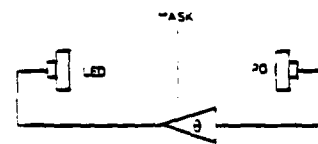
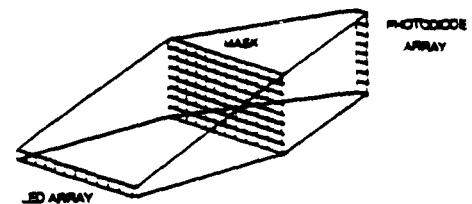


- Large NLO response discovered by A. Garito
- Numerous variants synthesized to tailor
 - NLO activity
 - Fabrication properties

Basic Structure of an Optical Neural Network



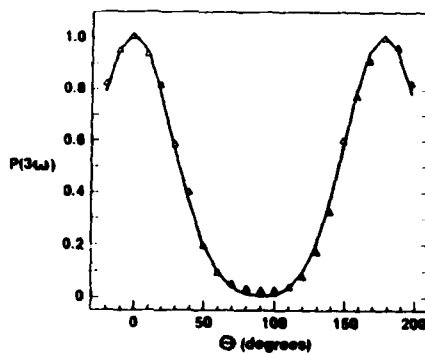
OPTOELECTRONIC IMPLEMENTATION OF A NEURAL NETWORK



ELECTRONIC FEEDBACK

- REGENERATING FEEDBACK - FORS OPTICAL STABILITY COMPENSABLE TO GAIN IN PUMP - PUMP FEEDBACK OF 100% PULSED PUMP
- LINEAR ARRAY OF OPTICAL REGENERABLE ELEMENTS THAT COULD REPLACE PHOTOELEMENTS

Angular Dependence of Reflected $\chi^{(3)}$ for Oriented Trans-Polyacetylene by Third Harmonic Generation



Third Order Response in Polyacetylene

• Resonant Process

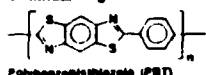
- Photoexcited Nonlinear Excitations
- Associated Structural Distortions (Solitons, Bipolarons, Polarons) Responsible for Large Shifts of Oscillator Strength Observed With Resonant Pumping
- Consequence of Electron-Phonon Interaction
- Electronic Resonant Enhancement
- Nonradiative Dissipation Produces Slower Response

• Reflected $\chi^{(3)}$

- $\theta \times 10^{-10}$ sec Parallel to Polymer Chain
- For Devices Polymer Must Be Able to Inherently Transmit or Guide Light

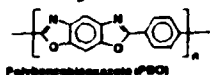
Third Order NLO Response of Ordered Polymers

• Collinear Rigid Rod



Polybenzobisthiazole (PBT)

• Planar Rigid Rod



Polybenzobisthiazole (PBO)

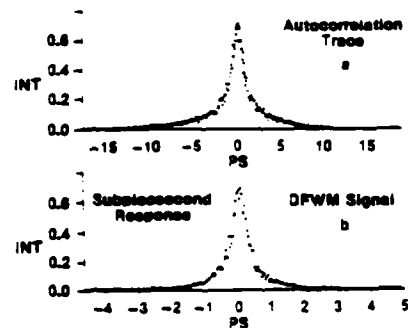
COMPARISON

Uniaxial PBT	— Third Harmonic Generation	— $\chi^{(3)} \approx 10^{-10}$ esu
Biaxial PBT	— Degenerate Four Wave Mixing (DFWM)	— $\chi^{(3)} \approx 10^{-11}$ esu
Uniaxial PBO	— Degenerate Four Wave Mixing	— $\chi^{(3)} \approx 2.5 \times 10^{-11}$ esu

- Requirement for Film Quality — Avoid inherently Grain or Fibrous Components Which Scatter Light

Degenerate Four Wave Mixing of Biaxial PBT Ordered Polymer Films

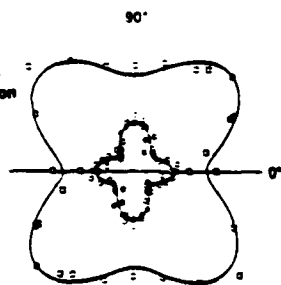
Poly (p-phenylenebenzobisthiazole) (PBT)



Nonresonant Third Order Susceptibility $\chi^{(3)}$ in Biaxial PBT

• Degenerate Four Wave Mixing

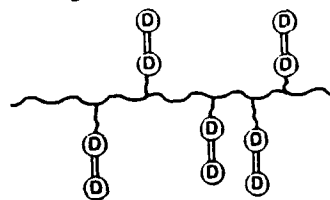
Polar Plot
 $\chi^{(3)}$ As a
Function of
Film Rotation
Angle



• New Feature for Third Order Devices

- Anisotropic $\chi^{(3)}$ Materials for Optically-Activated Birefringent Film Applications

$\chi^{(3)}$ Polymers for Fibers



- $\chi^{(3)}$ units have modest activity but very low absorption
- Polymer backbone confers secondary properties
 - Spinability
- Shear and elongational flow yield alignment

$\chi^{(3)}$ Materials

Thin Limit

Properties

- Near resonance
- High n_2
- High absorption (α)

Material

- Phthalocyanines

Application

- Etalons
- All optical SLM's

Advantages

- Fabrication ease
- Room temperature operation
- Potentially highest n_2 materials

Thick Limit

Properties

- Non resonant
- Lower n_2
- Very low absorption

Material

- Side chain polymer

Application

- NLO fibers
- All optical switching

Advantages

- Fiber spinning ease
- Potentially highest n_2/α materials

POLYALKYLTHIOPHENE

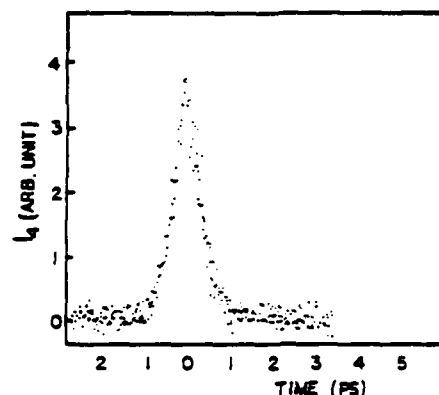
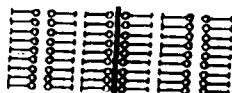


Fig. The degenerate four wave mixing signal obtained for a 20 layer thick Langmuir-Blodgett film of polyalkylthiophene shown as a function of the delay of the beam pump; the wavelength is 682 nm and the excitation pulsewidth is 348 fs.

POLYMER MULTIPLE QUANTUM WELLS



MOLECULAR ARCHITECTURE TAILORING

- LIQUID CRYSTALLINITY
- GUEST-HOST BLENDS
- IN-SITU POLYMERIZATION AND ORDERING
- RIGID/FLEXIBLE CHAIN CONFORMATIONS

NEW HYDROSTRUCTURE ASSEMBLIES

- GAST ANALOGS
- ROW GAST ANALOGS

QUANTUM DOT DOMAIN STRUCTURES

CHARGE CARRIER DYNAMICS

- CHARGE TRANSFER INTERACTIONS
- REDUCE DIMENSIONALITY OF CHARGE CARRIERS
- INTERFACE SING
- PICOSECOND TRANSIENT ABSORPTION/SCATTEING
- TRANSIENT ETALON EFFECTS/PHONON INDUCED PROCESSES

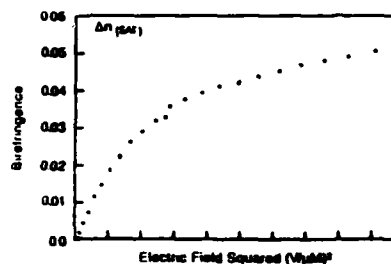
$$\chi^{(3)} = 0^{-9} \text{ esu}$$

LCC Composite

New LCC's



- $d \ll \lambda$ (Rayleigh scattering regime)
- Randomly oriented LC microdroplets
- Low scattering - hazy blue to transparent
- Kerr material with positive n_2



A-12

ADVANCED POLYMER BLENDS AND OPTICS

NLO POLYMERS

GENERATION	SECOND ORDER NLO <i>g</i> (2)	THIRD ORDER NLO <i>g</i> (3)
I (1980 - 1990)	HOMOPOLYMERS	
	0 ISOTROPIC	0 BOND ALTERNATION
	0 POLED	0 LADDER
	0 ORIENTED	0 ORDERED
II (1990 - ?)	POLYMER - POLYMER INTERACTIONS { BLENDS - ALLOYS MOLECULAR COMPOSITES }	
	0 SELF-INDUCED POLARIZATION	0 NEAR-OFF RESONANCE
	0 SELF-ORGANIZING	0 PLASMA

IMPROVEMENTS IN CALCULATION OF NLO SINGLE-MOLECULE PROPERTIES

PARALLEL COMPUTING

ABSORPTION LINEWIDTHS

MOLECULAR CONFORMATIONS AND DEFECTS

DEVELOPMENT OF ALTERNATIVE METHODOLOGIES, SUCH AS FINITE FIELD APPROXIMATIONS

GENERALIZATION OF SINGLE-MOLECULE TO BULK NLO PROPERTIES

STATISTICAL AVERAGING OF ORIENTATION (FROZEN GAS MODEL)

STATISTICAL AVERAGING OF CHAIN LENGTHS

EFFECTS OF INTERMOLECULAR INTERACTIONS ON SINGLE MOLECULE NLO PROPERTIES

EFFECTS OF INTERMOLECULAR INTERACTIONS ON MOLECULAR CONFORMATION AND STRUCTURE

EFFECT OF INTERMOLECULAR INTERACTIONS ON MATERIAL ULTRASTRUCTURE

THE KEY: INTERMOLECULAR INTERACTIONS!

Status of Understanding for Polymer Design

Detailed Mechanism(s) of Nonlinear Optical Activity in Delocalized Electron Polymers Have Yet to Be Defined

- Nonlinear Optical Activity May Not Be Simply Related to Bandgap
- Potential Contributions of D Orbitals to NLO (S-D Cross-Terms)
- Role of Electron-Phonon Interactions
- A Quantitative Correlation Between $\chi^{(2)}$ and Electron Delocalization Length
- Effect of Doping and Intermolecular Charge Transfer Needs to Be Clarified
- Quantitative Theory Looking to Predict macromolecules With Large Second Order (Pockel) and Third Order (Kerr) Molecular Susceptibilities

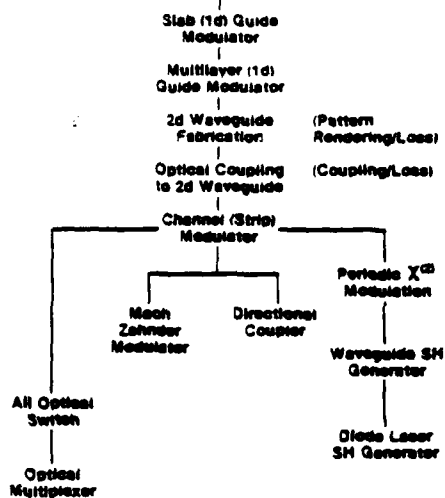
State-of-Art $\chi^{(2)}$ Devices

• Traveling-Wave Electrode Mach-Zehnder Electrooptic Modulator

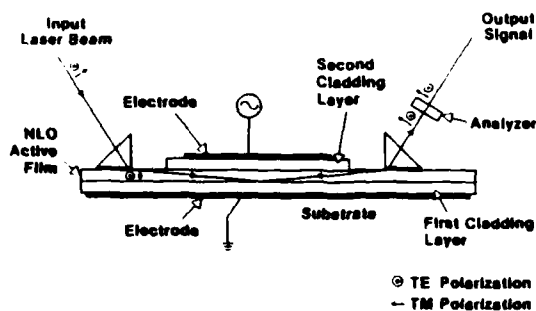
	LiNbO ₃ Modulator	Polymer Modulator
Switching Voltage (V)	3 1/2 - 10 1/2	1.3 (0.7 With Higher $\chi^{(2)}$)
Power Requirement (W)	0.5 - 5	0.03
Maximum Frequency (GHz)	8 - 24	> 50

- No Expected Velocity Mismatch Implies Higher Frequency Devices are Possible With Polymers
- Electrooptic Bragg Cell
 - High Speed Radar Signal Processing
 - 20 GHz as a Target
- Second Harmonic Generation
 - High Efficiency Doubling of a Diode Laser

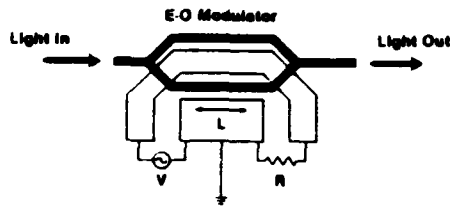
Waveguide Devices



Polymeric Electrooptic Modulator



Traveling-Wave Waveguide



• Voltage Varies Along the Length
($L \geq \lambda$ Electrical)

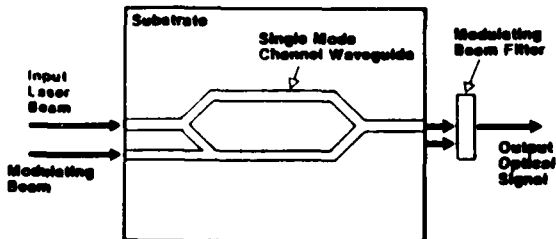
• Important Device Parameters:

- Voltage
- Optical Mode Size
- Drive Power
- Speed
- Length
- Impedance

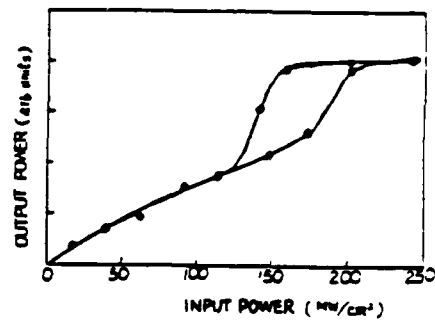
State-of-Art $\chi^{(3)}$ Devices

- Far Less Progress Than $\chi^{(2)}$
- Large Payoff in Multiplexing and Demultiplexing
 - High Speed
 - Handle Many Inputs
 - Very High $\chi^{(3)}$
- Can Lead to:
 - All Optical Interferometer and Optical Switch
 - Optical Stability and Digital Optical Information Processing
 - Optically Induced Dynamic Grating and Real-Time Holography
- Device Performance Depends on Material Properties in a Complicated Way
 - Determined by Device Architecture
 - Parallel/Analog Processing of 2D Image
 - Phase Conjugate Optics and Image Processing
 - Self Focusing/Defocusing Applications

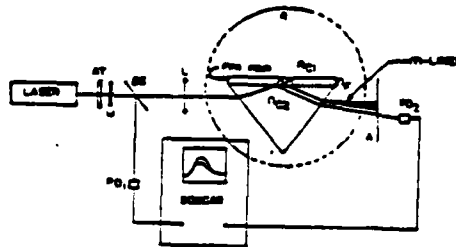
Mach-Zehnder All Optical Modulator



OPTICAL STABILITY IN A
NONLINEAR POLYMER
FABRY-PEROT ETALON



OPTICAL BISTABILITY IN A POLYMER
QUASI-WAVE GUIDE INTERFEROMETER



RESULTS:

- (1) OBTAIN LINEAR REFRACTIVE INDEX AND FILM THICKNESS
- (2) OBTAIN BOTH MAGNITUDE AND SIGN OF $\chi^{(2)}$

Ref 28

OPTICAL BISTABILITY IN A
NONLINEAR POLYMER
QUASI-WAVEGUIDE INTERFEROMETER

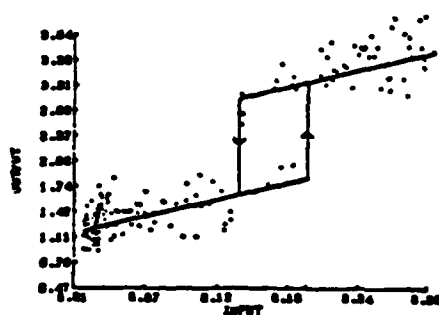


FIGURE 1. The observed optical bistability behavior in the poly-4-vinylpyridine quasi-waveguide interferometer. The decreasing angle is 45° .

Summary

Second Order

- Poled Polymer Films
 - Close to Achieving Levels of Response for Electrooptic Device Application
- First Polymers Comparable to Lithium Niobate Reported
- Focus for Research to Achieve Optimum Electrooptic Modulation
 - $\chi^{(2)}$ Parallel to Film Surface

Third Order

- Nonlinearities of 10^{-8} esu Large for Nonresonance but Still Needs to be Larger ($\approx 10^{-7}$ esu) for Broad Device Application
- State-of-Art of 10^{-8} esu WILL Find Applications in Optical Wave Guide Devices Such as Optical Switches and Optically Controlled Modulators
- Thin Film Applications Such as Etalons Unlikely Unless Significant Advances in Larger Nonlinearities, Optical Flatness and Optical Clarity

B-1

P. N. Prasad
State University of New York at Buffalo

NONLINEAR OPTICAL EFFECTS
IN POLYMERIC FILMS

B-2

NONLINEAR OPTICAL EFFECTS

SECOND ORDER NONLINEAR OPTICAL PROCESSES

N

CURRENT STATUS

POLYMERIC FILMS

PARAS M. PRASAD

DEPARTMENT OF CHEMISTRY

STATE UNIVERSITY OF NEW YORK AT BUFFALO

BUFFALO, NEW YORK 14214

1. PREDICTABILITY OF STRUCTURE
FOR MOLECULAR ENGINEERING
→ REASONABLE

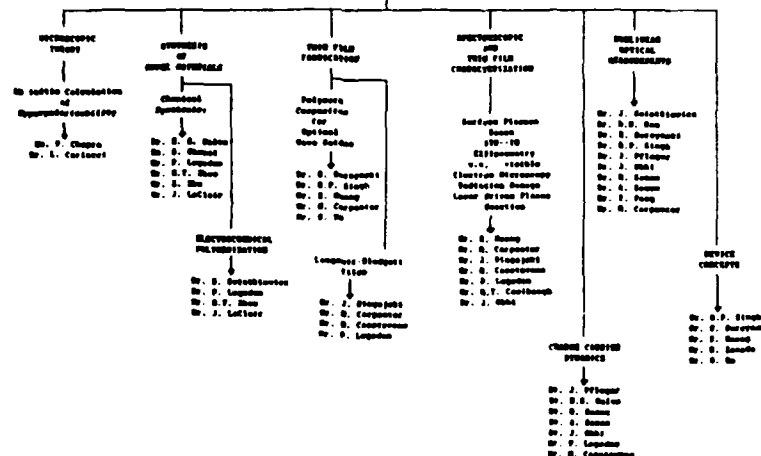
2. LARGE $\chi^{(2)}$
FAST RESPONSE TIME → ALREADY ACHIEVED
LOW DC DIELECTRIC CONSTANT

3. GUIDED WAVE PROCESSES - ALREADY DEMONSTRATED

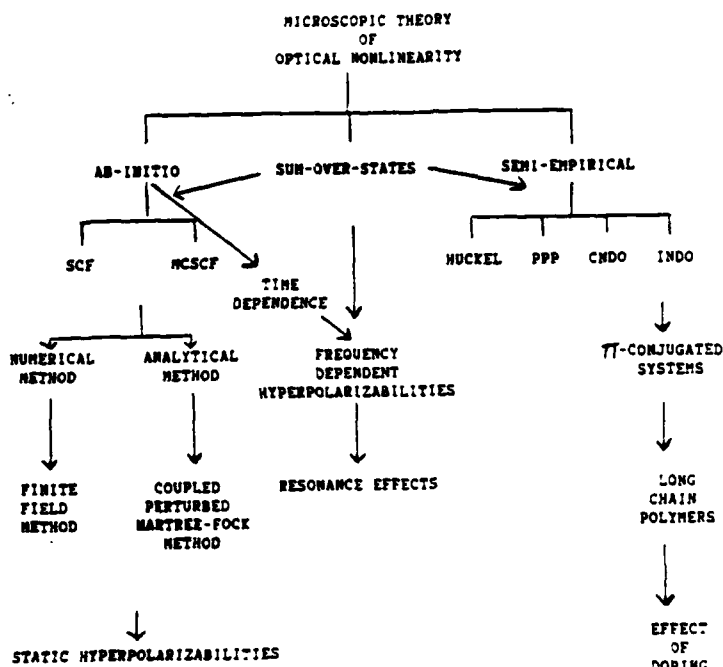
4. POLYMERIC STRUCTURES
NOT REQUIRED, BUT MAY BE DESIRABLE FOR MATERIALS
PROCESSING AND DEVICE APPLICATIONS
DOPED POLYMERS, LIQUID CRYSTALLINE POLYMERS, ETC.

5. DEVICES (?) : RESTRICTED BY MATERIALS LIMITATION

ORGANIC NONLINEAR OPTICS PROGRAM



B-3



AB-INITIO CALCULATIONS OF SECOND HYPERPOLARIZABILITIES (2)

OBJECTIVE: Relative importance of σ and π contributions
 comparison of various π electron structures
 π -electron conjugation effect
 Sign of γ
 Anisotropy of γ tensor
 Effect of substituents
 Conformational effect
 Effect of Structural (conformational defects)
 such as solitons, polarons and bipolarons

Identify Structural Parameters
 for enhancing γ (3)

SEMI-EMPIRICAL APPROACH

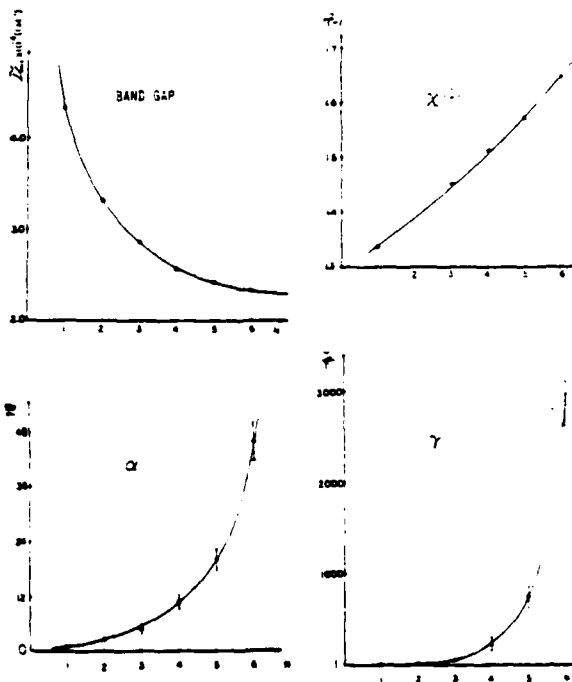
DEFINE MOLECULAR HAMILTONIAN INCLUDING
 FIELD DEPENDENT STARK TERM
 CONSTRUCT $LCAO + MO + \pi$ SLATER DETERMINANTS
 WITH A CHOICE OF 40 BASIS SET
 OPTIMIZE THE GEOMETRY USING SCF
 CALCULATE DIPOLE MOMENT AS A FUNCTION OF FIELD
 POLYNOMIAL FIT TO GET γ
 CHANGE FIELD DIRECTIONS TO CALCULATE
 DIFFERENT COMPONENTS OF γ
 ORBITAL TRANSFORMATION TO SEPARATE
 σ AND π -CONTRIBUTIONS
 CONTOUR PLOTS TO OBTAIN FIELD INDUCED
 CHARGE REDISTRIBUTION
 STATIC SECOND HYPERPOLARIZABILITIES (4)
 NONRESONANT VALUE
 MERITS OF THIS APPROACH:
 ONLY GROUND STATE PROPERTIES NEED
 TO BE DEFINED
 IN PERTURBATIVE CALCULATIONS INVOLVING
 EXCITED STATES EXPANSION, EXCITED STATE
 PROPERTIES NEED TO BE CALCULATED

B-4

SOME CONCLUSIONS OF THEORETICAL STUDIES OF MICROSCOPIC NONLINEARITY

1. THE CHOICE OF BASIS, PARTICULARLY THE INCLUSION OF DIFFUSE POLARIZATION FUNCTIONS, IS IMPORTANT IN DESCRIBING THE HYPERPOLARIZABILITIES OF CONJUGATED SMALL MOLECULES.
2. γ IS ANISOTROPIC, WITH THE COMPONENT γ_{zzzz} ALONG CHAIN GROWING RAPIDLY FOR THE CONJUGATED HYDROCARBONS SERIES POLYENES, POLYINES AND CUMULENES AS THE CHAIN LENGTH GROWS.
3.2
3. FOR POLYENES, CHAIN LENGTH DEPENDENCE OF N IS FOUND.
5 5.3
FREE ELECTRON MODEL AND HUCKEL MODEL PREDICT N^5 AND $N^{5.3}$ RESPECTIVELY.
4. THE CORRESPONDING ORBITAL ANALYSIS SHOWS THAT THE SIGMA AND π -ELECTRON CONTRIBUTIONS TO γ ARE OF OPPOSITE SIGNS.
5. CONTOUR MAP OF THIRD DERIVATIVE OF CHARGE DENSITY WITH RESPECT TO FIELD (REGIONAL CONTRIBUTION ANALYSIS OF γ) CONDUCTED FOR POLYINES, INDICATES THAT THE NONLINEAR ELECTRONIC DISTORTION IS A CO-OPERATIVE EFFECT WITH A SUBSTANTIAL CHARGE TRANSFER ALONG THE ENTIRE LENGTH OF THE CHAIN.
6. OUR SCF CALCULATION RESULTS FOR α COMPARE WELL WITH THOSE OF THE SOS METHOD, BUT γ VALUES DO NOT AGREE.
7. IN THE SERIES $R1 - C \equiv C - R2$, THE LONGITUDINAL COMPONENT γ_{zzzz} INCREASES AS THE ELECTRON WITHDRAWS GROUPS AT $R1$ OR $R2$ ARE SUBSTITUTED.
8. A COMPARISON OF γ FOR CIS-BUTADIENE, TRANS-BUTADIENE AND THIOPHENE REVEALS THE FOLLOWING ORDER:
TRANS-BUTADIENE) THIOPHENE) CIS-BUTADIENE

THIOPHENE OLIGOMERS
REPEAT UNIT DEPENDENCE



B-5

DEPENDENCE OF α AND γ ON NUMBER OF REPEAT UNITS (N)

$F = A + B \ln \delta^{-1}$	$F = \alpha$ OR γ
EXPT	FOR $\langle \alpha \rangle = 1.88$ FOR $\gamma = 1.45$
OUR AB-INITIO CALCULATION ON POLYENES	FOR $\alpha = 0.13 \pm 0.15$ FOR $\gamma = 3.2 \pm 3.4$
FREE ELECTRON MODEL	FOR $\alpha = 0.3$ FOR $\gamma = 1.5$
OUR MODEL	$\alpha = 0.23$ $\gamma = 5.3$

FOR THERMOC

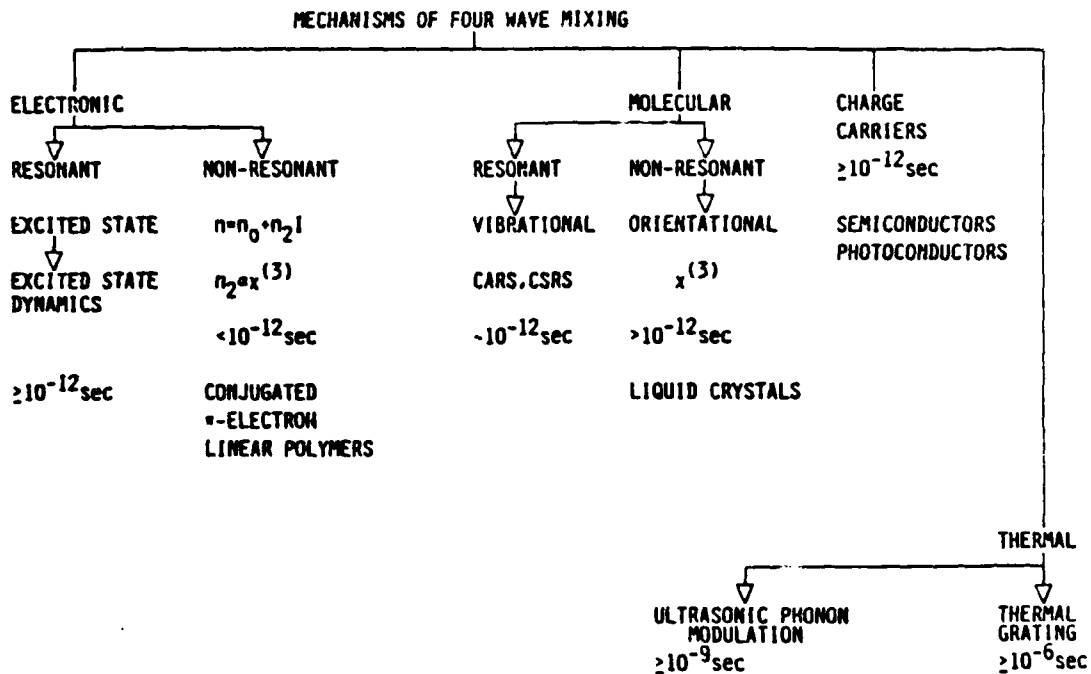
$\langle \alpha \rangle$	$\langle \gamma \rangle$
AB-INITIO CALCULATION	$8.2 \times 10^{-24} \text{ cm}^{-1}$
EXPT. VALUE	9.8×10^{-24}

FOR ETHYLENE

$\langle \alpha \rangle$
AB-INITIO CALCULATION
EXPT. VALUE

- CONSIDERATION OF $\alpha^{(2)}$
RELEVANT PARAMETERS
1. MAGNITUDE OF $\alpha^{(2)}$
 2. RESONANCE TIME
 3. ANISOTROPY OF $\alpha^{(2)}$
 4. ORDER OF $\alpha^{(2)}$
 5. POLARIZABILITY
 6. LOCAL FIELD EFFECT
 7. ELECTRONIC RESONANCE ENHANCEMENT
 8. VIBRATIONAL RESONANCE ENHANCEMENT
- TECHNIQUE USED

EXPERIMENTAL TECHNIQUE FOR WAVE MIXING
OPTICAL WAVELENGTH
NON-LOCAL FIELD EFFECT
SURFACE PLASMON
TWO-WAVELENGTH GENERATION
TWO-WAVELENGTH GENERATION



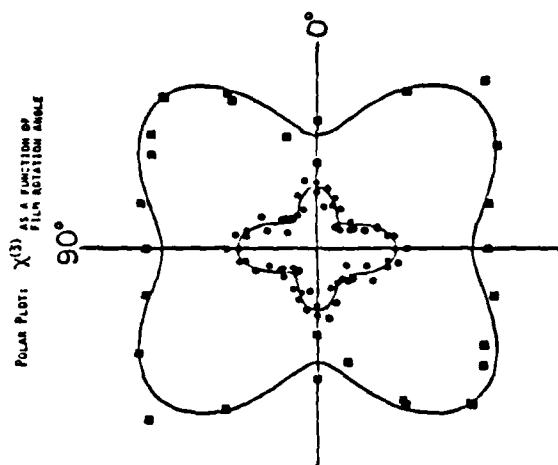
MEASUREMENTS OF $\chi^{(3)}$

RELEVANT PARAMETERS:

1. MAGNITUDE OF $\chi^{(3)}$
2. RESPONSE TIME
3. ANISOTROPY OF $\chi^{(3)}$
FOURTH RANK TENSOR
4. SIGN OF $\chi^{(3)}$
5. REAL OR COMPLEX (?)
6. LOCAL FIELD EFFECT
7. ELECTRONIC RESONANCE ENHANCEMENT
8. VIBRATIONAL RESONANCE ENHANCEMENT

TECHNIQUES USED:

FEMTOSECOND DEGENERATE FOUR WAVE MIXING
OPTICAL WAVEGUIDE
NON-LINEAR FABRY PEROT
SURFACE PLASMON
THIRD HARMONIC GENERATION
KERR GATE EXPERIMENT



B-6

FEEDBACK $\chi^{(3)}$ BY FOUR WAVE MIXING ELECTRONIC FEEDBACK

SYSTEM	MECHANISM	RESPONSE TIME	$\chi^{(3)}$
PVDF	CORRELATED ELECTRO- MECHANICAL	100 ns	10^{-11} esu
POLYETHYLENE FIBER	SOLUTION POLARIZ- ATION	ns	10^{-9} esu
ETHANOLAMINE (IN FILM)	ELECTROLYTIC	ns	10^{-8} esu
POLYTHIOPHENE ELECTROCHEMICALLY DEPOSITED	POLARIZABLE	ns	10^{-9} esu
POLYETHYLENE GLASSY CARBON FILM (IN FILM)	POLARIZABLE	ns	10^{-9} esu

CAUTION

$\chi^{(3)}$ DEPENDENT ON POLARIZATION STATE
 $\chi^{(3)}$ BY A FACTOR OF 10 IN ETHANOLAMINE

B-7

NON LINEAR OPTICAL EFFECTS IN CONJUGATED POLYMERS WITH CONFORMATIONAL DEFECTS (Bond Alternation)

NONRESONANT CASE: Charge on Polymer Backbone can be Varied in a Controlled way - Tune $\chi^{(3)}$

RESONANT CASE: Photoinduced Solitons and Bipolarons create Mid Gap States

Redistribution of Oscillator Strength

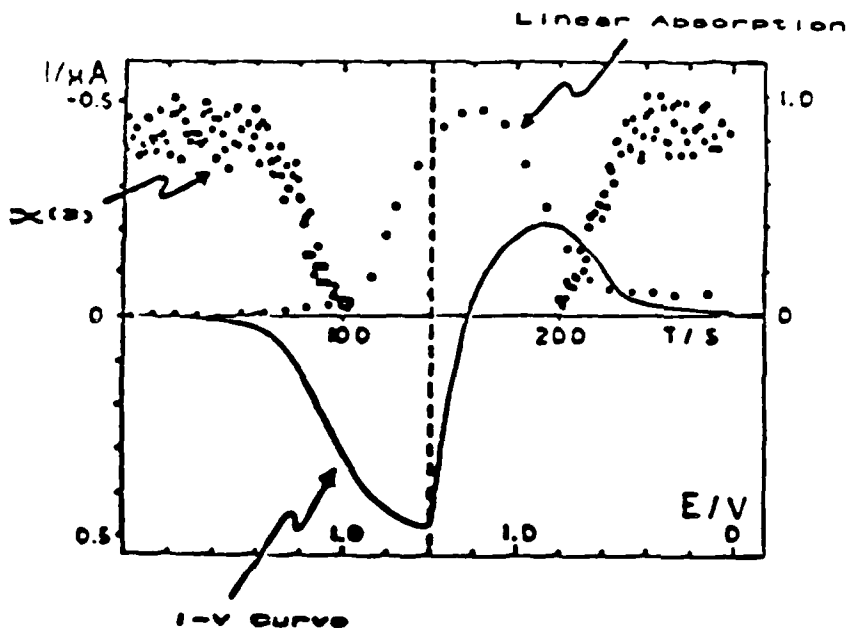
Large $\chi^{(3)}$ with Fast Response

A NEW PHENOMENON

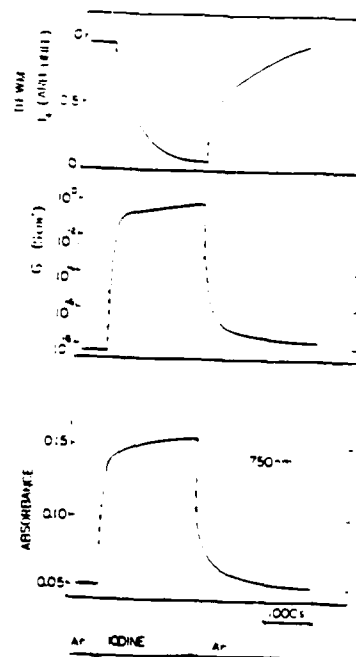
Chemical or Electrochemical Switching of $\chi^{(3)}$ Between High and Low States

IN-SITU ELECTROCHEMICAL STUDY OF $\chi^{(3)}$ IN POLYTHIOPHENE

REDUCED FORM \leftrightarrow OXIDIZED FORM \leftrightarrow REDUCED FORM



SMIATKIEWICZ, JANISZEWSKA AND PRASAD

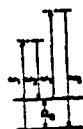


POLYALKYLTHIOPHENE - LB FILMS
IODINE DOPING

B-8

PICOSECOND TIME-RESOLVED COHERENT RAMAN SCATTERING

$\chi^{(3)}$

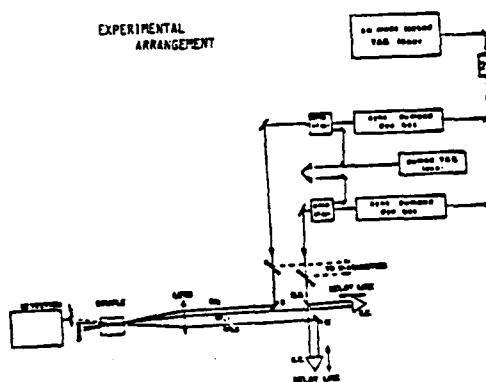


CARS

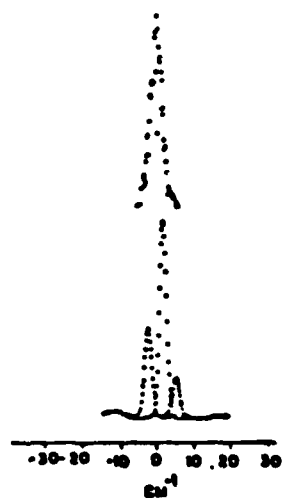


CSRS

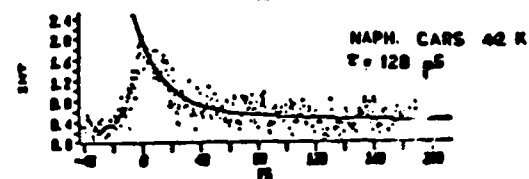
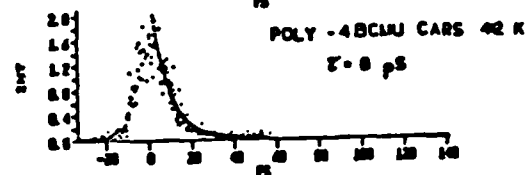
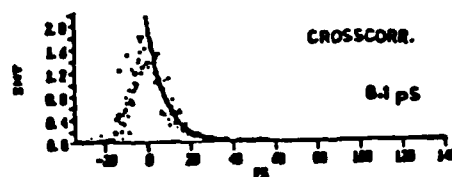
EXPERIMENTAL ARRANGEMENT



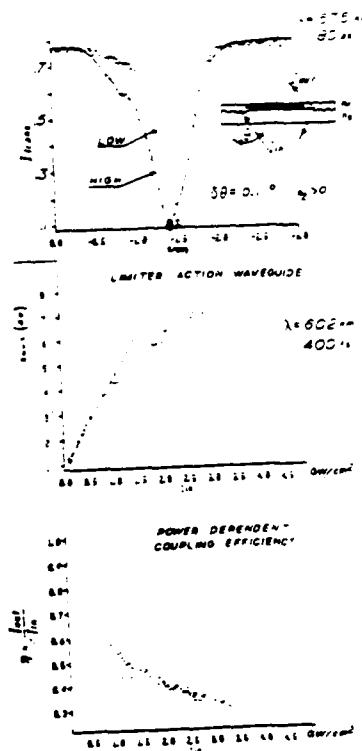
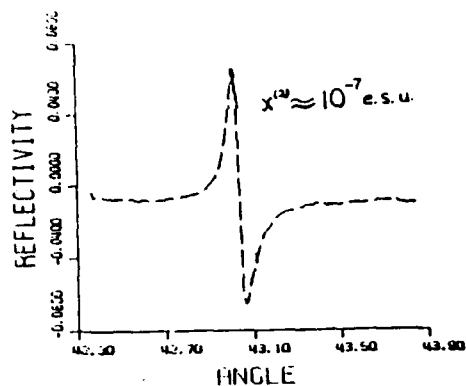
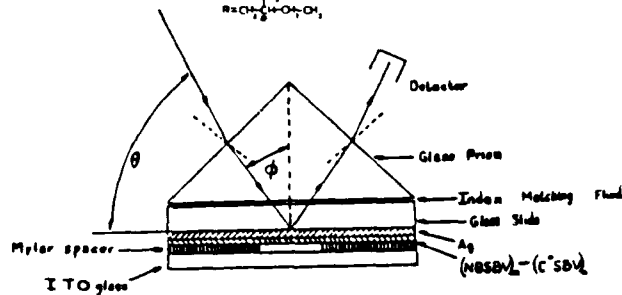
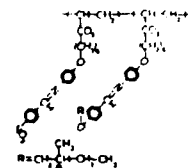
POLY - 4BCM (LOW MOL. WT), 42 K



CROSSCORR.



- 1 SURFACE PLASMON ELECTRO-OPTIC MODULATION IN THE ELECTRO-OPTICALLY POLED POLYMERIZED LANGMUIR-BLODGETT FILMS OF A LIQUID CRYSTALLINE POLYMER
- 2 FABRY-PEROT ETALON OPTICAL SWITCHING AND OPTICAL ISOLATION
BOTH ABSORPTIVE AND DISPERSIVE
- 3 QUASI-WAVEGUIDE INTERFEROMETER OPTICAL ISOLATION
- 4 WAVEGUIDE MAY BE ONLY EXAMPLE OF $\chi^{(3)}$ POLYMER WAVEGUIDE
LIMITED ACTION INTENSITY DEPENDENT PHASE SHIFT
INTENSITY DEPENDENT COUPLING ANALOG
FREQUENCY SPECTRUM SHAPING IN WAVEGUIDE PROPAGATION
- 5 HOLLOW FIBERS FILLED WITH NONLINEAR MATERIALS LOW SCATTERING, GAIN AND AMPLIFICATION



B-10

HERE DO WE GO NOW?

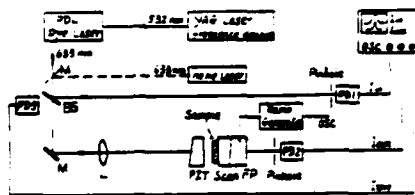


FIG. 1. EXPERIMENTAL SETUP FOR THE OBSERVATION OF OPTICAL BISTABILITY.

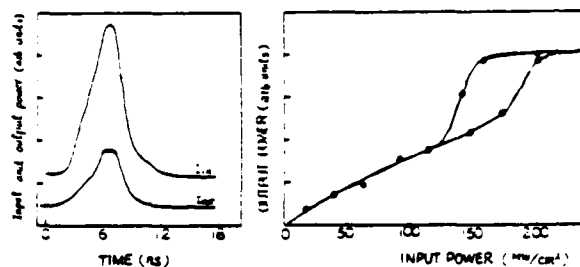


FIG. 2. LEFT: INPUT AND OUTPUT PULSES
RIGHT: INPUT-OUTPUT CHARACTERISTICS

ENHANCEMENT OF $\chi^{(3)}$

(A) DO WE NEED EXTENSIVE π - ELECTRON DELOCALIZATION?

BAND GAP REDUCES. PROBLEM WITH NONRESONANT WIDTH

PROBLEM WITH DISTRIBUTION OF CONJUGATION LENGTH

A BROAD DISTRIBUTION OF BAND GAPS.

(B) DO WE NEED A HIGH MOLECULAR WEIGHT POLYMER?

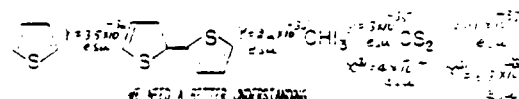
PROBLEM WITH SOLUBILITY

DERIVATIZE WITH LONG ALKYL CHAIN, REDUCES PACKING DENSITY

PROBLEM WITH DISTRIBUTION OF MOLECULAR WEIGHT

REFRACTIVE INDEX INHOMOGENEITIES

(C) DO WE NEED π ELECTRONS?



WE NEED A BETTER UNDERSTANDING

OF STRUCTURE-PROPERTY RELATIONSHIP

THEORETICAL STUDIES
OF MICROSCOPIC NONLINEARITIES

BULK
EFFECTS

EXPERIMENTAL STUDIES OF
SEQUENTIALLY BUILT
AND SYSTEMATICALLY
DERIVATIZED STRUCTURES

2. OPTICAL QUALITY MATERIALS

PROCESSABLE MATERIALS

STRUCTURAL CONTROL, CHARACTERIZATION AND MATERIALS PROCESSING FOR LOW
OPTICAL LOSS SYSTEMS

3. DEVICE PHYSICS AND DEVICE STRUCTURES

EXPERIMENTS WITH CHANNELLED WAVEGUIDES, CATALONS, FIBERS

ACKNOWLEDGEMENT

DR. J. SVIATEKIEWICZ	DR. D.N. RAO
DR. R. BURZYNSKI	DR. S.P. SINGH
DR. S. GHOSHAL	DR. J. PFLEGER
DR. H.S. NALWA	DR. L. JANI-SZEWIEKA
MR. P. GHORRA	MR. X. HUANG
MR. L. GARLAGEI	MR. Y. FANG
MR. S. GHOSH	MR. H. CARPENTER
MR. J. BIEGAUSKI	MR. P. LOBBON
MR. M.T. COOLBAUGH	MR. H. CASSTEVEN
MR. R. SAWADA	MR. M.T. ZHANG

DR. DONALD R. ULRICH (AFOSR)

SUPPORT

AIR FORCE OFFICE
OF
SCIENTIFIC RESEARCH

C-1

A. F. Garito
University of Pennsylvania

RECENT ADVANCES IN NONLINEAR
OPTICAL PROPERTIES OF ORGANIC
AND POLYMER SYSTEMS

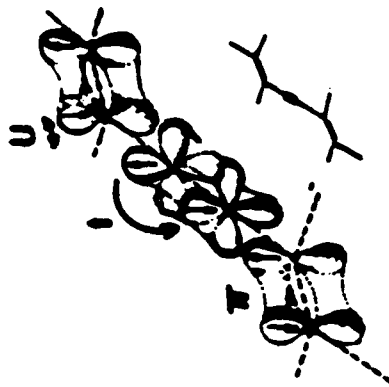
C-2

**RECENT ADVANCES IN NONLINEAR OPTICAL PROPERTIES
OF ORGANIC AND POLYMER SYSTEMS**

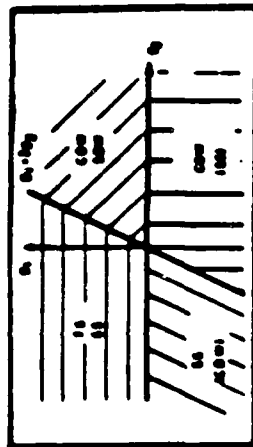
**A.F. Garito
Department of Physics
University of Pennsylvania
Philadelphia, PA 19104-6396**

**ELECTRON CORRELATED STATES: ORIGIN OF THIRD ORDER NONLINEAR
OPTICAL SUSCEPTIBILITY OF CONJUGATED LINEAR CHAINS**

FERMI GAS WITH ELECTRON-ELECTRON INTERACTIONS



QFT



$\theta_1 = \theta_2$

TIGHT BINDING : HUCKEL
 $H = \sum_{ij} t_{ij} c_{i\sigma}^\dagger c_{j\sigma}$
 $E = \alpha + 2t \cos ka$
 • INDEPENDENT ELECTRONS
 • EXCITONS

ELECTRON DELOCALIZATION

SCF - MO - MCI
 $H = \sum_{ij} t_{ij} c_{i\sigma}^\dagger c_{j\sigma} + \sum_{ij} U_{ij} c_{i\sigma}^\dagger c_{i\sigma} c_{j\sigma}^\dagger c_{j\sigma}$
 $+ \sum (-1 - \sum U_{ij}) c_{i\sigma}^\dagger c_{i\sigma} + \sum U_{ij}$
 • ALL VALENCE ELECTRONS
 • S.D.T.O. CI
 • 2 PHOTON STATES

HUBBARD
 $H = t \sum_{ij} c_{i\sigma}^\dagger c_{j\sigma} + U \sum_i n_{i\uparrow} n_{i\downarrow}$
 • ELECTRON CORRELATION
 • 2 PHOTON STATES
 • SDWs
 • CDWs

HEISENBERG
 $H = \sum_{ij} J_{ij} \cdot \vec{S}_i \cdot \vec{S}_j$
 $J_{ij} = -2 t_{ij}^2 / U$
 • 1D MAGNETIC CHAINS
 • SDWs

$U/t \rightarrow \infty$

$U/t \rightarrow 0$

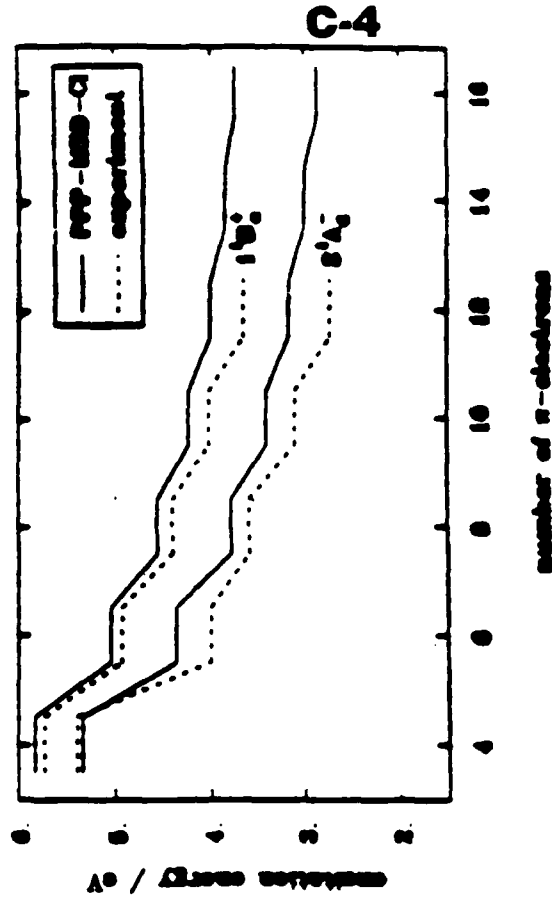
$U/t \rightarrow 0$

COMPUTATION

ELECTRON CORRELATION AND RESONANT PROCESSES



- π -ELECTRON STATES DOMINATED BY
ELECTRON CORRELATIONS
- TWO PHOTON 2^1A_g STATE EXISTS BELOW
FIRST OPTICALLY ALLOWED 1^1B_u STATE
- PPP AND HUBBARD MODELS OBTAIN
CORRECT STATE ORDERING WITH INCLUSION
OF AT LEAST DOUBLY EXCITED
CONFIGURATIONS (DCI)



FROM TAVAN AND SCHULTEN, J. CHEM. PHYS. 85,
6602 (1986)

ELECTRONIC STATES OF OT

SYMMETRY	ENERGY (eV)	$\mu_{Ag}(D)$	$\mu_{1B_{u,g}}(D)$
5'B _u	7.30	1.14	0.00
6'A _g	7.16	0.00	13.24
4'B _u	7.01	1.11	0.00
3'B _u	6.47	0.01	0.00
5'A _g	6.07	0.00	1.11
4'A _g	6.00	0.00	2.84
3'A _g	5.19	0.00	0.07
2'B _u	4.79	0.86	0.00
1'B _u	4.42	7.81	0.00
2'A _g	4.15	0.00	2.82

1'A_g —



OT (octatetraene)

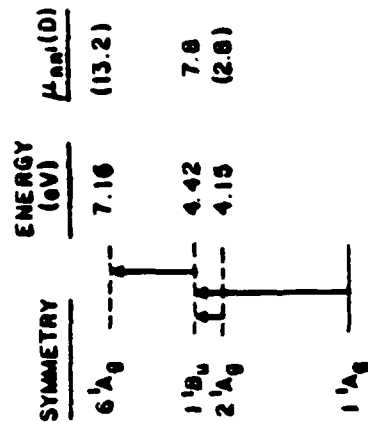
VERTICAL EXCITATION ENERGIES: CHAIN LENGTH

N(sites)	1'B _u (eV)		2'A _g (eV)	
	Exp.	Theo.	Exp.	Theo.
4	5.91	5.77	5.4(0-0)	5.31
6	4.93	4.94	4.0(0-0)	4.59
8	4.40	4.42	3.97	4.15
10	4.02	4.07	3.48	3.90
12	3.65	3.83	2.91	3.74

OT

- DOMINANT 1 PHOTON STATE: 1'B_u
 - LOW-LYING 2'A_g EXCITED STATE:
- ELECTRON CORRELATION

MICROSCOPIC ORIGIN OF $\gamma(-3\omega; \omega, \omega, \omega)$ FOR LINEAR CONJUGATED CHAINS

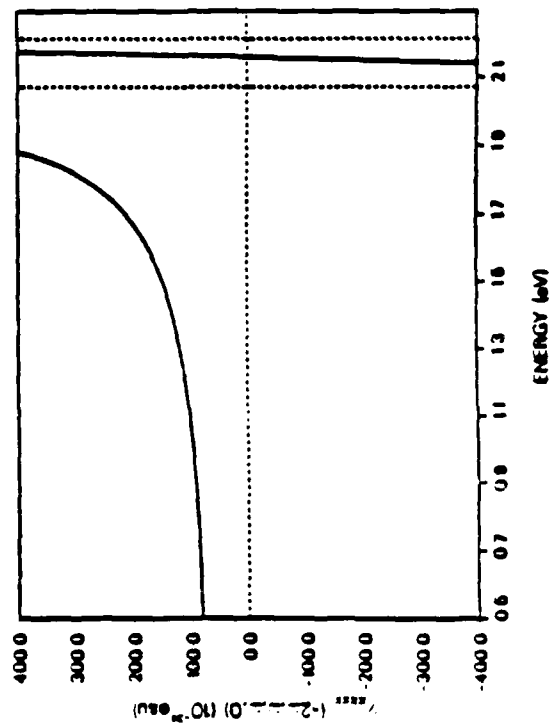
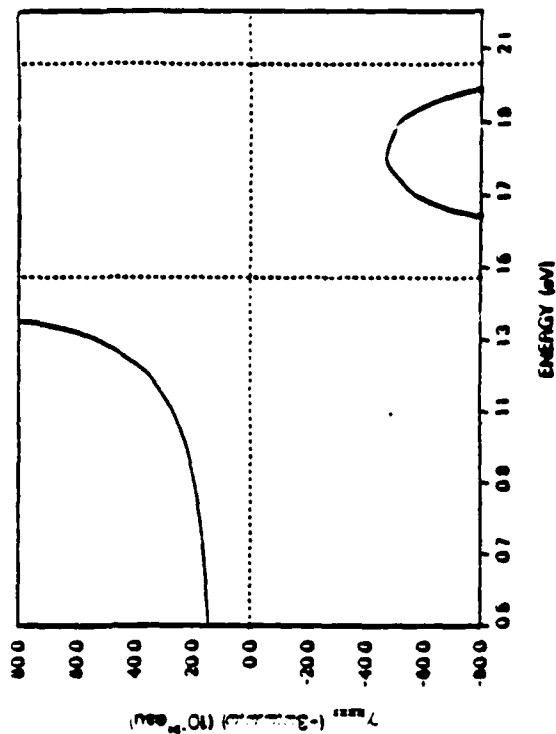


OT

- $\gamma_{xxxx}(-3\omega; \omega, \omega, \omega) = 15.5 \times 10^{-36} \text{ esu}$
 $\gamma_g(-3\omega; \omega, \omega, \omega) = 3.4 \times 10^{-36} \text{ esu}$ ($\omega = 0.65 \text{ eV}/\hbar$)

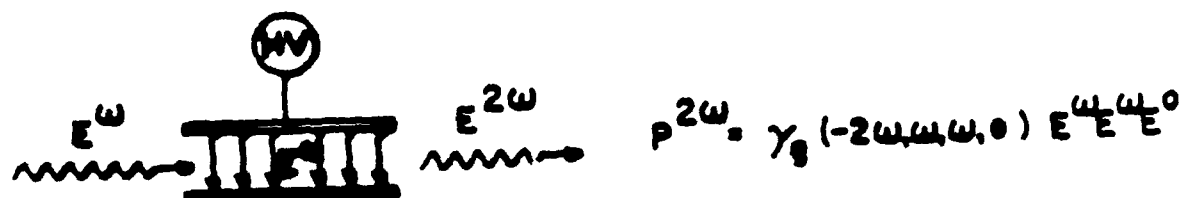
- ONLY CONTRIBUTIONS: $g \rightarrow ^1B_u \rightarrow ^1A_g \rightarrow ^1B_u \rightarrow g$
- 1A_g STATES: THOSE WITH LARGEST μ_{nn} WITH DOMINANT 1B_u STATE
- 2 PHOTON 1A_g STATES CRITICAL IN THIRD ORDER PROCESSES

C-6



C-7

DC INDUCED SECOND HARMONIC GENERATION AND γ_g



$$\gamma_g(-2\omega; \omega, \omega, 0) = \frac{1}{5} \left[\sum_i \gamma_{iiii} + \frac{1}{3} \sum_{i,j} (\gamma_{iiij} + \gamma_{ijij} + \gamma_{ijji}) \right] + \frac{1}{5} \frac{\mu}{kT} \beta_z(-2\omega; \omega, \omega)$$

• SECOND ORDER CONTRIBUTION β_z VANISHES BY SYMMETRY

γ_g VALUES (IN UNIT OF 10^{-36} esu) AT 1.787 eV:

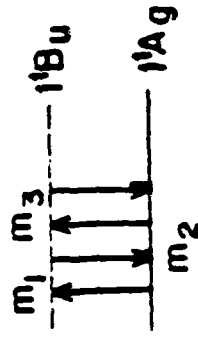
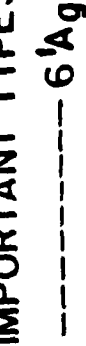
	γ_g (THEORY)	γ_g (EXPERIMENT)
BUTADIENE (N=4)	3.6	3.45 ± 0.2
HEXATRIENE (N=6)	13.9	11.3 ± 1.05
(60% \uparrow - 40% \downarrow)	(12.9)	

• CALCULATED γ_g AGREES WITH EXPERIMENT BOTH FOR THE MAGNITUDE AND SIGN

MICROSCOPIC ELECTRONIC ORIGIN OF $\gamma(-3\omega; \omega, \omega, \omega)$

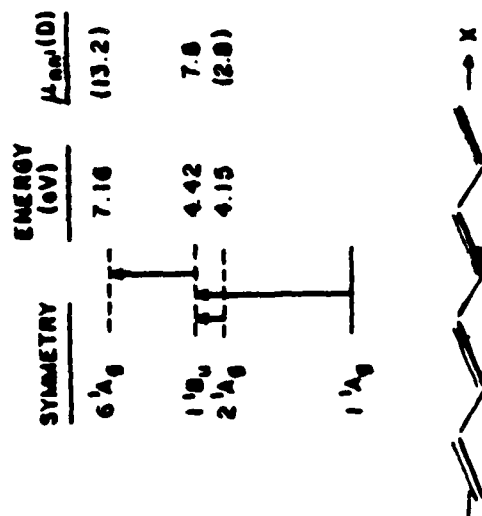
$$\chi_{ijkl}(-3\omega; \omega, \omega, \omega) = \frac{e^4}{4\hbar^3} \sum_{m_1, m_2, m_3} \frac{\langle g | r_i | m_3 \rangle \langle m_3 | r_j | m_2 \rangle \langle m_2 | r_k | m_1 \rangle \langle m_1 | r_l | g \rangle}{(\omega_{m_1 g} - \omega)(\omega_{m_2 g} - 2\omega)(\omega_{m_3 g} - 3\omega)} + \dots$$

TWO IMPORTANT TYPES OF CONTRIBUTING TERMS



- INTERMEDIATE STATE m_2 IS THE GROUND STATE ITSELF
- NUMERATOR IS POSITIVE
- $(\omega_{gg} - 2\omega)$ TERM IN DENOMINATOR IS NEGATIVE
- NEGATIVE CONTRIBUTION TO γ
- INTERMEDIATE STATE m_2 IS THE UPPER $6'A_g$ STATE
- NUMERATOR IS POSITIVE
- $(\omega_{m_2 g} - 2\omega)$ TERM IN DENOMINATOR IS POSITIVE
- POSITIVE CONTRIBUTION TO γ

TRANSITION DENSITY MATRIX DIAGRAMS

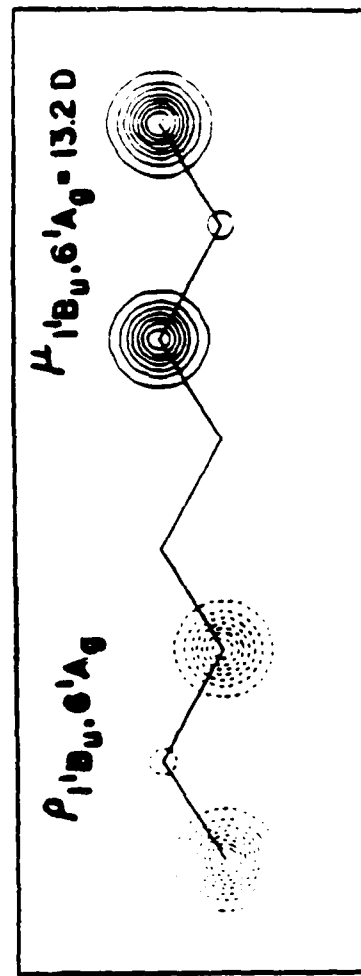
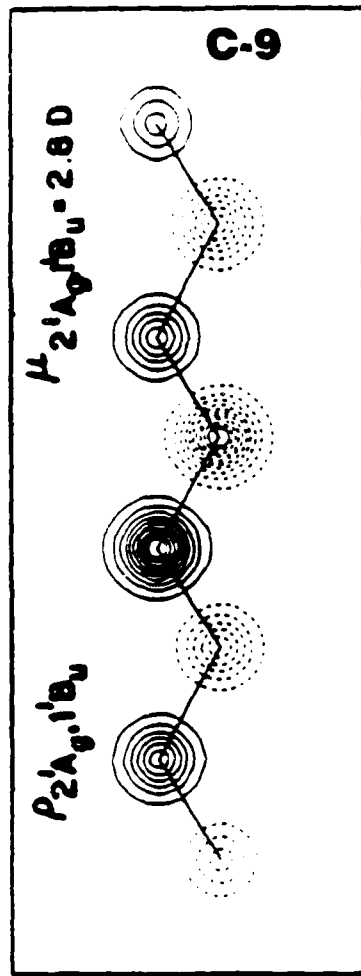
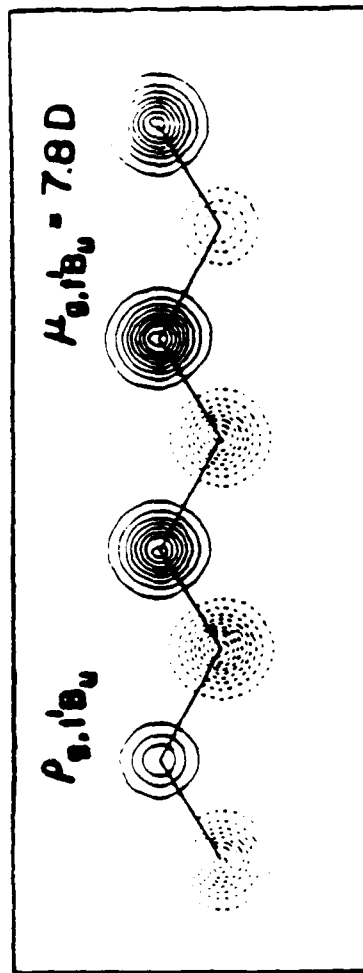


OT

$$\bullet \langle \mu_{\text{ext}} \rangle = \int \rho_{\text{ext}}(r) dr$$

• CORRELATION OCCURS ACROSS ENTIRE CHAIN LENGTH

• $\mu_{1'B_u, 6'A_g} \gg \mu_{2'A_g, 1'B_u}$: CHARGE SEPARATION IS LARGEST IN $\rho_{1'B_u, 6'A_g}$



DEPENDENCE OF $\gamma(-3\omega_i, \omega_i, \omega_i)$ ON NUMBER OF SITES

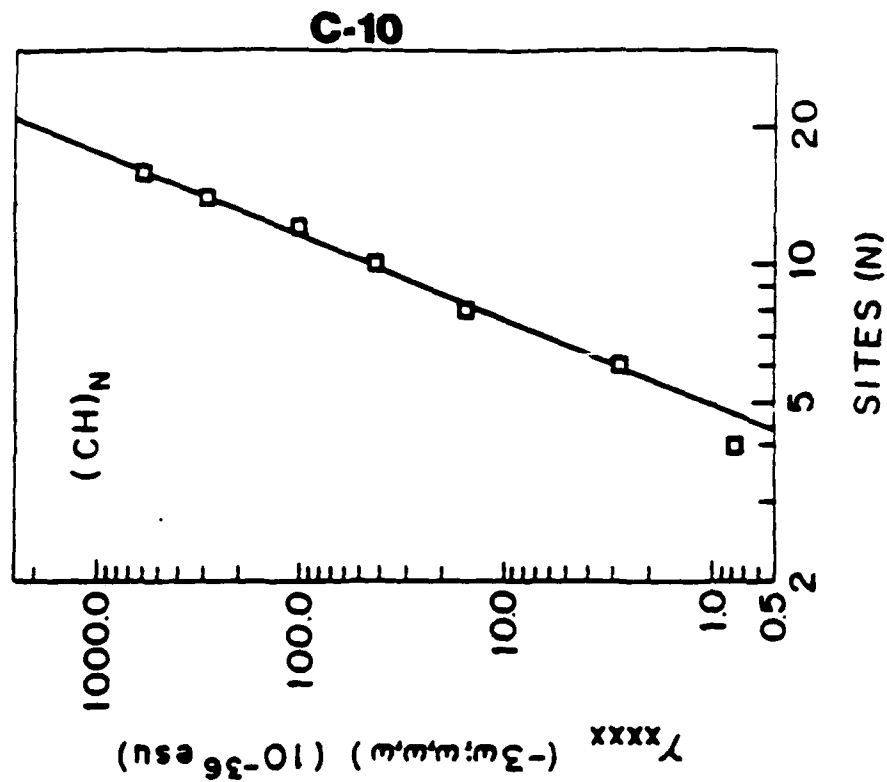
- FINITE CHAIN LIMIT: POWER LAW DEPENDENCE

$$\gamma_{xxxx} \propto N^{5.4}$$

- DECREASED EXCITATION ENERGY
- INCREASED TRANSITION MOMENTS
- INCREASED NUMBER OF CONTRIBUTING EXCITED STATE TERMS

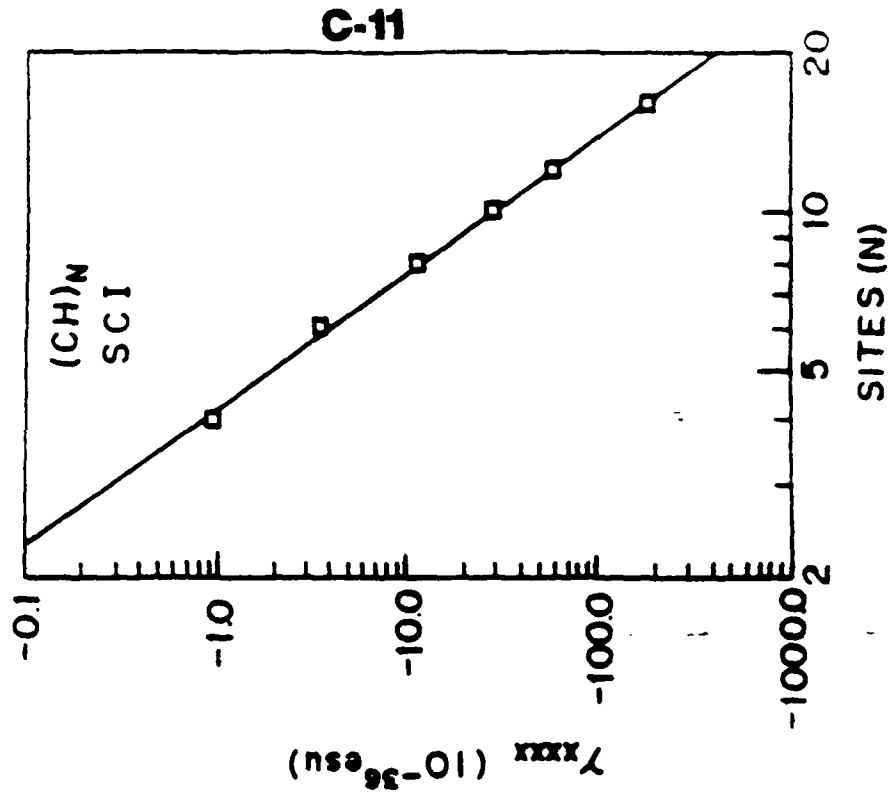
- POLYMER CHAINS: $\chi^{(3)} \sim 10^{-9}$ esu

- 50 SITES (60 Å)



INCOMPLETE DESCRIPTION OF ELECTRON CORRELATION

- SCI ONLY; OTHERWISE IDENTICAL TO FULL. SDCI
- NEGATIVE SIGN FOR γ_{HSH} FOR ALL CHAIN LENGTHS
- SCI POWER LAW EXPONENT IS 3.9 AS COMPARED TO 5.4 OF SDCI



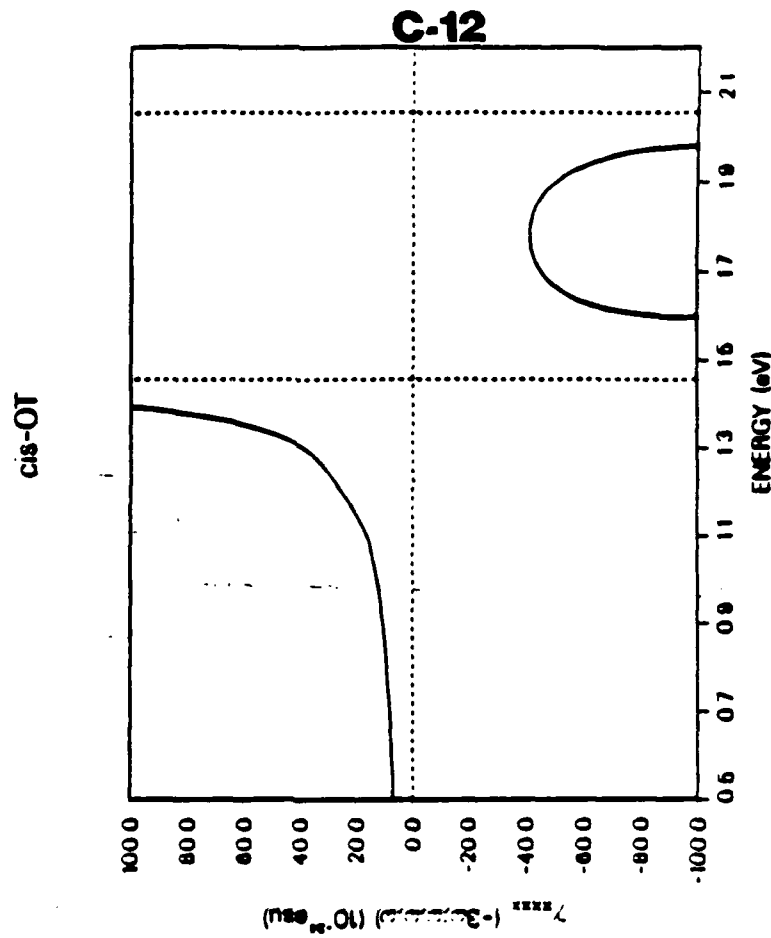
MICROSCOPIC ORIGIN OF $\gamma(-3\omega; \omega, \omega, \omega)$ FOR CIS - POLYENES



cis - OCTATETRAENE (cis-OT)

- $\gamma_{xxxx}(-3\omega; \omega, \omega, \omega) = 7.7 \times 10^{-36} \text{ esu}$
($\omega = 0.65 \text{ eV}/\hbar$)
- $\gamma_g(-3\omega; \omega, \omega, \omega) = 1.6 \times 10^{-36} \text{ esu}$

- ONLY CONTRIBUTIONS: $g \rightarrow {}^1B_u \rightarrow {}^1A_g \rightarrow {}^1B_u \rightarrow g$
- 1A_g STATES: THOSE WITH LARGEST $\mu_{nn'}$ WITH DOMINANT 1B_u STATE
- 2 PHOTON 1A_g STATES CRITICAL IN TUNING ORDER PROCESSES

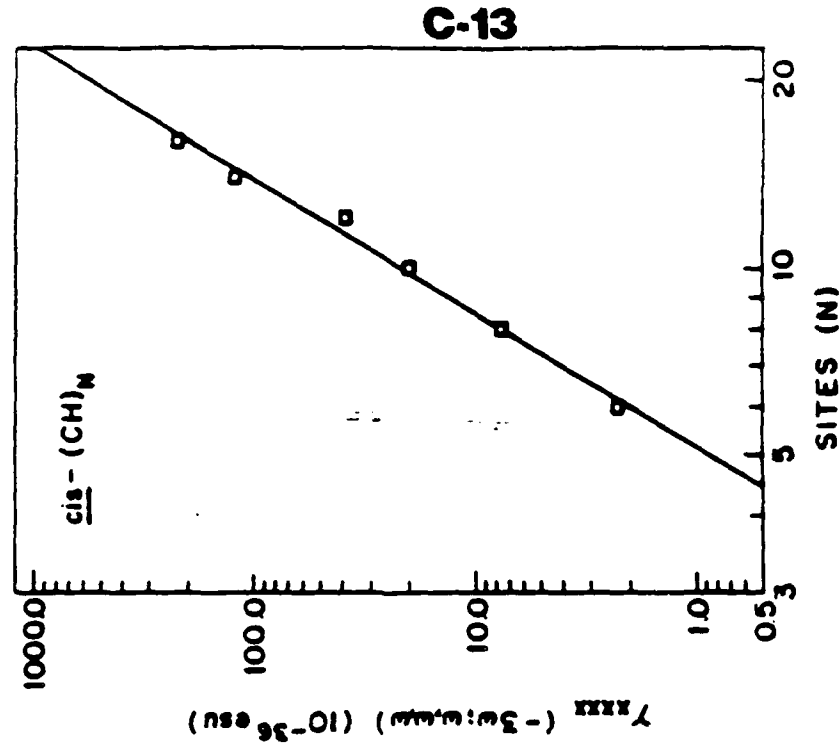


DEPENDENCE OF $\gamma(-3\omega; \omega, \omega, \omega)$ ON NUMBER OF SITES

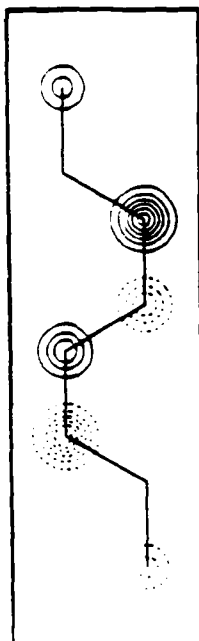
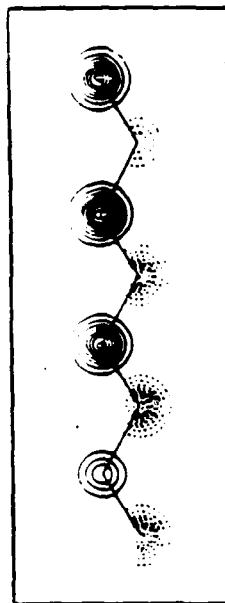
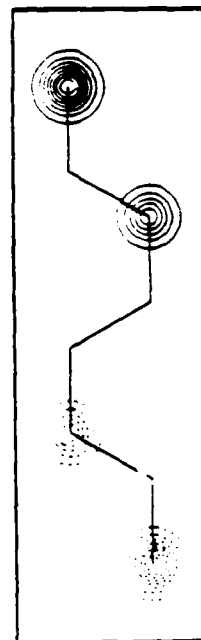
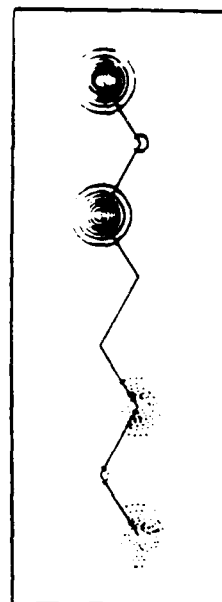
- FINITE CHAIN LIMIT: POWER LAW DEPENDENCE

$$\gamma_{\text{max}} \propto N^{4.7}$$

- DECREASED EXCITATION ENERGY
- INCREASED TRANSITION MOMENTS
- INCREASED NUMBER OF CONTRIBUTING EXCITED STATE TERMS

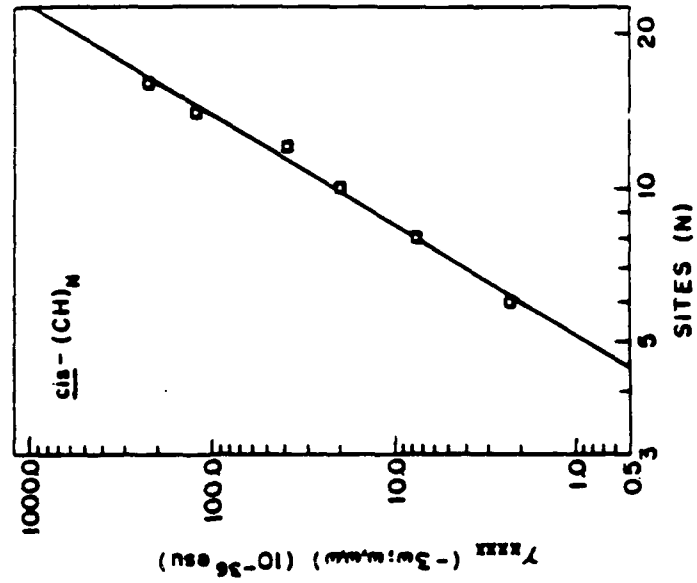


TRANSITION DENSITY MATRIX DIAGRAMS

 $\rho_{g,i}B_u$ $\mu_{g,i}B_u = 7.90$  $\mu_{g,i}B_u = 7.80$  $\rho_{i'1}B_u, 6'A_g$ $\mu_{i'1}B_u, 6'A_g = 12.00$  $\mu_{i'1}B_u, 6'A_g = 13.20$ 

• CHARGE REDISTRIBUTION ESSENTIALLY
THE SAME FOR cis AND trans
CONFORMATIONS

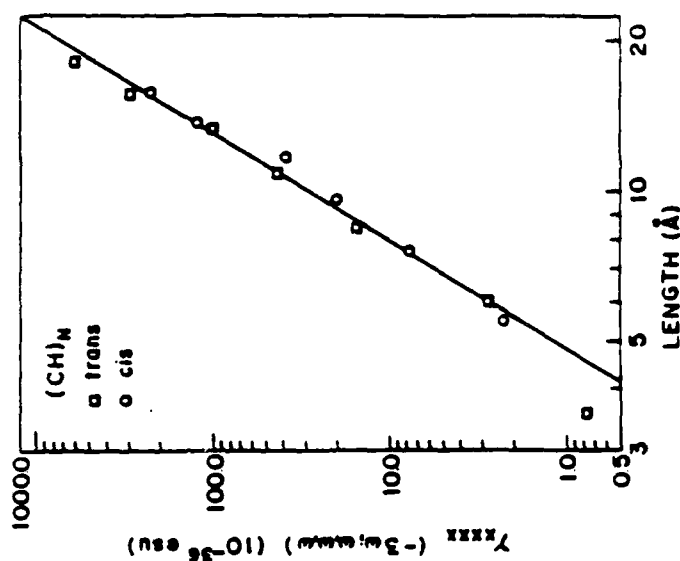
DEPENDENCE OF $\gamma(-3\omega_i, \omega_i, \omega_i)$ ON NUMBER OF SITES



- FINITE CHAIN LIMIT: POWER LAW DEPENDENCE

$$\gamma_{RR} \propto N^{4.7}$$

- DECREASED EXCITATION ENERGY
- INCREASED TRANSITION MOMENTS
- INCREASED NUMBER OF CONTRIBUTING EXCITED STATE TERMS

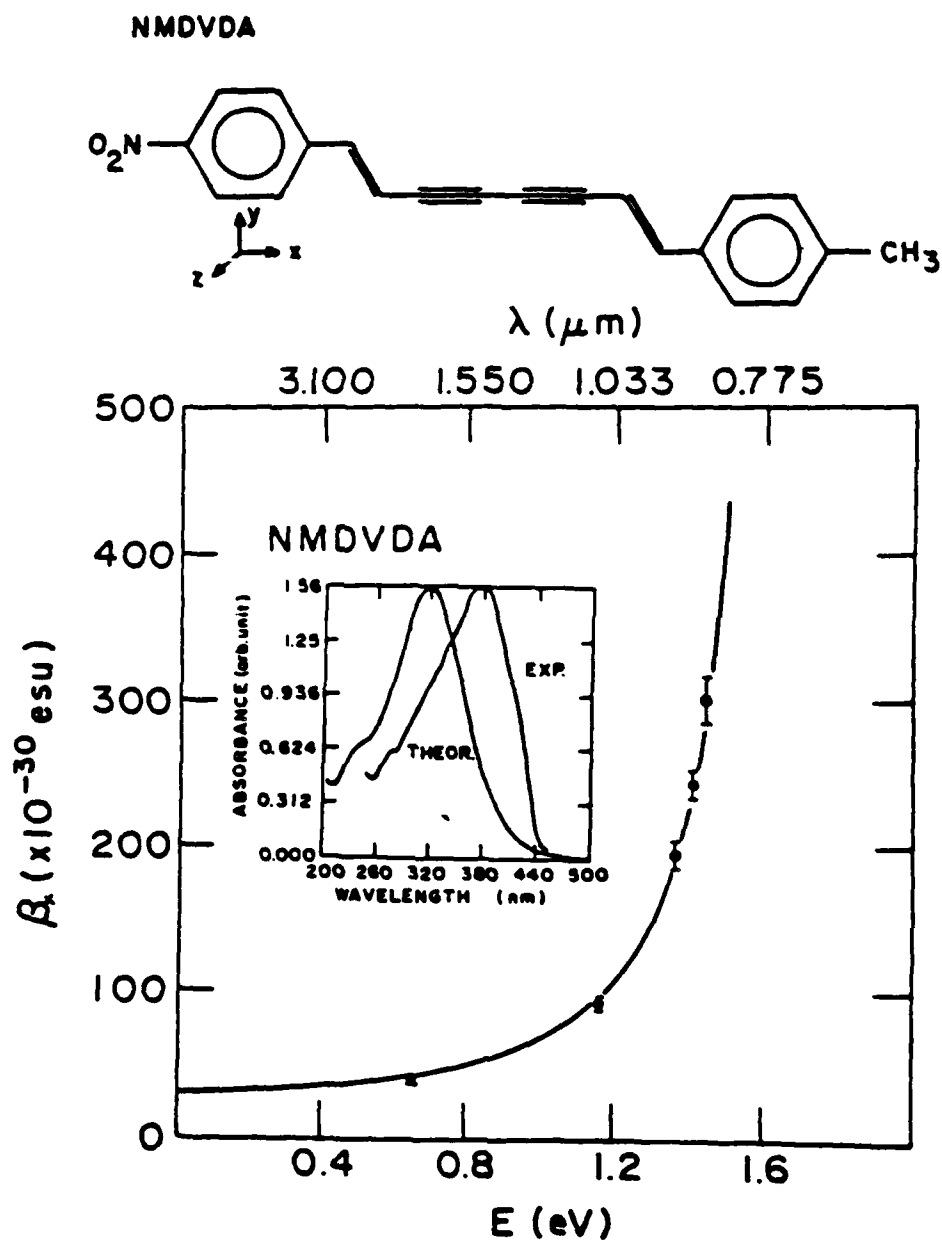


DEPENDENCE OF $\gamma(-3\omega; \omega, \omega)$ ON CHAIN LENGTH

- FINITE CHAIN LIMIT : $\gamma_{xxxx} \propto L^{4.6}$
- $\gamma_{xxxx}(-3\omega; \omega, \omega)$ FOR cis IS SMALLER THAN THAT FOR trans OF SAME NUMBER OF SITES
- DIFFERENCE IN $\gamma_{xxxx}(-3\omega; \omega, \omega)$ IS ACCOUNTED FOR BY DIFFERENCE IN LENGTH IN X-DIRECTION
- $\gamma_{xxxx}(-3\omega; \omega, \omega)$ MUCH MORE SENSITIVE TO CHAIN LENGTH THAN CONFORMATION

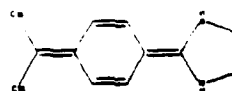
C-17

ELECTRON CORRELATED STATES: ORIGIN OF SECOND ORDER NONLINEAR OPTICAL SUSCEPTIBILITY OF CONJUGATED CYCLIC CHAINS

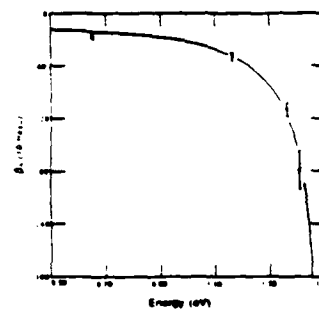
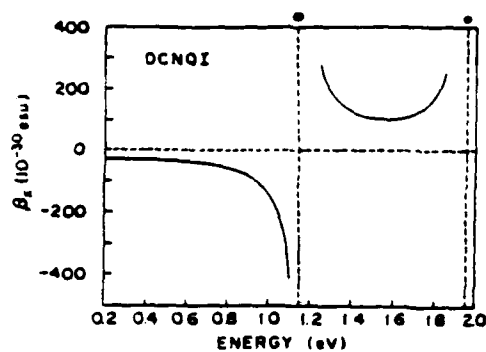
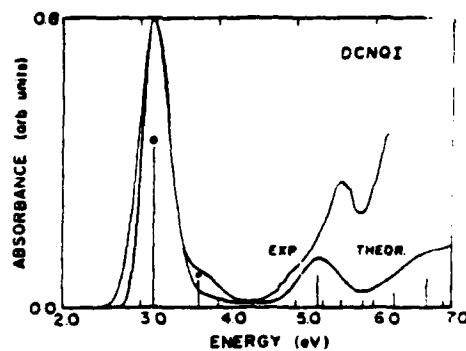


C-18

DCNQI



SYMMETRY C_{2v}	ENERGY (eV)	μ_{nq}^x (D)	$\Delta\mu_n^x$ (D)
$\bullet 3A_1$	3.92	3.1	-6.8
$1B_2$	3.78	0.0	-3.1
$\bullet 2A_1$	2.31	9.0	-4.1
$1A_1$			



DCNQI	Experimental	SDCI	SCI
μ_x (Debye)	17.5 ± 0.8	17	18.4
β_x (10^{-30} esu)	-27 ± 3	-19.7	-73.2
$\mu_x \beta_x$ (10^{-48} esu)	-474 ± 52	-335	-1347

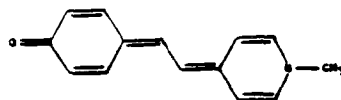
Comparison of Experimental and SDCI,SCI Values of Dipole Moment and the Second Order Microscopic Susceptibility at 0.65 eV.

	SDCI	SCI
$\beta_{diag}^{(H)}$	44%	85%
$\beta_{off}^{(H)}$	56%	15%

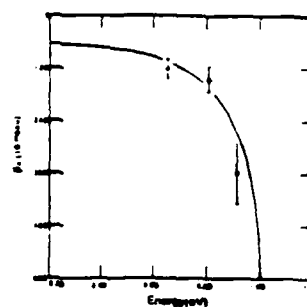
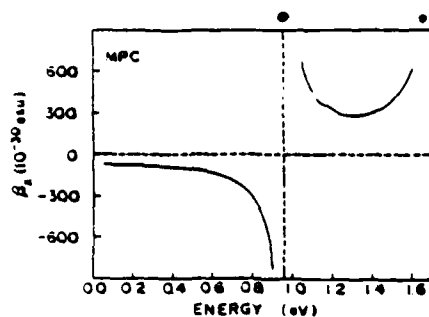
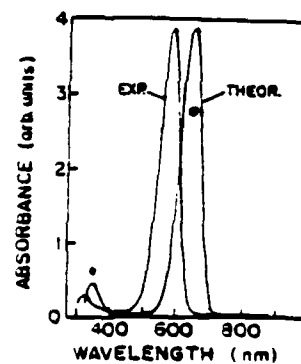
The percentage Contributions of Diagonal Term and Off-diagonal Term.

C-19

MPC



SYMMETRY C_s	ENERGY (eV)	μ_{ng}^x (D)	$\Delta\mu_{ng}^x$ (D)
$\bullet 5A'$	3.69	4.7	-8.3
$1A'$	3.69	0	-20.0
$4A'$	3.54	0.4	-13.8
$3A'$	2.42	0.1	-14.1
$\bullet 2A'$	1.92	12.0	-4.4
$1A'$			



MPC	Experimental	SDCI	SCI
μ_s (Debye)	17.4 ± 2.5	21.4	25.1
β_2 (10^{-30} esu)	-123 ± 22	-104.7	-236.4
$\mu_s \beta_2$ (10^{-48} esu)	-2140 ± 390	-2240	-5933

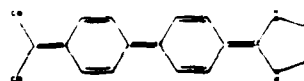
Comparison of Experimental and SDCI,SCI Values of Dipole Moment and the Second Order Microscopic Susceptibility at 0.65 eV.

	SDCI	SCI
β_{TXX}^W	55.5%	86.4%
β_{TYY}^W	44.5%	13.6%

The percentage Contributions of Diagonal Term and Off-diagonal Term.

C-20

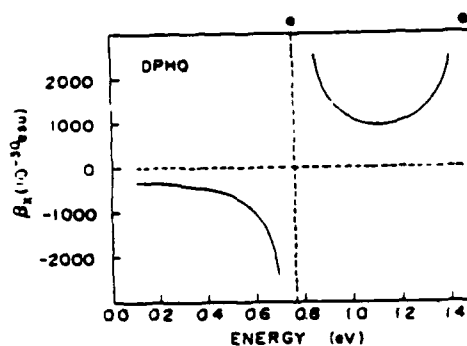
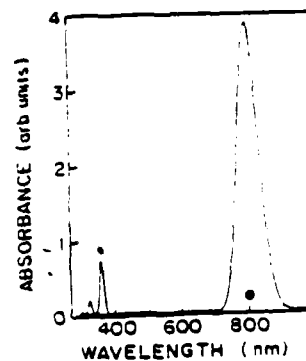
DPHQ



SYMMETRY C_{2v}

• $3A_1$
 $1B_2$
 • $2A_1$
 $1A_1$

ENERGY (eV)	μ_{ng}^x (D)	$\Delta\mu_n^x$ (D)
3.41	4.2	-8.6
3.18	0	-9.4
1.54	14.4	-7.7



DPHQ	SDCI	SCI
μ_x (Debye)	25.4	30.5
β_x (10^{-30} esu)	-1410	-628
$\mu_x \beta_x$ (10^{-48} esu)	-35800	-19100

Comparison of Experimental and SDCI,SCI Values of Dipole Moment and the Second Order Microscopic Susceptibility at 0.65 eV.

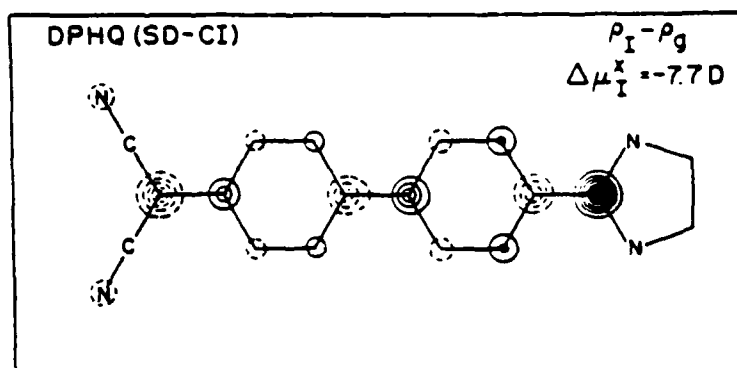
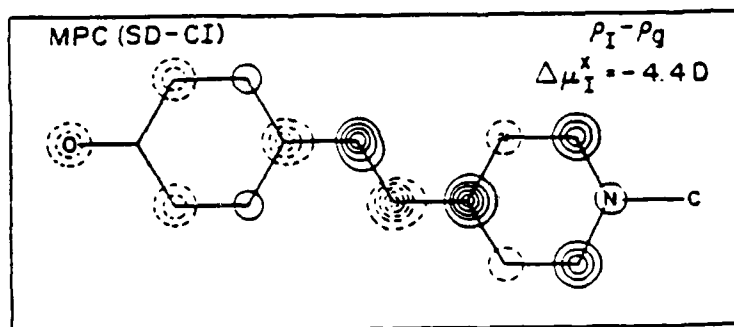
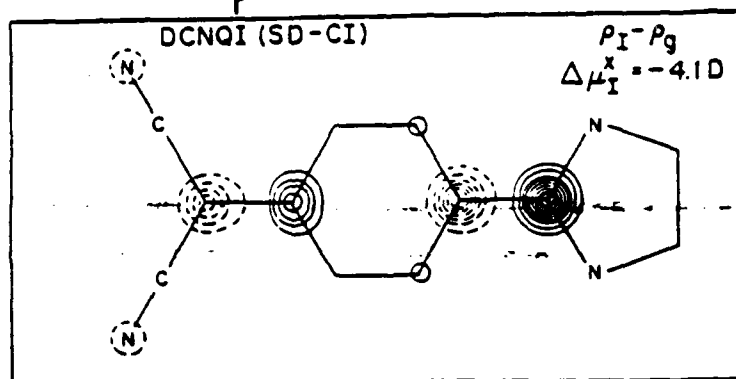
	SDCI	SCI
β_{TXX}^{nw}	72%	85%
β_{TXX}^{nw}	28%	15%

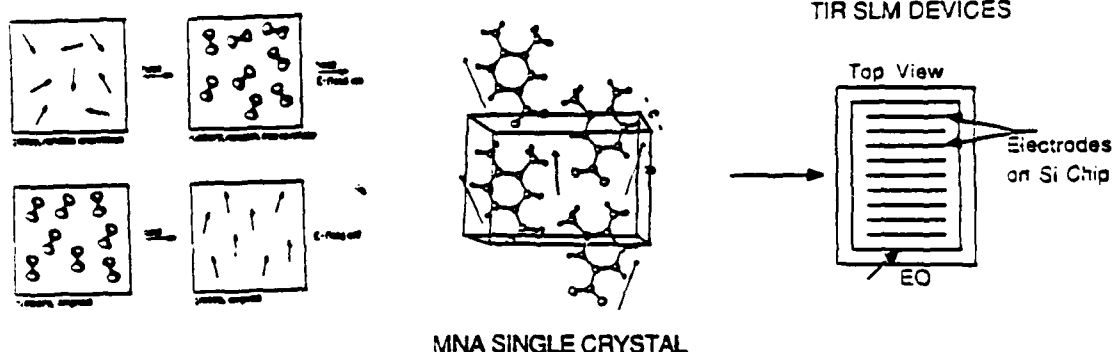
The percentag , Contributions of Diagonal Term and Off-diagonal Term.

C-21

ELECTRON DENSITY CORRELATION DIAGRAMS

$$\langle \Delta \mu_n \rangle = e \int r (\rho_n - \rho_g) dr$$





MNA SINGLE CRYSTAL

Orientational Order

$$\chi_{111}^{(2)} = N \frac{\beta_{xxx} \mu_x E}{k_B T} f^2 \omega (f^2 \omega)^2 \left(\frac{1}{5} + \frac{4}{7} \langle P_2 \rangle + \frac{8}{35} \langle P_4 \rangle \right)$$

CLASS	SYSTEM	$\mu_x \beta_x$ ($10^{-30} \text{cm}^2 \text{Desu}^{-1}$)	d_{11} (10^{-9}esu) ($\lambda = 1.907 \mu\text{m}$)	r_{11} (10^{-12}m/V) ($\lambda = 0.633 \mu\text{m}$)
RESONANT RING	MNA	66	0.8	0.3
	AZO DYE	530*	6*	2.5
	MNA SINGLE CRYSTAL		230	67
LINEAR CHAIN	NMDVOA	200	2.3	0.9
CYCLIC CHAIN	MPC	2100	24	10
	DCNQI	470	5.3	2.2
	DPHQ	36000	410	170

*Measured at $\lambda = 1.58 \mu\text{m}$

RELATED REFERENCES

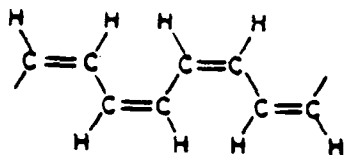
1. Third harmonic generation study of orientational order in nematic liquid crystals, Phys. Rev. **A34**, 5051 (1986).
2. Microscopic origin of second order nonlinear optical properties of organic structures, in Nonlinear Optical and Electroactive Polymers (Plenum, New York, 1988).
3. Recent developments in microscopic descriptions of the nonlinear optical properties of organic and polymer structures, in Proceedings SPIE 825 (1988).
4. Nonlinear optical properties of linear chains and electron correlation effects, Phys. Rev. B - Rapid Communications (in press).
5. Symmetry controlled electron correlation mechanism for third order nonlinear optical properties of conjugated linear chains, in Electroresponsive Polymers, Special Issue, Mol. Cryst. Liq. Cryst. (1988).
6. Nonlinear optical properties of polyenes: Electron correlation and chain conformation, in Nonlinear Optical Properties of Polymers (Materials Research Society, Boston, 1988) **109**, p. 91.

D-1

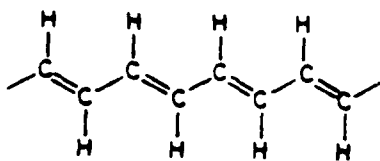
S. Etemad
Bell Communications

CONJUGATED POLYMERS
AND
NONLINEAR OPTICS

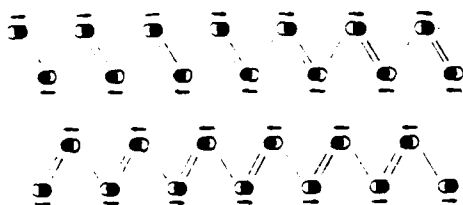
D-2



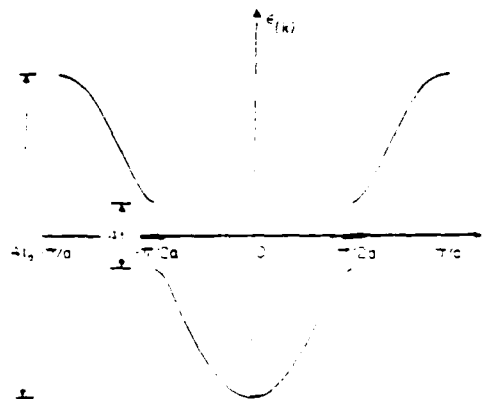
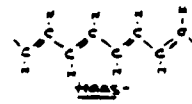
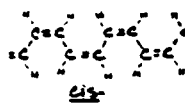
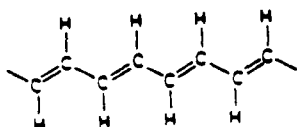
(a)



(b)



trans-(CH)₄



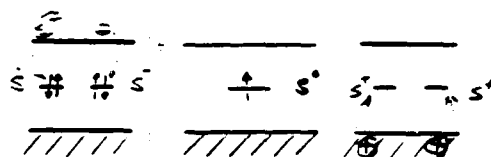
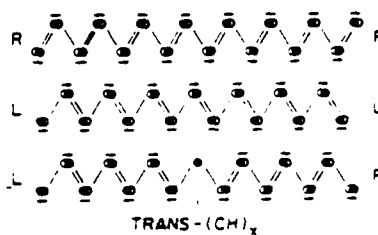
trans-(CH)₄

$$E_g = 2.5 - 3.0 \text{ eV}$$

$$2\Delta = 4E_g = 1.5 \text{ eV} \quad \text{c.f. a.s.}$$

$$E_g = 0.05 \text{ eV}$$

REVERSED CHARGE SPIN



D-3

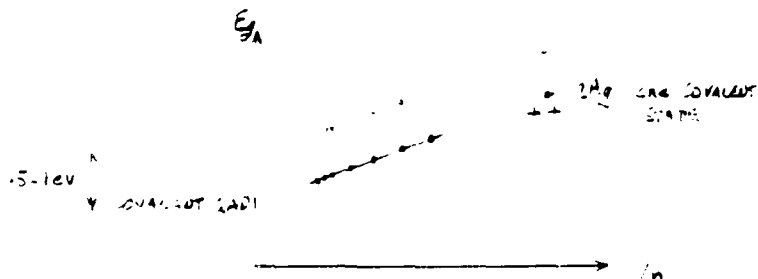
CHEMISTRY VIEW



HIGHLY CORRELATED STATES

(MANY BODY)

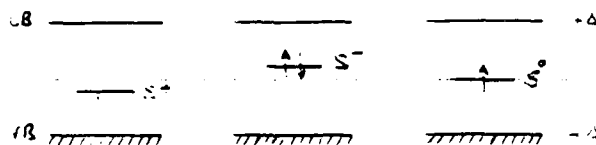
CASE STUDY: FINITE POLYMER



n IS CONFIGURATION LENGTH

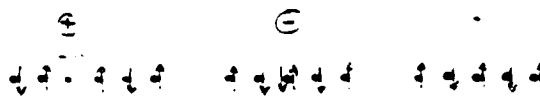
COULOMB INTERACTIONS

PERTURBATION APPROACH



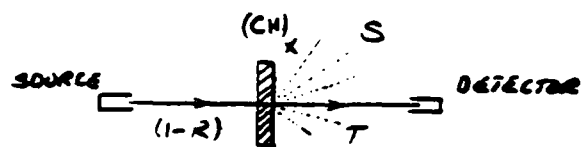
"MID-GAP" TRANSITIONS

HIGHLY CORRELATED STATES

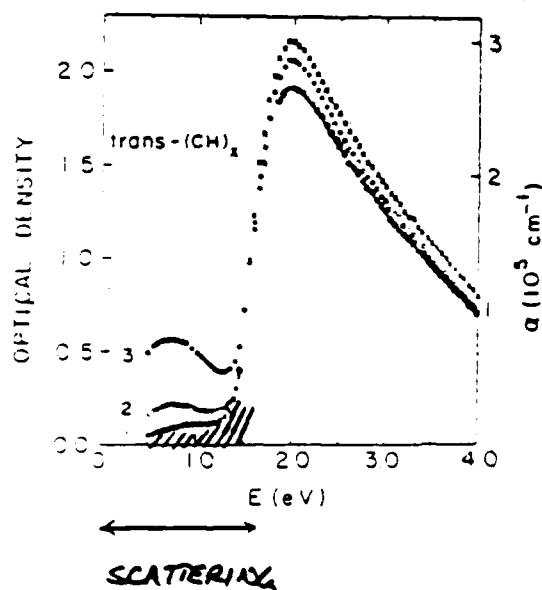


LOWEST ENERGY TRANSITIONS

S^+ ABSORPTION AT BAND GAP

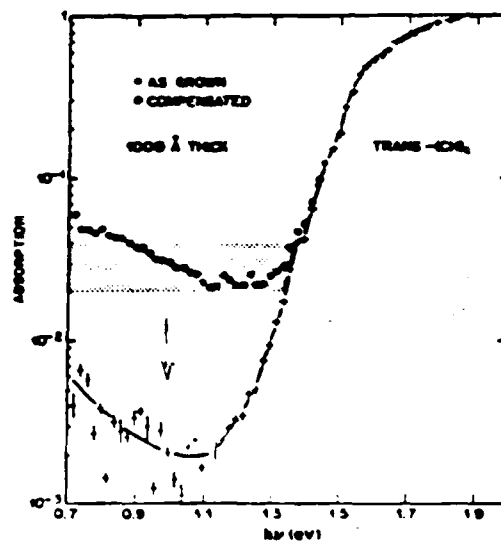


$$1-R = T + S + R$$

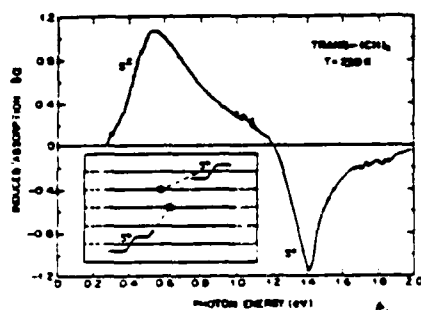


LONG TIME BEHAVIOR

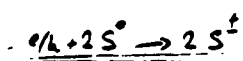
EFFECT OF COMPENSATION
WITH NH_3



MOL. CRYST. LIQ. CRYST. 17, 275.



A. J. J. E. 1974

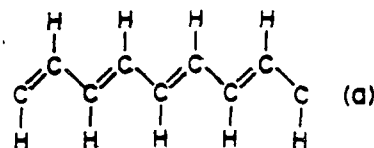


PRL 30, 786 (74)

λ^+

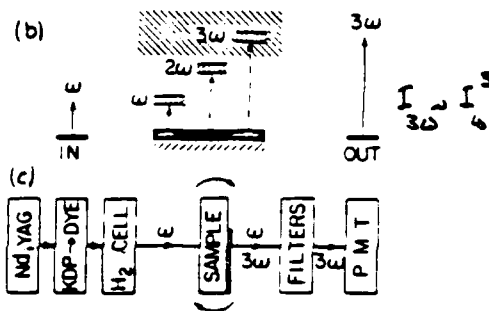
2.

COVALENT
GAS



WHERE IS THE 2^{nd} 'COVALENT GAP'
WITH RESPECT TO 13_{th} 'IONIC GAP'

THIRD HARMONIC GENERATION



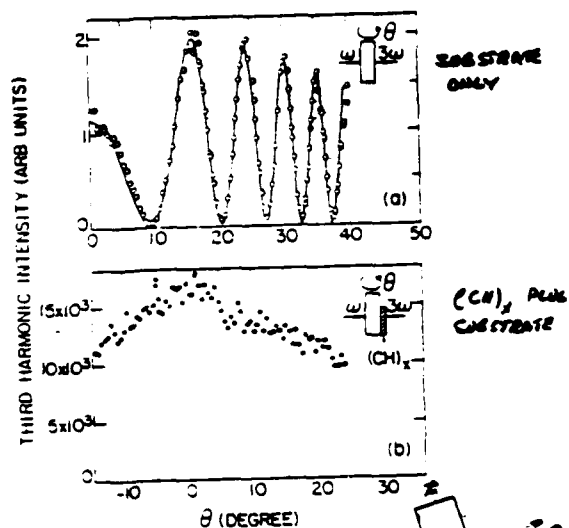
FILM. COMPENSATED $(CH_3)_X$ Fig. 1
700 Å THICK; UNIFORM

$$\chi^{(3)}(3\omega; \omega, \omega, \omega) = \sum_{n_1 n_2 n_3} \Omega_{n_1} \Omega_{n_2} \Omega_{n_3} \Omega_{n_1 + n_2 + n_3} \left[\frac{1}{(E_{n_1} - 3\omega)(E_{n_2} - 2\omega)(E_{n_3} - \omega)} + \frac{1}{(E_{n_2} + \omega)(E_{n_3} - 2\omega)(E_{n_1} - \omega)} + \frac{1}{(E_{n_3} + \omega)(E_{n_1} + 2\omega)(E_{n_2} - \omega)} + \frac{1}{(E_{n_1} + 3\omega)(E_{n_2} + 2\omega)(E_{n_3} + \omega)} \right]$$

TRANSITIONS BETWEEN ALL STATES
IRRESPECTIVE OF SYMMETRY

D-6

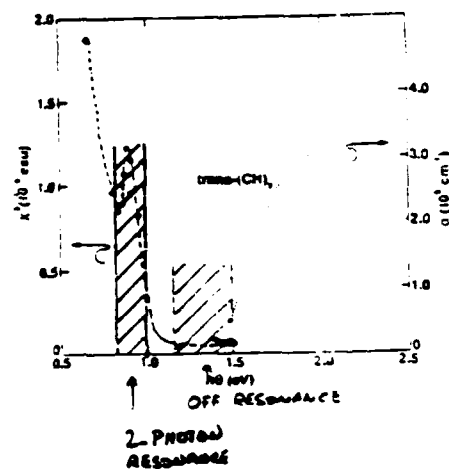
$\chi^{(3)}$ OF $(CH)_x$: CALIBRATION



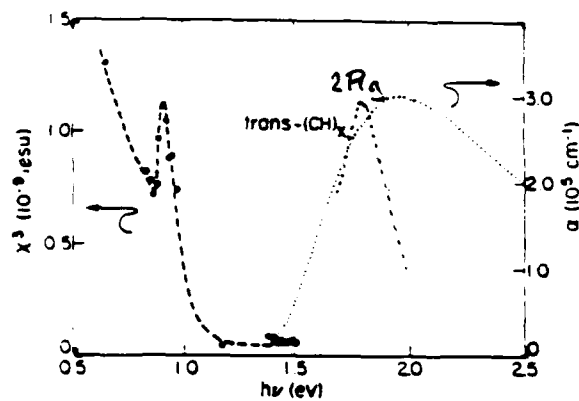
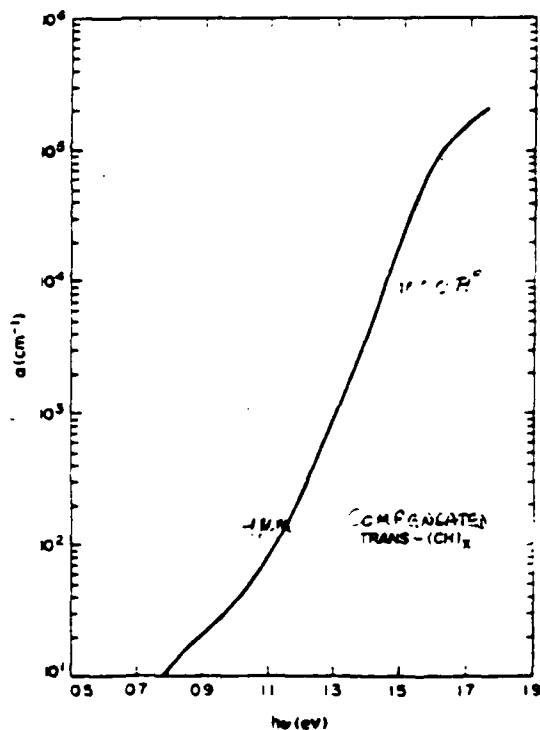
$$L = \frac{\lambda \omega}{6(n_0 - n_{3\omega})}$$

$$\frac{I_{3\omega}}{I_0} \sim I_0^3 \cdot |\chi^{(3)}|^2 \cdot \sin^2\left(\frac{\pi \cos \theta}{2L}\right)$$

$\chi^{(3)}$: BEG LARGE
 $\chi^{(3)} \sim 0.5 \times 10^{-10}$ esu



$\chi^{(3)}$ LARGE

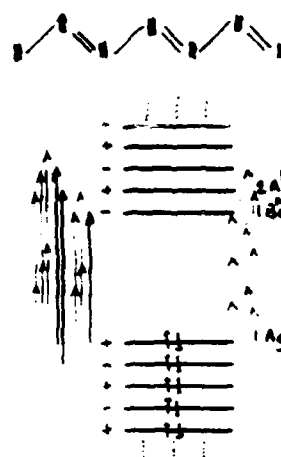


$2R_1$ STATE IS CLOSE TO $1B_u$ STATE?!

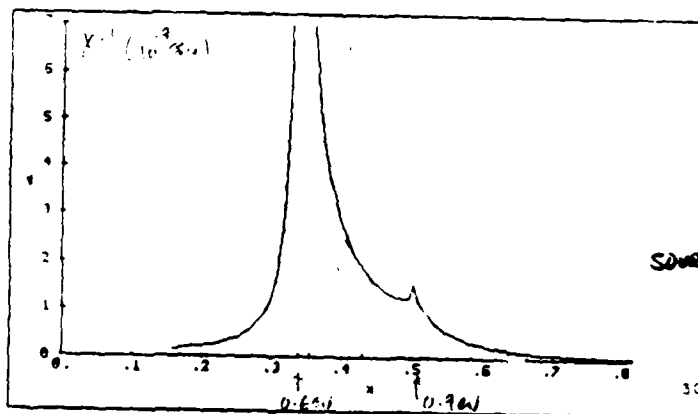
FREE ELECTRON LASER (FEL)

INTENSE TUNABLE IR RADIATION
1 → 100 KW IN 2-10 μm RANGE

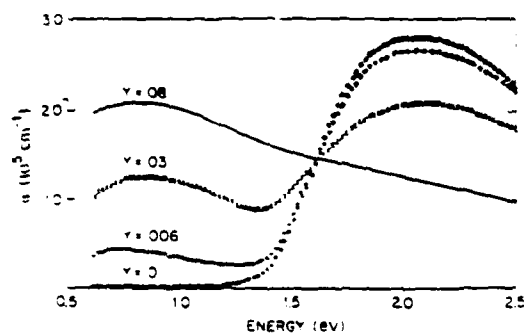
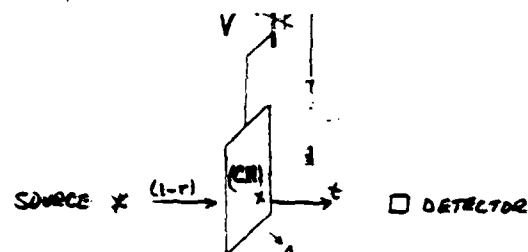
STANFORD → DUKE



- < PARTICLE IN A BOX
- < DIMERIZATION
- < IONIC & COVALENT STATES



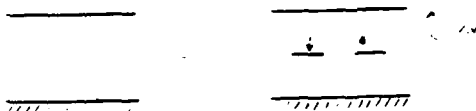
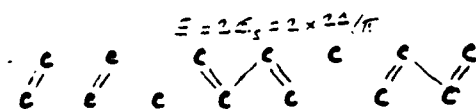
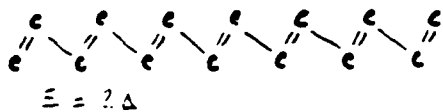
$U=0$ CALCULATION $W < W_u$



$$\chi_{EL} = 1.1 \times 10^{-17} \text{ cm}^2 \cdot \text{eV} / \text{injected charge}$$

ENHANCED BY $\sim 1/a$

DOPING & SOLITON FORMATION



NO SPIN.

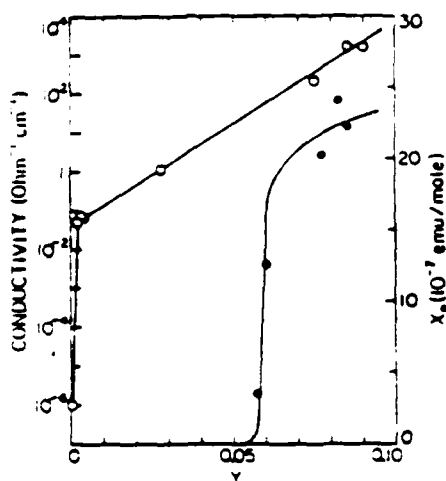
SIGNATURES OF SOLITON

DOPING

APPEARANCE OF ABSORPTION BAND
NEAR 1100 CM⁻¹

APPEARANCE OF ENHANCED IR ACTIVE
LOCAL MODES

NO INCREASE IN χ



Hirai, et al. PRB 29, 2341 (1984)

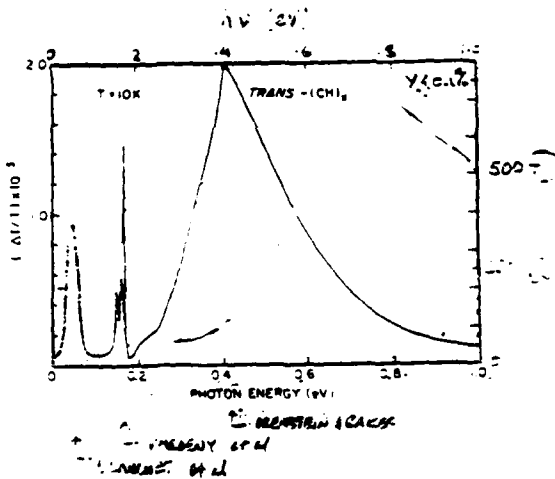
D-9

PHOTOELECTRIC
IN PHOTOELECTRIC

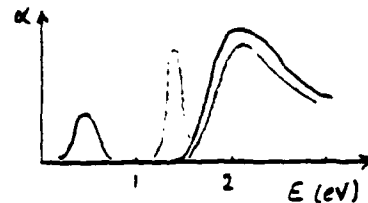
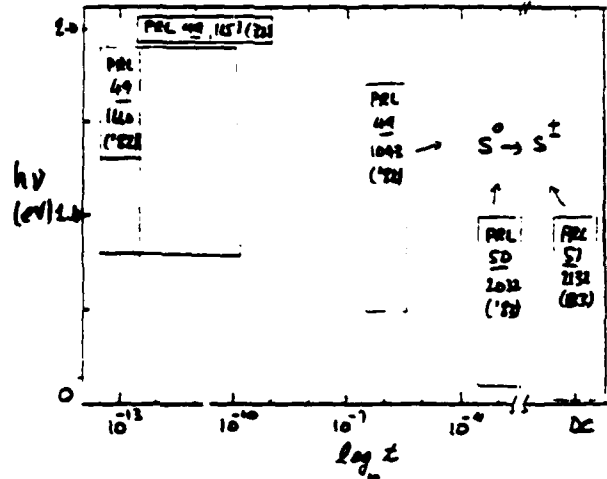
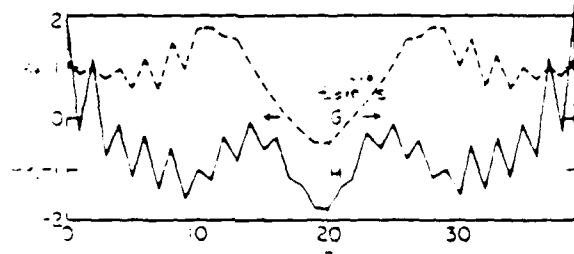
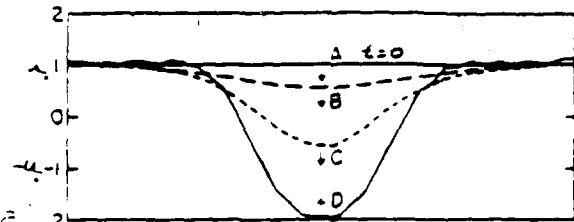
Su & Schrieffer Proc. Nat. Acad. Sci. USA
77 5426 (1980)

SPEED OF RESPONSE RESONANCE

$t > 10^{-2}$ sec.

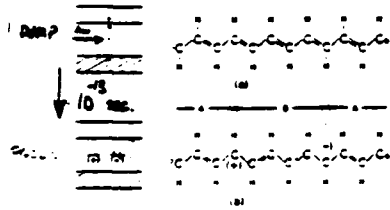


ELECTRONICALLY ENHANCED IR MODES
→ SELF TRAPPED CHARGE IN C60



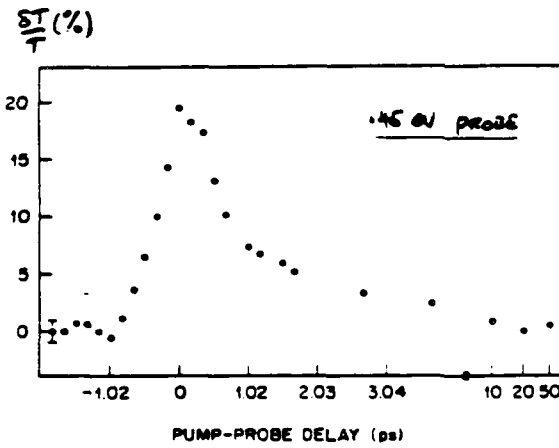
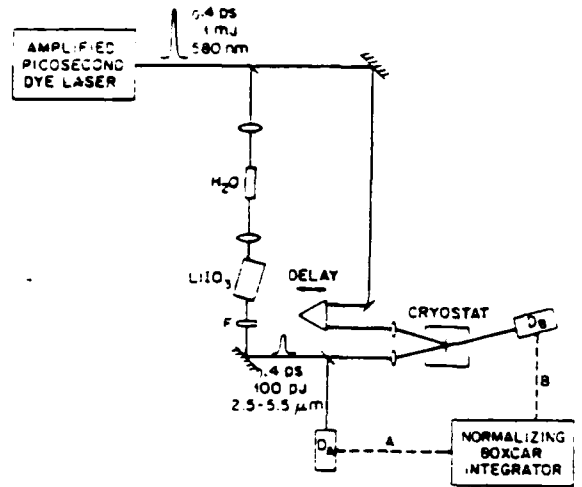
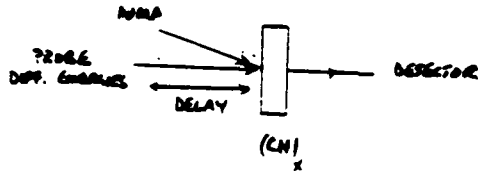
D-10

SU & SCHRIEFFER, *Proc. Natl. Acad. Sci.* 77, 5626 (80)

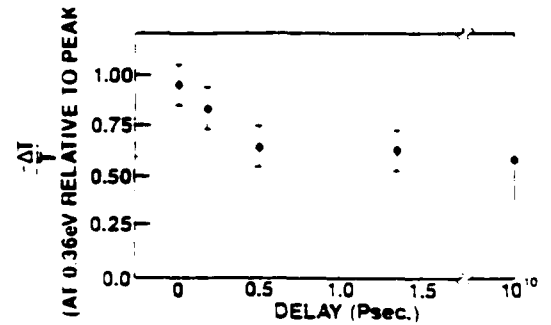
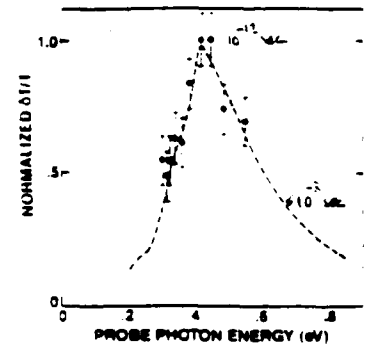


$$E_{ph} > E_{23} \quad (E_2 \approx \frac{24}{h})$$

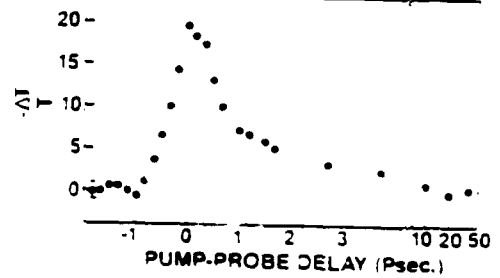
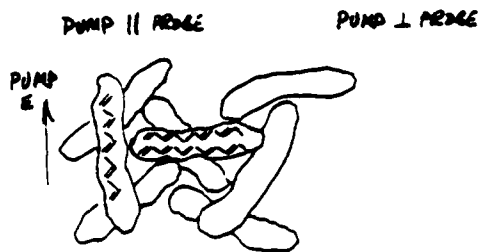
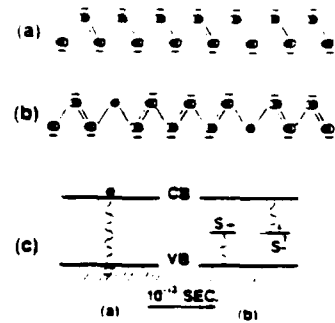
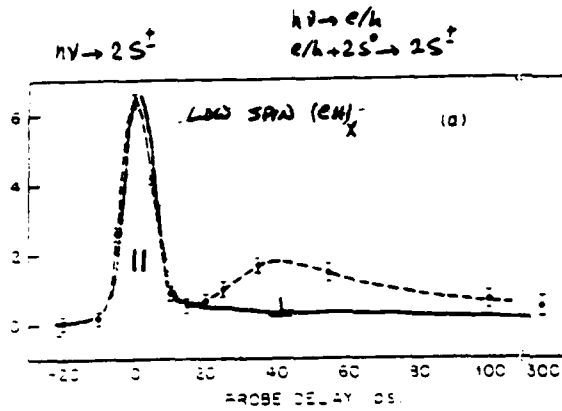
$$\tau = 1/\omega_{ph} \quad (10^{-13} \text{ sec})$$



< 0.1 ps RISE TIME
 ~ 0.5 ps LIFETIME
 POWER DECAY (10 DIFF. ?)

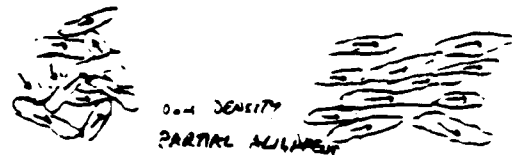


D-11

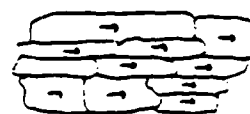


MAGNITUDE OF $\chi^{(3)}$

SHIRAKAWA (CH)



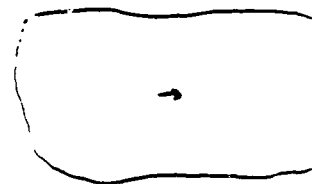
x OFF RESONANCE TRANSPARENT (CH)



DURHAM (CH)

100% ALIGNMENT
100% SPACE FILLING
MACROSCOPIC DOMAINS

x POTENTIAL APPLICATIONS



WINNER'S (CH)

D-12

* INTRINSIC ABSORPTION IS SMALL $2 \times 10^{-3} \mu$
 * SCATTERING LONGER MORPHOLOGY DEPENDENT

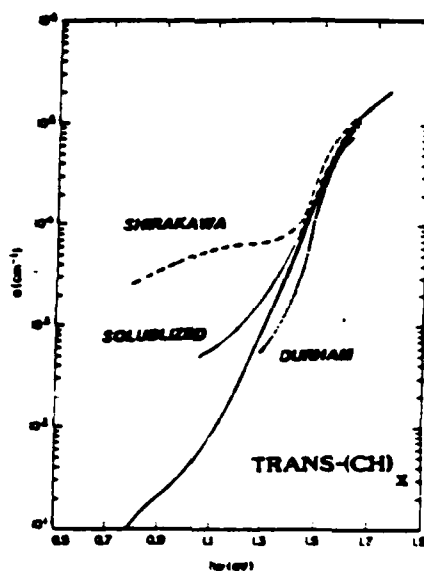


FIGURE OF MERIT

$$K \propto \chi^3 / \alpha_{\text{TOTAL}}$$



FOR n -WAVE DIFFERENTIAL Δn IS NOT LARGE

$$K \propto \alpha_{\text{TOTAL}} = \alpha_{\text{ABS}} + \alpha_{\text{SCATTERING}}$$

→ PROCESSABILITY (1 μm \times 1 μm - THICK FILMS)
 EASE OF FABRICATION

E-1

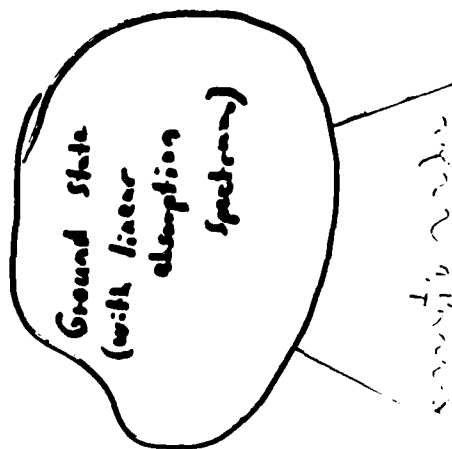
A. J. Heeger

University of California at Santa Barbara

ANISOTROPY OF THE THIRD ORDER
NONLINEAR OPTICAL SUSCEPTIBILITY
IN CONJUGATED POLYMERS

"Instantons" as the source of
Nonlinear Optical Properties
of Polyacetylene

Nonlinear Optics



Acknowledgement:

M. Sinclair

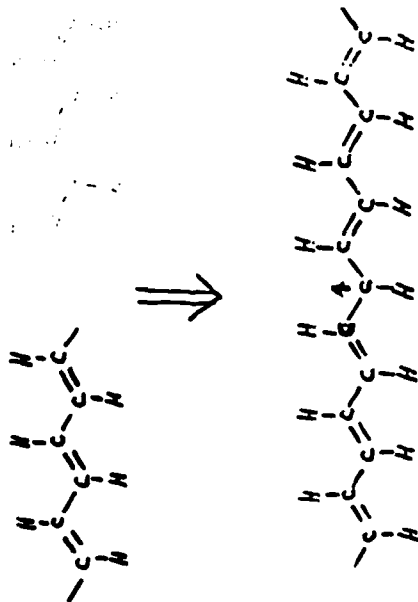
D. Moses

W.-P. Su

E-2

trans - (CH)₂

Broken symmetry with 2-fold
degenerate ground state



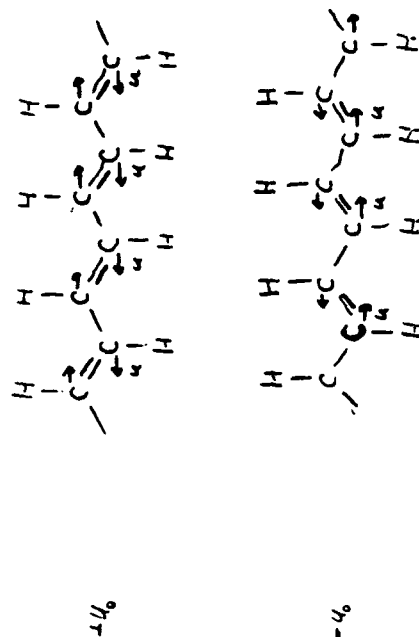
Bond-alternation domain wall or "Soliton"

a "particle" consisting of
structural distortion

localized non-bonding electronic state
p_z

M₁ ~ 5 me

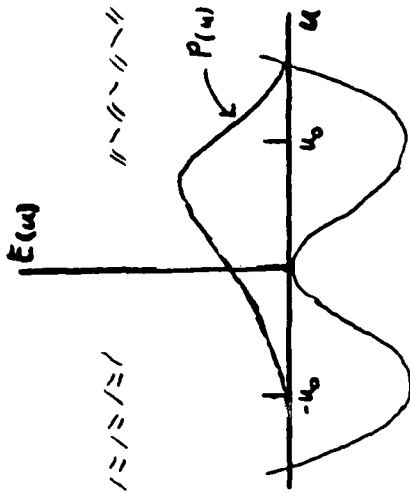
trans - (CH)₂ : two-fold degenerate ground state



E-3

Quantum (zero point) fluctuations
are important!

"Instantons" as the Source of χ'' in $T_{\text{exp}} - (CH)_x$



Order parameter $Q = \pm (-i)^N u_N \stackrel{\text{(classical)}}{=} \pm u_0$

Classical:



Quantum:



"Instanton" = nonlinear zero-point fluctuation

Instantons in polyacetylene

The effect of nonlinear ground state fluctuations on the photoproduction of charged solitons

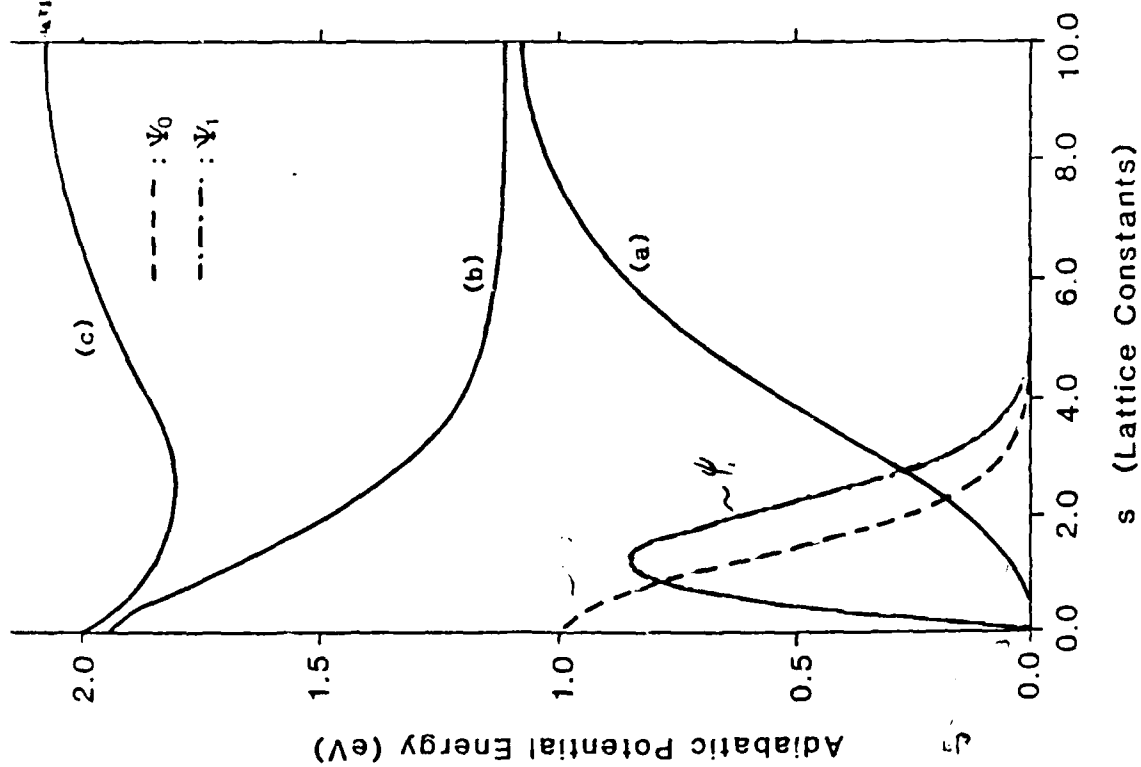
Creation energy for soliton-antisoliton pair

$$\underline{2E_s = \frac{2}{\pi} E_g < E_g}$$

E-4

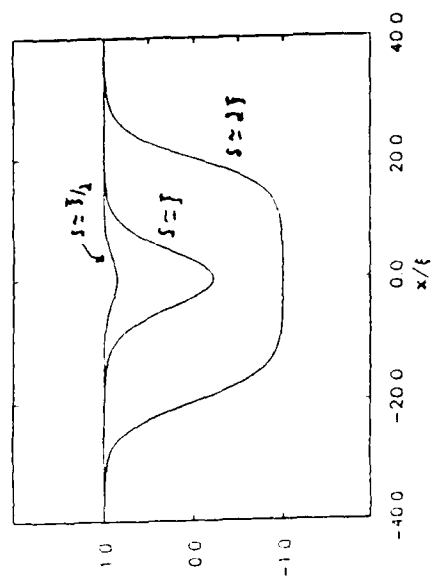
Can one get direct photogeneration of solitons for $\hbar\omega < E_g$?

Yes --- with help from ground state fluctuations !!

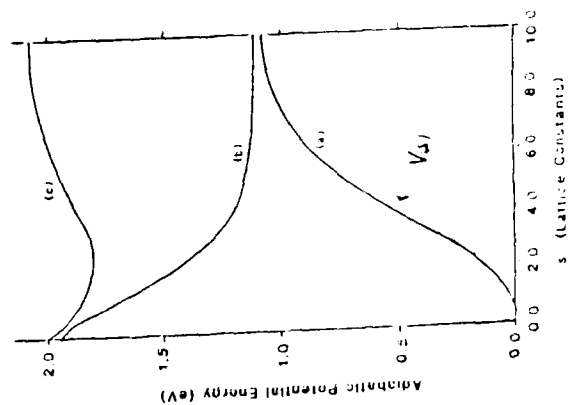


ψ_0, ψ_1 (Lattice Constants)

$$\phi(x=na) = q_0 [1 - \tanh(2s/\xi) \tanh(x-s/\xi) - \tanh(x+s/\xi)]$$



E-5



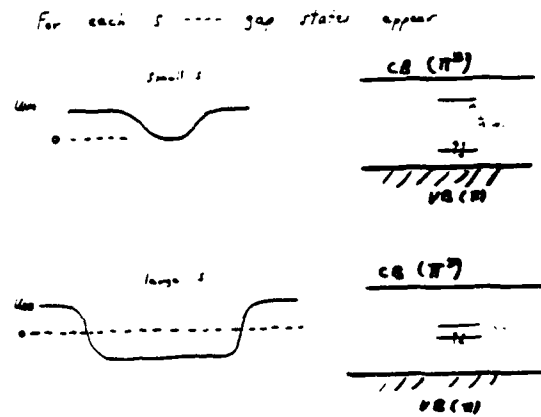
$$U(s) = \frac{1}{2} m \dot{s}^2 - V(s)$$

4 solve

$$\psi_0, \psi_1 = \psi$$

transformed problem

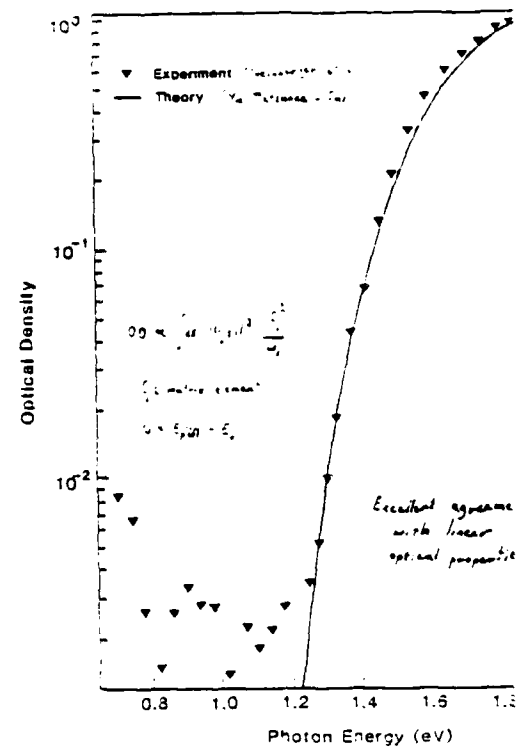
E-6



$$\Delta E = \frac{\gamma}{\pi} \Delta + \hbar \omega_0(\omega)$$

$$E_g = 2.4 = 1.8 - 1.9 \text{ eV}$$

$$\frac{\gamma}{\pi} \Delta \approx 1.15 \text{ eV (threshold)}$$



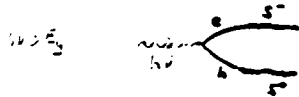
The connection to resonant

nonlinear optical properties

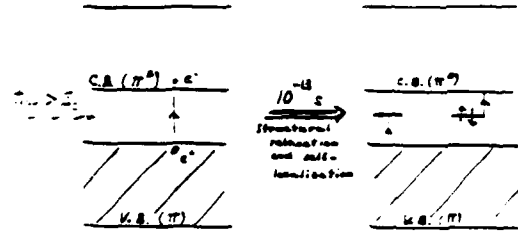
E-7

Soliton Photogeneration & Confinement in $(CH)_x$

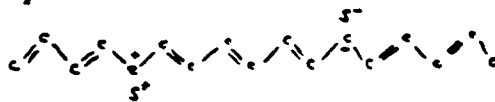
Dynamical calculations (Su & Schrieffer) show that after photogeneration of e-h pair, lattice distortion forms in very short time ($\sim 10^{-13}$ sec) leading to photogenerated S^+ and S^- pairs



Photogeneration of Solitons



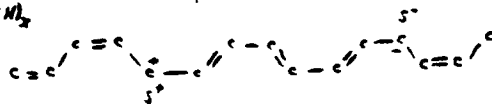
Trans- $(CH)_x$



Two states are equivalent --- S^+ and S^- "free"

Higher energy region

cis- $(CH)_x$



S^+ and S^- are "confined"

Sum Rule

$$\int_{-\infty}^{\infty} \left[\frac{\epsilon''(\omega)}{\omega} \right] d\omega = \int_{-\infty}^{\infty} \left[\frac{\epsilon''(\omega)}{\omega} \right] d\omega \Rightarrow \chi^{(3)} \approx 5 \times 10^{-12} \text{ (resonant)}$$

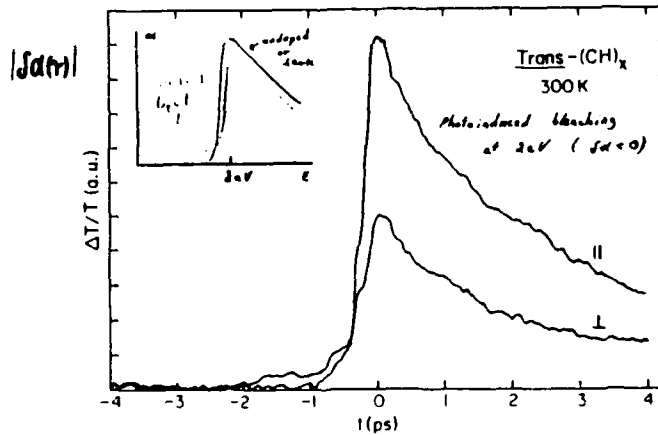
Nonlinear Optics

Index of refraction is different after absorption of 1st photon

Resonant A.C. process

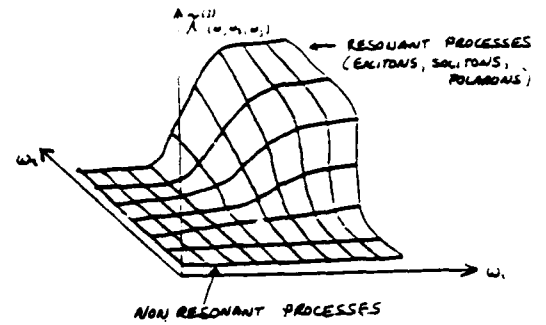
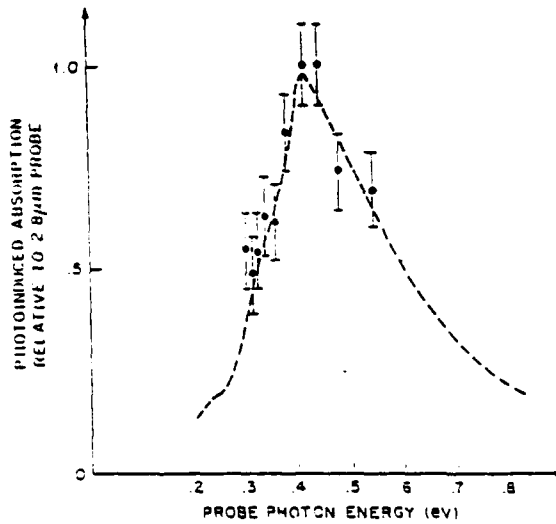
Vardeny, Stuart, Moss, Chou & ASH

PRL (1988)



E-8

Robing, Etend et al



we have seen how solitons lead directly to resonant NLO

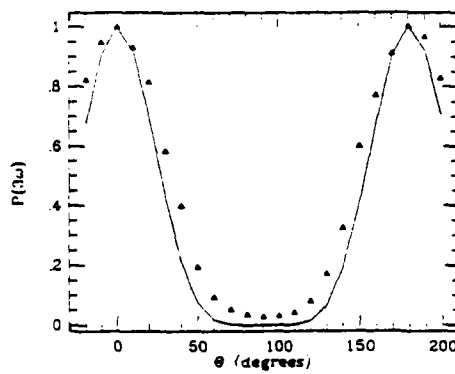
What about non-resonant NLO?

(i.e. for $\hbar\omega < \frac{E_g}{2}$... we have $\frac{E_g}{2}$)

Yes ---- Instantons

THIRD HARMONIC GENERATION IN ORIENTED C_6H_6

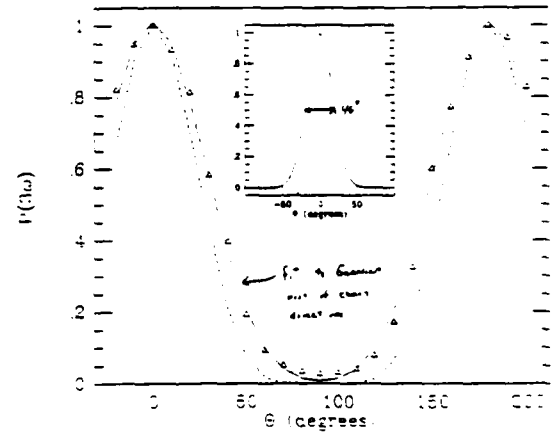
$$P(3\omega) \propto \chi_{11}^{(3)} E_{11}^3 = \chi_{11}^{(3)} E^3 \cos^3 \theta$$



Alignment Direction

Polarization direction

$$\chi_{11}^{(3)}(3\omega, \omega, \omega) = (4 \pm 1) \times 10^{-10} \text{ esu}$$



711 Nonlinearity associated with
-Electron reorganization
-Polarization

E-9

$$N_{\text{chains}} \chi^{(2)}(s, \omega, \omega)$$

Third order perturbation theory on the excited states of the s-configuration yields

$$\begin{aligned} \chi^{(2)} &= N_0 \sum_{\alpha} \langle \alpha | \mu | 0 \rangle \langle 0 | \mu | \alpha \rangle \times \\ & \left[\frac{1}{(E_0 - E_{\alpha} - 3\omega)(E_0 - 2\omega)(E_0 - \omega)} + \frac{1}{(E_0 - \omega)(E_0 - 2\omega)(E_0 - \omega)} \right] \\ & + \frac{1}{(E_0 - \omega)(E_0 - 2\omega)(E_0 - \omega)} + \frac{1}{(E_0 - \omega)(E_0 - 2\omega)(E_0 - 3\omega)} \end{aligned}$$

where $E_0 = E_{s,0} - E_{s,0}$

$E_{s,0}$ is the ground state energy

$E_{s,\alpha}$ ($\alpha = 1, 2, \dots$) are the energies of excited states of the s-configuration

μ_{α} are the dipole matrix elements

N_0 is the density of chains per unit area, where $N_0 = 1/L^2$ is the phase space for soliton pairs on a chain of L and L is the density of chains per unit area.

The sum is over all excited states with symmetry opposite to α and α is an excited state with the same symmetry as α .

(1)

(2)

(3)

(4)

(5)

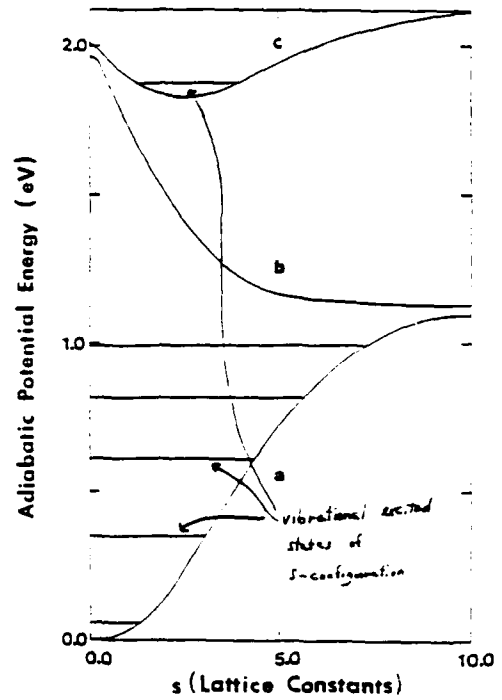


Fig. 1. Potential energy

To estimate the magnitude of $\chi^{(2)}$ we consider the term in the full sum

where the matrix elements go from $\alpha = E_{s,0} \rightarrow \alpha = E_{s,1} \rightarrow \alpha = E_{s,2} \rightarrow \alpha = E_{s,3}$ we

ignore the various vibrational states of the s-configuration and consider only

the single contribution ($\chi^{(2)}_{11}$):

$$\begin{aligned} \chi^{(2)}_{11} &= N_0 \sum_{\alpha} \langle \alpha | \mu | 0 \rangle \langle 0 | \mu | \alpha \rangle \times \\ & \left[\frac{1}{(E_0 - E_{\alpha} - 3\omega)(E_0 - \omega)} + \frac{1}{(E_0 - \omega)(E_0 - 3\omega)} \right] \end{aligned}$$

For $3\omega = E_0$

$$\chi^{(2)}_{11} = 4N_0 \sum_{\alpha} \langle \alpha | \mu | 0 \rangle \langle 0 | \mu | \alpha \rangle \times \left[\frac{1}{(E_0 - E_{\alpha} - 3\omega)(E_0 - \omega)} + \frac{1}{(E_0 - \omega)(E_0 - 3\omega)} \right]$$

where μ_{α} is the matrix element between the ground state with wave function

$\psi_0(s)$ and the excited state with energy E_{α} relative to the ground state

Since

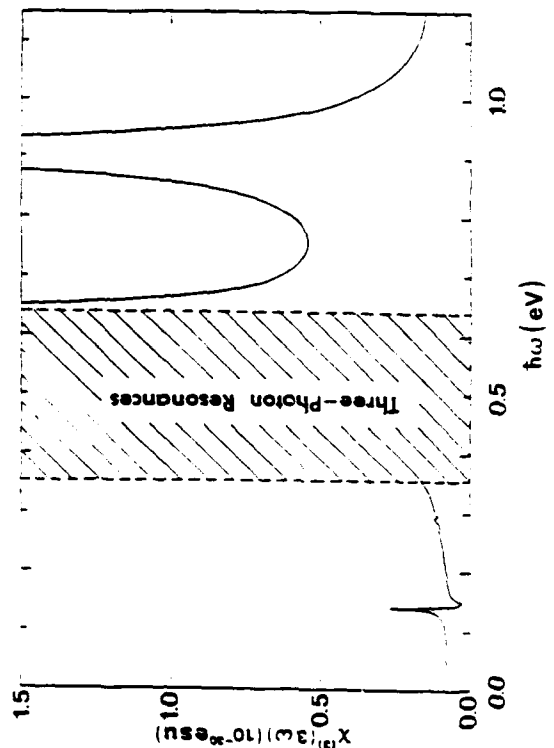
$$\alpha = N_0 \sum_{\alpha} \langle \alpha | \mu | 0 \rangle \langle 0 | \mu | \alpha \rangle$$

is the linear term in the polarizability

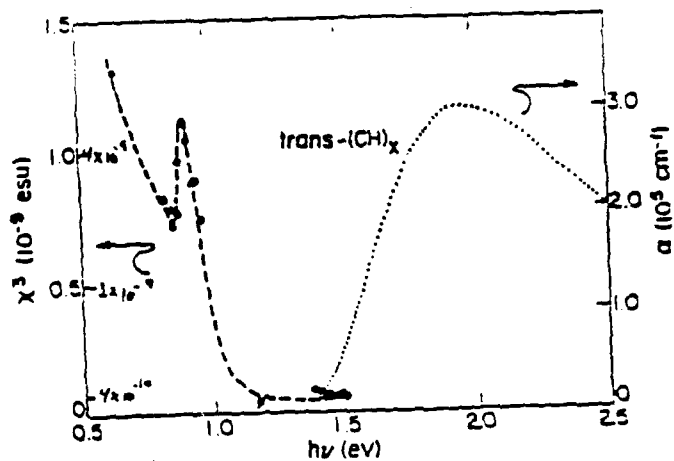
$$\chi^{(2)}_{11} = 4\alpha \sum_{\alpha} \langle \alpha | \mu | 0 \rangle \langle 0 | \mu | \alpha \rangle$$

$$\chi^{(2)}_{11} = (8\alpha^2 / N_0) \sum_{\alpha} \langle \alpha | \mu | 0 \rangle \langle 0 | \mu | \alpha \rangle$$

$$\chi^{(2)}_{11} = 3 \times 10^{-10} \text{ esu}$$



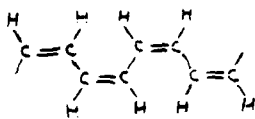
E-10



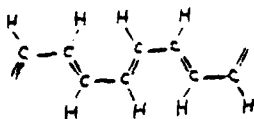
Kajzar, Steward, Morrison & Baker
 Synth Met 17, 563 (1987)

with the ground-state absorption

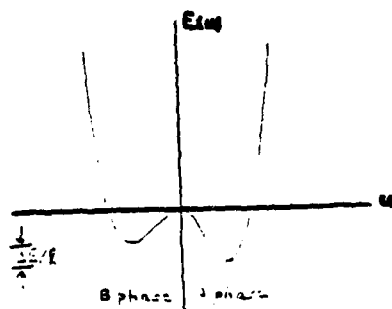
Not
 equivalent



A phase

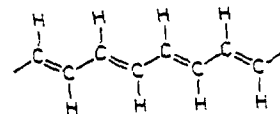


B phase

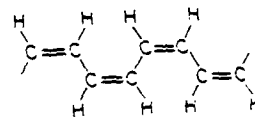


Symmetry breaking origin of $\chi^{(2)}$ Component at

Measurement of $\chi^{(2)}$ in the π and π^* bands of $(CH)_x$



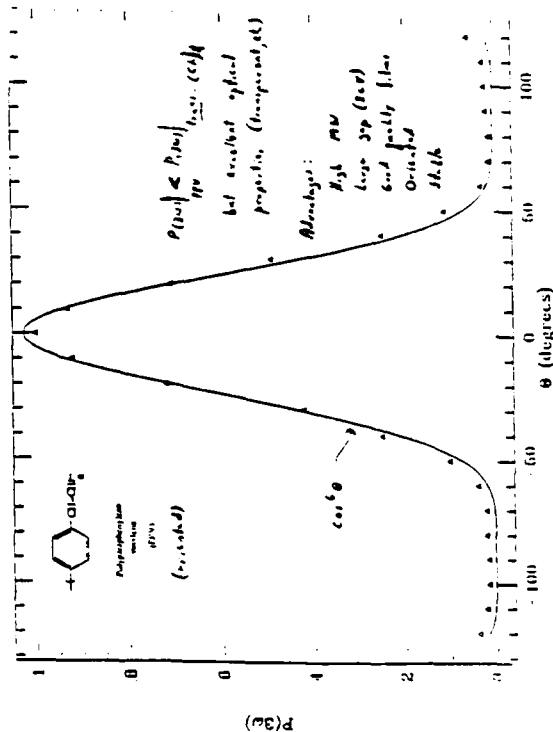
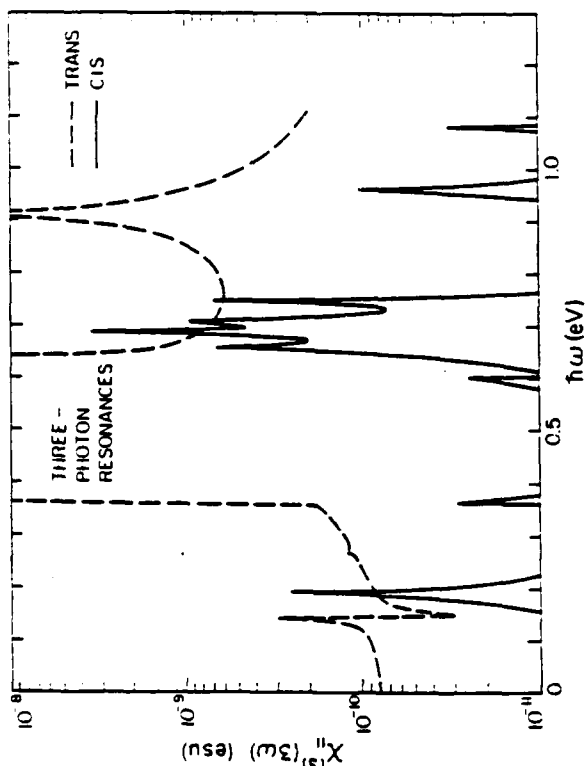
TRANS



CIS

$$\chi^{(2)}_{\text{trans}} < \chi^{(2)}_{\text{cis}}$$

$$\chi^{(2)}_{\text{trans}} = 1/15 \sim 10^{-11} \text{ esu}$$



Conclusions

- 1) Large $\chi^{(3)}$, are a general feature of conjugated polymers
- 2) Mechanism is associated with the π -electrons
- 3) At 1064 nm $\chi^{(3)}_{\text{trans}} \approx \chi^{(3)}_{\text{cis}}$ but large anisotropy $\chi^{(3)}_{\text{trans}} \gg \chi^{(3)}_{\text{cis}}$ is certainly larger by considerable factor
- 4) For isotropization $\chi^{(3)}_{\text{trans}} > 16 \chi^{(3)}_{\text{cis}}$

- 5) Mechanism from rigid bond structure is not dominant contribution for trans

Questions:

- 1) Why is $\chi^{(3)}_{\text{trans}} - \chi^{(3)}_{\text{cis}}$ special?
- 2) How is second anisotropy $\chi^{(2)}$ or known relevant properties?

F-1

K. D. Singer

AT&T

NONLINEAR OPTICS IN
ORDERED MOLECULAR SYSTEMS

F-2

NONLINEAR OPTICS IN ORDERED MOLECULAR SYSTEMS

K.D. SINGER and M.G. KUZYK
AT&T Engineering Research Center, Princeton, NJ

OUTLINE

R.B. COMIZZOLI

D.L. FISH

W.R. HOLLAND

H.E. KATZ

L.A. KING

M.L. SCHILLING

J.E. SOHN

- NONLINEAR OPTICS IN MOLECULAR ENSEMBLES
- FILMS POLED UNDER UNIAXIAL STRESS
- NEW POLYMERS
 - MATERIALS
 - CORONA POLING
 - NONLINEAR OPTICAL PROPERTIES
 - MOLECULAR ORIENTATION DISTRIBUTION

MOLECULAR MATERIALS

- MACROSCOPIC POLARIZATION

$$P_i(t) = \chi_i^{(0)} + \chi_i^{(1)}(t)E_j(t) + \chi_{ijk}^{(2)}(t)E_j(t)E_k(t) + \chi_{ijkl}^{(3)}(t)E_j(t)E_k(t)E_l(t) + \dots$$

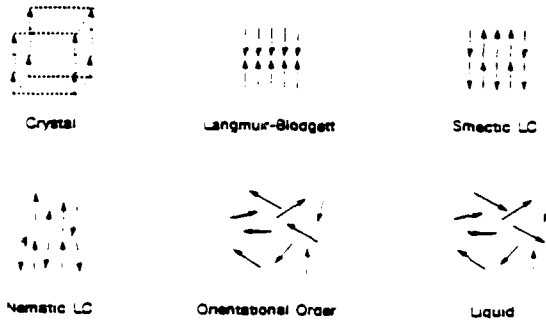
- MICROSCOPIC POLARIZATION

$$p_i(t) = \mu_i^{(0)} + \alpha_{ij}(t)F_j(t) + \beta_{ijk}(t)F_j(t)F_k(t) + \gamma_{ijkl}(t)F_j(t)F_k(t)F_l(t) + \dots$$

- VAN DER WAALS MATERIALS

$$P_i(t) = \frac{1}{V} \langle p_i(t) \rangle_i$$

MATERIAL CLASSES



MOLECULAR ORDER

- MOLECULES FIXED IN LATTICE

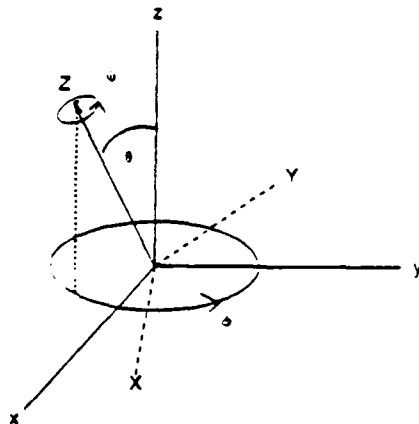
$$\chi_{ijkl...}^{(n)} = N_s \sum_{I,J,K,L,...,s=1}^s a_{iI}(s) a_{jJ}(s) a_{kK}(s) \cdots \xi_{IJKL...}(s)$$

- THERMODYNAMIC ENSEMBLE

EULER ANGLES

$$\chi_{ijkl...}^{(n)} = N \langle \xi_{IJKL...} \rangle_{ijkl...}$$

$$\langle \xi_{IJKL...} \rangle_{ijkl...} = \int_0^{2\pi} d\phi \int_0^\pi \sin\theta d\theta \int_0^{2\pi} d\psi \xi_{IJKL...} a_{iI} a_{jJ} a_{kK} \cdots G(\phi, \theta, \psi)$$



F-4

SYMMETRY CLASSES

$\chi^{(2)}$ components for point group ∞/mmm

	1	2	3
1	0	0	$\chi_{111}^{(2)}$
2	0	0	$\chi_{111}^{(2)}$
3	0	0	$\chi_{111}^{(2)}$
4	0	$\chi_{111}^{(2)}$	0
5	$\chi_{111}^{(2)}$	0	0
6	0	0	0

$\chi^{(3)}$ components for point group ∞/mmm

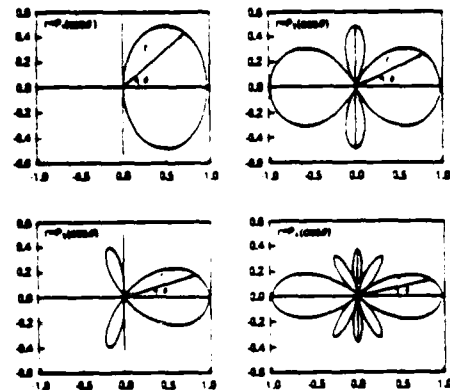
	1	2	3	4	5	6
1	$\chi_{111}^{(3)}$	$\chi_{111}^{(3)}$	$\chi_{111}^{(3)}$	0	0	0
2	$\chi_{111}^{(3)}$	$\chi_{111}^{(3)}$	$\chi_{111}^{(3)}$	0	0	0
3	$\chi_{111}^{(3)}$	$\chi_{111}^{(3)}$	$\chi_{111}^{(3)}$	0	0	0
4	0	0	0	$\chi_{111}^{(3)}$	0	0
5	0	0	0	0	$\chi_{111}^{(3)}$	0
6	0	0	0	0	0	$\chi_{111}^{(3)}$

Row and column labels: 1=11; 2=22; 3=33; 4=23,32; 5=31,13; 6=12,21

DISTRIBUTION FUNCTION

$$G(\theta) = \sum_{l=0}^{\infty} \frac{(2l+1)}{2} A_l P_l(\cos\theta)$$

LEGENDRE POLYNOMIALS



ELECTRIC FIELD POLING

SUSCEPTIBILITIES

$$\chi_{12...}^{(2n)} = \sum_{m=0}^{2n} u_{12...}^{(2n-m)} \langle P_{2n-m} \rangle$$

$$\chi_{12...}^{(2n-1)} = \sum_{m=0}^{2n-1} u_{12...}^{(2n-1-m)} \langle P_{2n-1-m} \rangle$$

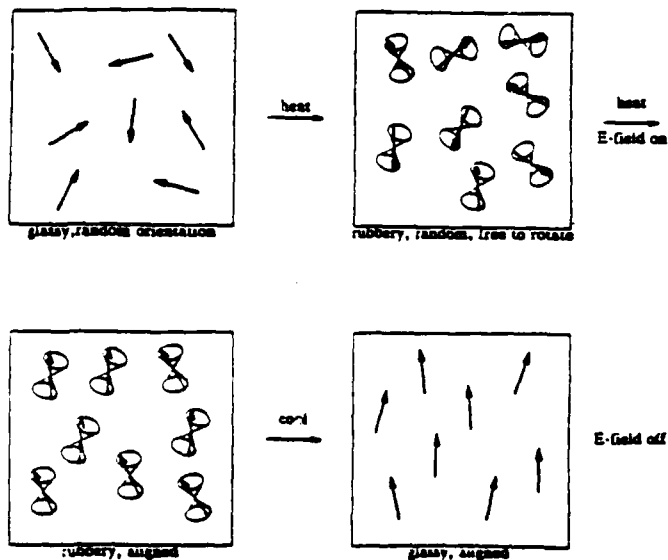
• SECOND ORDER

$$\chi_{33}^{(2)} = N B_m \left[\frac{3}{5} \langle P_1 \rangle - \frac{2}{5} \langle P_3 \rangle \right]$$

$$\chi_{11}^{(2)} = \chi_{11}^{(2)} = \chi_{11}^{(2)} = N B_m \left[\frac{1}{5} \langle P_1 \rangle - \frac{1}{5} \langle P_3 \rangle \right]$$

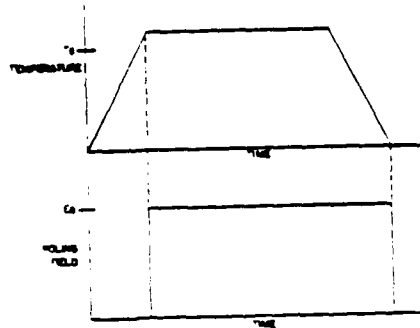
• THIRD ORDER

$$\chi_{333}^{(3)} = N \gamma_m \left[\frac{1}{5} - \frac{4}{7} \langle P_2 \rangle - \frac{8}{35} \langle P_4 \rangle \right]$$



F-5

POLED MATERIALS



$$G_v(\Omega, E_p) = \frac{\exp\left[-\frac{1}{kT}(\sum_v U_{vv} - m_v^* \cdot E_p)\right]}{\int d\Omega \exp\left[-\frac{1}{kT}(\sum_v U_{vv} - m_v^* \cdot E_p)\right]}$$

$$\chi_{ijk}^{(2)} = v_{ijk}^{(0)} \langle P_3 \rangle + v_{ijk}^{(2)} \langle P_2 \rangle + v_{ijk}^{(4)} \langle P_4 \rangle$$

POLING UNDER UNIAXIAL STRESS

- SECOND HARMONIC TENSOR PROPERTIES
- MOLECULAR DISTRIBUTION

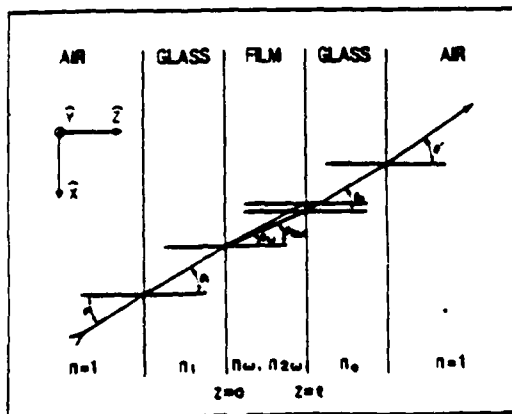
SECOND HARMONIC GENERATION

$$P^{(2)}(2\omega) = 2d_{31}(-2\omega; \omega, \omega)E_1(\omega)E_3(\omega)$$

$$P^{(2)}(2\omega) = 2d_{31}(-2\omega; \omega, \omega)E_2(\omega)E_3(\omega)$$

$$P^{(2)}(2\omega) = d_{31}(-2\omega; \omega, \omega) \left[E_1^2(\omega) - E_2^2(\omega) \right] + d_{33}(-2\omega; \omega, \omega)E_3^2(\omega)$$

EXPERIMENTAL GEOMETRY



SECOND HARMONIC INTENSITY

$$P_T = \frac{512\pi^3}{A} |d_{33}|^2 \epsilon_0^4 T_{2\omega}^2 r_0^2 P^2(\theta) I_\omega^2 \left[\frac{1}{n_\omega^2 - n_{2\omega}^2} \right]^2 \sin^2 \psi$$

- P-POLARIZED INCIDENT LIGHT

$$p(\theta) = (a \cos^2 \theta_\omega - \sin^2 \theta_\omega) \sin \theta_{2\omega} + 2a \cos \theta_\omega \sin \theta_\omega \cos \theta_{2\omega}$$

- S-POLARIZED INCIDENT LIGHT

$$p(\theta) = a \sin(\theta_{2\omega})$$

$$a = \frac{d_{31}}{d_{33}}$$

F-6

ORDERING ENERGY

$$G_u(\Omega) = \frac{\exp\left[-\frac{U}{kT}\right]}{\int d\Omega \exp\left[-\frac{U}{kT}\right]}$$

• ELECTRIC FIELD POLING

$$U_E = m^* E_p$$

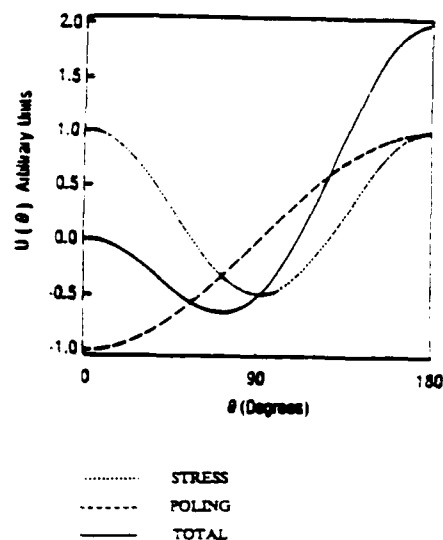
$$\chi_{33}^{(2)} = N\beta_{33} \frac{m^* E_p}{kT} \left(\frac{1}{5} + \frac{4}{7} \langle P_2 \rangle + \frac{8}{35} \langle P_4 \rangle \right)$$

$$\chi_{11}^{(2)} = \chi_{31}^{(2)} = \chi_{31}^{(2)} = N\beta_{33} \frac{m^* E_p}{kT} \left(\frac{1}{15} + \frac{1}{21} \langle P_2 \rangle - \frac{4}{35} \langle P_4 \rangle \right)$$

• UNIAXIAL STRESS

$$U_T = U_p + U_E = bP_2(\cos\theta) - m^* E_p P_1(\cos\theta)$$

ORDERING ENERGY

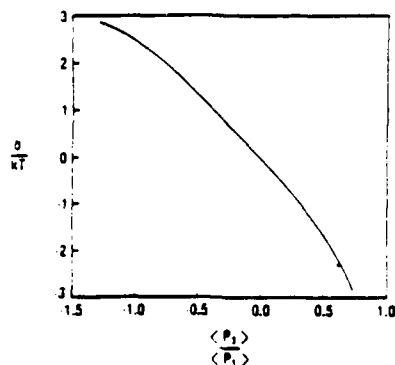


STRESS POTENTIAL

$$\frac{\exp\left[-\frac{(U_p - U_E)}{kT}\right]}{\left[\frac{m^* E}{kT}\right]} = a_1 \left(\frac{b}{kT}\right) P_1(\cos\theta) + a_3 \left(\frac{b}{kT}\right) P_3(\cos\theta)$$

$$\frac{\langle P_3 \rangle}{\langle P_1 \rangle} = \frac{3 a_3}{5 a_1}$$

b = magnitude of stress potential



DISTRIBUTION FUNCTION

$$\langle P_1 \rangle = \frac{2}{3} \frac{m^* E_p}{kT} \frac{a_1}{A_n}$$

$$\frac{\langle P_3 \rangle}{\langle P_1 \rangle} = \frac{1-3a}{1+2a}$$

$$\langle P_2 \rangle = \frac{1}{2} \left(\frac{\langle P_1 \rangle}{\left[\frac{m^* E_p}{3kT} \right]} - 1 \right)$$

$$\langle P_4 \rangle = \frac{1}{4} \left(\frac{\langle P_3 \rangle}{\left[\frac{m^* E_p}{7kT} \right]} - 3 \langle P_2 \rangle \right)$$

F-7

FILMS POLED UNDER STRESS

- DISPERSE RED 1 DYE DISSOLVED IN PMMA

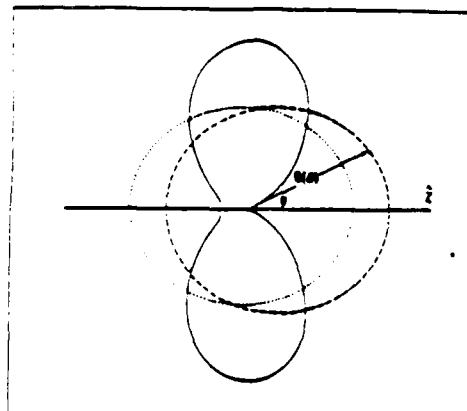
Film #	Dye Number Density $N \times 10^{20}/\text{cm}^3$	Thickness $l(\mu\text{m})$	Poling Field $E_p(\text{MV/cm})$	Stress $\sigma(\text{dynes/cm}^2 \times 10^7)$
1	2.42	4.0	0.60	0.00
2	1.08	4.9	0.25	3.71

- RESULTS

Film #	d	$\frac{\mu^* E_p}{kT}$	$\frac{b}{kT}$	$\langle P_1 \rangle$	$\langle P_2 \rangle$	$\langle P_3 \rangle$	$\langle P_4 \rangle$	Δn
1	0.33	0.50	0.00	0.16	-0.020	0.00	0.015	0.0014
2	0.7	0.20	1.2	0.041	-0.20	-0.019	-0.02	-0.0043

NEW MATERIALS

DISTRIBUTION FUNCTION



..... ISOTROPIC
 - - - - - POLED
 ——— STRESS + POLED

$$r \approx d \approx N \beta \mu E_p$$

- MOLECULES
- CORONA POLING
- POLYMERS

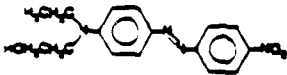
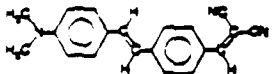
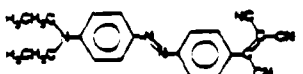
MOLECULES

$\beta \mu$ MEASURED BY EFISH

- DIRECT MEASUREMENT IN DIPOLAR SOLVENT, DMSO
- INFINITE DILUTION TECHNIQUE

F-8

RESULTS

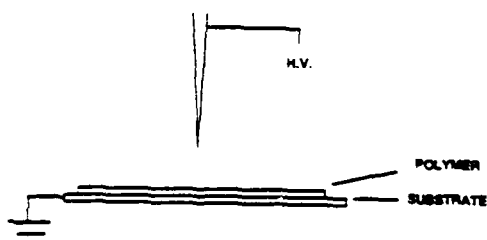
	Molecule	$\beta\mu^*$
DR1		1090 ^r
DCV		2850 ^r
TCV		4110 ^g

* $\beta\mu$ in $10^{-30} \text{ cm}^5 \text{ D/esu}$

† $\lambda = 1.356 \mu\text{m}$

‡ $\lambda = 1.58 \mu\text{m}$

CORONA POLING

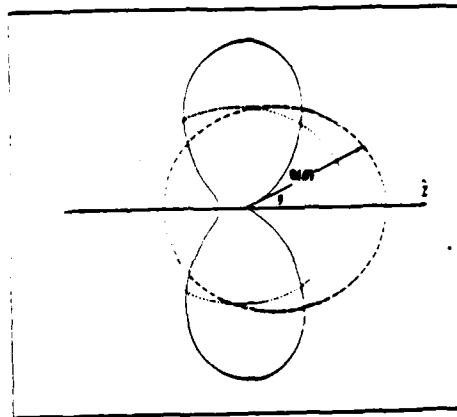


- NO ELECTRODE DEPOSITION
- HIGHER POLING FIELD

F-9

- RESTRICTED MOTION
 - REDUCES POSSIBLE SUSCEPTIBILITY
 - REDUCES DECAY MECHANISM
- CORONA POLING ALTERS MOLECULAR DISTRIBUTION

DISTRIBUTION FUNCTION



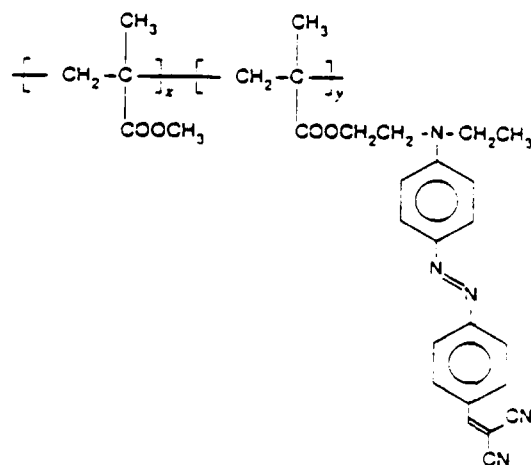
..... ISOTROPIC
----- ELECTRODE POLED
———— CORONA POLED

SUMMARY

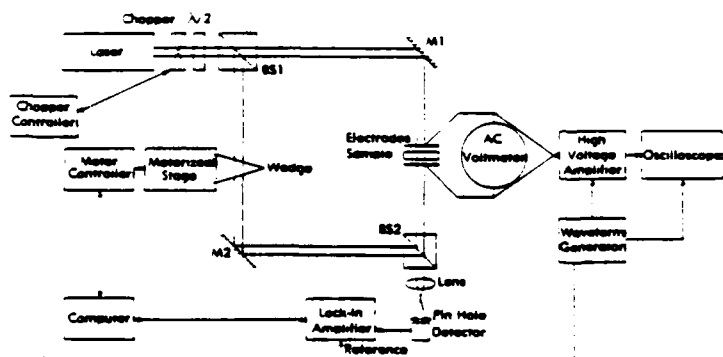
- NONLINEAR OPTICS CAN REVEAL MOLECULAR DISTRIBUTION
 - INTERNAL AND EXTERNAL FORCES
- CORONA POLING
- NEW MATERIALS

SIDE-CHAIN POLYMERS

- HIGHER NUMBER DENSITY
- RESTRICTED MOTION
 - EFFECT ON POLING
 - EFFECT ON RELAXATION LIFETIME

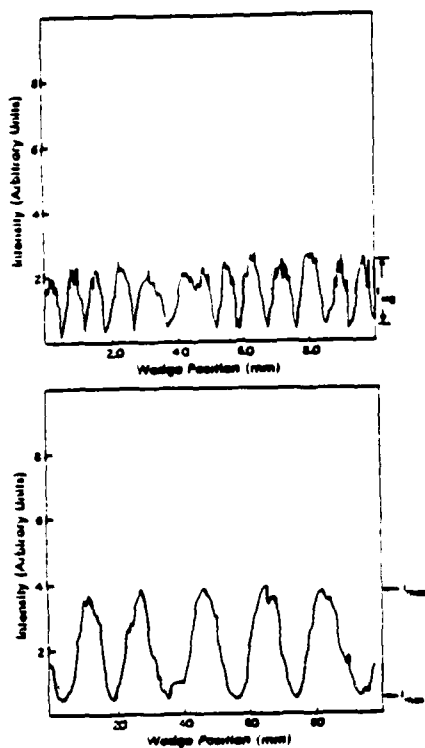


ELECTRO-OPTIC MEASUREMENT



F-11

ELECTRO-OPTIC MEASUREMENT



RESULTS

MATERIAL	N (10^{20} cm^{-3})	n	d_0 (10^{-6} cm)	d_r (10^{-6} cm)	r_{11}^d (10^{-12} m/V)	r_{33}^d (10^{-12} m/V)
DCV/MMA (corona)	~8	1.58 ($\lambda = 0$)	$d_{33} = 29$ $d_{31} = 20$	$d_{33} = 28$ $d_{31} = 18$	$r_{33}^d = 9$ $r_{31}^d = 6$	$r_{33}^d = 9$ $r_{31}^d = 6$
DCV/PMMA (corona)	2.3	1.53 ($\lambda = 0$)	$d_{33} = 34$ $d_{31} = 17$	$d_{33} = 9$ $d_{31} = 4.5$		
DR 1/PMMA (corona)	2.3	1.52 ($\lambda = 0$)	$d_{33} = 13$ $d_{31} = 6$			
DR 1/PMMA (electrode)	2.7	1.52 ($\lambda = 0$)	$d_{33} = 6$ $d_{31} = 2$			

G-1

H. Nakanishi

Research Institute
for Polymers and Textiles, Japan

SEVERAL SERIES OF NOVEL
POLYDIACETYLENES FOR NONLINEAR OPTICS

G-2

Several Series of Novel Polydiacetylenes for Nonlinear Optics

by

Machiro NAKANISHI

(Res.Inst.for Polymers & Textiles)

1. Significance of Crystal Engineering for Aromatic Substituted Polydiacetylenes (APDA)
2. APDAs by a Hydrogen-Bonding Effect
3. APDAs by a Bending Effect (I)
4. APDAs by a Bending Effect (II)
5. APDAs by an Anchor-Void Effect
6. APDAs by a Fluorine-Substitution Effect
7. APDAs by Complex Effects
8. Preliminary Evaluation of $\chi^{(3)}$ of APDAs
9. Conclusion

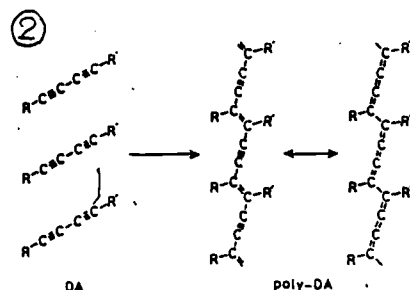
Covorkers : H. Matsuda

S. Okada

M. Kato

S. Takaraki

M. Ohtsuka



ポリアセチレン化合物および共役系分子の3次の非線形光学効果

化合物	測定方向	$\chi^{(3)}$ (10^{-10} esu)
TCDAモノマー	—	—
TCDAモノマー	—	1.2 ± 0.5
TCDAモノマー	—	1.1 ± 0.5
TCDAモノマー	—	270 ± 140
TCDAモノマー	—	700 ± 500
PTCモノマー	—	1600 ± 1000
PTCモノマー	—	5000 ± 5000
PTCモノマー	—	4000 ± 2000 (10.5 μm)
PTCモノマー	—	400 ± 200 (10.5 μm)

C. Sauteret et al. (1976)

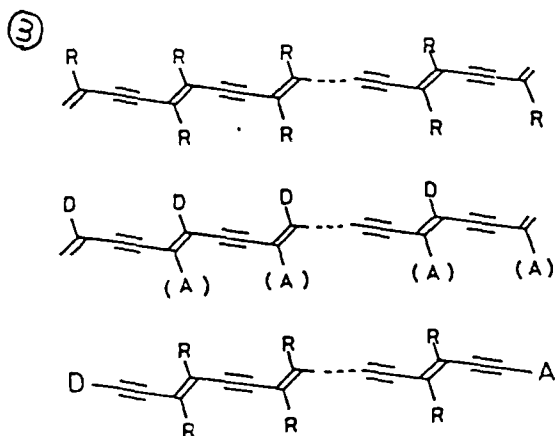
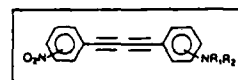
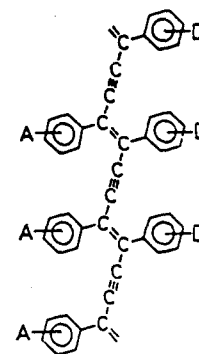


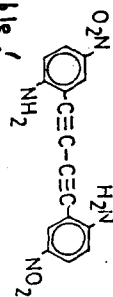
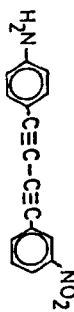
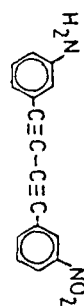
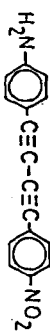
Fig. 1 Interesting polydiacetylene structures for NLO. (R=Ar)

④

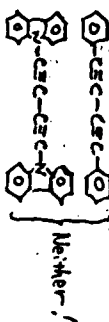
Bandwidths(BV), Bandgaps(Eg), and Ionization Potentials(IP) for Acetylenic(A) and Butatrienic(B) Polydiacetylenes By VEH Calculation.

Substituents	BV	Eg	IP
H in A	3.972	2.596	5.338
C ₆ H ₅ in A	1.116	1.769	4.903
CH ₃ in A	3.265	2.449	5.039
H in B	4.816	0.154	4.277
C ₆ H ₅ in B	1.878	0.215	4.133
CH ₃ in B	4.136	0.435	4.032

B.J.Orchard & S.K.Tripathy, Macromol., 19, 1884 (1986).



Not polymerizable!



表了 Substitue Photo-Bromide of Derivative of Diphenylmethane as Depictor from Nature as
 Problem of the Substitutess in the Phenyl Ring!

	Substance	Yields	Boiling pt. °C.	color	Crystal Shape	Solubility in DMF
I	H	①	no	-	needles	yes
II	-HO ₂	2	3.0	red	needles	yes
III	-HO ₂	3	3.5	red	needles	yes
IV	-HO ₂	②	no	-	needles	-
V	-HO ₂	4	no	-	plates	-
VI	-HO ₂	5	no	-	plates	-
VII	-HO ₂	6	no	-	needles	-
VIII	-HO ₂	③	10	red-brown	needles	no
IX	-HO ₂	7	35	green-brown	needles	yes
X	-HO ₂	④	no	-	needles	-
XI	-HO ₂	8	6.2	light purple	needles	yes
XII	-HO ₂	9	3.0	white	needles	yes
XIII	-HO ₂	⑤	no	-	needles	-
XIV	-HO ₂	10	4.0	light blue	changed plates	yes
XV	-HO ₂	11	13	green-black	changed plates	no
XVI	-HO ₂	⑥	no	-	changed plates	-

1. ^a For the synthesis of 15, 17, 18, 19, 20, 21, 22, 23, 24, 25, 26, 27, 28, 29, 30, 31, 32, 33, 34, 35, 36, 37, 38, 39, 40, 41, 42, 43, 44, 45, 46, 47, 48, 49, 50, 51, 52, 53, 54, 55, 56, 57, 58, 59, 60, 61, 62, 63, 64, 65, 66, 67, 68, 69, 70, 71, 72, 73, 74, 75, 76, 77, 78, 79, 80, 81, 82, 83, 84, 85, 86, 87, 88, 89, 90, 91, 92, 93, 94, 95, 96, 97, 98, 99, 100, 101, 102, 103, 104, 105, 106, 107, 108, 109, 110, 111, 112, 113, 114, 115, 116, 117, 118, 119, 120, 121, 122, 123, 124, 125, 126, 127, 128, 129, 130, 131, 132, 133, 134, 135, 136, 137, 138, 139, 140, 141, 142, 143, 144, 145, 146, 147, 148, 149, 150, 151, 152, 153, 154, 155, 156, 157, 158, 159, 160, 161, 162, 163, 164, 165, 166, 167, 168, 169, 170, 171, 172, 173, 174, 175, 176, 177, 178, 179, 180, 181, 182, 183, 184, 185, 186, 187, 188, 189, 190, 191, 192, 193, 194, 195, 196, 197, 198, 199, 200, 201, 202, 203, 204, 205, 206, 207, 208, 209, 210, 211, 212, 213, 214, 215, 216, 217, 218, 219, 220, 221, 222, 223, 224, 225, 226, 227, 228, 229, 230, 231, 232, 233, 234, 235, 236, 237, 238, 239, 240, 241, 242, 243, 244, 245, 246, 247, 248, 249, 250, 251, 252, 253, 254, 255, 256, 257, 258, 259, 260, 261, 262, 263, 264, 265, 266, 267, 268, 269, 270, 271, 272, 273, 274, 275, 276, 277, 278, 279, 280, 281, 282, 283, 284, 285, 286, 287, 288, 289, 290, 291, 292, 293, 294, 295, 296, 297, 298, 299, 300, 301, 302, 303, 304, 305, 306, 307, 308, 309, 310, 311, 312, 313, 314, 315, 316, 317, 318, 319, 320, 321, 322, 323, 324, 325, 326, 327, 328, 329, 330, 331, 332, 333, 334, 335, 336, 337, 338, 339, 340, 341, 342, 343, 344, 345, 346, 347, 348, 349, 350, 351, 352, 353, 354, 355, 356, 357, 358, 359, 360, 361, 362, 363, 364, 365, 366, 367, 368, 369, 370, 371, 372, 373, 374, 375, 376, 377, 378, 379, 380, 381, 382, 383, 384, 385, 386, 387, 388, 389, 390, 391, 392, 393, 394, 395, 396, 397, 398, 399, 400, 401, 402, 403, 404, 405, 406, 407, 408, 409, 410, 411, 412, 413, 414, 415, 416, 417, 418, 419, 420, 421, 422, 423, 424, 425, 426, 427, 428, 429, 430, 431, 432, 433, 434, 435, 436, 437, 438, 439, 440, 441, 442, 443, 444, 445, 446, 447, 448, 449, 450, 451, 452, 453, 454, 455, 456, 457, 458, 459, 460, 461, 462, 463, 464, 465, 466, 467, 468, 469, 470, 471, 472, 473, 474, 475, 476, 477, 478, 479, 480, 481, 482, 483, 484, 485, 486, 487, 488, 489, 490, 491, 492, 493, 494, 495, 496, 497, 498, 499, 500, 501, 502, 503, 504, 505, 506, 507, 508, 509, 510, 511, 512, 513, 514, 515, 516, 517, 518, 519, 520, 521, 522, 523, 524, 525, 526, 527, 528, 529, 530, 531, 532, 533, 534, 535, 536, 537, 538, 539, 540, 541, 542, 543, 544, 545, 546, 547, 548, 549, 550, 551, 552, 553, 554, 555, 556, 557, 558, 559, 560, 561, 562, 563, 564, 565, 566, 567, 568, 569, 570, 571, 572, 573, 574, 575, 576, 577, 578, 579, 580, 581, 582, 583, 584, 585, 586, 587, 588, 589, 590, 591, 592, 593, 594, 595, 596, 597, 598, 599, 600, 601, 602, 603, 604, 605, 606, 607, 608, 609, 610, 611, 612, 613, 614, 615, 616, 617, 618, 619, 620, 621, 622, 623, 624, 625, 626, 627, 628, 629, 630, 631, 632, 633, 634, 635, 636, 637, 638, 639, 640, 641, 642, 643, 644, 645, 646, 647, 648, 649, 650, 651, 652, 653, 654, 655, 656, 657, 658, 659, 660, 661, 662, 663, 664, 665, 666, 667, 668, 669, 670, 671, 672, 673, 674, 675, 676, 677, 678, 679, 680, 681, 682, 683, 684, 685, 686, 687, 688, 689, 690, 691, 692, 693, 694, 695, 696, 697, 698, 699, 700, 701, 702, 703, 704, 705, 706, 707, 708, 709, 710, 711, 712, 713, 714, 715, 716, 717, 718, 719, 720, 721, 722, 723, 724, 725, 726, 727, 728, 729, 730, 731, 732, 733, 734, 735, 736, 737, 738, 739, 740, 741, 742, 743, 744, 745, 746, 747, 748, 749, 750, 751, 752, 753, 754, 755, 756, 757, 758, 759, 760, 761, 762, 763, 764, 765, 766, 767, 768, 769, 770, 771, 772, 773, 774, 775, 776, 777, 778, 779, 780, 781, 782, 783, 784, 785, 786, 787, 788, 789, 790, 791, 792, 793, 794, 795, 796, 797, 798, 799, 800, 801, 802, 803, 804, 805, 806, 807, 808, 809, 810, 811, 812, 813, 814, 815, 816, 817, 818, 819, 820, 821, 822, 823, 824, 825, 826, 827, 828, 829, 830, 831, 832, 833, 834, 835, 836, 837, 838, 839, 840, 841, 842, 843, 844, 845, 846, 847, 848,

G. Wegner (1971)

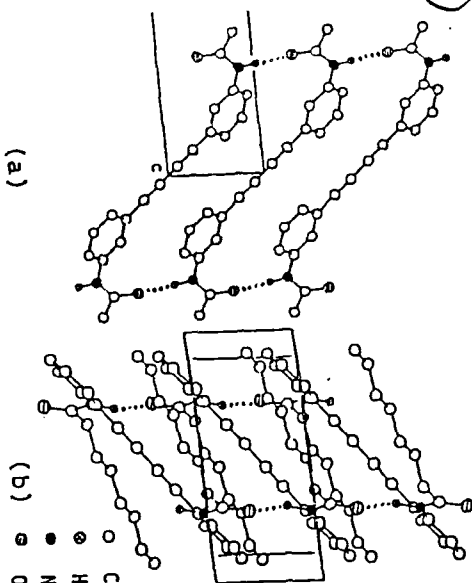


図 2 2と3の結晶構造

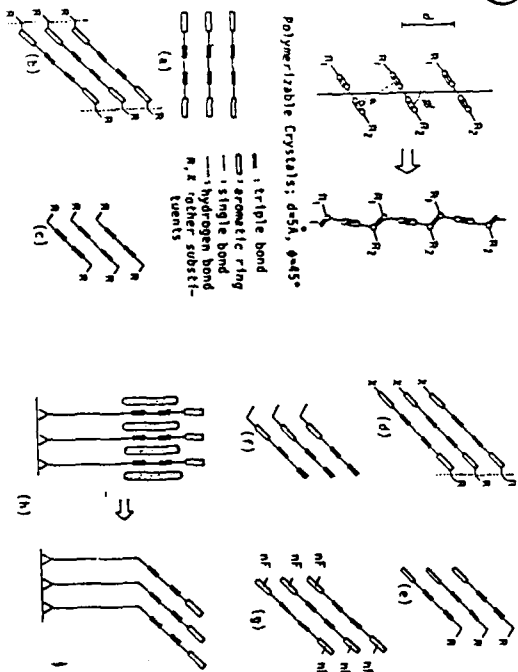
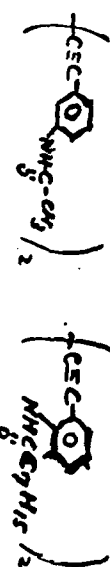
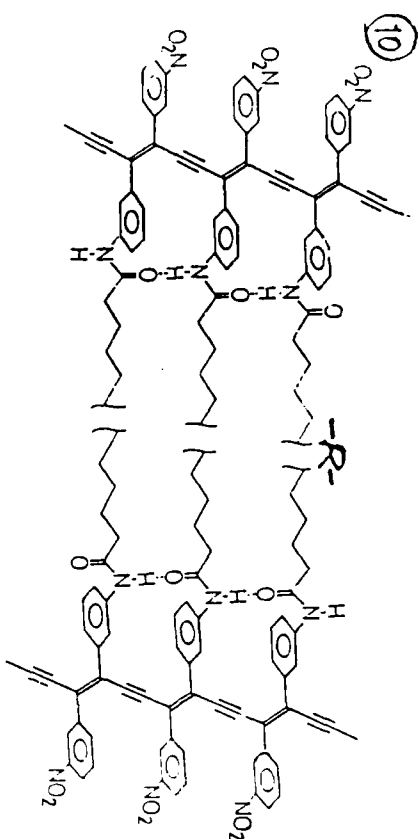
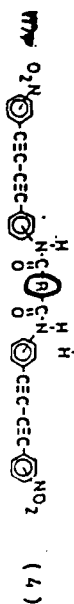
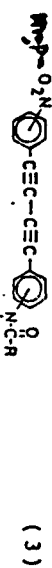


Fig. 2 Crystal engineering of polydiacetylenes with π -conjugation between main chain and

(9) 表 2 アミド基を持つ新規ジアセチレンの
固 相 重 合 性

Structure	Substituent of -N-C-R position (R) H O	Reactivity	Polymer Yield(%)
(3)	o (-C ₁₇ H ₃₅) m (-C ₁₇ H ₃₅) p (-C ₁₇ H ₃₅) m (-C ₇ H ₁₄ COOH) m (-C ₁₈ H ₃₆ COOH)	+ + - + +	13.4 8.9 - 13.8 -
(4)	m (none) m (-C ₄ H ₈ -) m (-C ₇ H ₁₄ -) m (-C ₈ H ₁₆ -) m (-C ₁₈ H ₃₆ -)	- + - ++ ++	- - 58.8 92.9

* ⁶⁰Co γ ray at the dose of ca. 100 Mrad.
- stable, + reactive, ++ highly reactive.



(11) Table Reactivity of A-n

n	Reactivity	IR ν _{C=O} (cm ⁻¹)	mp(°C)
7	-	1672	208
8	++	1656	189
9	+	1667	155
10	++	1647	194
11	+	1661	159
18	+++	1658	175

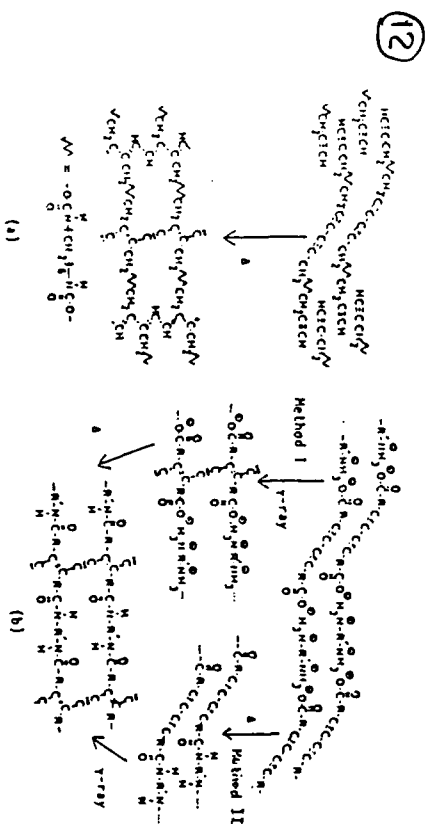


Figure 1. Schematic presentation of 2-D solid-state polymerization of diacetylene-acetylenes (a) and diacetylene nylon salts (b).

(13)

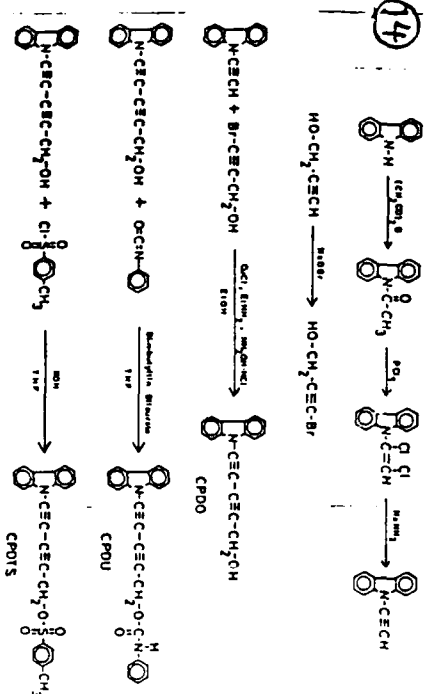
$R_1 \backslash R_2$	A	B	C	D	E	F
A	86.0	—	—	—	—	—
B	129	>240	—	—	—	—
C	68.3	132	113	145	96.0	153
D	70.8	160	93.0	114	123	125
E	64.8	111	625.	112	123	125
F	—	—	—	—	—	—

$R_1-C \equiv C-C \equiv C-R_2$

m.p./°C
reactivity

- stable, + reactive, ** highly reactive

(14)



Scheme of synthetic procedures of CPDO and the derivatives.

(15)

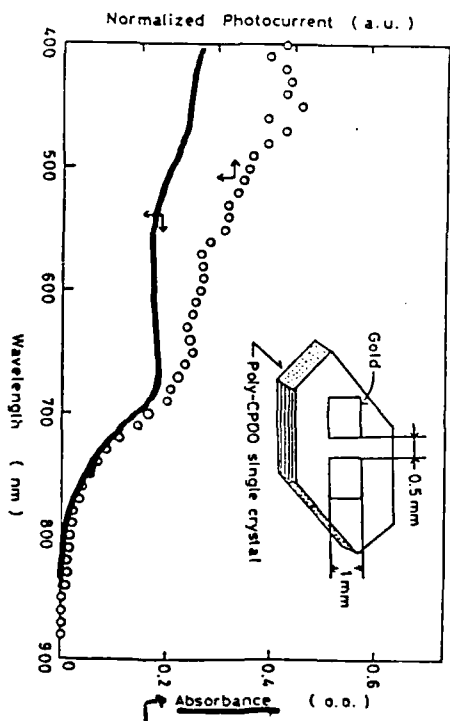


Fig. 7 Action spectrum of photocurrent (O) and absorption spectrum (—) of poly-CPDO.

(16)

Table 3 Band Gap Energies and Ionization Potentials of Polydiacetylenes

Polydiacetylene	Eg (eV)	I.P. (eV)
poly-PTS	2.1	(5.3)*
poly-DCIID	2.3	
poly-CPDO	1.6	4.4

* Calculated

(17)

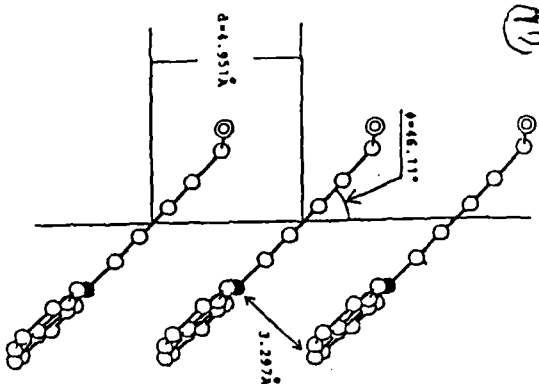
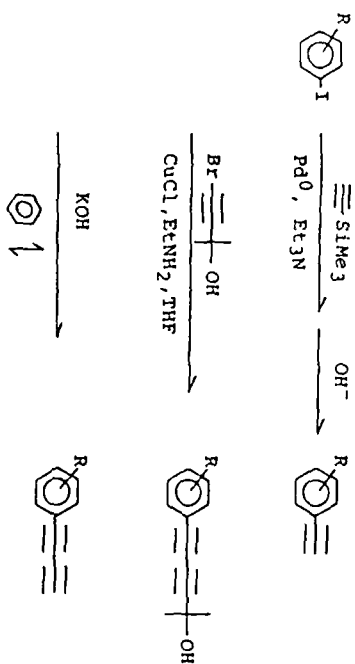


Table Crystallographic data of CPD's.

Formular	Monomer	Polymer
$C_{17}H_{11}NO$	$C_{17}H_{11}NO$	$C_{17}H_{11}NO$
Mr	245.3	245.3
Crystal System	Monoclinic	Monoclinic
Space Group	$P2_1/a$	$P2_1/a$
a (Å)	16.249(3)	16.494(6)
b (Å)	4.951(1)	4.873(3)
c (Å)	17.360(4)	19.513(8)
β (°)	113.53(2)	124.27(3)
V (Å ³)	1280.4(5)	1296 (1)
Z	4	4
Dx (Mg m ⁻³)	1.27 _x	1.25 _x
Dm (Mg m ⁻³)	1.27	1.26

(19)



(20)

Table Solid state polymerizability of Phenylbutadiyne derivatives.

NO.	R	UV	Y	Δ	重合収率 (%)	[γ 球量 MRad]
1	2-NO ₂	O	O	O	95.6	[70.0]
2	3-NO ₂	O	O	O	94.3	[25.5]
3	4-NO ₂	X	X	O	—	[50.0]
4	2-NH ₂	O	O	O	99.0	[70.0]
5	3-NH ₂	O	O	O	100	[27.0]
7	2-NH ₂	O	O	O	100	[156.0]
	5-NO ₂					

O : active
X : inactive

(18)

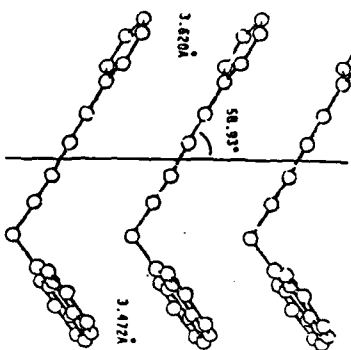


Table Crystallographic data

Formular	$C_{21}H_{15}N$
Mr	305.4
Crystal System	Monoclinic
Space Group	$P2_1/c$
a (Å)	13.180 (4)
b (Å)	4.256 (1)
c (Å)	28.776 (2)
β (°)	91.71 (3)
V (Å ³)	1628 (1)
Z	4
Dx (Mg m ⁻³)	1.246
Dm (Mg m ⁻³)	1.244
R	0.077

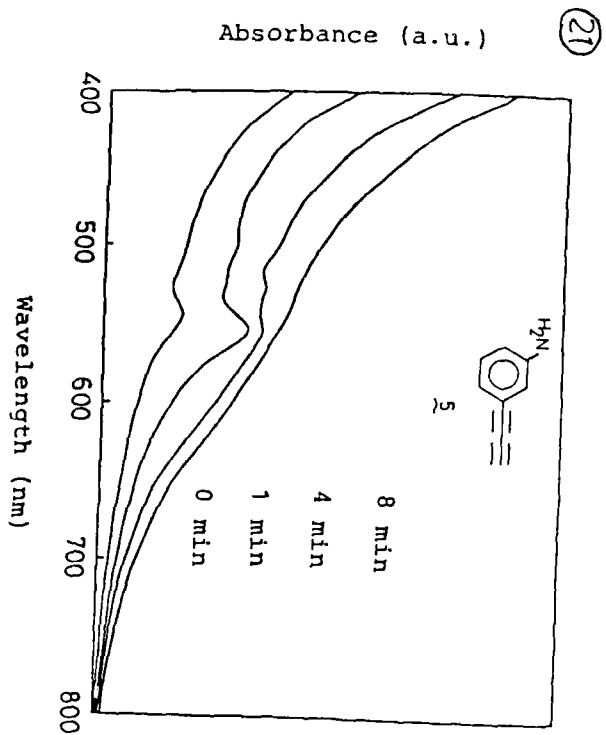


Fig. Absorption spectra of 5 with changing UV irradiation time.

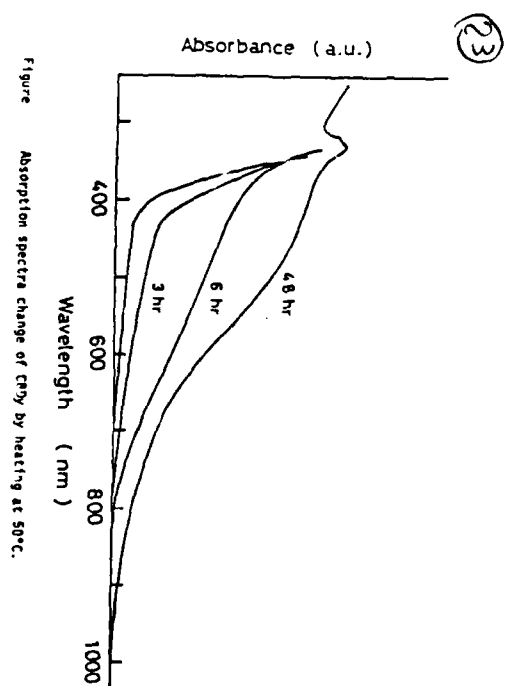
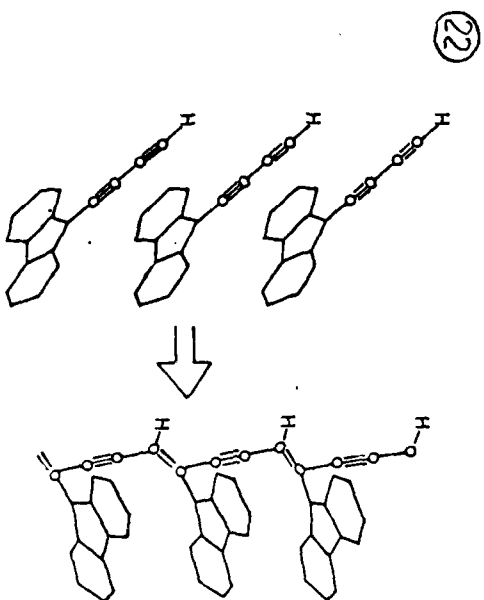


Figure Absorption spectra change of CBDy by heating at 50°C.

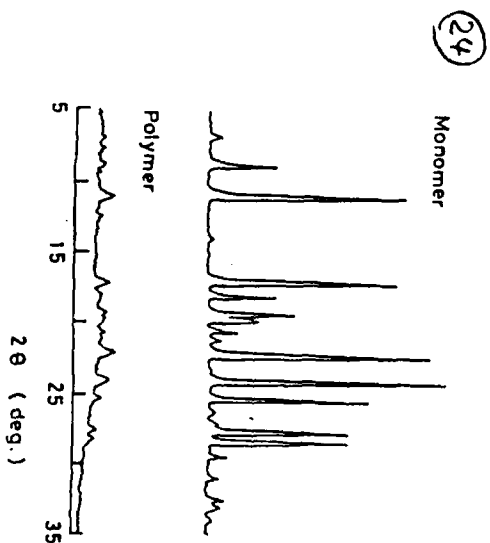
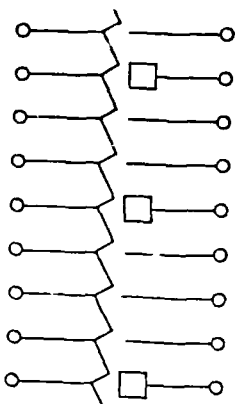
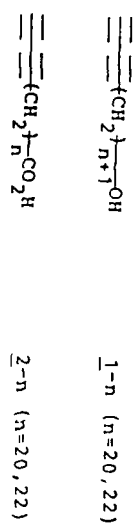


Figure X-ray powder diffraction patterns of CBDy.

(25)



G-8

(26)

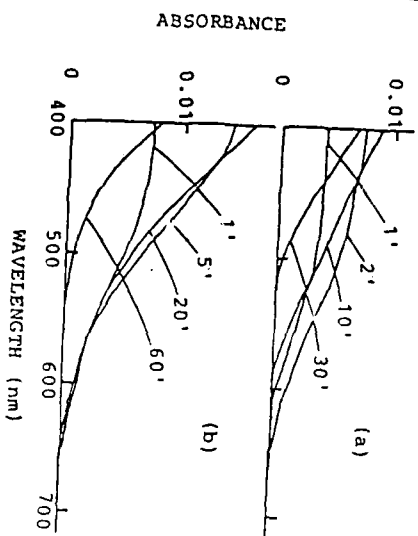
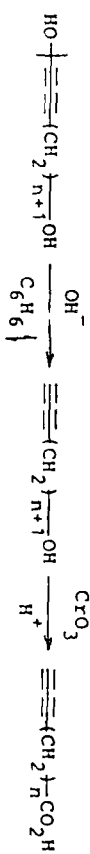
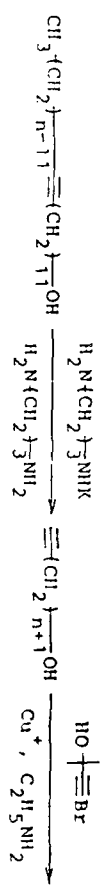
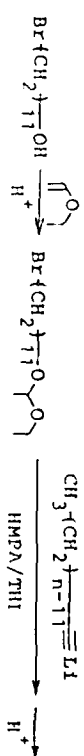
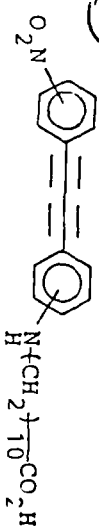


Fig. 4. Visible spectra of 20 layers of 1-20(a) and 2-20(b).

(27)

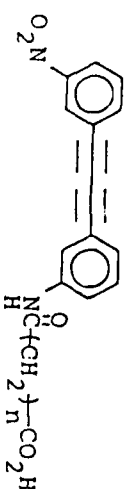


(28)

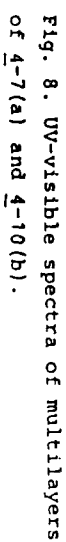


3-m (3,3'-substituted)

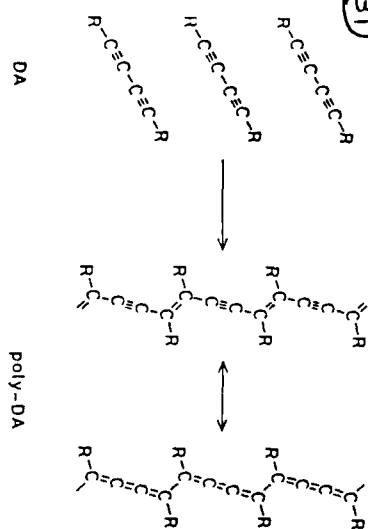
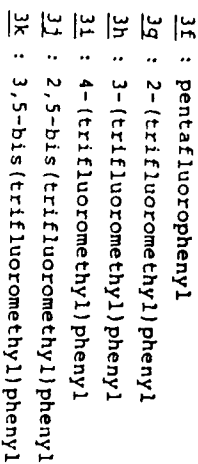
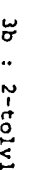
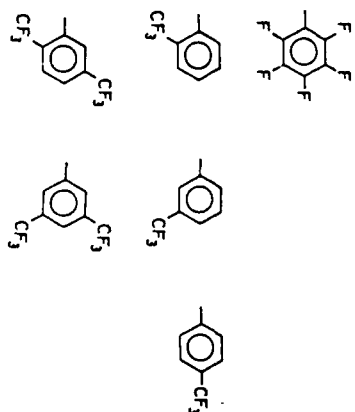
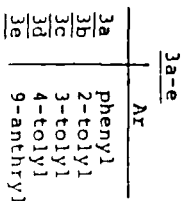
3-p (4,4'-substituted)



4-n (n=7, 10)



30



33

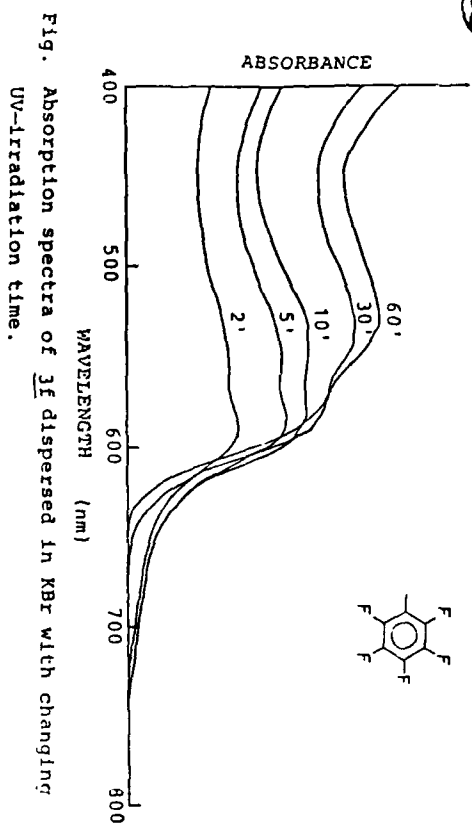


Fig. Absorption spectra of 3f dispersed in KBr with changing UV-irradiation time.

34

Table Polymer yield by γ -ray irradiation.

Substituents of phenyl group	γ -ray dose (Mrad)	Polymer yield (%)
—	19.7	2
pentafluoro	19.7	82
2-(trifluoromethyl)	100	11
3-(trifluoromethyl)	100	1>
4-(trifluoromethyl)	100	18
2,5-bis(trifluoromethyl)	50.3	98
3,5-bis(trifluoromethyl)	50.3	1>

35

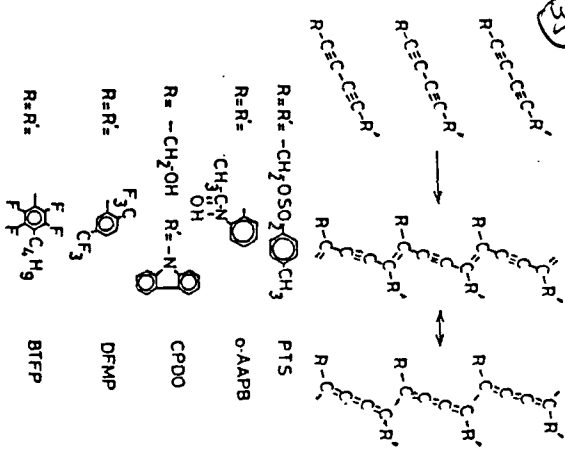


Fig. 1 Solid-state polymerization scheme and polydiacetylene derivatives.

36

Table 1 $X^{(3)}$ values of polydiacetylene thin films

Poly-DA	Thickness (μm)	$X^{(3)} \times 10^{11}$ (esu)		
		Pumping Wavelength (μm)		
		1.83	1.88	1.94
DFMP	1.09	2.4	3.5	2.6
	0.98	3.7		2.4
BTFP	0.070	28	32	13
	0.054	26		15
PTS	1.35			1.1

Reference: fused quartz, $X^{(3)} = 3 \times 10^{-14}$ esu at 1.89 μm

H-1

F. Kajzar
CEN Saclay, France

RESONANCE EFFECTS
IN CUBIC HYPERPOLARISABILITIES
OF CONJUGATED POLYMERS

RESONANCE EFFECTS IN CUBIC HYPERPOLARISABILITIES OF CONDENSED POLYMERS

Francis KAZZAR

Commissariat à l'Energie Atomique
Institut de Recherche Technologique et de Développement Industriel
Division d'Electronique, de Technologie et d'Instrumentation
Département d'Electronique et d'Instrumentation Nucléaire
Laboratoire de Physique Electronique des Matériaux
CEA Saclay, 91191 Gif sur Yvette, France

- THIN FILM PREPARATION TECHNIQUES (polyacetylenes)
- THIRD ORDER OPTICAL HYPERPOLARISABILITY DETERMINATION TECHNIQUES

Third Harmonic Generation

Electric Field Induced Second Harmonic Generation

- NONLINEAR SPECTROSCOPY IN PDA THIN FILMS

Multiresonance phenomena

Two photon resonances → Kerr susceptibility
intensity dependent index of refraction

Temperature variation of cubic susceptibility

Nonlinear Optical Dichroism

- POLARISATION EFFECTS IN PDA THIN FILMS

PDA THIN FILM PREPARATION TECHNIQUES

- Langmuir - Blodgett technique
- Solution casting
- Dipping technique from a polymer solution
- Evaporation technique (sublimation coating)
- Shear technique (thin noncrystalline films)

Why thin films (0.003 μ m up to a few tens of microns)?

- Nonlinear optical properties characterisation

$$1 \ll l_e \quad l_e = \lambda_F / 2(n_F - n_F)$$

$$j = \begin{cases} 2 & \text{EFISH} \\ 3 & \text{THG} \end{cases}$$

$$\begin{aligned} I_{2\omega} &\sim I_{\omega}^2 \\ I_{3\omega} &\sim I_{\omega}^3 \end{aligned} \quad \text{"phase matching"}$$

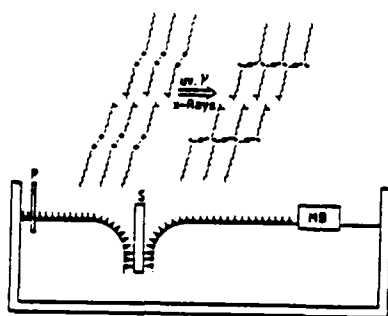
- Nonlinear spectroscopy
harmonic light within absorption range

- Integrated optics
- Thin film devices

LANGMUIR-BLODGETT METHOD OF THIN FILM DEPOSITION

Disubstituted monomers:

$$R_1 = C_6H_4 - C \equiv C - C_6H_4 - R_2$$



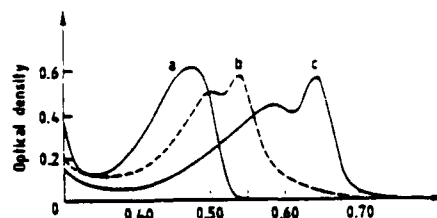
P - pressure sensor MB - mobile barrier S - substrate

Transfer: layer by layer of monomer film

Polymerisation of monomer film by UV, X-Ray radiation

Polymerisation of the monomer film on water subphase

Transfer of polymer monolayer ~ 30 Å thick, on a substrate



Optical absorption spectra of different disubstituted polymers:

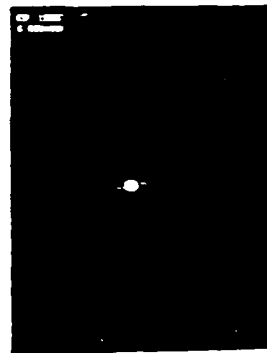
- a - yellow form (polymer solution amorphous phase)
- b - red form (stable)
- c - blue form

H-3



1000 Å

Electron micrograph of a 20,000-angstrom monolayer



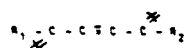
Electron diffraction pattern of a 20,000-angstrom monolayer

PRINCIPAL PROPERTIES OF LB FILMS

- Control over thin films with controllable thickness each layer $\sim 10^2$ Å thick.
- Thickness limited to a few thousand Angstroms
- Two-dimensional order
- Films composed from polycrystallites
large light scattering

SOLUTION CASTING

Soluble polymers



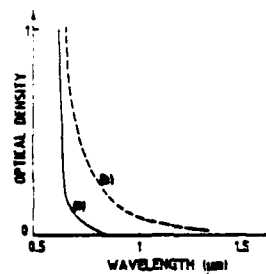
3-BCMU	$R_1, R_2 = (CH_2)_3OCOMCH_2COOC_6H_9$
4-BCMU	$R_1, R_2 = (CH_2)_4OCOMCH_2COOC_6H_9$
TS-12	$R_1, R_2 = (CH_2)_{12}OSOC_6H_4CH_3$

Thin films with thickness varying from a few thousand Angstroms to a few tens of microns

Crystallites - large light scattering

Large surface roughness - light scattering by surface

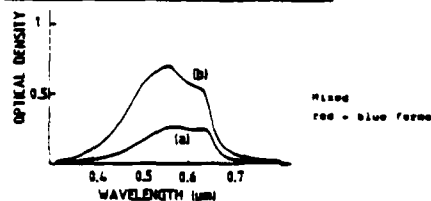
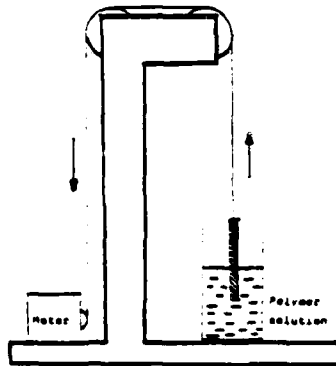
Surface light scattering effects in solution cast 4-BCMU film (see fig. 6)



Teil of optical absorption spectrum of a 50 μm thick native 4-BCMU film (a) and after an annealing at 400° C under vacuum and a simultaneous cooling of a silica plate on free film face (b).

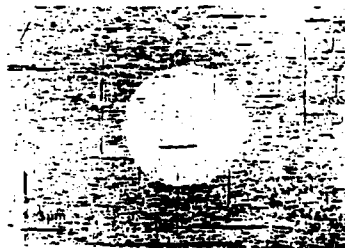
H-4

DIPPING TECHNIQUE FROM A POLYMER SOLUTION

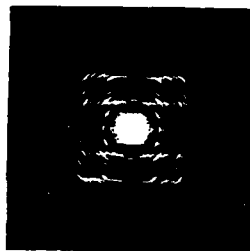


Absorption spectra of a 200 Å (a) and 2150 Å (b) thick polymer films obtained by dipping technique from 3-OCNV solution in CHCl₃.

EPITAXY ON SINGLE CRYSTAL SUBSTRATE



Electron micrograph of a bi-oriented 3-OCNV film (250 Å) evaporated on KBr single crystal substrate.

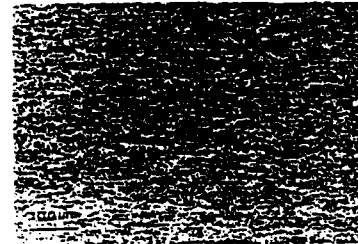


Electron diffraction of a central part of bi-oriented 250 Å thick 3-OCNV film.

MONOMER EVAPORATION TECHNIQUE - SUBLIMATION

High vacuum - 10⁻⁶ Torr

WORKS FOR PRACTICALLY ALL 24 MONOMERS SOLUBLE IN THE CASE OF MONOMERS POLYMERIZING THERMALLY LIKE 1,3,5-PTS, DCH YIELDS HOMOGENEOUS THIN FILMS WITH THICKNESS VARYING FROM A FEW HUNDREDS TO A FEW TENS OF MICRONS.



Electron micrograph of a 3-OCNV (R₁R₂CH₂CH₂CH₂CH₃) thin film showing an isotropic orientation of crystallites.

Light scattering by crystallites - this can be reduced by a cooling of substrate - diminution of the crystallite size.

THIRD HARMONIC GENERATION EXPERIMENTS

$$\text{IN TRANSPARENT } E_{1\omega}^2 = E_{2\omega}^2 - E_{3\omega}^2$$

$$\text{OR } |E_{1\omega}^2| \gg |E_{2\omega}^2|$$

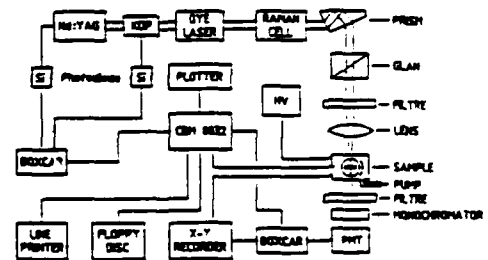
NONLINEAR SUSCEPTIBILITY
(For a transparent film)

$$J_{3\omega} = \frac{2304\pi^2}{C} \left(\frac{\omega}{\omega_0} \right)^2 \left(\frac{1}{n_0} \right) |A|^2 J_0$$

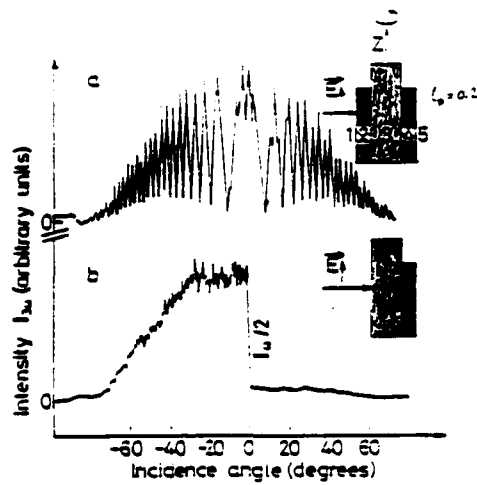
OR FOR COATING ON THE REFRACTIVE INDEX DISCONTINUITY "SHARP RESONANCE"

For an absorbing film at harmonic frequency

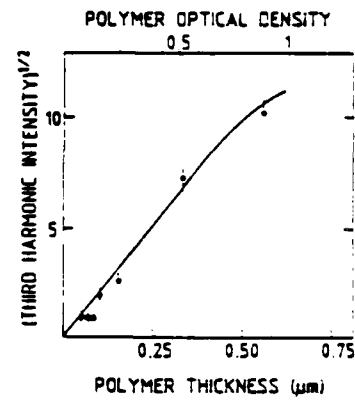
$$J_{3\omega} = \frac{2304\pi^2}{C} \left(\frac{\omega}{\omega_0} \right)^2 J_0^2 \quad J_0 = \frac{(1 - \exp(-\alpha_{3\omega} L))}{[\alpha_{3\omega}^2 - (\alpha_{2\omega}^2 - \alpha_{1\omega}^2)]} = \frac{(1 - \exp(-\alpha_{3\omega} L))}{[\alpha_{3\omega}^2 - (\alpha_{2\omega}^2 - \alpha_{1\omega}^2)]}$$



EXPERIMENTAL SET-UP FOR THIRD HARMONIC GENERATION EXPERIMENTS.



Third harmonic intensity from an LB PUA film as function of rotation angle.



$\chi^3(-2\omega; \omega, \omega, \omega)$ phase determination

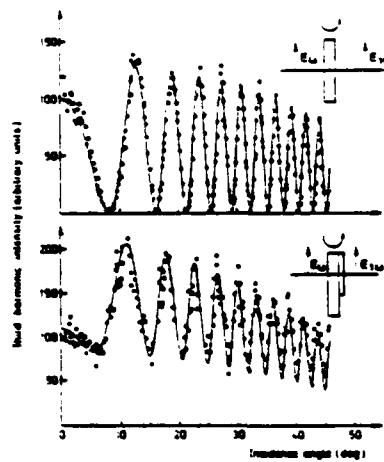


FIG. 4. Third harmonic intensity as function of incidence angle for (a) glass plate and (b) glass plate + polymer film in vacuum. Points represent measured values and solid lines the calculated ones with tabulated values of refractive indices for glass.⁷

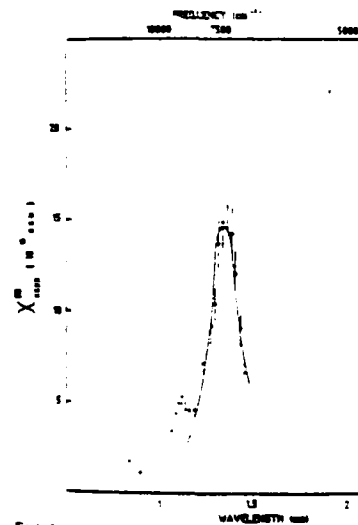


Fig. 1. Calculated intensity $X^{(3)}_{eff} = 10^{-11} \text{ esu}$ for silicon, covering the entire spectrum, as a function of the laser wavelength. The experimental data is shown as a solid line in the plot.

Kagley, Messner, and Rosen

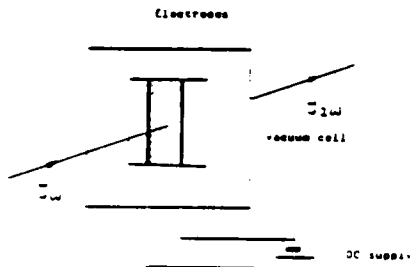
J. Appl. Phys., Vol. 60, No. 5, 1 November 1986

H-6

ELECTRIC FIELD INDUCED OPTICAL SECOND HARMONIC GENERATION

DEVELOPMENTS - CONTOURMETRIC STRUCTURE
NO SECOND HARMONIC GENERATION

By applying an external DC field
CONTROLMETRY BECOMES
SECOND HARMONIC GENERATION



Comparison with a single crystal quartz standard (Q)

$$\langle \chi^{(2)}(\omega_1, \omega_2, \omega_3) \rangle = \frac{1}{2\pi} \int_{-\infty}^{\infty} dt \int_{-\infty}^{\infty} dt' \int_{-\infty}^{\infty} dt'' \langle \chi^{(2)}(t, t', t'') \rangle e^{-i(\omega_1 t + \omega_2 t' + \omega_3 t'')} \quad (e.s.u.)$$

f - polymer film

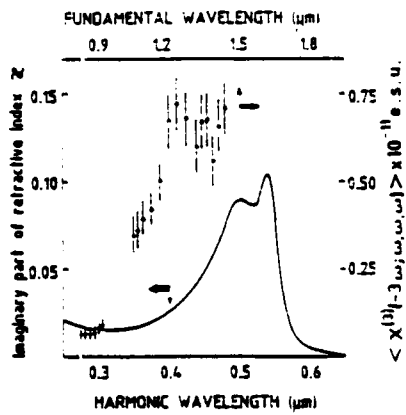


Fig. 3 LB film - red form

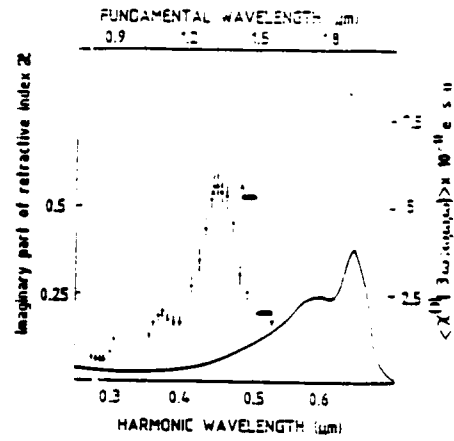
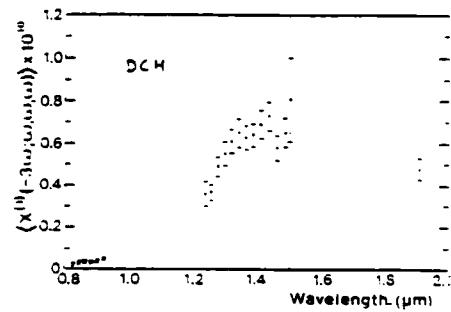
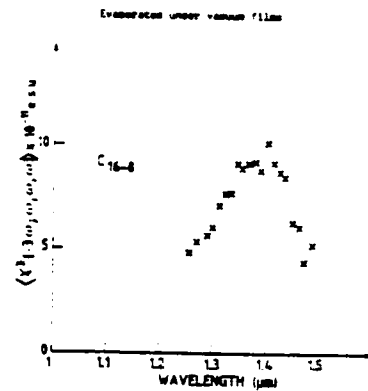
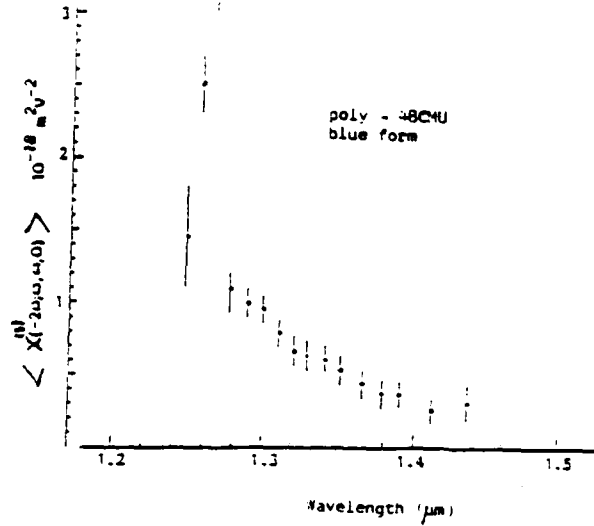
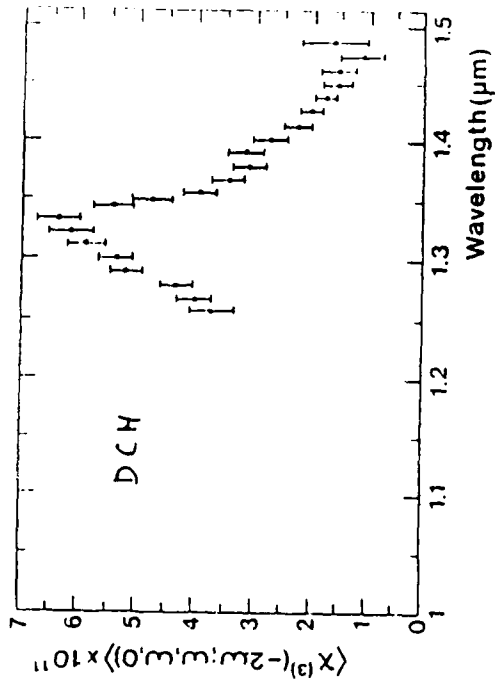


Fig. 4 LB film - blue form



H-7



Tensor elements contributing to $\chi^{(3)}(-2\omega; \omega, \omega, 0)$ (EFGH):

	Contribution to $\chi^{(3)}$ from two-photon resonance $\propto 1/(E_1 - E_2 - \hbar\omega)$	Contribution to $\chi^{(3)}$ from three-photon resonance $\propto 1/(E_1 - E_2 - \hbar\omega)$
	$\langle \chi^{(3)}(-2\omega; \omega, \omega, 0) \rangle = \frac{1}{2} \frac{1}{E_1 - E_2 - \hbar\omega} \langle \chi^{(3)}(-2\omega; \omega, \omega, 0) \rangle$	$\langle \chi^{(3)}(-2\omega; \omega, \omega, 0) \rangle = \frac{1}{2} \frac{1}{E_1 - E_2 - \hbar\omega} \langle \chi^{(3)}(-2\omega; \omega, \omega, 0) \rangle$
	$\langle \chi^{(3)}(-2\omega; \omega, \omega, 0) \rangle = \frac{1}{2} \frac{1}{E_1 - E_2 - \hbar\omega} \langle \chi^{(3)}(-2\omega; \omega, \omega, 0) \rangle$	$\langle \chi^{(3)}(-2\omega; \omega, \omega, 0) \rangle = \frac{1}{2} \frac{1}{E_1 - E_2 - \hbar\omega} \langle \chi^{(3)}(-2\omega; \omega, \omega, 0) \rangle$
	$\langle \chi^{(3)}(-2\omega; \omega, \omega, 0) \rangle = \frac{1}{2} \frac{1}{E_1 - E_2 - \hbar\omega} \langle \chi^{(3)}(-2\omega; \omega, \omega, 0) \rangle$	$\langle \chi^{(3)}(-2\omega; \omega, \omega, 0) \rangle = \frac{1}{2} \frac{1}{E_1 - E_2 - \hbar\omega} \langle \chi^{(3)}(-2\omega; \omega, \omega, 0) \rangle$
	$\langle \chi^{(3)}(-2\omega; \omega, \omega, 0) \rangle = \frac{1}{2} \frac{1}{E_1 - E_2 - \hbar\omega} \langle \chi^{(3)}(-2\omega; \omega, \omega, 0) \rangle$	$\langle \chi^{(3)}(-2\omega; \omega, \omega, 0) \rangle = \frac{1}{2} \frac{1}{E_1 - E_2 - \hbar\omega} \langle \chi^{(3)}(-2\omega; \omega, \omega, 0) \rangle$

J. P. Ward, Rev. Mod. Phys., 27, 1 (1955)

— two-photon resonance
 with a same symmetry as
 fundamental level
 - - - three-photon resonance
 . . . one-photon resonance

Tensor elements contributing to $\chi^{(3)}(-2\omega; \omega, \omega, 0)$ (EFISHG):

	Contribution to $\chi^{(3)}$ from two-photon resonance $\propto 1/(E_1 - E_2 - \hbar\omega)$	Contribution to $\chi^{(3)}$ from three-photon resonance $\propto 1/(E_1 - E_2 - \hbar\omega)$
	$\langle \chi^{(3)}(-2\omega; \omega, \omega, 0) \rangle = \frac{1}{2} \frac{1}{E_1 - E_2 - \hbar\omega} \langle \chi^{(3)}(-2\omega; \omega, \omega, 0) \rangle$	$\langle \chi^{(3)}(-2\omega; \omega, \omega, 0) \rangle = \frac{1}{2} \frac{1}{E_1 - E_2 - \hbar\omega} \langle \chi^{(3)}(-2\omega; \omega, \omega, 0) \rangle$
	$\langle \chi^{(3)}(-2\omega; \omega, \omega, 0) \rangle = \frac{1}{2} \frac{1}{E_1 - E_2 - \hbar\omega} \langle \chi^{(3)}(-2\omega; \omega, \omega, 0) \rangle$	$\langle \chi^{(3)}(-2\omega; \omega, \omega, 0) \rangle = \frac{1}{2} \frac{1}{E_1 - E_2 - \hbar\omega} \langle \chi^{(3)}(-2\omega; \omega, \omega, 0) \rangle$
	$\langle \chi^{(3)}(-2\omega; \omega, \omega, 0) \rangle = \frac{1}{2} \frac{1}{E_1 - E_2 - \hbar\omega} \langle \chi^{(3)}(-2\omega; \omega, \omega, 0) \rangle$	$\langle \chi^{(3)}(-2\omega; \omega, \omega, 0) \rangle = \frac{1}{2} \frac{1}{E_1 - E_2 - \hbar\omega} \langle \chi^{(3)}(-2\omega; \omega, \omega, 0) \rangle$
	$\langle \chi^{(3)}(-2\omega; \omega, \omega, 0) \rangle = \frac{1}{2} \frac{1}{E_1 - E_2 - \hbar\omega} \langle \chi^{(3)}(-2\omega; \omega, \omega, 0) \rangle$	$\langle \chi^{(3)}(-2\omega; \omega, \omega, 0) \rangle = \frac{1}{2} \frac{1}{E_1 - E_2 - \hbar\omega} \langle \chi^{(3)}(-2\omega; \omega, \omega, 0) \rangle$
	$\langle \chi^{(3)}(-2\omega; \omega, \omega, 0) \rangle = \frac{1}{2} \frac{1}{E_1 - E_2 - \hbar\omega} \langle \chi^{(3)}(-2\omega; \omega, \omega, 0) \rangle$	$\langle \chi^{(3)}(-2\omega; \omega, \omega, 0) \rangle = \frac{1}{2} \frac{1}{E_1 - E_2 - \hbar\omega} \langle \chi^{(3)}(-2\omega; \omega, \omega, 0) \rangle$
	$\langle \chi^{(3)}(-2\omega; \omega, \omega, 0) \rangle = \frac{1}{2} \frac{1}{E_1 - E_2 - \hbar\omega} \langle \chi^{(3)}(-2\omega; \omega, \omega, 0) \rangle$	$\langle \chi^{(3)}(-2\omega; \omega, \omega, 0) \rangle = \frac{1}{2} \frac{1}{E_1 - E_2 - \hbar\omega} \langle \chi^{(3)}(-2\omega; \omega, \omega, 0) \rangle$
	$\langle \chi^{(3)}(-2\omega; \omega, \omega, 0) \rangle = \frac{1}{2} \frac{1}{E_1 - E_2 - \hbar\omega} \langle \chi^{(3)}(-2\omega; \omega, \omega, 0) \rangle$	$\langle \chi^{(3)}(-2\omega; \omega, \omega, 0) \rangle = \frac{1}{2} \frac{1}{E_1 - E_2 - \hbar\omega} \langle \chi^{(3)}(-2\omega; \omega, \omega, 0) \rangle$
	$\langle \chi^{(3)}(-2\omega; \omega, \omega, 0) \rangle = \frac{1}{2} \frac{1}{E_1 - E_2 - \hbar\omega} \langle \chi^{(3)}(-2\omega; \omega, \omega, 0) \rangle$	$\langle \chi^{(3)}(-2\omega; \omega, \omega, 0) \rangle = \frac{1}{2} \frac{1}{E_1 - E_2 - \hbar\omega} \langle \chi^{(3)}(-2\omega; \omega, \omega, 0) \rangle$
	$\langle \chi^{(3)}(-2\omega; \omega, \omega, 0) \rangle = \frac{1}{2} \frac{1}{E_1 - E_2 - \hbar\omega} \langle \chi^{(3)}(-2\omega; \omega, \omega, 0) \rangle$	$\langle \chi^{(3)}(-2\omega; \omega, \omega, 0) \rangle = \frac{1}{2} \frac{1}{E_1 - E_2 - \hbar\omega} \langle \chi^{(3)}(-2\omega; \omega, \omega, 0) \rangle$

J. P. Ward, Rev. Mod. Phys., 27, 1 (1955)

— two-photon resonance with
 the same symmetry (as funda-
 mental) level
 - - - two-photon resonance with
 opposite (to fundamental)
 symmetry level
 . . . one-photon resonance

Tensor elements contributing to optical Kerr susceptibility $\chi^{(3)}$ $\omega = \omega_1, \omega_2, \omega_3$

Diagram	Expression for $\chi^{(3)}$	Expression for $\chi^{(3)}$
	$\chi^{(3)}_{1111} = \frac{1}{4} \frac{(\mu_{12})^4}{\omega_{12}^2 \omega_{13}^2 \omega_{14}^2}$	$\chi^{(3)}_{1111} = \frac{1}{4} \frac{(\mu_{12})^4}{\omega_{12}^2 \omega_{13}^2 \omega_{14}^2}$
	$\chi^{(3)}_{1111} = \frac{1}{4} \frac{(\mu_{12})^4}{\omega_{12}^2 \omega_{13}^2 \omega_{14}^2}$	$\chi^{(3)}_{1111} = \frac{1}{4} \frac{(\mu_{12})^4}{\omega_{12}^2 \omega_{13}^2 \omega_{14}^2}$
	$\chi^{(3)}_{1111} = \frac{1}{4} \frac{(\mu_{12})^4}{\omega_{12}^2 \omega_{13}^2 \omega_{14}^2}$	$\chi^{(3)}_{1111} = \frac{1}{4} \frac{(\mu_{12})^4}{\omega_{12}^2 \omega_{13}^2 \omega_{14}^2}$
	$\chi^{(3)}_{1111} = \frac{1}{4} \frac{(\mu_{12})^4}{\omega_{12}^2 \omega_{13}^2 \omega_{14}^2}$	$\chi^{(3)}_{1111} = \frac{1}{4} \frac{(\mu_{12})^4}{\omega_{12}^2 \omega_{13}^2 \omega_{14}^2}$
	$\chi^{(3)}_{1111} = \frac{1}{4} \frac{(\mu_{12})^4}{\omega_{12}^2 \omega_{13}^2 \omega_{14}^2}$	$\chi^{(3)}_{1111} = \frac{1}{4} \frac{(\mu_{12})^4}{\omega_{12}^2 \omega_{13}^2 \omega_{14}^2}$
	$\chi^{(3)}_{1111} = \frac{1}{4} \frac{(\mu_{12})^4}{\omega_{12}^2 \omega_{13}^2 \omega_{14}^2}$	$\chi^{(3)}_{1111} = \frac{1}{4} \frac{(\mu_{12})^4}{\omega_{12}^2 \omega_{13}^2 \omega_{14}^2}$
	$\chi^{(3)}_{1111} = \frac{1}{4} \frac{(\mu_{12})^4}{\omega_{12}^2 \omega_{13}^2 \omega_{14}^2}$	$\chi^{(3)}_{1111} = \frac{1}{4} \frac{(\mu_{12})^4}{\omega_{12}^2 \omega_{13}^2 \omega_{14}^2}$
	$\chi^{(3)}_{1111} = \frac{1}{4} \frac{(\mu_{12})^4}{\omega_{12}^2 \omega_{13}^2 \omega_{14}^2}$	$\chi^{(3)}_{1111} = \frac{1}{4} \frac{(\mu_{12})^4}{\omega_{12}^2 \omega_{13}^2 \omega_{14}^2}$
	$\chi^{(3)}_{1111} = \frac{1}{4} \frac{(\mu_{12})^4}{\omega_{12}^2 \omega_{13}^2 \omega_{14}^2}$	$\chi^{(3)}_{1111} = \frac{1}{4} \frac{(\mu_{12})^4}{\omega_{12}^2 \omega_{13}^2 \omega_{14}^2}$
	$\chi^{(3)}_{1111} = \frac{1}{4} \frac{(\mu_{12})^4}{\omega_{12}^2 \omega_{13}^2 \omega_{14}^2}$	$\chi^{(3)}_{1111} = \frac{1}{4} \frac{(\mu_{12})^4}{\omega_{12}^2 \omega_{13}^2 \omega_{14}^2}$

conduction band
valence band
two-photon band

valence band

Band structure of the PDA molecule

J.F. Ward, Rev. Mod. Phys. 37, 1 (1965)

— two photon resonance
- - - one photon resonance

Intensity dependent index of refraction

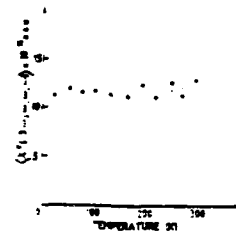
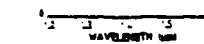
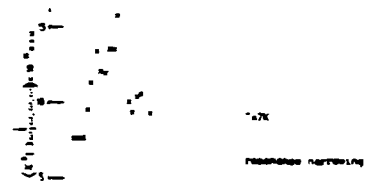
$$n = n_0 + n_2 I$$

$$n_2 = \frac{12\pi^2}{c^2} \frac{(\mu_{12})^4}{\omega_{12}^2 \omega_{13}^2 \omega_{14}^2}$$

At two photon resonance $\chi^{(3)}$ is complex

active optical bistability

Temperature variation of $\chi^{(3)}$ - Jero, et al



Constant of $\chi^{(3)}$ - Jero, et al. vs temperature - quantum origin of cubic hyperpolarizability - one-site filling model - Schmidt-Rink et al Phys. Rev. B 32, 1995

H-9

NONLINEAR OPTICAL DISSONANCE

Enhanced I_{SH} - due to E_{DC} in direction of polymer chain

θ - angle between incident electric field and polymer chain

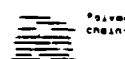
Harmonic intensity

$$I_{SH} \sim \cos^2 \theta$$



Example: oriented OCH thin film

same orientation of polymer chains mutually perpendicular



In linear optics: crossed polarizers, linear optics, dissipation

$$I = I_0 \cos^2 \theta + \cos^2(90^\circ - \theta) = I_0$$

In the experiments

$$I_{SH} = A \cos^2 \theta + B \sin^2 \theta$$

Harmonic field

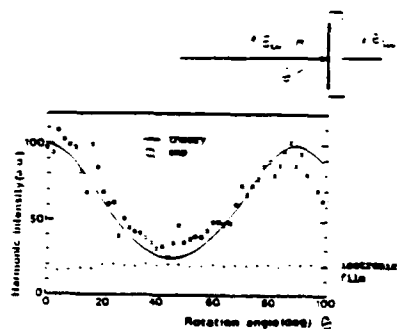
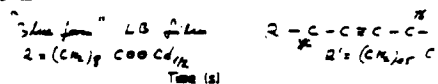
$$I_{SH} = I_{SH}^0 + A^2 \cos^2 \theta + B^2 \sin^2 \theta$$

Harmonic intensity

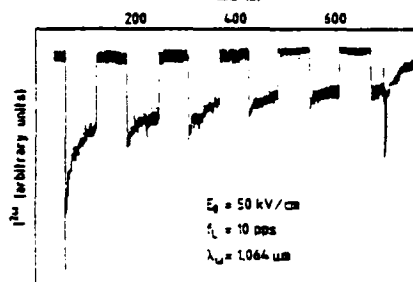
θ - angle between incident electric field and polymer chain

POLARIZATION EFFECTS

LB film

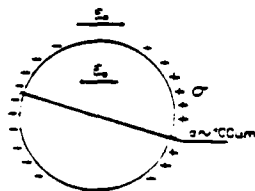


Third harmonic intensity from a 10-nm-thick LB film obtained by rotating on a Si/SiO₂ substrate.



Decrease of SH intensity due to an internal polarization creation of π -n dipoles and their orientation in external DC field

H-10



Setting of the magnetic polarization by charge unbalance at the laser tube boundaries.

CONCLUSIONS

ADVANTAGES

Large $\tau^{(3)}$ with fast response time 20
 The photon resonance in telecommunications window 1.3 - 1.5 μ m
 Active optical bistability
 Simple system
 Thin film feasibility by different techniques
 Oriented thin films
 Stationary
 Optical gap and physico-chemical properties can be modified
 by a choice of size groups

PROBLEMS

Light scattering
 anisotropic thin film
 Photoconduction
 Chemical stability PTS
 blue-red transformation in some cases

WORKERS

Jean HESSIER - chief of the laboratory
 Pierre-Alain CHOLLET
 Dominique GREG
 Jean-Marc NUNZI
 Fabrice CHARRA - graduate student
 Jacques BANIDE
 Roger CRAS - technical staff
 Andre LORIN

EXTERNAL COLLABORATIONS

Isabelle LEDOUX - CNET Bagneux
 Jacques ZYSS - CNRS Toulouse
 Alain BOUDET
 Jacques LENOIGNE - CRM Strasbourg
 Anne THIERRY
 Shashu ETENAD - Bellcore
 Lewis ROTHBERG - AT&T Murray Hill
 Michel DUMONT
 Jean-Claude LOULERGUE - Institut d'Optique Orsay
 Yves LEVY
 Gerardo MEYER - MPI Mainz

I-1

Y. R. Shen

University of California at Berkeley

NONLINEAR OPTICAL MEASUREMENTS
ON LIQUID CRYSTALS
AND
QUASI-LIQUID CRYSTALS

Optical Nonlinearities
 of
 Liquid Crystals
 and
 Quasi-Liquid Crystals

Motivation:

Liquid crystal molecules are
 highly nonlinear

Existence of many liquid crystals
 with different molecular structures

Dependence of nonlinearities on
 molecular structure

Gary Berkovic
 Theo Rasing

I-3

Technique for measuring $\vec{\chi}^{(2)}$

SHG from molecular monolayer
spread on water

$$\chi_{ijk}^{(2)} = N L_{ii} L_{jj} L_{kk} \langle G_{ijk}^{\alpha\beta\gamma}(\Omega) \rangle \alpha_{\alpha\beta\gamma}^{(2)}$$

If $\Omega \equiv \theta$ and L 's are known,

then the n elements of $\vec{\chi}^{(2)}$
can be deduced from measurements
of $n+1$ independent components
of $\vec{\chi}^{(2)}$.

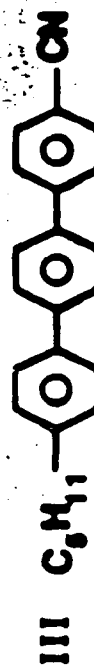
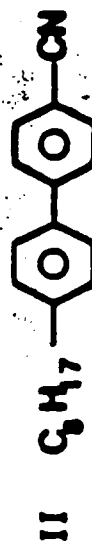
Advantages:

1. Molecular density can be a variable.
2. Local field effect could be less important.

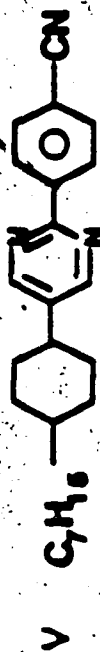
Disadvantages:

1. Not all molecules are spreadable on water.
2. Molecules could interact with water.

ALKYL-CYANO-(POLY)-PHENYLS



ALKYL-CYANO-PHENYL PYRIMIDINES



ALKOXY-CYANO-BIPHENYL



1-5

TABLE 1 Second order polarizabilities, $\alpha_{eff}^{(2)}$, for molecules I - VI. θ_0 is the average orientation angle of the molecular long axis to the surface normal, as calculated from the SHG data.

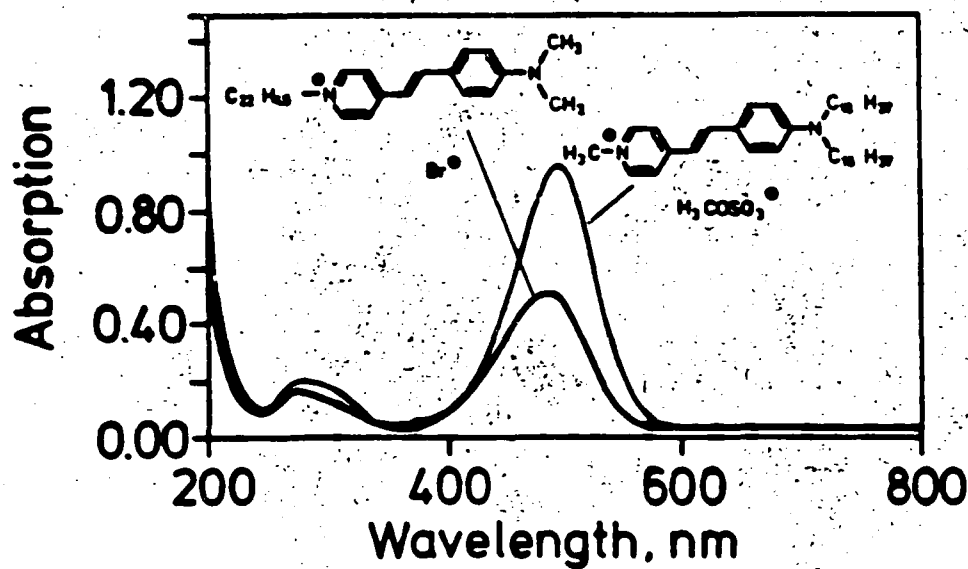
	$ \alpha_{eff}^{(2)} $ (10^{-30} esu)		θ_0 ($^\circ$)
	at 2 ω resonance	at 1.08 μ m	
I	4	8	80 ± 10
II	25	3	71 ± 2
III	13	8	69 ± 2
IV	8	8	79 ± 3
V	8	8	82 ± 4
VI	40	5	78 ± 2

Results:

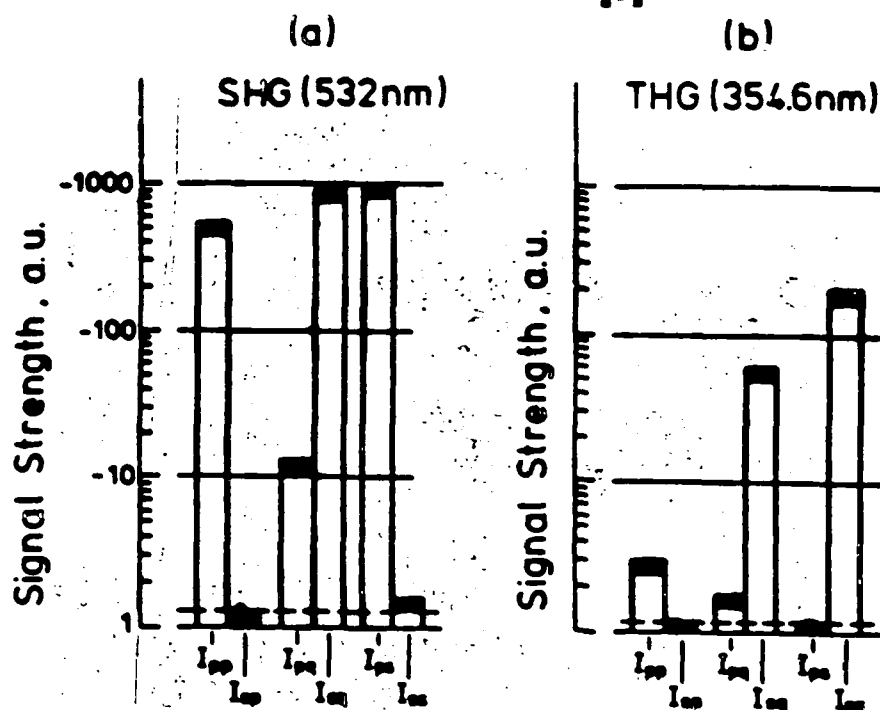
1. $\alpha^{(2)} \sim 10^{-29}$ esu
2. CN is a better electron donor than COOH.
3. Interruption of electron delocalization decreases $\alpha^{(2)}$
4. Triphenyl is worse than biphenyl presumably because of twist between phenyl rings.

Nonlinearities of Hemicyanine Dyes and the Environmental Effect

G. Marowsky
L. F. Chi
D. Mobius
R. Steinkeff
D. Dorsch
B. Rieger



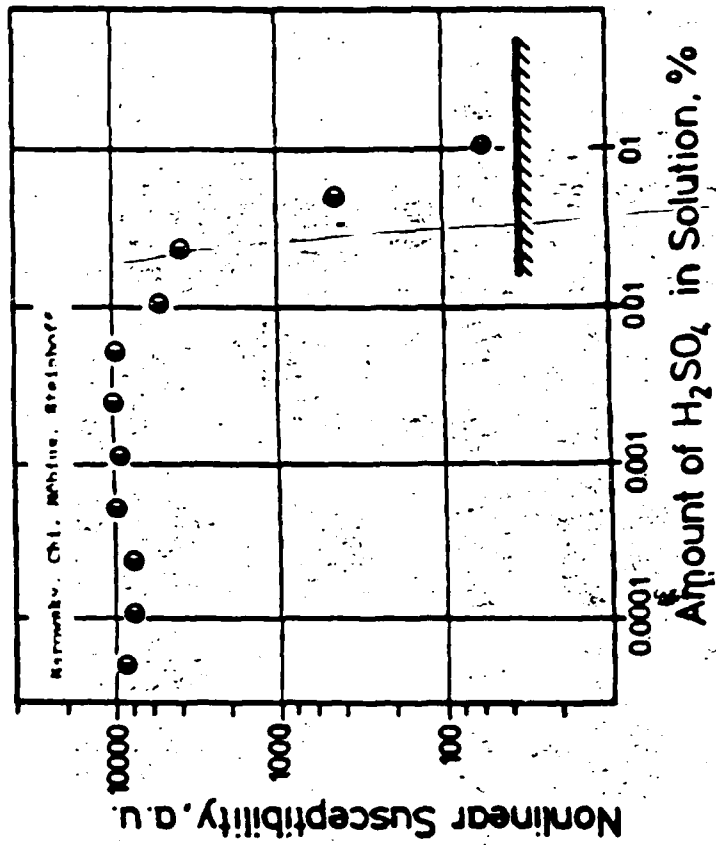
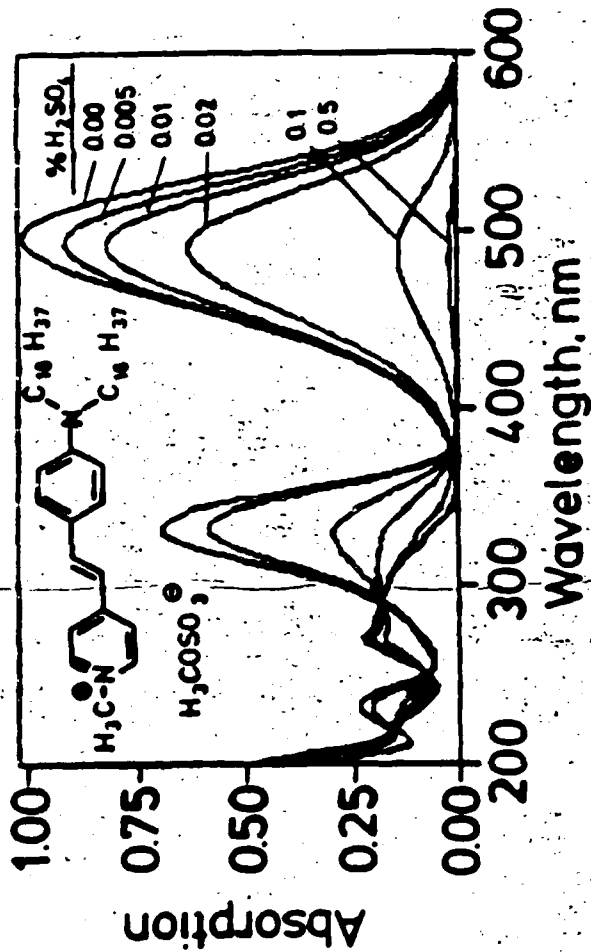
I-7



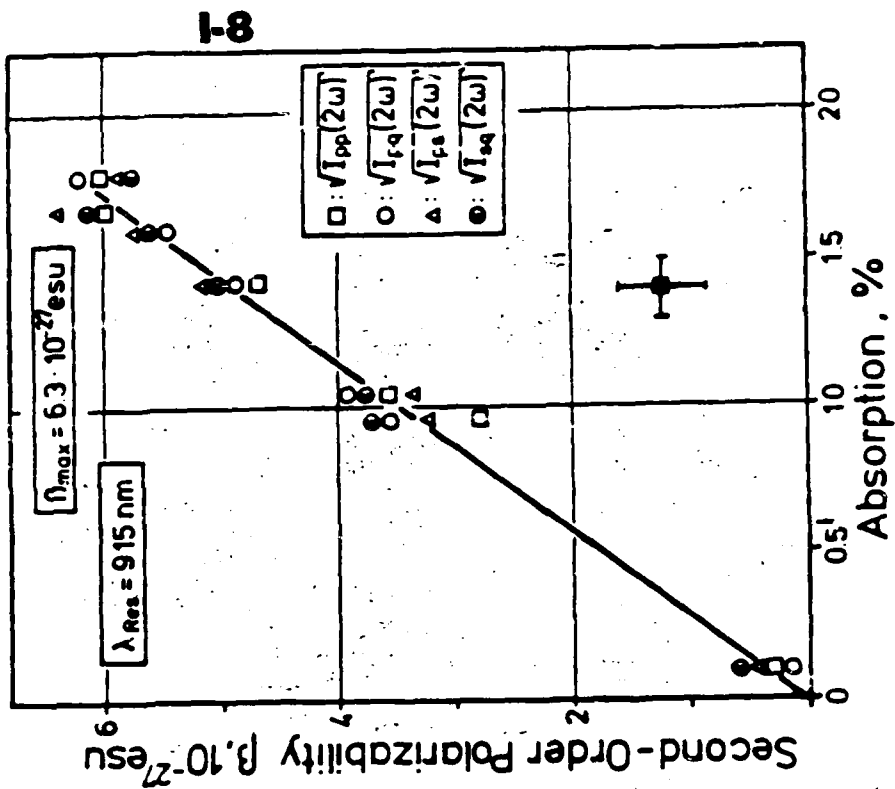
Barovsky, Chi, Möbius, Steinhoff,
Shen, Dorech, Rieger: Nonlinear
Optical Properties ...
Fig. 2

Effects of Protonation

1. Suppresses charge-transfer absorption
2. Drastically reduces $\chi^{(2)}$
3. $\chi^{(2)} \propto$ charge-transfer absorption
 $\propto N_{\text{unprotonated}}$
4. UV absorption band has little effect
on $\chi^{(2)}$.



Karosky, Chi, Möbius, Steinbock,
 Shen, Dorsch, Biegert, Nonlinear
 Optical Properties



Poling

on

Quasi Liquid Crystal films

Theory of Poling.
Assume $\alpha^{(1)}$ and \vec{p} dominated by $\alpha_{333}^{(1)}$ and p_3 \vec{E} along \hat{x}

$$\chi_{xxx}^{(2)} \propto \alpha_{333}^{(2)} \langle \cos^3 \theta \rangle$$

$$\chi_{yyx}^{(2)} \propto \alpha_{y33}^{(2)} [\langle \cos \theta \rangle - \langle \cos^3 \theta \rangle]$$

$$\langle \cos^n \theta \rangle = \int_{-1}^1 \cos^n \theta e^{-V/kT} d(\cos \theta) / Z$$

$$V = V_N - U \cos \theta - p E \cos \theta$$

$$V_N = -U_3 P_3(\cos \theta) - U_4 P_4(\cos^4 \theta) -$$

$$\langle \cos^n \theta \rangle \cong \int_{-1}^1 \cos^n \theta \left(1 + \frac{U + pE}{kT} \cos \theta\right)^n \frac{V_N/k}{Z_N} \times d(\cos \theta)$$



SPIROPYRAN

MEROCYANINE

$$= \langle \cos^n \theta \rangle$$

$$= \frac{U + pE}{kT} \langle \cos^{n+1} \theta \rangle \quad n \text{ odd}$$

H. Haung
T. Rasing
F.P. Jkrventzman
I.R. Cabrera
V.A. Krongauz

$$\langle Cn^2\theta \rangle = \langle Cn^2\theta \rangle_0 \quad \text{indep of } E$$

$$\langle P_2(Cn\theta) \rangle = \frac{1}{2}(3\langle Cn^2\theta \rangle - 1) = \langle P_2(Cn\theta) \rangle_0 \\ \equiv S$$

obtained from birefringence

$$\langle Cn\theta \rangle = \langle Cn^2\theta \rangle_0 \left(\frac{u + pE}{kT} \right)$$

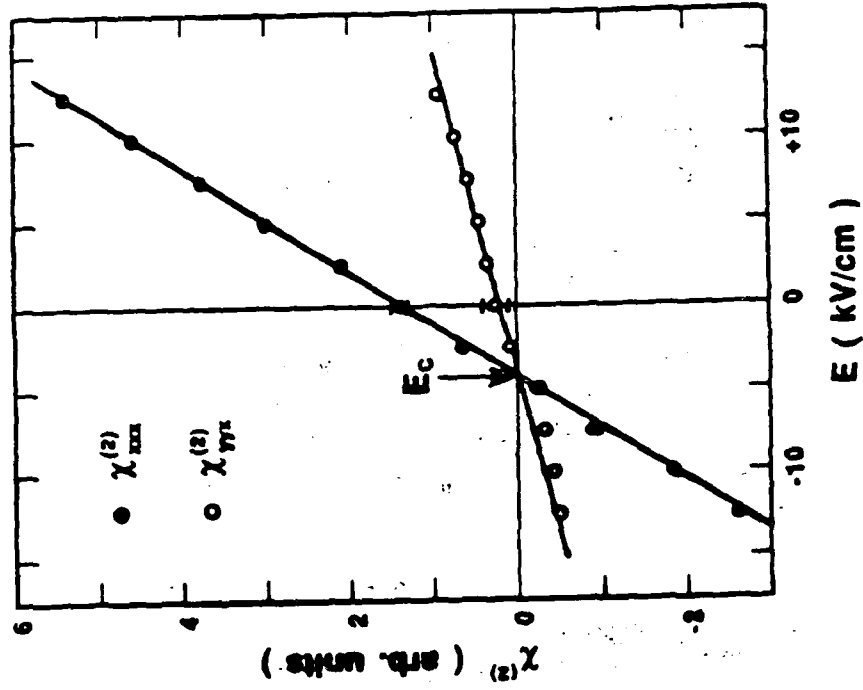
$$\langle Cn^3\theta \rangle = \langle Cn^4\theta \rangle_0 \left(\frac{u + pE}{kT} \right)$$

$$\chi_{xxx}^{(2)} \propto \langle Cn^4\theta \rangle_0 \left(\frac{u + pE}{kT} \right)$$

$$\chi_{yyx}^{(2)} \propto [\langle Cn^2\theta \rangle_0 - \langle Cn^4\theta \rangle_0] \left(\frac{u + pE}{kT} \right)$$

Measurements of $\chi_{xxx}^{(2)}$ and $\chi_{yyx}^{(2)}$ versus E allow the determination of $\langle Cn^4\theta \rangle_0$, u , and p .

I-10



J-1

**D. J. Gerbi
3M Co.**

**NONLINEAR OPTICAL EFFECTS
IN
CONJUGATED SYSTEMS**

**SECOND ORDER NONLINEAR OPTICAL EFFECTS
IN CONJUGATED SYSTEMS**

DIANA GERBI

G. T. BOYD

D. A. ENDER

R. M. HENRY

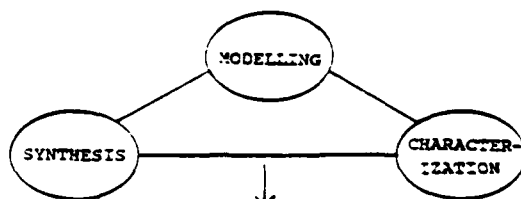
K. K. KAM

P. C. W. LEUNG

J. J. STOFKO

ADVANCED OPTICAL MATERIALS
SCIENCE RESEARCH LABORATORY
3M CORPORATE RESEARCH LABORATORIES

**ADVANCED OPTICAL MATERIALS PROGRAM
(ORGANIC-BASED DEVICES)**



DEVELOPMENT AND APPLICATIONS

- IDENTIFY CANDIDATE MATERIALS
- UNDERSTAND AND MAINTAIN MOLECULAR ORDER
- DETERMINE APPLICATIONS OF MATERIALS. FEASIBILITY IN DEVICES

$X^{(2)}$

OPTICAL COMMUNICATIONS

FIBER OPTICS LAB
TELCOMM
3M DOWMAN
EOTEC

$X^{(3)}$

OPTICAL SIGNAL PROCESSING

INFORMATION AND
IMAGING TECHNOLOGIES

SENSORS

FIBER OPTICS LAB

**OPTICAL SIGNAL PROCESSING
OPTICAL SENSOR PROTECTION**

APOSIR

OUTLINE

- I. REVIEW OF SECOND ORDER NONLINEAR OPTICS, CHARACTERIZATION METHODS AND DEVICE CONFIGURATIONS
- II. ADVANTAGES OF ORGANIC NONLINEAR OPTICAL MATERIALS
- III. MATERIALS PROCESSING/APPLICATIONS
- IV. ELECTRO-OPTIC MATERIALS - CRYSTALS AND POLED POLYMER SYSTEMS

MACROSCOPIC POLARIZATION:

$$P_i = P_{i0} + \chi_{ij}^{(1)} E_j + \chi_{ijk}^{(2)} E_j E_k + \chi_{ijkl}^{(3)} E_j E_k E_l + \dots$$

MICROSCOPIC POLARIZATION:

$$P_i = P_{i0} + \alpha_i E_i + \beta_{ijk} E_j E_k + \gamma_{ijkl} E_j E_k E_l + \dots$$

REVIEW OF SECOND ORDER NONLINEAR OPTICAL EFFECTS

ELECTRO-OPTIC EFFECT:

Index of refraction changes with applied voltage

$$n = n_0 + \Delta n(E) \\ \Delta n \propto \chi^{(2)}$$

SUM FREQUENCY GENERATION:

Output frequency = sum of input frequencies

$$w(\text{out}) = w_1 + w_2 \\ \text{SHG: } I(2w) \propto [\chi^{(2)}]^2 [I(w)]^2$$

DIFFERENCE FREQUENCY GENERATION:

Output frequency = difference of input frequencies

$$w(\text{out}) = w_1 - w_2$$

CHARACTERIZATION METHODS FOR SECOND ORDER NONLINEAR OPTICAL MATERIALS

POWDER SHG

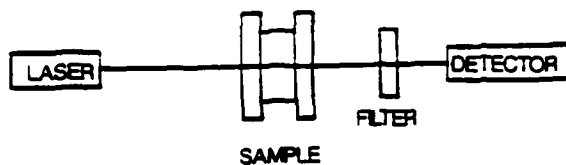
SINGLE CRYSTAL SHG

EFISH

POLYMER POLING

ELECTRO-OPTIC EFFECT

POWDER SHG



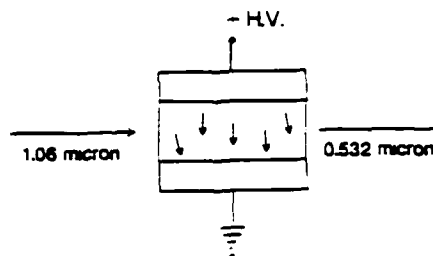
$$\eta = \frac{I(2w)_{\text{sample}}}{I(2w)_{\text{urea}}}$$

MATERIAL FORM: MICROCRYSTALLINE POWDER

ADVANTAGES: USEFUL FOR SCREENING

DISADVANTAGES: CANNOT RESOLVE MICRO- AND MACROSCOPIC CONTRIBUTIONS TO NONLINEARITY

EFISH



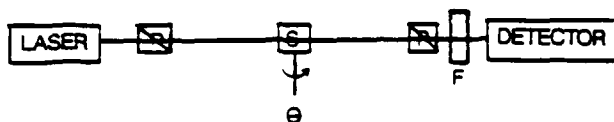
MATERIAL FORM: SOLUTION (LOW POLARITY SOLVENTS)

ADVANTAGES: OBTAIN MOLECULAR PROPERTIES.

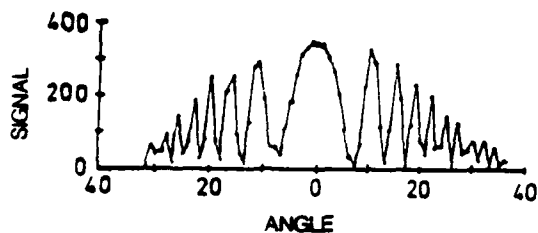
COMPARISONS

DISADVANTAGES: MOLECULAR PROPERTIES ARE SUBJECT TO ENVIRONMENT

SINGLE CRYSTAL SHG



MAKER FRINGE



MATERIAL FORM: LARGE SINGLE CRYSTAL (mm to cm)

ADVANTAGES: MEASURES TENSOR ELEMENTS $\chi^{(2)}$

DISADVANTAGES: REQUIRES CRYSTAL ORIENTATION, INDICES OF REFRACTION, POLISHING

POLYMER POLING

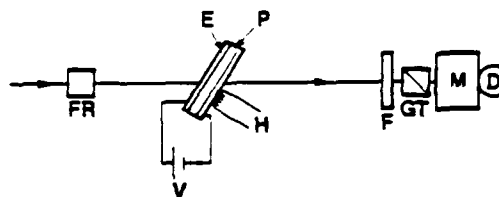


Figure 2. Experimental set-up for thin film SHG measurement using Fresnel rhombs. FR, Faraday Rotator; E, polarizer; P, half-wave plate; H, half-wave plate; GT, Glan-Thompson prism; M, monochromator; D, detector.

MATERIAL FORM: POLYMER SYSTEM

ADVANTAGES: REAL LIFE ENVIRONMENT,

EASY SIGNAL DISCRIMINATION

DISADVANTAGE: NOT A DIRECT MEASUREMENT FOR E-O

ELECTRO-OPTIC EFFECT

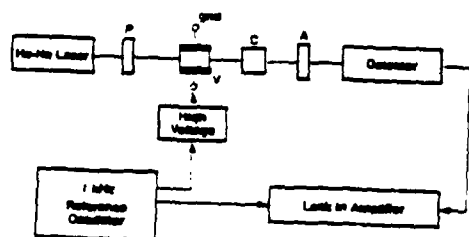


Figure 1. Experimental set-up for electro-optic measurements using polarizer P, analyzer A, and Babinet-Solai compensator C.

MATERIAL FORM: POLYMER SYSTEMS, CRYSTALS

ADVANTAGES: DIRECT MEASUREMENT (DEVICE FORM)

DISADVANTAGES: LESS SENSITIVE THAN SHG
NOT AN IN-SITU TEST
CRYSTALLOGRAPHIC ORIENTATION
FOR CRYSTALS

ADVANTAGES OF ORGANIC MATERIALS

- * SYNTHETIC TAILORABILITY VIA DELOCALIZATION/SUBSTITUENTS
- * SUBPICOSECOND RESPONSE TIMES
- * TRANSPARENCY
- * MECHANICAL AND STRUCTURAL STABILITY
- * HIGH RADIATION DAMAGE THRESHOLD
- * ENVIRONMENTAL STABILITY
- * PROCESSABILITY
- * ROOM TEMPERATURE OPERATION OF DEVICES

MATERIALS PROCESSING

SPIN-COATED POLYMERS

e.g. CHANNEL WAVEGUIDES

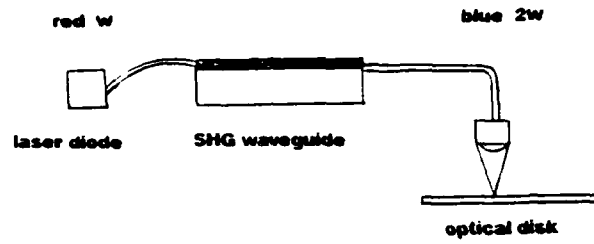
- REQUIRES LOW LOSS (<1 dB/cm)
- REPRODUCIBLE, WELL-KNOWN TECHNIQUES AVAILABLE
- INDUCE ORDER RATHER THAN RELY ON CRYSTAL PACKING

CRYSTALS

e.g. BULK CRYSTALS
CHANNEL WAVEGUIDES
VAPOR DEPOSITED FILMS

- REQUIRES LOW LOSS (<1 dB/cm)
- BULK CRYSTALS MUST BE DURABLE ENOUGH FOR CUTTING AND POLISHING
- COMPLETE CRYSTALLOGRAPHIC ORIENTATION IS REQUIRED
- PRINCIPAL OPTIC INDICES AND AXES RELATIVE TO EXTERNAL MORPHOLOGY MUST BE DETERMINED

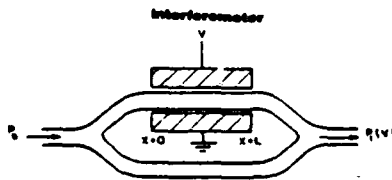
SECOND HARMONIC GENERATION APPLICATIONS



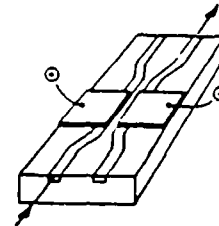
doubling optical frequency gives 4x storage density

APPLICATIONS — ELECTRO-OPTIC EFFECT

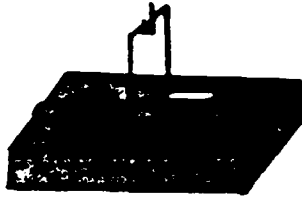
modulator



directional coupler



ELECTRO-OPTIC PHASE SHIFTER



MODULATOR, GYRO

* COMPARE LiNbO_3

$$\lambda = 850 \text{ nm}$$

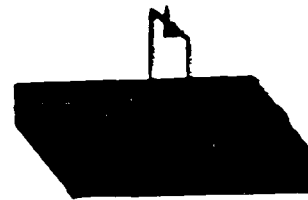
Insertion loss 6dB

$$\text{BW} = 3 \text{ GHz}$$

$$V_{\pi} = 5 \text{ V (4 cm)}$$

Room Temperature

ELECTRO-OPTIC PHASE SHIFTER



PZT CRYSTAL

$$\chi_{33}^{(2)} = \frac{\lambda n_e d}{2V\pi L}$$

$$\chi_{33}^{(2)} = 3 \times 10^{-7} \text{ esu} \approx 30 \cdot \chi^{(2)} \text{ (linear)}$$

POLED POLYMER

$$\chi^{(2)} = c N \mu \beta E \quad N = 1 \text{ Molar}$$

$$E = 0.4 \text{ MV/cm}$$

$$\Rightarrow \mu \beta = 50 \cdot \mu \beta \text{ (DPM)}$$

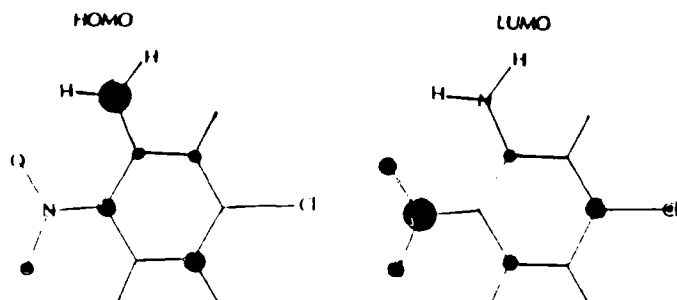
$$A < 0.1/\text{cm} \quad (1 \text{ dB/cm})$$

HALONITROANILINES	RELATIVE EFFICIENCY (UREA)	μ (DEBYE)
	20	4.471
	≤ 0.001	—
	≤ 0.001	9.400
	≤ 0.001	4.433
	2	7.722
	0.03	5.281
	≤ 0.001	8.023

MATERIAL	SPACE GROUP	a	b	c	α	β	γ	z
5-chloro-2-nitroaniline (phase I)	Pna2 ₁	30.844 Å	3.852 Å	6.004 Å	90°	90°	90°	4
5-bromo-2-nitroaniline (5-chloro-2-nitroaniline) (phase II)	P 1	7.344	7.844	7.091	97.98	116.69	83.23	2
2-chloro-4-nitroaniline*	Pna2 ₁	11.25	16.85	3.87	90	90	90	4
3-chloro-4-nitroaniline	P2 ₁ /C	3.813	12.531	14.467	90	91.20	90	4

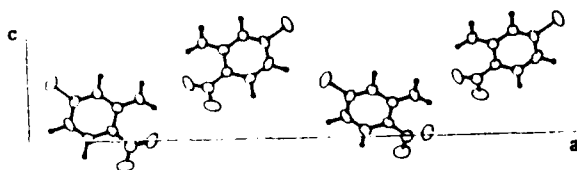
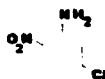
* A. T. McPhail and G. A. Sim, J. Chem. Soc., 227 (1965)

MOLECULAR MODELLING



$\beta \propto$ difference in ground state and excited state
dipole moments

5-CHLORO-2-NITROANILINE



a = 30.844 Å
b = 3.852
c = 6.004

SPACE GROUP
Pna2₁

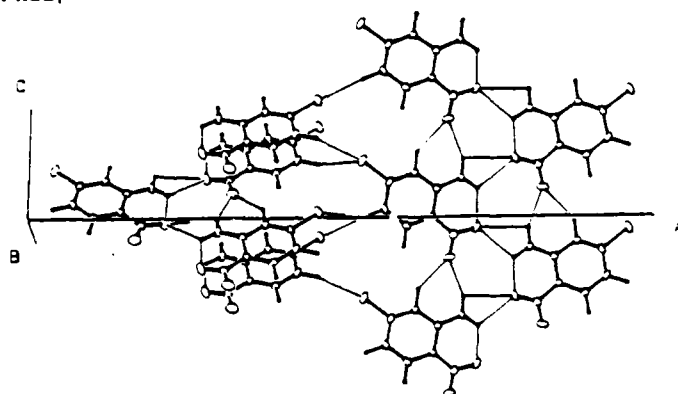


Figure 4. An illustration of the crystal structure of 5-chloro-2-nitroaniline. Significant intra- and intermolecular hydrogen bonding indicated by thin lines.

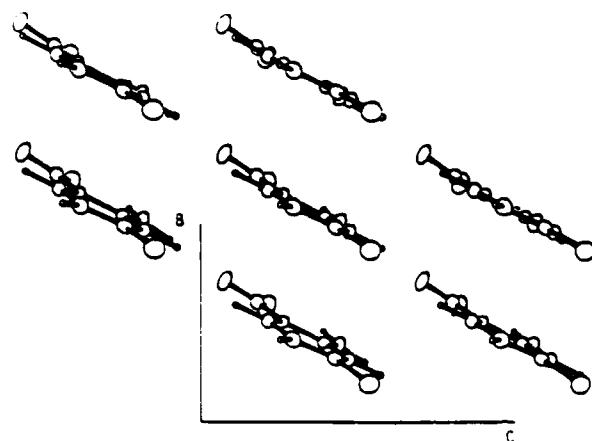


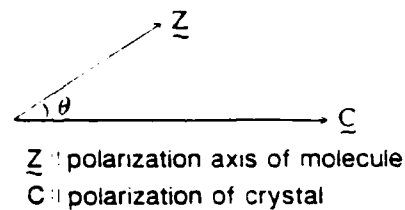
Figure 5. A projection of the ribbon-like packing structure of 5-chloro-2-nitroaniline. Molecules in each row are connected by significant intermolecular hydrogen bonding.

5-CHLORO-2-NITROANILINE

SPACE GROUP $Pna2_1$

polarization axis \parallel C-axis

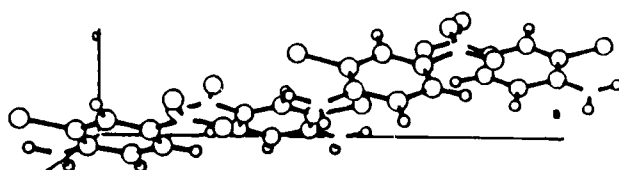
$$P \propto \chi(333) \propto \beta(zzz) \cos^3 \theta$$



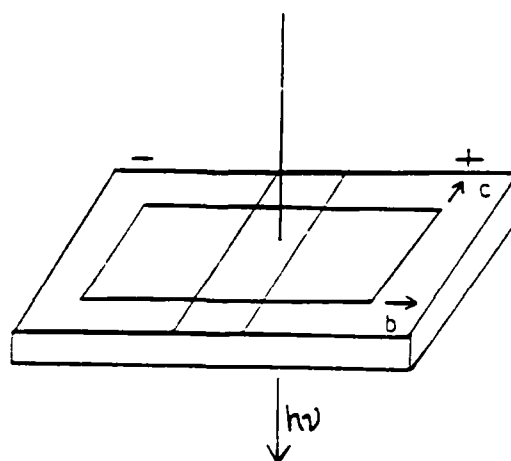
$$\underline{Z} \cdot \underline{C} = \cos \theta = 0.906$$

$$\text{SHG PACKING EFFICIENCY} \approx 0.74$$

2-CHLORO-4-NITROANILINE



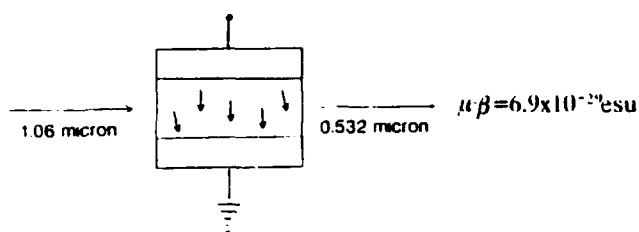
ELECTRODE CONFIGURATION
FOR MEASURING E-O EFFECT



$$\text{FIGURE OF MERIT} = \frac{1}{2} |n_{\text{TE}}^2 - n_{\text{TM}}^2| = 18 \text{ pm/v}$$

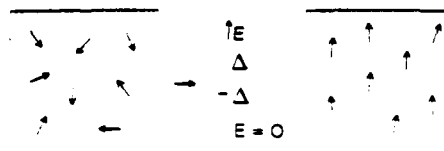
$$E^{\text{DC}} = \hat{y}$$

EFISH on 3-CHLORO-4-NITROANILINE



SHG STUDIES OF POLED POLYMERS

PRINCIPLE OF POLING GUEST/HOST SYSTEMS



INVESTIGATE:

- Extent of ordering
- In-situ β
- Poling dynamics

CONDITIONS FOR POLING

3-CHLORO-4-NITROANILINE IN PMMA



FIGURE 1. POLING OF 3-CHLORO-4-NITROANILINE IN PMMA

- 0.7 M in PMMA (10% by wt)
- $E = 6 \times 10^4$ V/cm
- $T = 110^\circ \text{C}$

RESULTS OF POLING EXPERIMENTS

- CALCULATED β AGREES WITH MEASURED
- OBSERVED DECREASE OF $\chi^{(2)}$ WITH TIME

CONDITIONS	$\chi^{(2)}$ (esu)
$E, 110^\circ \text{C}$	1×10^{-10}
E, RT	1×10^{-10}
$E = 0$ (30 sec), RT	0.5×10^{-10}
$E = 0$ (65 hr), RT	0.39×10^{-10}

POLED POLYMER SYSTEMS FOR ELECTRO-OPTIC EFFECT

GUEST	$\mu\text{-B}$ ($\times 10^{-28}$ D-esu) at 1.58 microns	A/molar			
		810 nm	1000 nm	1300 nm	1500 nm
3MX-40	37	84	51	30	27
3MX-3	19	1.5	0.13	0.09	0.1
3MX-36	18	0.6	0.3	0.3	0.3
3MX-2	15	0.5	0.6	0.6	0.6
3MX-1	11	0.07	0.06	0.05	0.07
3MX-8	10	0.03	0.04	0.04	0.04

K-1

G. R. Meredith
E. I. Dupont DeNemours and Co.

OPTICAL NONLINEARITY: MOLECULES,
ASSEMBLIES AND WAVE PHENOMENA

L-1

G. Khanarian
Hoechst-Celanese

CHARACTERIZATION OF POLYMERIC
NONLINEAR OPTICAL MATERIALS

Characterization of Nonlinear
Optical Organic Materials

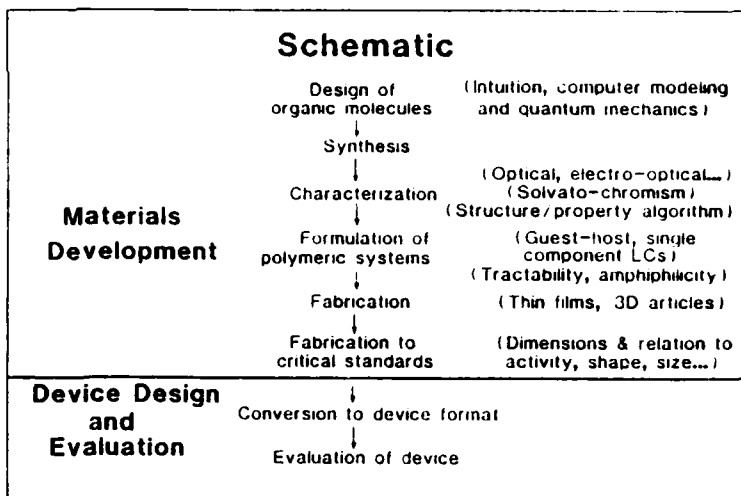
G. Khananan
Hoechst Celanese Corporation
Summit, New Jersey 07901

ACS Workshop
Virginia Beach, May, 1988

T. CHE
R. DEMARTINO
D. HAAS
T. LESLIE
H. MAN
J. STAMATOFF
C. TENG
H. YCCN

OUTLINE

- o Molecular Miller's Rule
- o Polymer Structure and
- o Measurement of $\chi^{(2)}$ by Second Harmonic Generation
- o Measurement of $\chi^{(2)}$ by the Pockels Effect
- o Results for MNA/PMMA
- o MNA/PMMA/Sol-Gel Glasses - Role of Molecular Motion
- o Langmuir Blodgett Films - Role of Internal Optical Field
- o Application to Devices



BASIC PHYSICS

MOLECULAR

$$P = \mu_e + eE + eE' + eE''$$

MATERIAL

$$P = x^{(1)}E + x^{(2)}E^2 + x^{(3)}E^3$$

$$\frac{d^2x}{dt^2} + 2\gamma \frac{dx}{dt} + \omega_0^2 x - \xi x^3 = -\frac{e}{m} E$$

$$x^{(1)}(\omega_0) = \frac{Ne^2}{m} \frac{1}{\omega_0^2 - 2i\gamma\omega_0 - \omega_0^2}$$

$$x^{(3)}(\omega_0, \omega_0) = -\frac{m\xi}{\sqrt{2}\gamma^3} [x^{(1)}(\omega_0)] [x^{(1)}(\omega_0)] [x^{(1)}(\omega_0 + \omega_0)]$$

ANHARMONIC OSCILLATOR MODEL

$$\epsilon_{\infty} = \frac{m\xi}{Ne^2}$$

m mass of electron

e charge of electron

N oscillator strength

\xi anharmonic constant

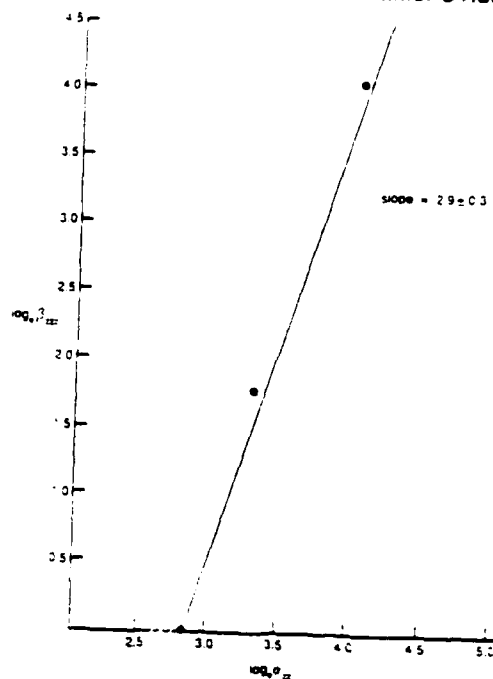
$$x^{(1)}$$

\omega angular frequency

L length of molecule

	Exp. (10 ¹⁸ esu)	Theory (10 ¹⁸ esu)
$\frac{m\xi}{Ne^2}$	1	3.0

$\log_e \beta_{xx}$ versus $\log_e \alpha_{xx}$
Verification of molecular Miller's Rule



- h = molecular height
- n = refractive index
- λ = wavelength of light
- ϵ = dielectric constant
- ρ = density
- K = Kerr constant
- γ_K = molar Kerr constant

$$\gamma_K = \frac{1}{310} \left(\frac{3n^2 - 1}{n^2 + 2} \right)^2 \left(\frac{3\rho^2}{4T} - \frac{3\rho^2}{4T} \right) = \frac{3\rho^2}{4T} \left(\frac{3n^2 - 1}{n^2 + 2} \right)^2 = 10^6$$

$$\beta_{zz} = \beta_{zz} - \bar{\beta}$$



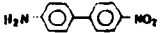

$$\beta_{zz} = \beta_{zz} - \bar{\beta} = \beta_{zz} - \bar{\beta} = \beta_{zz} - \bar{\beta}$$

$$\beta_z = \beta_{zzz} + \beta_{zzx} + \beta_{zyy} \quad (\text{1st hyperpolarizability})$$

- β = mean 2nd hyperpolarizability
- N_A = Avogadro's number
- k = Boltzmann's constant
- T = temperature
- $\bar{\beta}$ = mean polarizability
- μ = dipole moment

TABLE I





Molar Kerr constants γ_K ($\times 10^{-6}$ esu), linear polarizability α_{zz} ($\times 10^{-24}$ esu) and β_{zzz} ($\times 10^{-36}$ esu)

Compound	γ_K	α_{zz}	β_{zzz}
	0.985	13.2	1.0
	6.850	18.7	5.7
	14.5	29.5	20
	16.9	39.6	51

γ_K values are at 0.633 μ m. β_{zz} has been deduced from equation 1, and literature values for the dipole moment μ , and the average polarizability. α_{zz} values reported above are at 1.9 μ m. A dispersion formula has been used to go from 0.633 to 1.91 μ m. β_{zzz} are also at 1.91 μ m.

5.11 OF POLED FLEXIBLE DIPOLAR POLYMERS

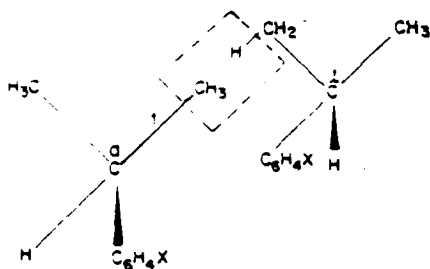
Types of Molecular Packing

Packing	Type	Order	Magnitude
	Non-centric	Second	Moderate
	Non-centric	Second	Strong
	Centric	Third	Strong
	Centric	Third	Weak

— +
→ Direction of dipole moment

● Theory same as for elish

● Exact calculations can be done for single chains - Flory Theory

FIG. 2. Designation of bonds of PPNS, $X = \text{NO}_2$.TABLE II. $\langle \mu \cdot \theta \rangle / x$ ($\times 10^{-48} \text{ cm}^2$) and $\langle \mu^2 \rangle / x$ ($\times 10^{-48} \text{ SC}^2 \text{ cm}^2$) of poly(p-nitrostyrene) vs tacticity p , $T = 298 \text{ K}$, $x = 200$ repeat units.

P	$\frac{\langle \mu \cdot \theta \rangle}{x}$	$\frac{\langle \mu^2 \rangle}{x}$
0.0 (isotactic)	21.5	10.7
0.2	16.6	8.27
0.4	16.3	8.12
0.6	16.8	8.36
0.8	16.4	8.17
1.0 (syndiotactic)	12.5	6.23

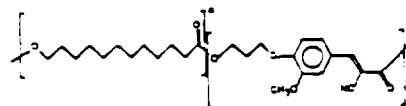


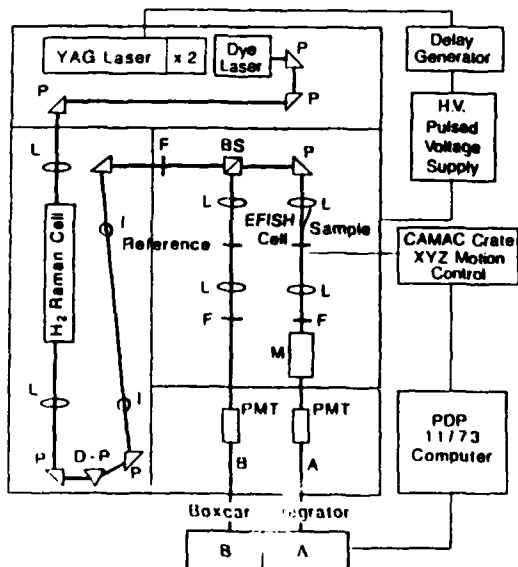
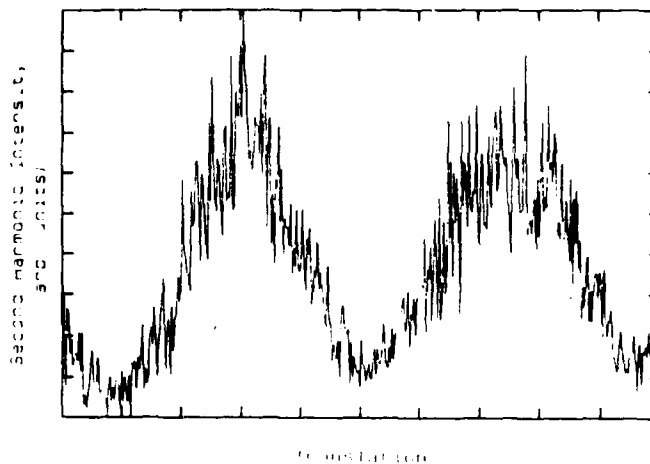
Table 2: Average Monomer Susceptibilities for Various Molecular Weight Copolymers.

Molecular Weight, M_n	Calculated Number of Monomer Units, n	$M_2 B_2 / n$ (10^{-48} esu)	Enhancement factor, G
NLO chromophore ^a	—	57	—
17,000	37	830	15
70,000	152	1140	20

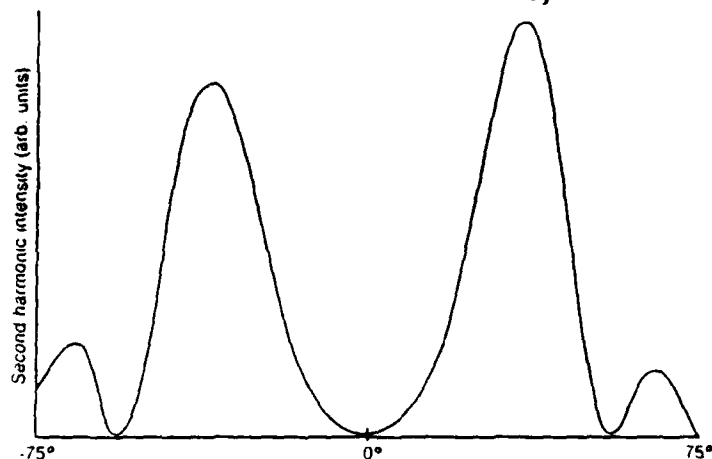
^a Determined by GPC relative to polystyrene.^b Structure II from Table 1.

C. S. Willard, S. E. Feth, M. Scotzava, and D. J. Williams
Corporate Research Laboratories, Eastman Kodak
Company, Rochester, N. Y.

G. D. Green,¹ J. I. Wenschink, III, H. K. Hall, Jr., and J. E. Mulvaney
C. S. Marvel Laboratories, Department of Chemistry,
University of Arizona, Tucson, Az.

Maker Fringe of EFISH of Dioxane at $\lambda = 1.535 \mu\text{m}$, $\text{HV} = 5.0 \text{ kv}$ 

Second Harmonic Intensity From a Poled MNA/PMMA Alloy

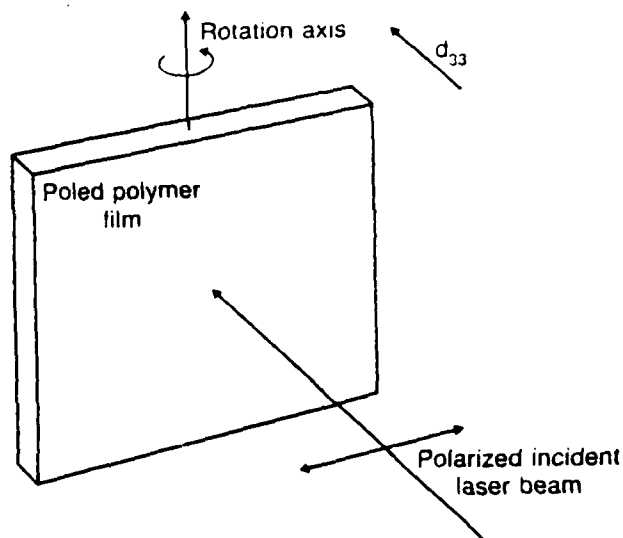


SECOND HARMONIC GENERATION FROM POLED POLYMERS

The second harmonic intensity is given by

$$\frac{I(2\omega)}{I(\omega)} = (T_d^2 p^2) \sin^2 \left(\frac{\pi}{2} \frac{L}{l_c} \frac{n}{n - \sin^2 \theta} \right)$$

- t, T Fresnel transmission factors
- d Second harmonic coefficient
- p Projection factor of d tensor onto optical electric field
- l_c Coherence length
- n Refractive index
- L Thickness of sample
- θ Angle of rotation



$$x^{(2)}(-2\omega, \omega, \omega) = 2d$$

When $\theta = 0$, $p = 0$ and there is no component of d along E , and there is no second harmonic observed

The Maker fringe arises from an interference between the fundamental beam and generated harmonic wave

THEORY OF MEASUREMENT FOR POCKELS AND KERR EFFECT

The birefringence Δn induced in a Kerr cell is:

$$\Delta n = \lambda B E^2$$

and in a Pockel cell:

$$\Delta n = 1/2 m' E$$

The birefringence results in a retardation τ :

$$\tau = \frac{2\pi \Delta n l}{\lambda}$$

in the small angle approximation, Equation 4 becomes:

$$\frac{1}{I} = \frac{1}{2} (1 + \tau)$$

A sinusoidal voltage is applied across the electro-optic cell

$$V = V_0 \sin \omega t$$

Substituting Equation 7 into Equation 5

$$I = \frac{I_0}{2} + \frac{\tau}{2} \frac{Kerr}{\lambda} + \frac{\tau}{2} \frac{Pockel \sin \omega t}{\lambda} + \frac{\tau}{2} \frac{Kerr \cos 2\omega t}{\lambda}$$

The apparent angular dependence of the Pockels effect arises from change of optical path length

$$\frac{d}{\cos \theta}$$

where d is the thickness of the sample

The analyzing light beam sees a different birefringence as a function of angle

$$\Delta n(\theta) = \Delta n(\theta = 90^\circ) \sin^2 \theta$$

θ is the angle between the normal axis of sample and the light beam

POCKELS EFFECT

The optical retardation is

$$\tau = \frac{2\pi}{\lambda} l \Delta n$$

l Optical path length

Δn Induced birefringence

λ Wavelength of light

The induced birefringence

$$\Delta n = \frac{1}{2} (n_1^2 r_{11} - n_1^2 r_{33}) E$$

r Pockels constant

n Refractive index

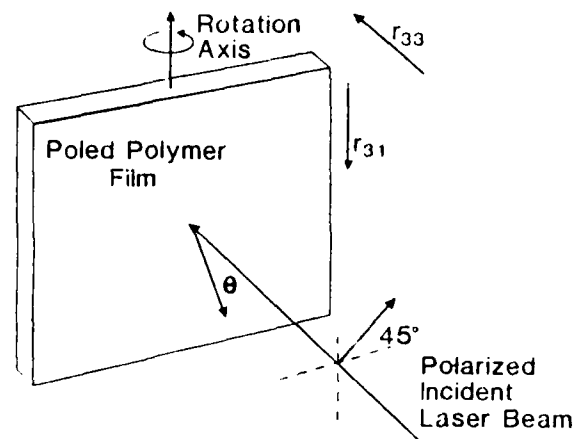
E Applied electric field

For poled materials

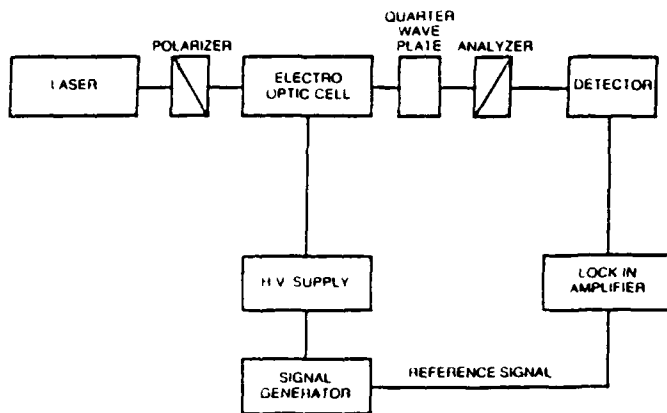
$$r_{11} = \frac{r_{33}}{3}$$

This result is obtained from a thermodynamic model for poling

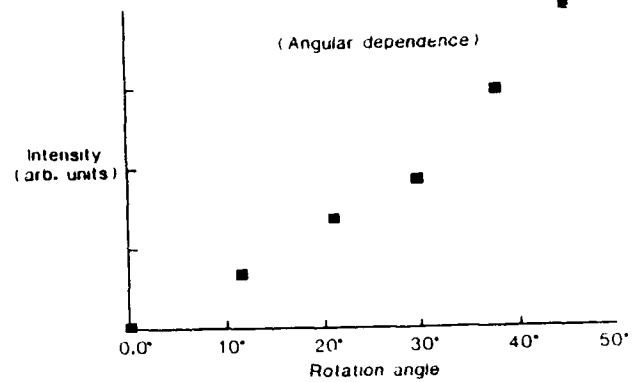
- Boltzmann statistics



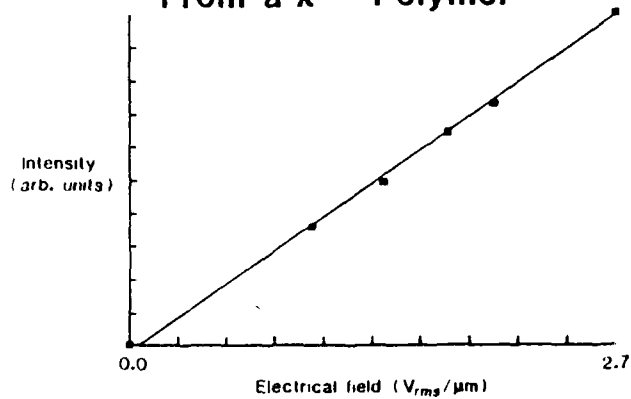
SCHEMATIC OF ELECTROOPTIC APPARATUS



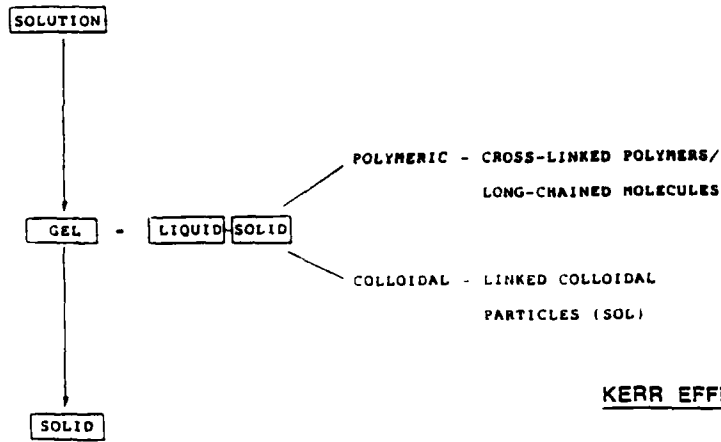
Pockels Effect from Poled MNA / PMMA Sample



Pockels Linear Electro-optic Effect From a $\chi^{(2)}$ Polymer



SOL-GEL TECHNOLOGY



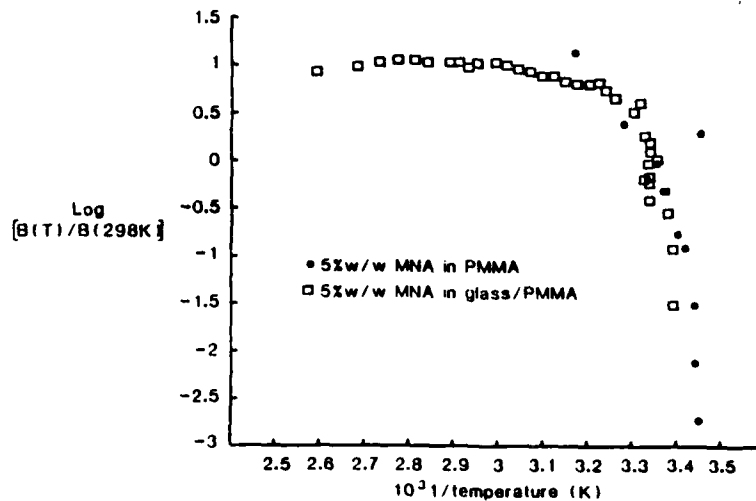
KERR EFFECT OF SOL-GEL GLASS

MNA added to sol-gel glass

PMMA is added to sol gel glass to give mechanical strength

Slab was cut and polished for electro-optic measurement

**Arrhenius Plot of Kerr Constant
for MNA Optical Composites**



THERMODYNAMIC MODEL

Assume that nonlinear optical molecules are distributed orientationally according to Boltzmann statistics.

$$\chi_{xxx}^{(2)}(-2\omega, \omega, \omega) = N f^3 \frac{\epsilon(n^2 + 2)}{n^2 - 2} \frac{\mu E}{5kT}$$

N	number density
f	internal field
s	hyperpolarizability
μ	dipole moment
E	poling field
k	Boltzmann constant
T	temperature
ϵ	dielectric constant
n	refractive index

RESULTS

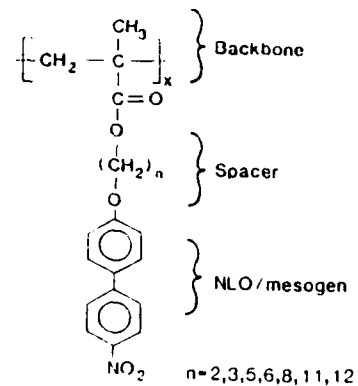
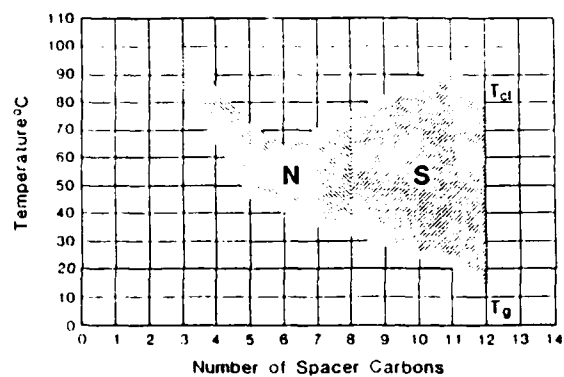
Sample	$\chi_{xxx}^{(2)}(-2\omega, \omega, \omega)$	$\chi_{xxx}^{(2)}(-\omega, \omega, 0)$	$\chi_{xxx}^{(2)}(\text{calc})$
10% MNA/PMMA	1.6	1.5	0.6

All $\chi^{(2)}$ values are $\times 10^{-11}$ esu and are at $1.06 \mu\text{m}$

$\chi_{xxx}^{(2)}(-2\omega, \omega, \omega)$ measured at $1.06 \mu\text{m}$

$\chi_{xxx}^{(2)}(-\omega, \omega, 0)$ measured at $0.63 \mu\text{m}$ and a dispersion relation was used to obtain values at $1.06 \mu\text{m}$

$\chi_{xxx}^{(2)}(\text{calc})$ used the thermodynamic model

NLO Side Chain Polymers
First GenerationDependence of Glass and Clearing Temperatures
on Carbon Spacer Length

NLO Polymer Properties

$\chi^{(2)}$ at 1.3 μm	> 50 pm/V
r (calculated)	> 14 pm/V
n (1.3 μm)	1.57
ϵ (DC)	3.5
ϵ (n^2)	2.6
waveguide loss at 1.3 μm	0.9 dB/cm

Spin coatable from common solvents

Poled for application

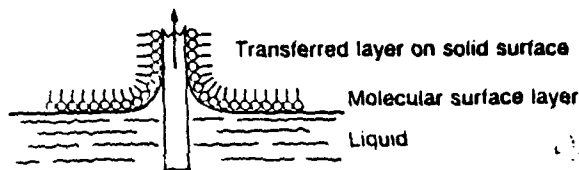
Stable (<10% loss) at >50°C for 5 years

LANGMUIR-BLODGETT FILMS

- 2D Material
- Orientation of Molecules by Surface
- Useful for Fundamental Studies of:
 - Interaction of radiation with molecules (spectroscopy)
 - Tilt angles
 - Hyperpolarizability
 - Molecule/surface interactions
 - Interaction between layers
 - Local optical electric field effects

Langmuir-Blodgett Film (LBF) Formation

- Is the deposition on a surface of a single molecular layer at a highly ordered state
- Sequential deposition leads to periodically structured films
- It is done by transfer of a compressed molecular surface layer on a liquid onto a solid surface by dipping



- Applications
 - Nonlinear optics: Bistable switches
Thin film SH and TH generation
 - Electro-optics: Thin film light modulator
 - Integrated optics: Planar dielectric wave guides

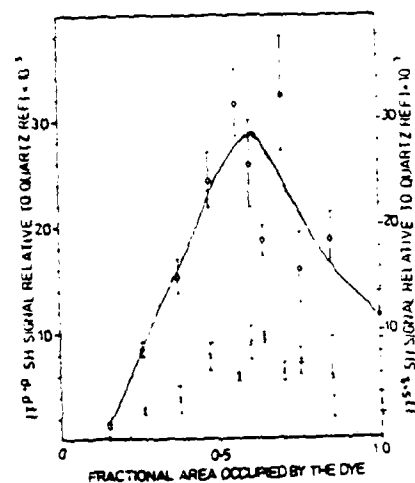


Fig. 5. Plot of the second-harmonic (SH) signals $17P-P$ (O) and $17S-S$ (x) relative to the quartz reference slab versus the area fraction occupied by the dye in the mixed monolayer.

Local Optical Electric Field

$$E_z = E_z - \alpha_{zz} E_z - (\beta_{zzz}) E_z^2 + (\gamma_{zzzz}) E_z^3$$

$$E_z = E_z + \sum_j T_{zz}^{(j)} P_z$$

$$T_{zz}^{(j)} = \frac{-4}{\epsilon_0^3}$$

μ , χ , β and γ are the dipole moments and polarizabilities

Z axis is normal to glass surface

Linear Mean Field Approximation

- Neglect fluctuation in dipole moment
- Assume that linear polarizability alone changes local dynamic optical field.

$$\begin{aligned} \sum_j T_{zz}^{(j)} &= \rho \int_0^a \frac{2\pi \mu \mu \rho}{r^3} \\ &= \frac{2\pi \rho}{a} \end{aligned}$$

ρ = surface density of dipoles

a = radius of nonlinear optical molecule

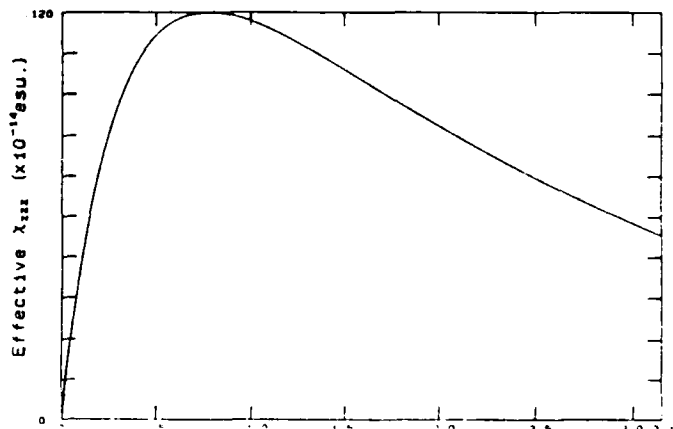
Results for the nonlinear

susceptibility

$$\chi_{zzz} = \frac{3a}{2\pi\alpha_{zz}} \frac{x}{(1+x)^2} - \frac{3\gamma\mu a}{2\pi\alpha_{zz}^2} \frac{x^2}{(1+x)^2}$$

$$x = \frac{2\pi\alpha_{zz}\rho}{a}$$

Variation of effective χ_{zzz} of a Langmuir Blodgett Film versus normalized concentration of active nonlinear optical molecule



CLASSES OF ORGANIC NLO DEVICES

● Electro-Optic Devices

- Control of light with electronics
- Based on the second order NLO susceptibility $\chi^{(2)}$
- Applications: Hybrid optical processing and optical communications

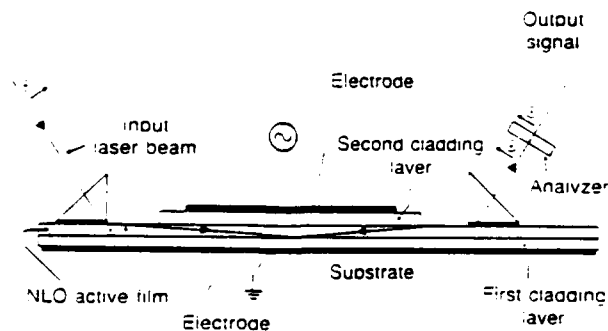
● All Optical Devices

- Control of light with light
- Based on the third order NLO susceptibility $\chi^{(3)}$
- Applications: All optical computing and ultra-fast optical communications

POLYMER GUIDE FABRICATION PROCESS

COMPONENTS

- Spin Coating (thin film formation)
- Buffer Layer and Substrate Materials
- Patterning
- Metallizing
- Beam Coupling



L-14

MODULATOR RESULTS

MATERIAL	LENGTH (CM.)	V _π (V)	Λ (nm)	F _{MAX} (MHz)	Γ ₃₃ (pm/V)
PMMA: pNA	1.0	450	633	30	.5
HCC #0520	1.0	45	633	0.5	3.5
HCC #1622	2.0	30	830	10*	3.75
HCC #1238	1.5	4.0	830	1	20

$$\Gamma_{33} = \frac{3 \lambda G}{2n^3 L V_{\pi} \Gamma}$$

Γ = .85 to .95 for these structures

OTHER MATERIAL PROPERTIES

> n FROM 1.61 TO 1.66

> g (100 KHz) = 3.5

SUMMARY

- Organic NLO research at HCC has developed outstanding NLO and EO polymers
- These materials, additionally, exhibit combination of excellent performance characteristics and fabrication properties for NLO and EO devices
- Initiative to develop a series of important NLO devices has been undertaken at HCC
- Fabrication science and technology for the materials is a key component of the initiative

M-1

T. Richardson

University of Oxford, U. K.

PREPARATION AND CHARACTERIZATION
OF
ORGANO-TRANSITION METAL
LANGMUIR-BLODGETT FILMS

M-2

THE PREPARATION AND CHARACTERISATION OF "GEMINO-TRANSITION METAL LANGMUIR-BLODGETT" FILMS

T. RICHARDSON, G.G. ROBERTS
UNIVERSITY OF OXFORD
DEPARTMENT OF ENGINEERING SCIENCE
PARKS ROAD, OXFORD, OX1 3PJ, ENGLAND

M.E.C. POLYMER, S.G. DAVIES
DYSON PERKINS LABORATORIES
UNIVERSITY OF OXFORD
SOUTH PARKS ROAD, OXFORD, OX1 3BY, ENGLAND

A SERIES OF NOVEL RUTHENIUM COMPOUNDS HAVE BEEN DEVELOPED FOR USE WITH THE LANGMUIR-BLODGETT DEPOSITION TECHNIQUE. COMPLEXING OF A 4- RUTHENIUM (CYCLOPENTADIENYL-BIS (TRIPHENYLPHOSPHINE)) HEAD GROUP TO A CYANOTERPHENYL LIQUID CRYSTAL MOLECULE HAS BEEN SHOWN TO INCREASE THE SECOND-ORDER NON-LINEAR OPTICAL HYPERPOLARIZABILITY AND FURTHERMORE INDUCE MULTILAYER FORMATION. OPTICAL ABSORPTION DATA HAVE REVEALED THE EXCELLENT REPRODUCIBILITY OF SUCCESSIVE MONOLAYER TRANSFER. SECOND HARMONIC GENERATION HAS BEEN OBSERVED AND THE EFFECT HAS BEEN INCREASED BY INCORPORATING UNSUBSTITUTED LIQUID CRYSTAL MOLECULES INTO THE VOIDS BETWEEN THE TERPHENYL CHAINS OF ADJACENT RUTHENIUM SUBSTITUTED MOLECULES. WE HAVE FURTHER OPTIMISED THE NON-LINEAR RESPONSE BY SYSTEMATICALLY VARYING THE ELECTRON-RELEASING CHEMICAL GROUP AND THE CONJUGATION WITHIN THE MOLECULE.

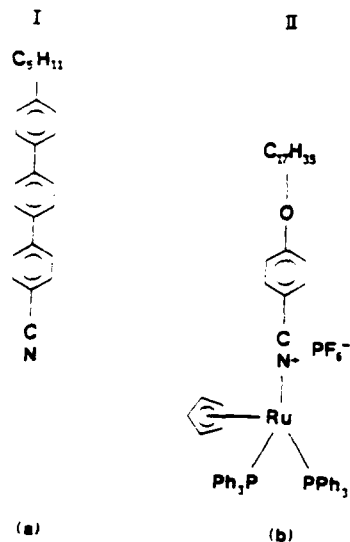


FIGURE 1

(A) A TYPICAL CYANO-TERPHENYL MOLECULE (I).
(B) THE $(C_5H_5)_2 Ru (PPh_3)_2$ SUBSTITUTED MOLECULE POSSESSES A LARGER SECOND-ORDER NON-LINEAR OPTICAL HYPERPOLARIZABILITY THAN COMPOUND (I).

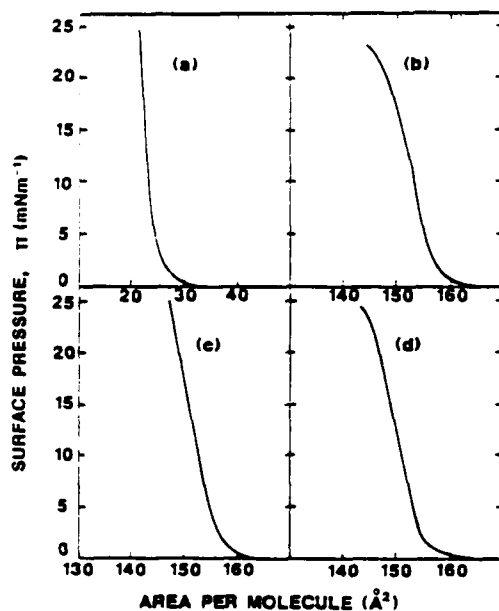


FIGURE 2

THE BEHAVIOUR OF MOLECULES OF COMPLEX I AND II UNDERGOING COMPRESSION ON THE WATER SURFACE. (A) COMPLEX I AT pH 5.8, (B, C AND D) COMPLEX II AT pH 5.8, 5.8 AND 8.7 RESPECTIVELY. THE MOLECULAR AREAS AT RELATIVELY HIGH SURFACE PRESSURE (20 mNm^{-1}) CORRESPOND ACCURATELY TO THE MEASURED CROSS-SECTIONAL AREA OF THE RUTHENIUM HEAD GROUP.

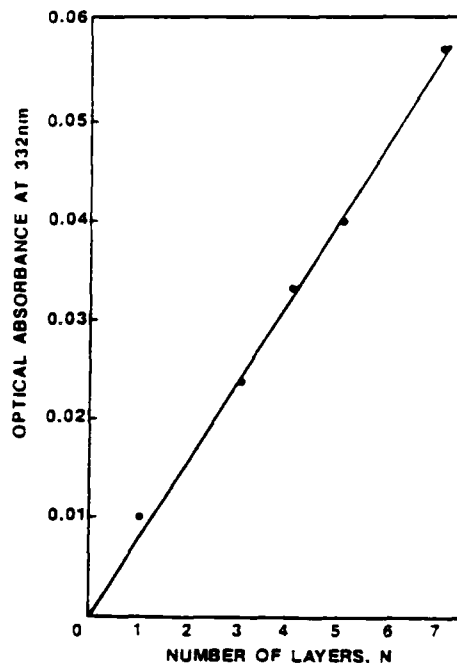


FIGURE 3

OPTICAL ABSORPTION VERSUS THE NUMBER OF TRANSFERRED MONOLAYERS. THE LINEAR RELATIONSHIP INDICATES THE REPRODUCIBILITY OF SUCCESSIVE MONOLAYER DEPOSITION.

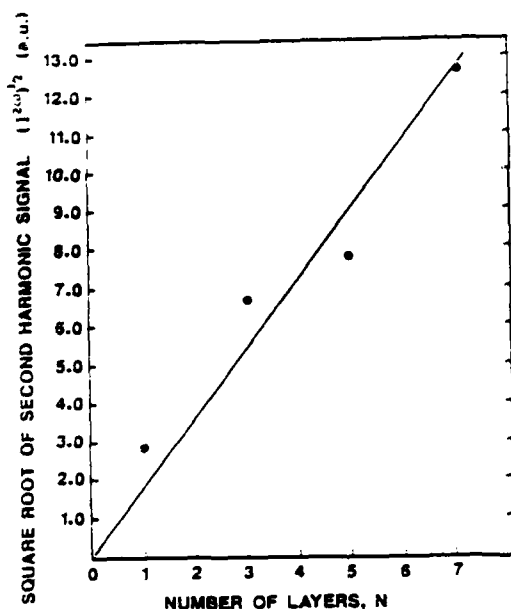
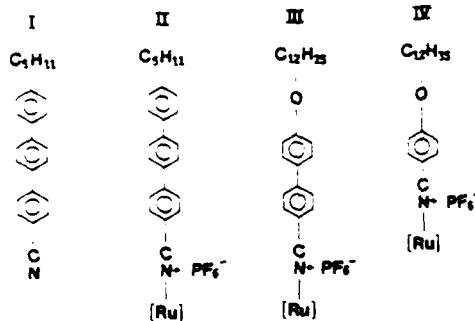


FIGURE 4

THE RELATIONSHIP BETWEEN THE SQUARE ROOT OF THE SECOND HARMONIC GENERATION SIGNAL AND STRENGTH THE THICKNESS OF THE FILM. THE APPROXIMATELY LINEAR RELATIONSHIP IMPLIES THE UNIDIRECTIONAL ALIGNMENT OF THE MOLECULES.



COMPLEX	SHG SIGNAL NORMALIZED TO II
II	1.0
II/I	1.5
III	11.0
IV	77.0

FIGURE 6

OPTIMISATION OF NON-LINEAR RESPONSE. THE SECOND HARMONIC SIGNAL IS HIGHLY DEPENDENT UPON THE ELECTRON DONOR AND THE DEGREE OF CONJUGATION.

(a) NO INCORPORATION



(b) INCORPORATED CTP MOLECULES

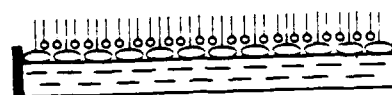


FIGURE 5

HIGH PACKING DENSITY STRUCTURES.

- (A) THE LIQUID CRYSTAL MOLECULES MAY REMAIN ON THE WATER SURFACE.
OR
(B) THEY MAY BE INCORPORATED INTO THE MATRIX FORMED BY THE RUTHENIUM SUBSTITUTED MOLECULES.

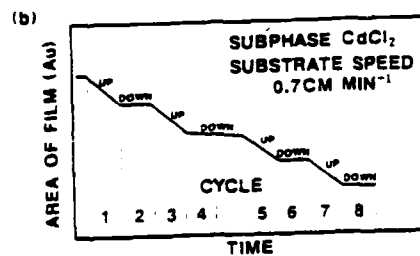
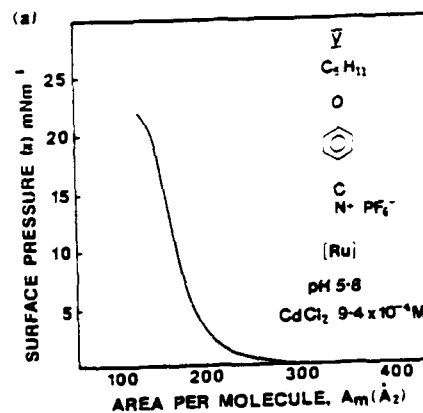


FIGURE 7

OPTIMISATION OF THE CARBON CHAIN LENGTH:-

- (A) II VS. A_m PLOT FOR COMPLEX V, SHOWN IN INSERT
(B) THE Z-TYPE DEPOSITION OF COMPLEX V. HIGHER RATES OF DEPOSITION ARE POSSIBLE WITH $CdCl_2$ IN THE SUBPHASE.

N-1

S. K. Tripathy
University of Lowell

OPTICAL PROPERTIES
OF
ORGANIZED ASSEMBLIES

OPTICAL PROPERTIES OF MOLECULAR ASSEMBLIES

SUKANT TRIPATHY
UNIVERSITY OF LOWELL
LOWELL, MA 01854

- Selected conjugated molecular and Macromolecular systems
- Organized mono and multilayer assemblies
- Characterization of microstructure and morphology
- Measurement and anticipation of electronic and optical properties

Selection of materials

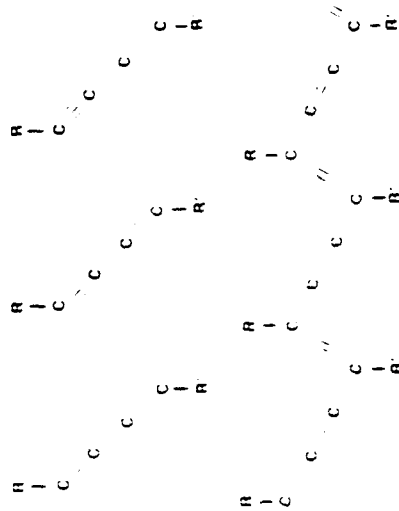
1. Linked donor-acceptor molecules.

anticipated large 2nd order effects.
example MNA

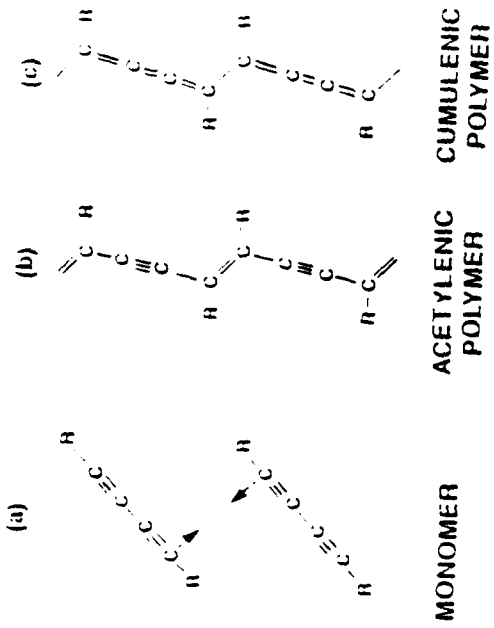
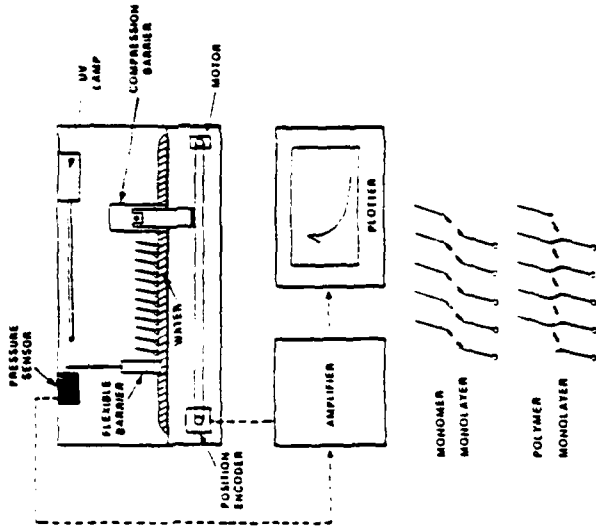
2. Polymers with delocalized backbone electronic structure.

anticipated large 3rd order susceptibilities.
example Polydiacetylenes

POLYDIACETYLENES



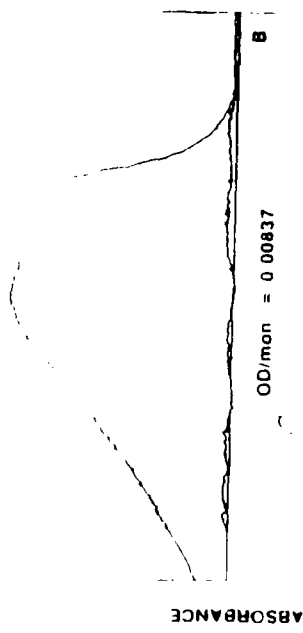
- Backbone Responsible for the Optical and the Nonlinear Optical Properties
- The Side Groups Provide a Handle for Fabrication and Structure Control



N-4

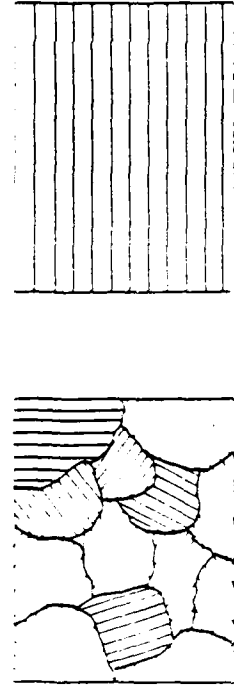
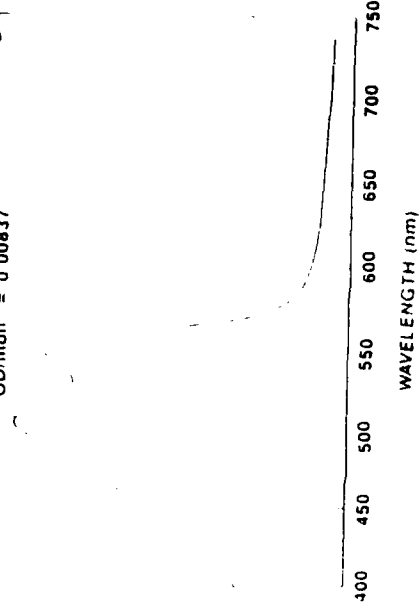
OD/mon. = 0.0039

A

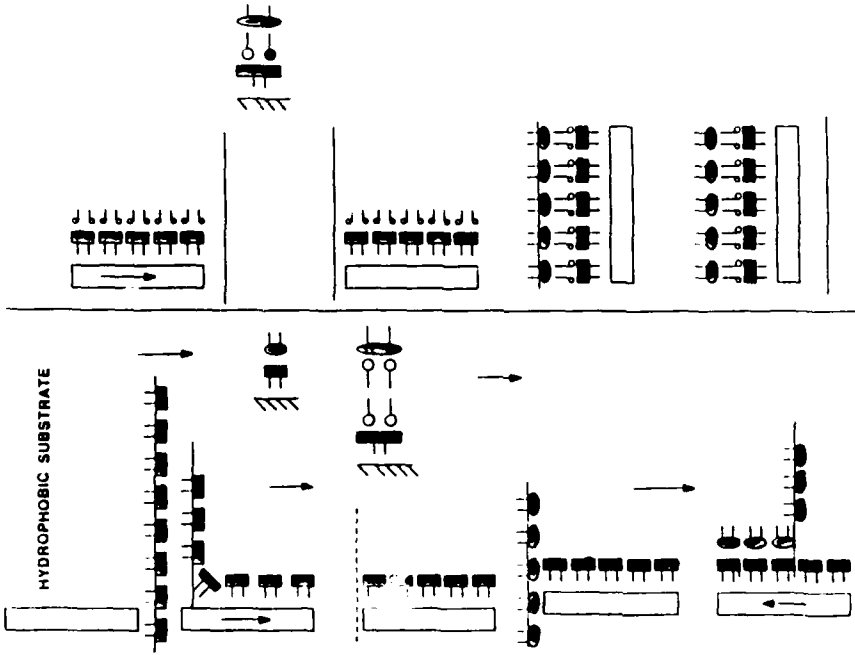


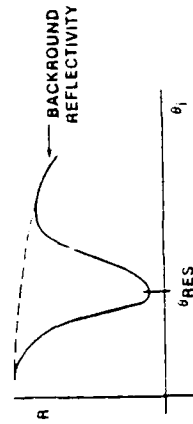
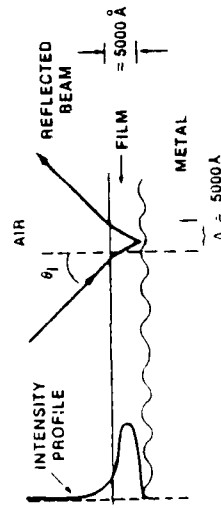
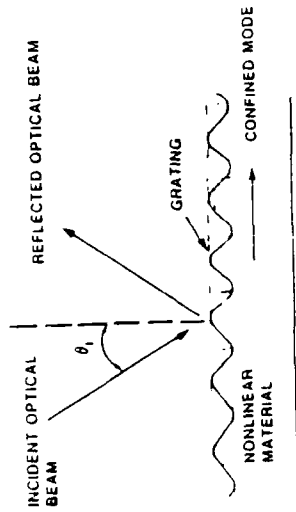
OD/mon. = 0.00837

B



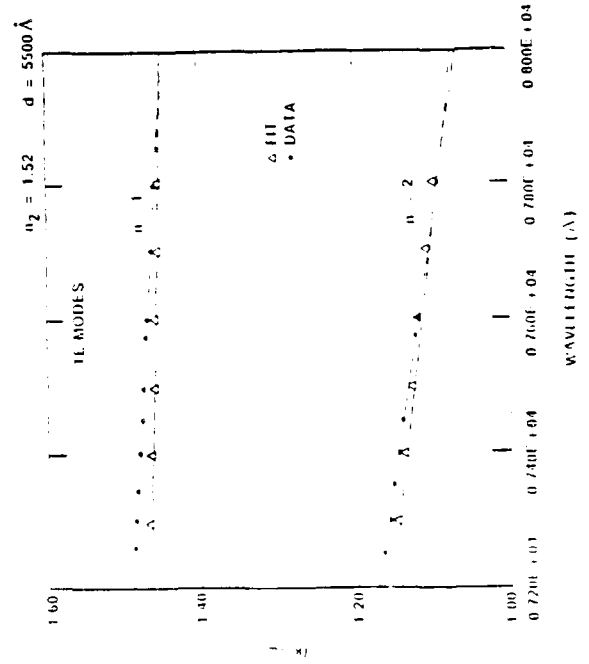
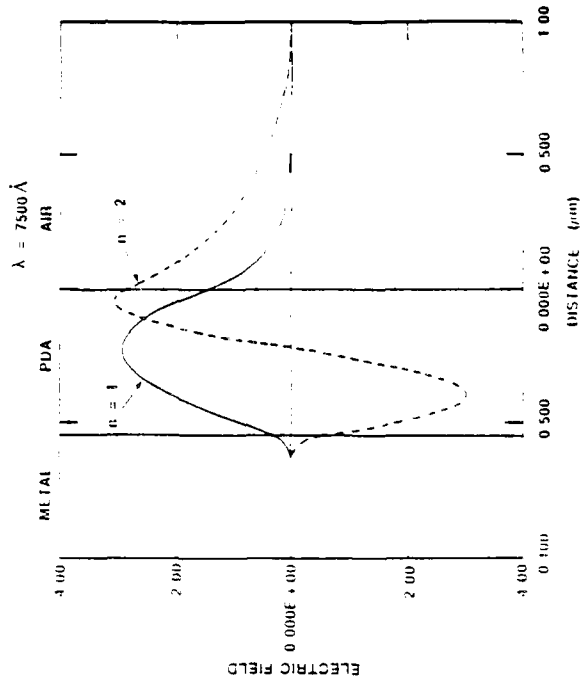
ARRANGING MONOLAYERS IN A PLANNED ORDER



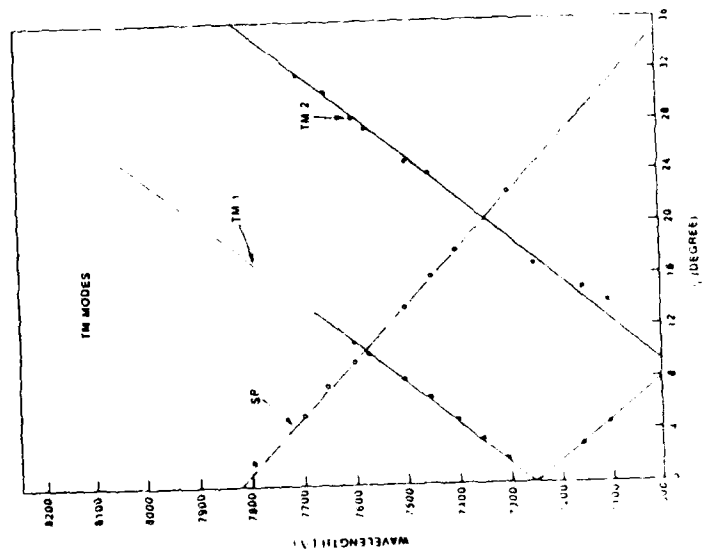
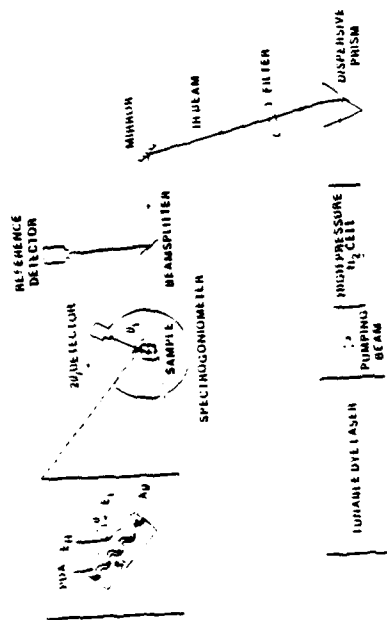
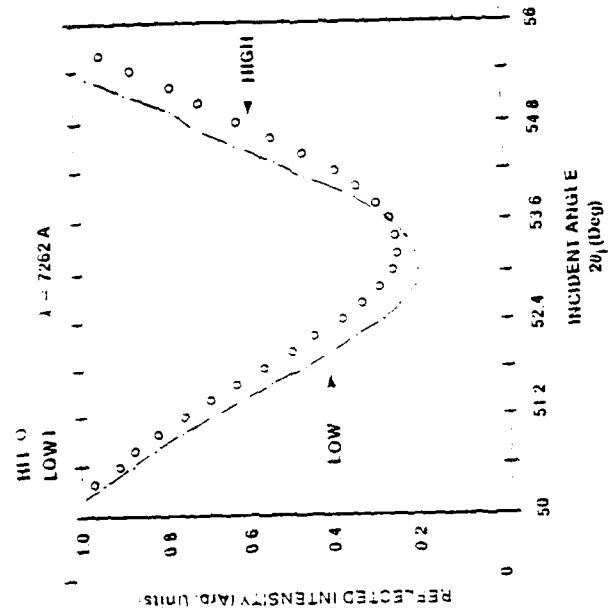
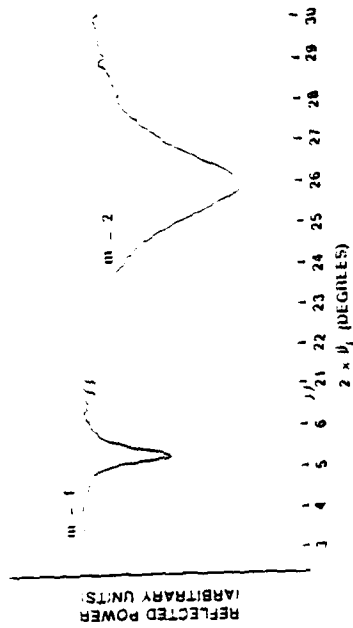


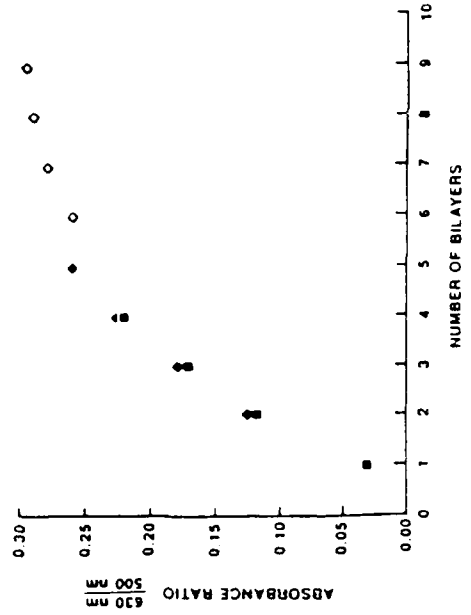
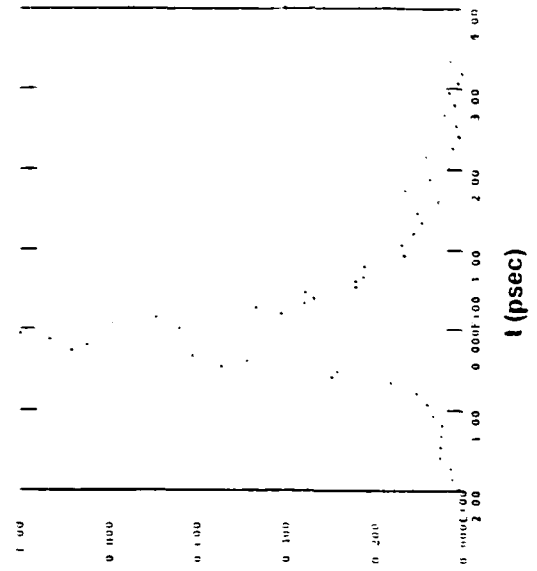
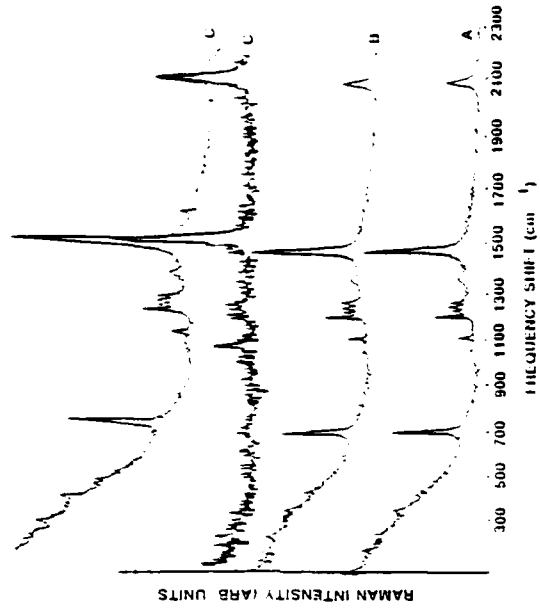
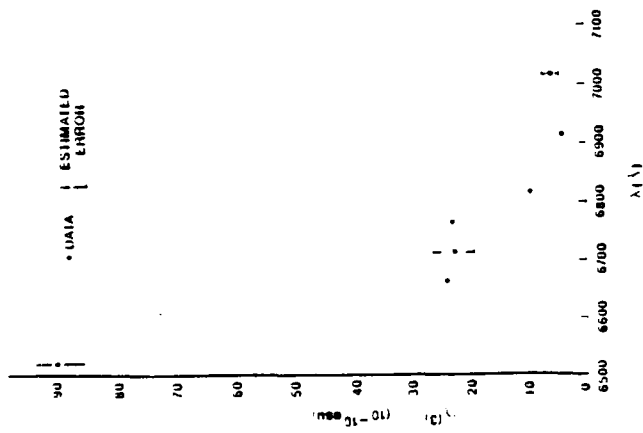
$$n_g = \lambda_0 / \lambda = \sin(\theta_{RES})$$

$$(n_g = k_0 / k_0)$$



N-6





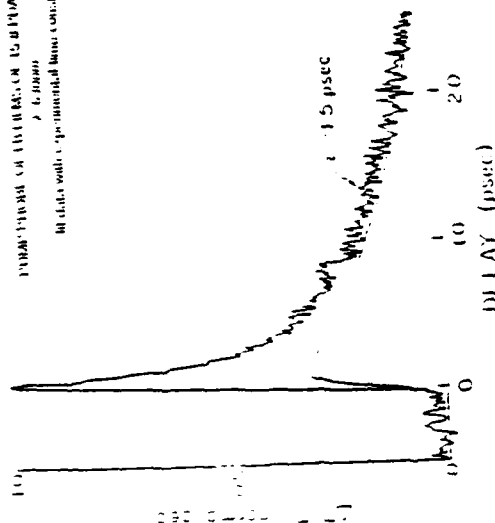
The diagram illustrates the experimental setup for measuring the photoacoustic effect. A continuum generation source (labeled 'continuum generation H') emits light through a series of mirrors and lenses. The light is focused onto a sample (labeled 'sample S'). The sample is a thin film on a substrate. The photoacoustic signal is measured by a microphone (labeled 'microphone'). The signal is then amplified by a 'lock-in amp.' and processed by a 'computer'. The computer is connected to a 'CPM' (Control Program Monitor) and a 'delay' unit. The 'delay' unit is connected to a 'chopper' and a 'copper vapor amplifier'. The 'chopper' is connected to the 'copper vapor amplifier' and the 'lock-in amp.'.

Figure 7.

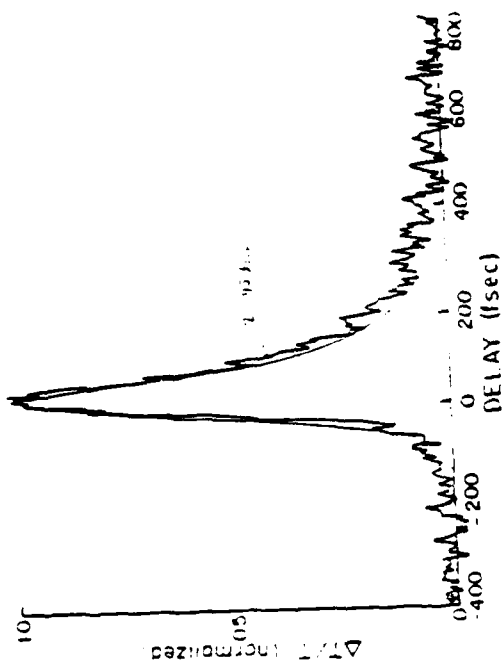
(continued)

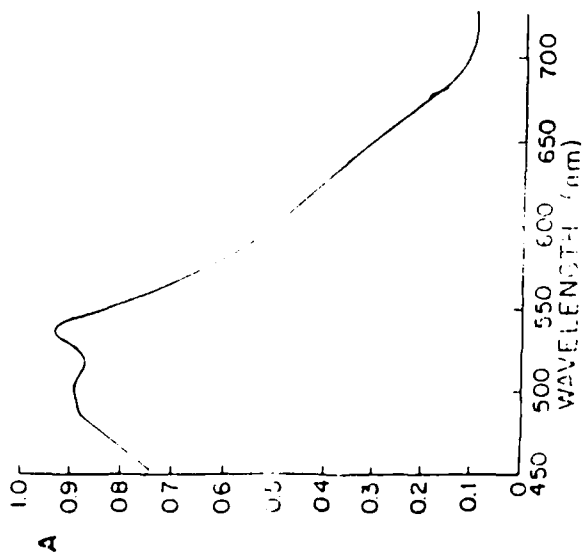
TABLE 9

Continued

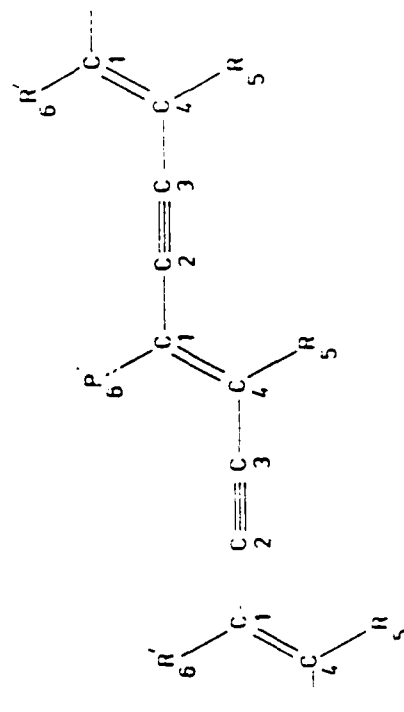


component of the data with long runs
concluded is submitted off





LINEAR ABSORPTION SPECTRUM OF LASER-INDUCED RED PHASE LB FILMS OF PDA 15-8



Structure of the polydiacetylene backbone. The numbers label the carbon atoms on the backbone and the single masses representing the side groups R and R' in the vibrational model

SCF ab initio Hartree-Rock

Semi empirical (EH)

VEH gives ab initio quality results

σ and π bonds treated equally

MINDO - Excellent geometry all electrons.

	ΔH_f	E_{tot}
PDA	498.6	-106275.8
PBT		-106158.7

Δ /rep. = 14.5 Kcals/Mole

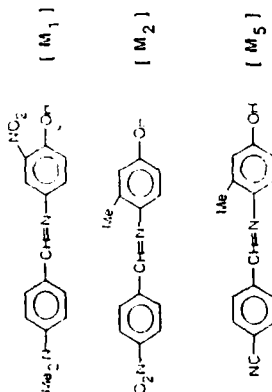
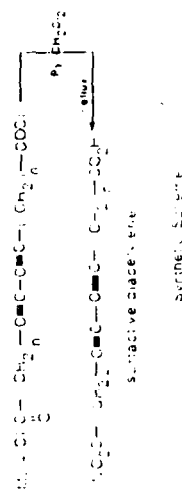
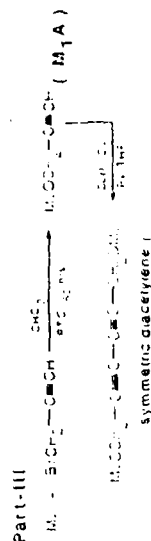
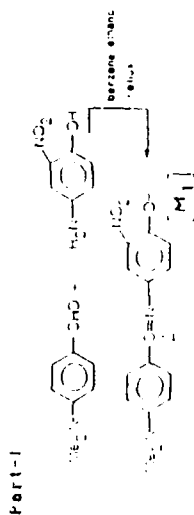
N-9

BANDGAP OF PDA AS A FUNCTION OF NONPLANARITY

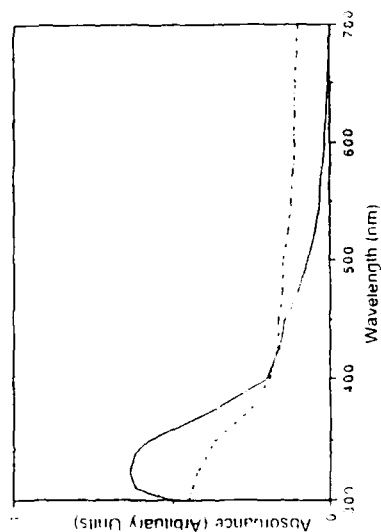
	0°	5°	10°	15°	20°
eV	2.596	2.550	2.585	2.612	2.721
cm^{-1}	20938	20631	20850	21070	21947
nm	478	485	480	475	456

EFFECT OF SUBSTITUENTS ON PDA ELECTRONIC STRUCTURE

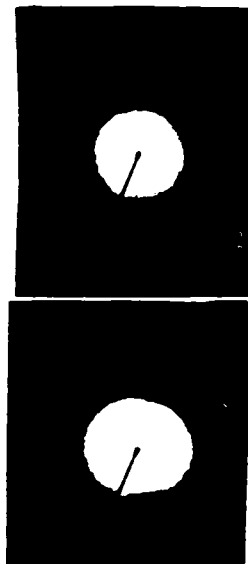
	BW	E_0	E_{ip}
PDA	3.972 (32043)	2.596 (20938)	5.338 (43056)
'2'-PDA	1.115 (8998)	1.769 (14266)	4.902 (39544)
$(CH_3)_2$ -PDA	3.265 (26337)	2.449 (19753)	5.039 (40642)



Molecular Structures of Some Representative Molecules



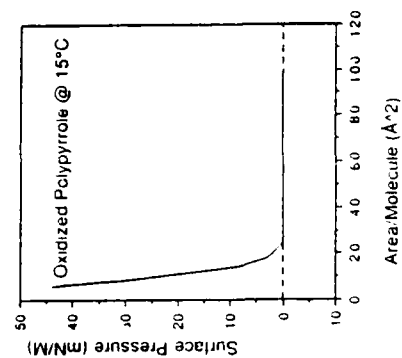
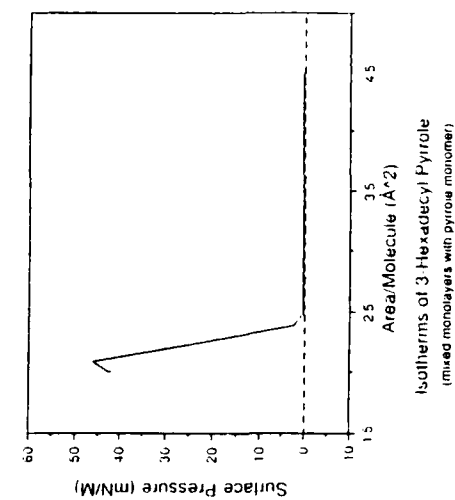
Visible Spectra of Partially Oxidized Polypyrrole in Solution

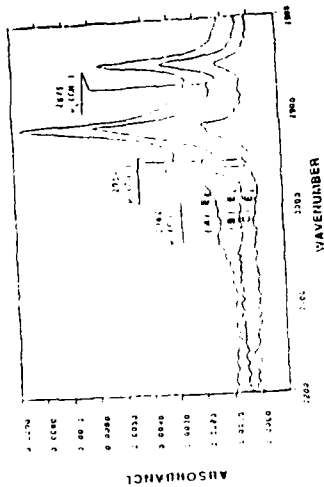
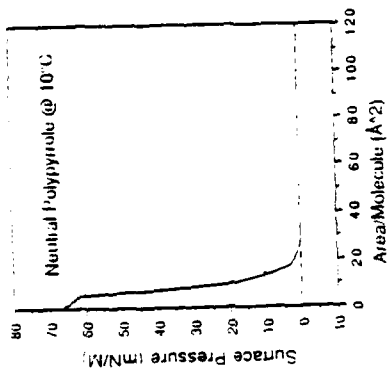
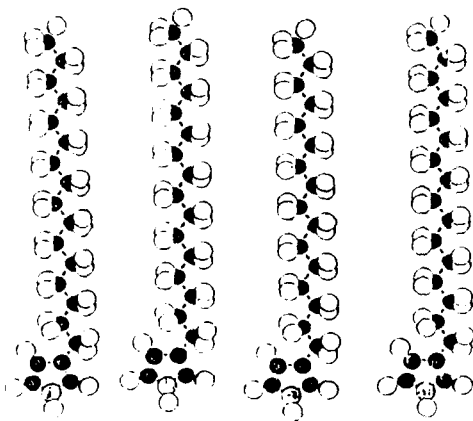


PYRROLE: HDP=500: 1 POLYPYRROLE

$d_1=2.58A$ $d_1=2.54A$
 $d_2=1.55A$ $d_2=1.55A$
 $d_3=1.33A$
 $d_4=1.01A$
 $d_5=0.90A$

N-11



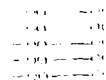
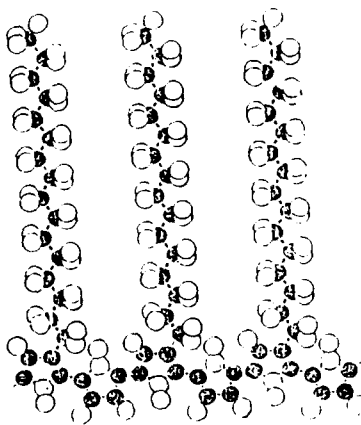


IR SPECTRA OF C₆H₁₂ PYRAOLE LB FILMS IN THE C-H STRETCHING REGION

- #### 4.1. TRANSMISSION OF 5 MONOLAYERS ON ZnSe

- # ANALYSIS OF MONOLAYERS ON PI

- (C) GIB OF 1 MICROLAYER ON PI



O-1

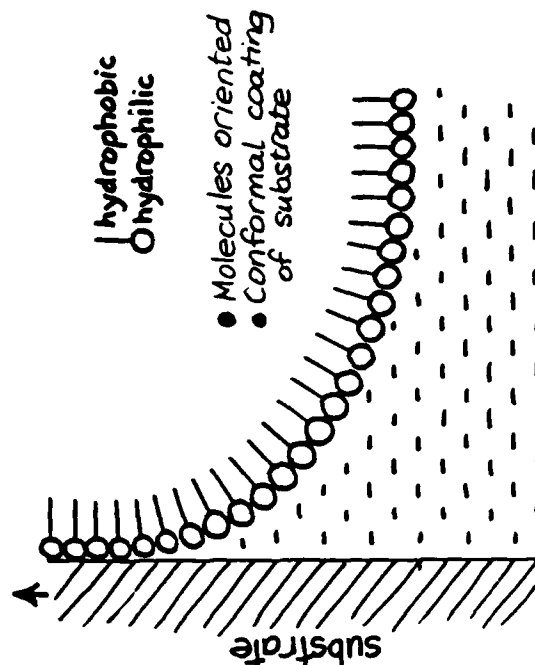
I. Peterson
GEC Research, Ltd., Great Britain

THE NONLINEAR OPTICS
OF
LANGMUIR-BLODGETT FILMS

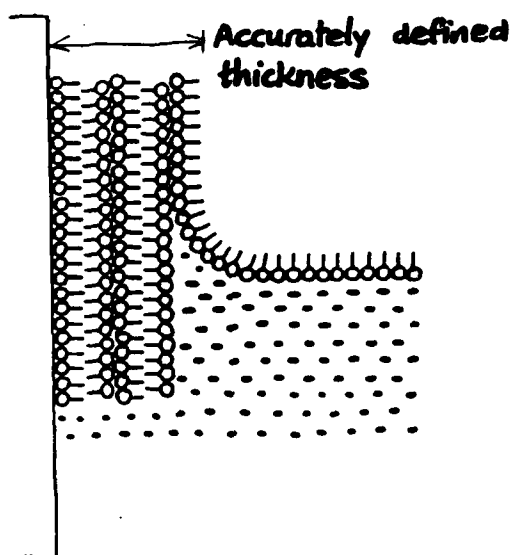
THE NONLINEAR OPTICS OF LANGMUIR-BLODGETT FILMS

Theoretical advantages:

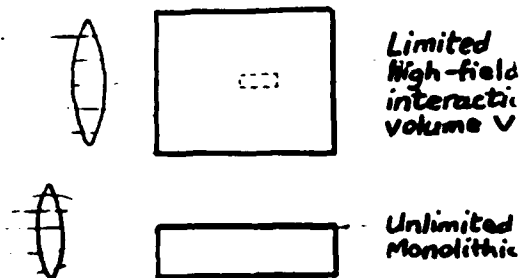
- Good geometry
- Chromophore alignment
- Dense packing



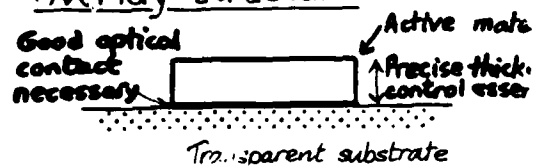
Building up thick films



Geometry



Overlay structure



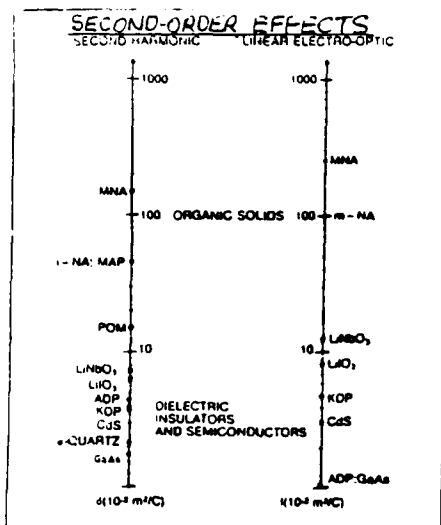


Fig 1 Comparison of nonlinear optical figures of merit for organic and inorganic solids. (d is measured at 1.05 μm ; r is the strain-free quantity measured at 0.633 μm , except for GaAs where it is measured at 0.9 μm)

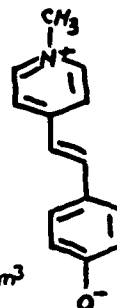
IF Garito & KD Singer
Laser Focus 80(1982)57

WHAT MOLECULE?



p-nitroaniline

$$\beta = 13 \times 10^{-50} \text{ CV}^{-2} \text{ m}^3$$



'Gedye'

merocyanine

$$\beta = 370 \times 10^{-50} \text{ CV}^{-2} \text{ m}^3$$

$$\frac{\beta}{\epsilon V}$$

$$65 \text{ pm/V}$$

$$1100 \text{ pm/V}$$

$$\text{cf. LiNbO}_3 \quad \chi_{\text{SHG}}^{(2)} = 10 \text{ pm/V}$$

Two-state Approximation

$$\beta = \frac{3e^3 \hbar^2}{2m} \frac{W_0}{(W_0^2 - 4W^2)(W_0^2 - W^2)} f \Delta\mu$$

W_0 State transition energy

W Photon energy $\hbar\omega$

f Oscillator strength

$\Delta\mu$ Dipole moment difference

The best materials have

- Long-wavelength absorption
- Strong absorption
- Charge transfer

Ian Girling } GEC
Graham Cross } Hirst
John Earls } Research

JOERS (LB nonlinear opt)

Durham Mike Petty
Lancaster Richard Tredgold
Hull George Gray
Plessey Jack Brettell
British Telecom
Roger Heckingbott

My new address.....

Institut für phys. Chemie
Universität Mainz FRG

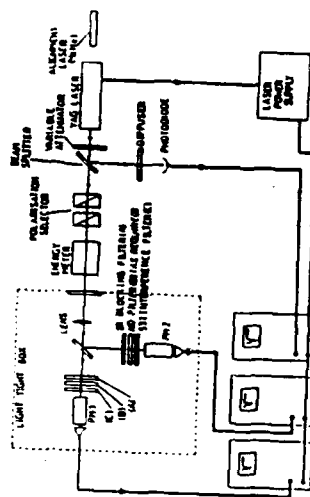
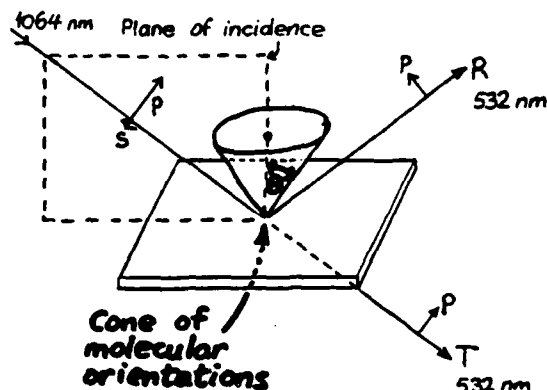


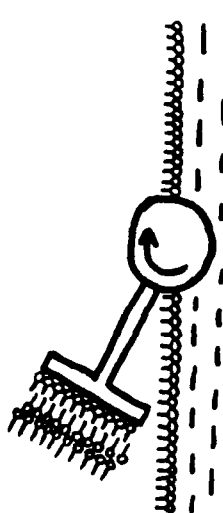
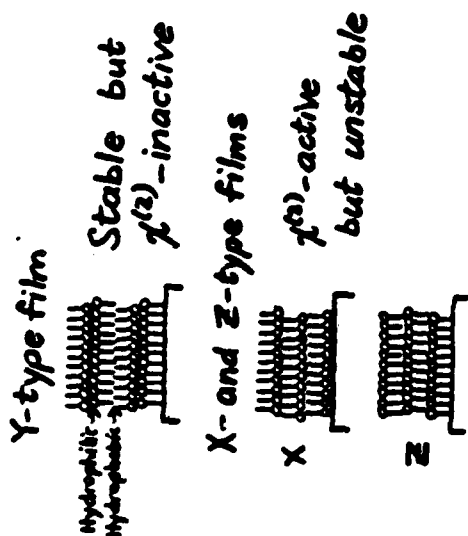
Fig. 1 Optical setup used for the SHG experiments

Second Harmonic Generation



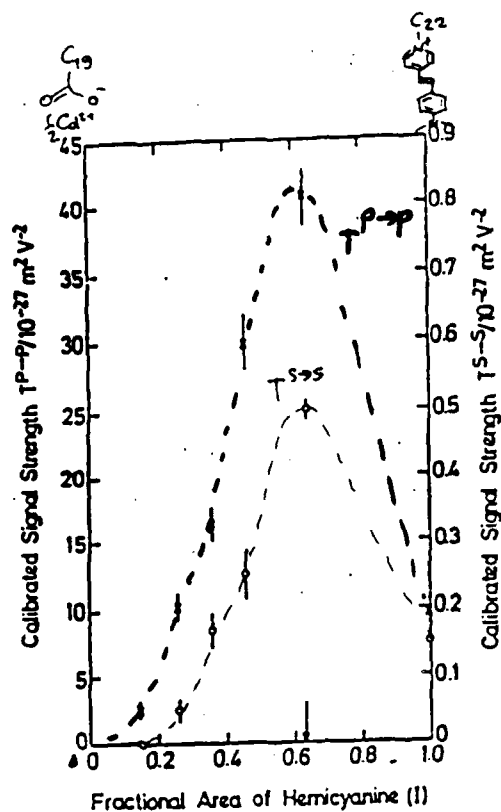
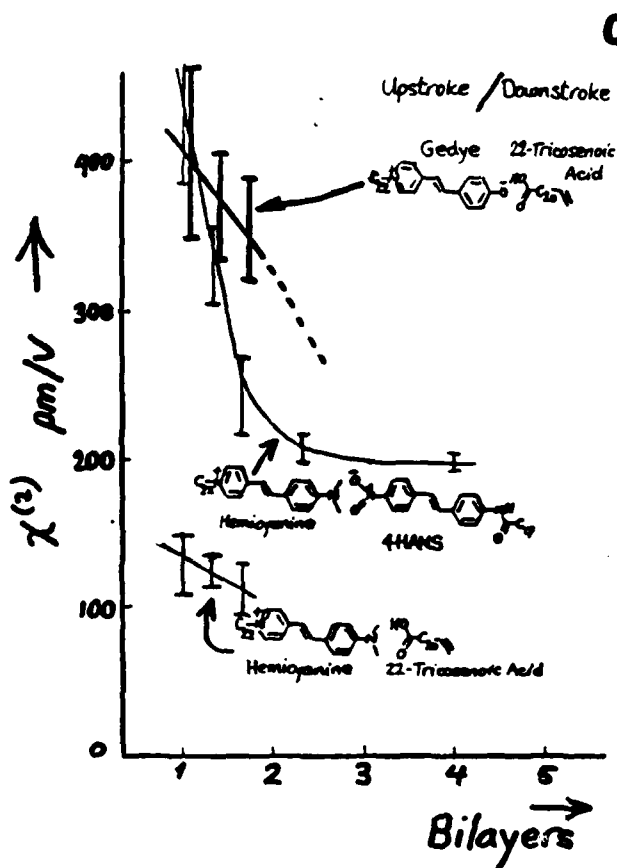
GEDYE MEROCYANINE MONOLAYERS

	$\chi^{(2)}$ (pm/v)	θ°
Low π	250	15
High π	1300	9



Deposition of $\chi^{(2)}$ -active

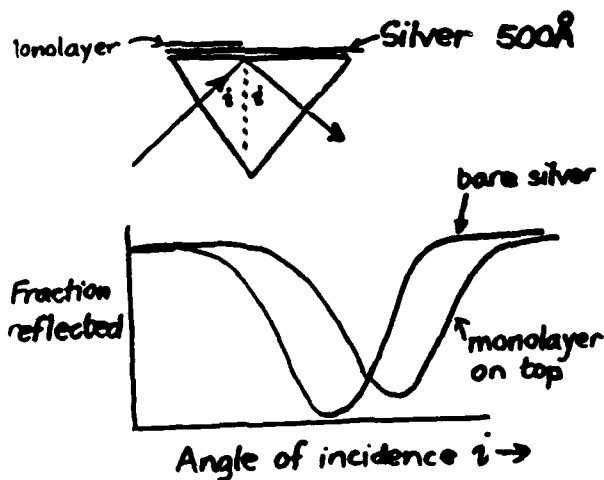
0-5

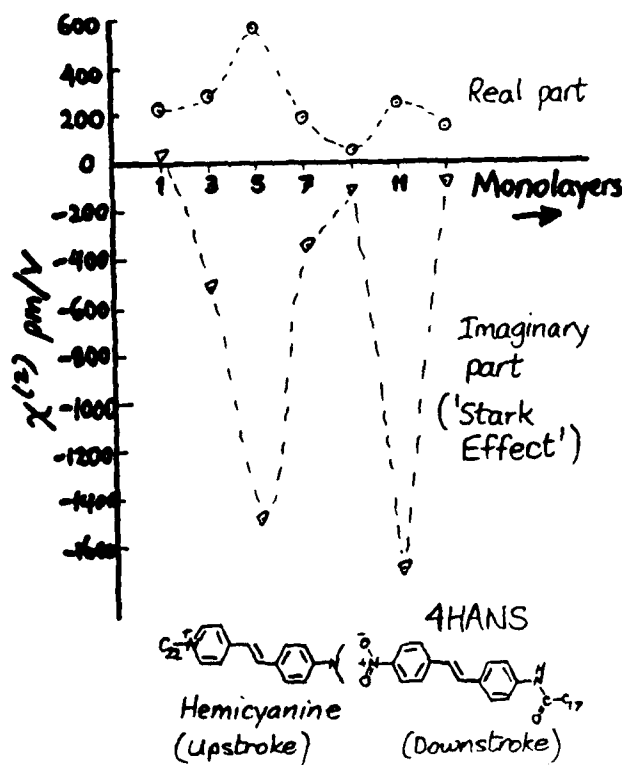
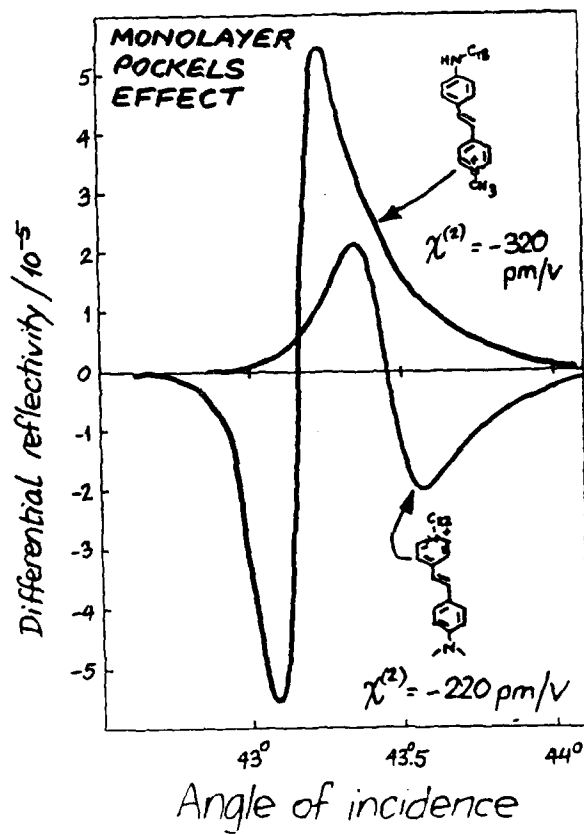
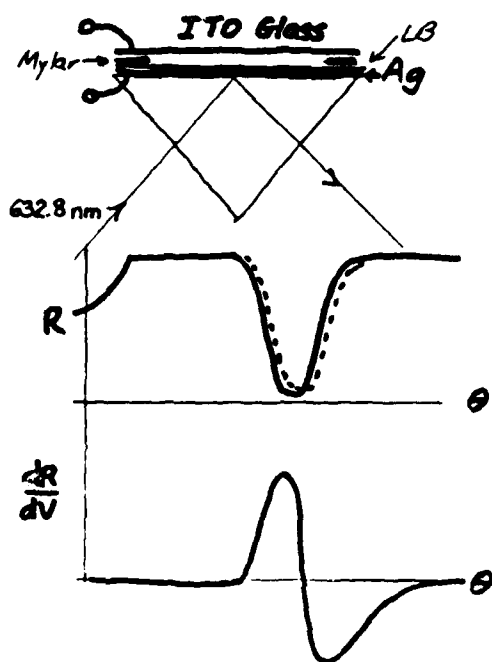


4 $T^{P+P}(x)$ and $T^{S+S}(o)$ second harmonic signal ($10^{-27} \text{ m}^2 \text{ V}^{-2}$) from mixed monolayer

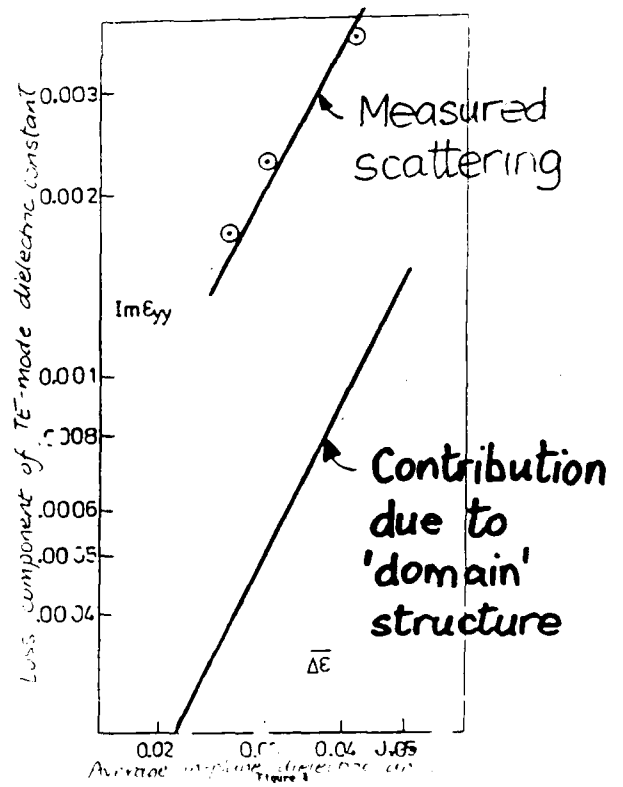
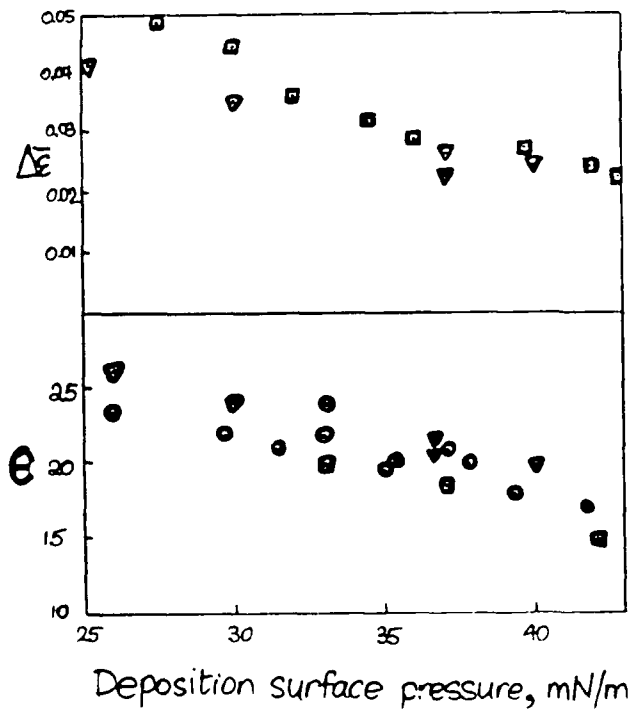
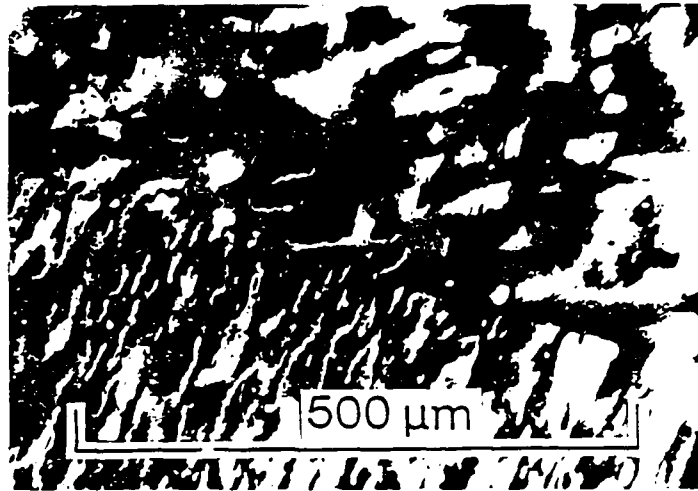
Measurement of refractive index

Surface plasmon Attenuated Total Reflection



Pockels-ATR Technique

0-7



P-1

R. S. Lytel
Lockheed Research and Development

ADVANCES
IN
ORGANIC ELECTRO-OPTIC DEVICES

R&DD
ORGANICS

LOCKHEED

ADVANCES IN ORGANIC ELECTRO-OPTIC DEVICES

MAY 19, 1988

R. LYTEL

Lockheed Research and Development Division
LOCKHEED MISSILES AND SPACE COMPANY INC.
3251 Hanover St. Palo Alto, California 94304

R&DD
ORGANICS
3/88

ACKNOWLEDGEMENTS

LOCKHEED

DARPA	U.S. ARMY	HOECHST CELANESE
J. NEFF	E. SHARP	J. STAMATOFF
	W. EISEN	D. DEMARTINO
AFOSR		U. YEH
D. BRUCH	U. PENN	
AFWAL/AFML	A. F. GARTO	U.S. MISS
P. JANI		A. GUNTER

R&DD
ORGANICS
3/88

THE LOCKHEED ORGANIC LOCKHEED DEVICES GROUP

SYNTHESIS	ANALYSIS	GRATINGS/FILTERS
S. ERMER	S. KWIATKOWSKI	M. STILLER
M. STILLER	G.F. LIPSCOMB	B. SULLIVAN
	R. LYTEL	
	D. SWANSON	
	A. TICKNOR	
CHARACTERIZATION	WAVEGUIDES	SPATIAL LIGHT MODULATORS
J. ALTMAN	G.F. LIPSCOMB	
K. ARON	R. LYTEL	D. ARMITAGE
P. ELIZONDO	M. STILLER	W. EADES
G. HANSEN	J. THACKARA	M. STILLER
G.F. LIPSCOMB	A. TICKNOR	J. THACKARA
R. STONE		

MAJOR BENEFITS OF NONLINEAR ORGANIC/POLYMERIC MATERIALS

* ORGANIC/POLYMERIC MATERIALS OFFER UNIQUE OPTICAL AND STRUCTURAL FEATURES FOR DEVICE APPLICATIONS

* MOLECULAR PROPERTIES CAN BE ENGINEERED TO ACHIEVE DESIRED MACROSCOPIC PROPERTIES

STRUCTURAL	OPTICAL
* MOLECULAR ENGINEERING	* LARGE, NONRESONANT RESPONSE
* THIN FILMS AND BULK CRYSTALS	* LOW DC DIELECTRIC CONSTANTS
* ROOM TEMPERATURE OPERATION	* FAST RESPONSE
* CHEMICAL/STRUCTURAL STABILITY	* HIGH OPTICAL DAMAGE THRESHOLD
* INTERNAL GRATINGS/STRUCTURE	* BROADBAND
* ARCHITECTURAL FLEXIBILITY	* LOW ABSORPTION

P-3

R&DD
ORGANICS
3/88

ORGANIC MATERIALS IN INTEGRATED OPTICS

LOCKHEED

- CURRENT TECHNOLOGY: FeLiNbO_3
 - Materials Dev. Began in 1960s
- $r = 32 \text{ pm/V}$
 - Larger Modulating Voltage
 - Little Improvement Expected
- LIMITED FABRICABILITY
 - 1000°C Processing
 - Depth Limited to 5 μm
 - Low Index Change Δn
 - Loss > 0.1 dB/cm
 - Optical Damage (Photorefractor)
- LARGE DIELECTRIC CONSTANT (28)
 - Longer Time Constants = RC
 - Large Velocity Mismatch in Traveling Wave Modulator
- MASS PRODUCTION DIFFICULT
 - * Saw Proc. Materials Research Society Boston, MA (12/87)
 - ** Current Lockheed/Hoechst Celanese Result
- PROPERTIES OF POLYMERIC ORGANIC E-O MATERIALS
 - Materials Dev. Began 1975
- $r = 14-53 \text{ pm/V}$ (poled films*)
 - Lower Modulating Voltage
 - Potentially Much Larger r
- FLEXIBLE FABRICATION
 - Low Temperature Processing
 - Flexible Dimensions
 - Controllable Index Change Δn
 - Loss < 0.8 dB/cm**
 - High Optical Damage Threshold
- LOW DIELECTRIC CONSTANT (4)
 - Shorter Time Constants = RC
 - Smaller Velocity Mismatch
- POTENTIAL FOR MASS PRODUCTION

R&DD
ORGANICS
3/88

ORGANIC MATERIALS IN OTHER DEVICES

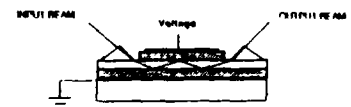
LOCKHEED

- | ELECTRO-OPTIC DEVICES | ALL-OPTICAL DEVICES |
|---|--|
| * SPATIAL LIGHT MODULATORS, TUNABLE FILTERS, SHUTTERS | * ETALON SWITCHES, ALL-OPTICAL FILTERS, NONLINEAR WAVEGUIDE DEVICES |
| * MATERIALS WITH LARGE r AND LOW DIELECTRIC CONSTANTS EXIST AND ARE AVAILABLE | * NONRESONANT NONLINEARITIES ARE STILL FAR TOO SMALL FOR MICRON-SIZED DEVICES. RESONANT MATERIALS REQUIRED |
| * FABRICATION UNDERWAY IN THIS PROJECT | * NONRESONANT MATERIALS NEARLY ADEQUATE FOR GUIDED WAVE DEVICES |

R&DD
ORGANICS
3/88

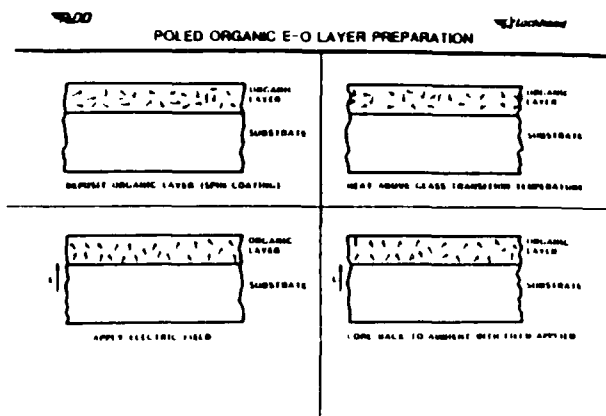
ORGANIC E-O THIN-FILM WAVEGUIDE MODULATORS

LOCKHEED



CONDUCTOR	BUFFER LAYERS	POLYMERS
COPPER ALUMINUM GOLD ITO	POLYSILOXANE RESIN UV CURABLE COATINGS SILICON DIOXIDE 2 COMPONENT EPOXY	MMA/PMMA PCSS C-22 MCC-1237 (new)

* TYPICAL LAYER THICKNESS OF OTHER 2 MICRONS
** LOSS ACCUMULATED PRIOR TO FINAL ASSEMBLY

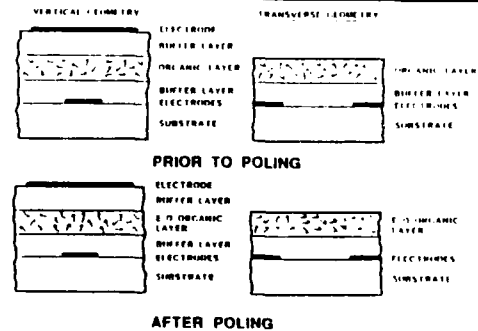


H&DU ORGANICS 3/88	POLED POLYMER FILMS AND SLAB WAVEGUIDE MODULATORS	LOCKHEED PC6S C-22
(wavelength = 0.83 μm)		
E-O COEFFICIENT (pm/V)	2.8	14.0
TM REFRACTIVE INDEX (POLED)	1.7	1.58
TM INDEX DIFFERENCE (POLED-UNPOLED)	0.06	0.005
WG LENGTH (cm)	1.8	2.5
MEASURED LOSS (dB/cm)	3.4	0.8
HALF-WAVE VOLTAGE (volts)	48	7

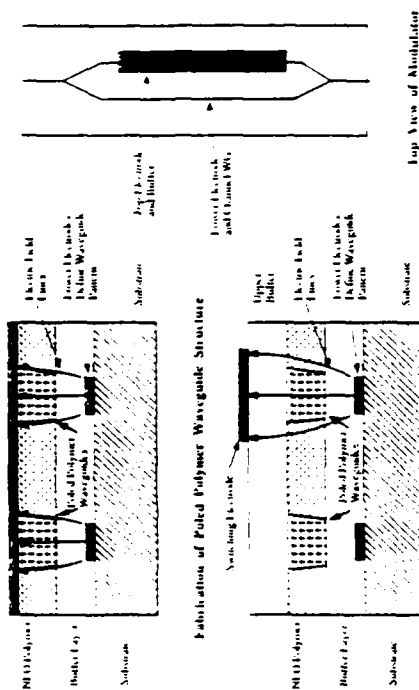
FABRICATION OF CHANNEL WAVEGUIDES BY SELECTIVE POLING

- * SINGLE POLARIZATION BURIED CHANNEL WAVEGUIDES CAN BE FABRICATED BY SELECTIVE ELECTRIC FIELD POLING IN THIN FILM POLYMERS USING VERTICAL OR TRANSVERSE ELECTRODES
- * POLING PRODUCES HIGHER INDEX, E-O CHANNELS BURIED IN SURROUNDING, UNPOLED, LOWER INDEX POLYMER
- * WAVEGUIDE PATTERN DEFINED BY PHOTOLITHOGRAPHY
- * RELATIVELY LOW TEMPERATURE PROCESSING, 100-200 C
- * FLEXIBLE DIMENSIONS IN HEIGHT AND WIDTH, 1-100 MICRONS
- * VARIABLE INDEX DIFFERENCE $\Delta n=0.001-0.05$
- * CAN MODE MATCH TO STANDARD SINGLE MODE FIBER
- * CONCEPT PROVED IN DEVICE STRUCTURES: MACH-ZEHNDER INTERFEROMETER, COUPLER, TRAVELING WAVE MODULATOR

VERTICAL AND TRANSVERSE POLING OF GLASSY POLYMER FILMS/WAVEGUIDES

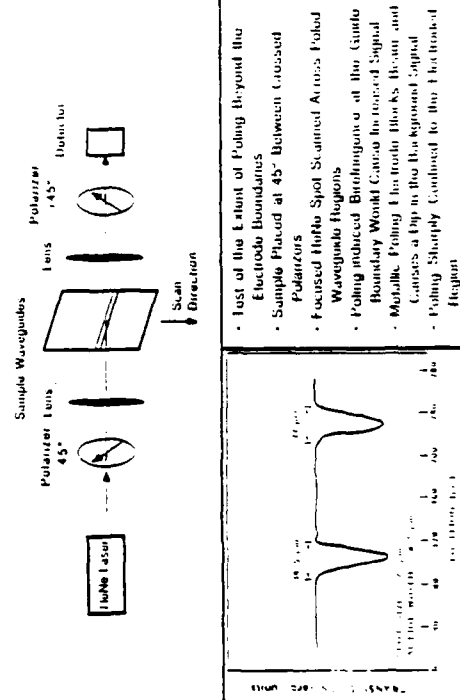


ORGANICS 3/88 INTEGRATED OPTIC MODULATOR FABRICATION

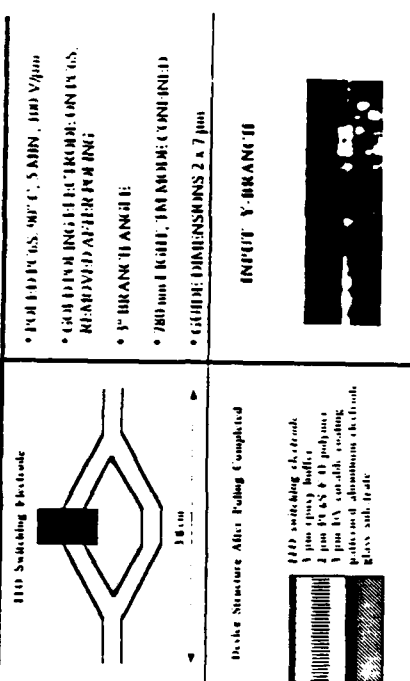


Optical Modulation By Electro-Optic Modulation

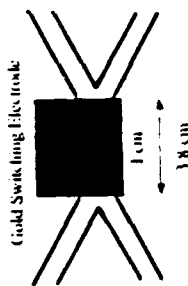
ORGANICS 3/88 CHANNEL BOUNDARY IN SELECTIVELY-POLED GUIDES



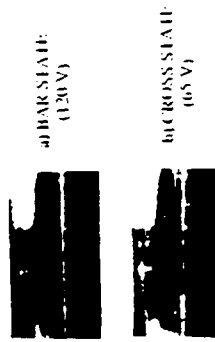
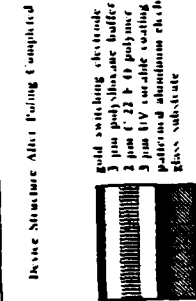
ORGANICS 3/88 FABRICATION AND OPERATION OF A SELECTIVELY-POLED M-Z INTERFEROMETER



STOCKHOLM



- POLY(4-C, 22, 105°C, 15 MIN., 90 V/μm)
- 3° COUPLING ANGLE
- 830 nm LIGHT, 1000000 COUNTS
- INSITU/OUT OF FOCUS 2 K / μm
- COUPLING GROUND: 2 K 1 μm



Q-1

B. K. Nayar

British Telecom Research Laboratories, U. K.

**ORGANIC NONLINEAR OPTICAL DEVICES
AND
MATERIAL CONSIDERATIONS**

ORGANIC NONLINEAR OPTICAL DEVICES
AND MATERIAL CONSIDERATIONS

B K NAYAR

British Telecom Research Laboratories
Martlesham Heath
Ipswich
Suffolk IP5 7RE
United Kingdom

ACKNOWLEDGEMENTS

BTRL

STRATHCLYDE UNIVERSITY

K I WHITE

J N SHERWOOD

R KASHYAP

F R CRUICKSHANK

G HOLDCROFT

S M G GUTHRIE

J RUSH

B J McARDLE

P DUNN

H MORRISON

Ipswich

E A SHEPHERD

Suffolk IP5 7RE

C S YOON

United Kingdom

Q.2



NON-LINEAR OPTICAL PROCESSES

OUTLINE

1. Review of device requirements for optical signal processing
2. Why organics?
3. Bulk devices
4. Guided wave devices
5. Crystal cored fibres
6. Material requirements dictated by the device design
7. Review of the present status

$$P_i = \epsilon_0 \left[\chi_{ij}^{(1)} E_j + \chi_{ijk}^{(2)} E_j E_k + \chi_{ijkl}^{(3)} E_j E_k E_l + \dots \right]$$

• $\chi_{ij}^{(1)}$

Linear susceptibility

• $\chi_{ijk}^{(2)}, \chi_{ijkl}^{(3)}, \dots$

Non-linear

susceptibilities

$\chi_{ijk}^{(2)} = 0$ in centrosymmetric media

NONLINEAR OPTICAL DEVICES FOR SIGNAL PROCESSING

- Amplitude/Phase Modulators
- Switching Matrices
- Bistable Elements
- Frequency Convertors
- Tunable Sources
- Amplifiers
- Real-time phase conjugators

WHY ORGANIC MATERIALS?

- Large optical nonlinearities
- Fast response times
- High optical damage thresholds
- Large birefringence
- Material optimisation using "Molecular Engineering"

Q.4



DISADVANTAGES OF ORGANIC MATERIALS

- Low melting points
- Mechanically weak
- Susceptible to chemical attack
- Complex transmission spectra
- Health hazards

MATERIAL SYSTEMS

SINGLE CRYSTAL

- Bulk
- Thin film
- planar
- overlays
- Confined growth
- channels
- fibres

POLYMER FILMS

- LC polymers
- Guest-host polymers
- LB films

Q:5

BULK ORGANIC DEVICES

BULK MBA-NP CRYSTAL GROWTH

- Material Purification
 - column chromatography
 - successive recrystallisations
- Selection of perfect seeds
 - X-ray topography
- Solution growth by temperature lowering of a seeded saturated methanol solution

DEVICE TYPE	MATERIALS
SHG	DAN, mNA, MBA-NP, MAP, NPP, POM, Urea
SFG	Urea
OPA	POM, NPP
OPE	POM
OPO	Urea

2.6

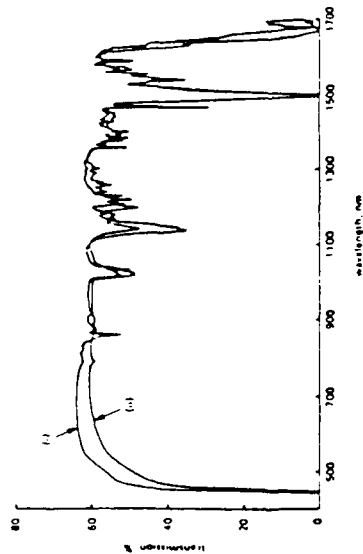


© British Telecommunications plc

© British Telecommunications plc

MBA-NP CRYSTAL TRANSMISSION SPECTRA

Crystal Cut: (001); Propagation: [001]
Input Polarisation: (i) [100] and (ii) [010]



© British Telecommunications plc



MBA-NP SHG RESULTS

- Large single crystal growth

— $5 \times 3 \times 3 \text{ cm}^3$

- Type I Phase-Matched SHG

— $d_{\text{eff}} = 3.4 \times 10^{-12} \text{ m/V}$

- $d_{22} = 25 \times 10^{-12} \text{ m/V}$

Q-7

© British Telecommunications plc



ADVANTAGES OF GUIDED WAVE NONLINEAR INTERACTIONS

- Semiconductor laser powers adequate
- Long interaction lengths
- Phase-matching using modal dispersion
- Ease of coupling to optical fibres

ACTIVE WAVEGUIDE TYPES

• PLANAR

- Two-dimensional eg slab
- Three-dimensional eg channel

• FIBRE

- Polished/D-shaped fibres with overlays
- Crystal cored fibres
- Doped fibres

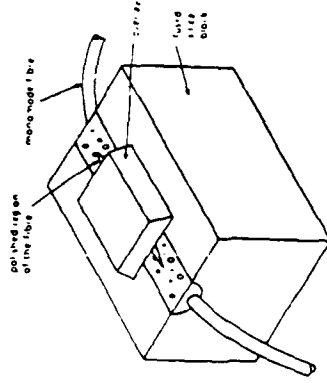
Q. 8



ACTIVE WAVEGUIDE DEVICE TYPES

- Waveguide
- Directional Coupler
- Waveguide Interferometers
 - Mach-Zehnder, Ring Resonator etc
- Waveguide Fabry-Perot

POLISHED / D-SHAPED FIBRES WITH NONLINEAR OVERLAYS



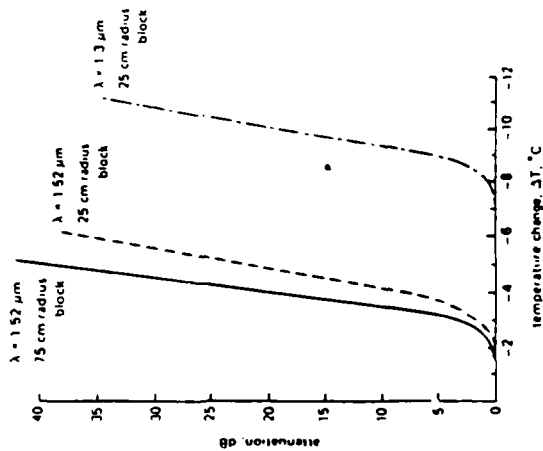
Q.9

- Evanescent mode field interacts with the Nonlinear Overlay eg

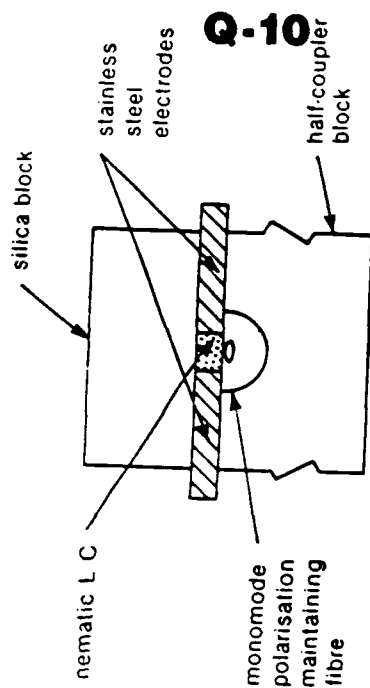
— Change in the overlay index can be used to modulate Amplitude or Phase of the fibre mode

ATTENUATION OF A POLISHED FIBRE WITH A REDUCTION IN THE OIL OVERLAY TEMPERATURE ie INCREASE IN INDEX

$$\frac{dnD}{dT} = -3.7 \times 10^{-4} \text{ } ^\circ\text{C}$$



SCHEMATIC OF A FIBRE E-O MODULATOR WITH A NEMATIC LC OVERLAY



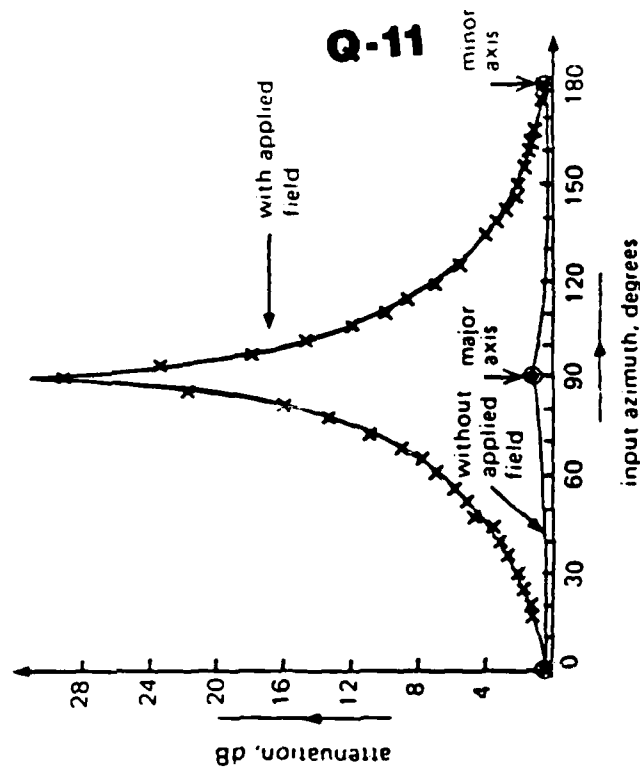
CHARACTERISTICS OF A FIBRE E-O AMPLITUDE MODULATOR WITH A NEMATIC LIQUID CRYSTAL OVERLAY

• Insertion Loss

— Horz Pol: 1.2dB and Vert Pol: 0.5dB

- Modulation Depth (Vert Pol): >30dB
- Switching Voltage: 5V
- Switching Field Strength: 0.2V/ μ m
- Response Times: $\tau_r = 2.5$ ms and $\tau_f = 160$ ms

EXTINCTION RATIO OF A LC FIBRE MODULATOR WITH INPUT AZIMUTH ANGLE

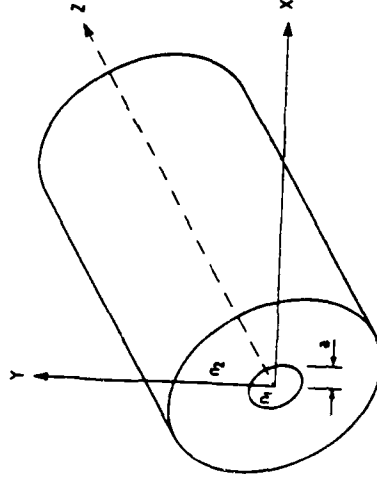


WHY CRYSTAL CORED FIBRES?

- Peak intensity in the core
- Good geometrical uniformity
- Large choice of cladding glasses
- Encapsulation of crystal core
- In-line fibre device

CRYSTAL CORED FIBRES

- Cylindrical waveguiding structure



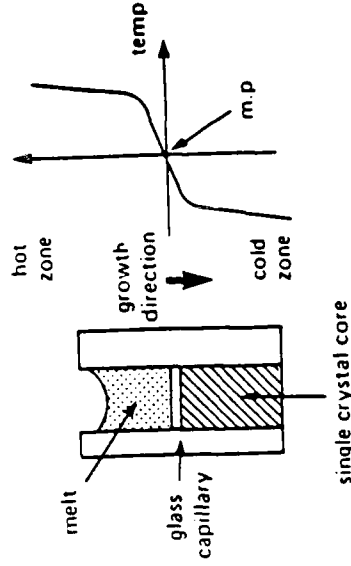
Q-12

- For optical guidance $n_1 > n_2$
- Applications: Three-wave and Four-wave mixing processes

FABRICATION PROCESS

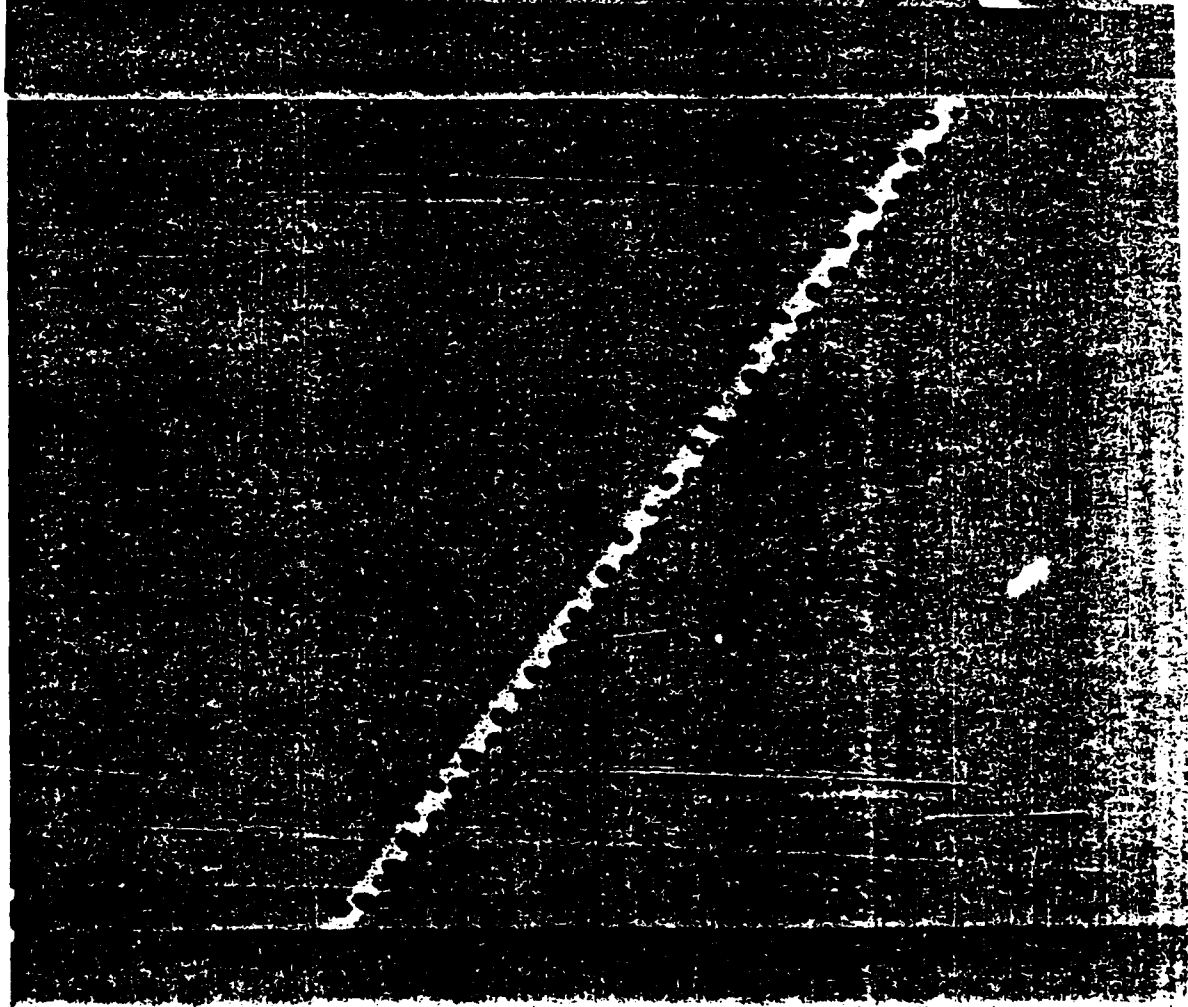
- Selection of suitable cladding glass
 — $\Delta n = n_c - n_{cl} < 0.05$
- Drawing of small bore capillaries
 — Bore diameter = 2 to 10 μm
- Capillaries filled with the crystal melt
- Growth of single orientated crystal

CRYSTAL CORED FIBRE FABRICATION

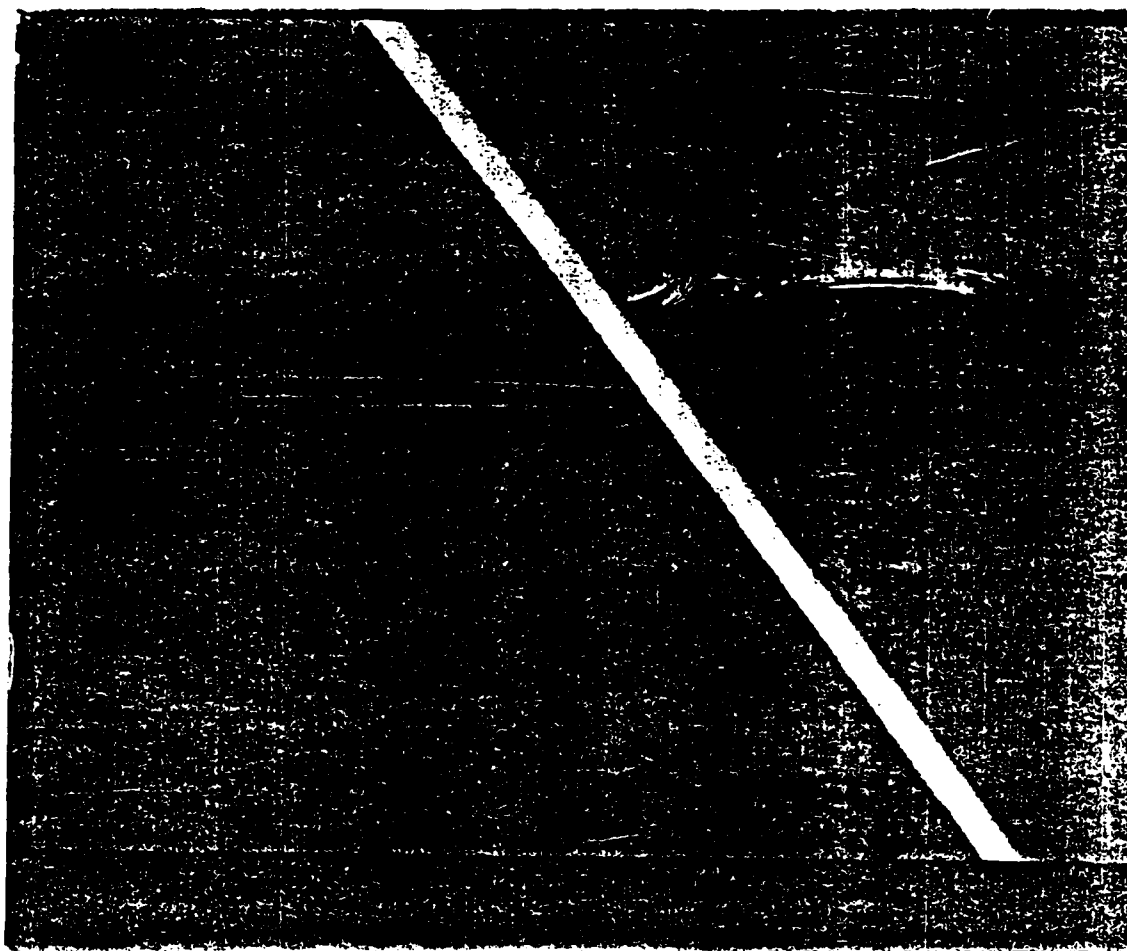


Q-13

Defects in CCFs



SINGLE CRYSTAL CORE



**FACTORS INFLUENCING DEFECT FREE
CRYSTAL GROWTH**

- Material Purity
- Adsorbed Oxygen
- Bubbles
- Temperature Gradient
- Growth Rate
- Vibration

**MATERIAL REQUIREMENTS FOR
GROWTH IN GLASS CAPILLARIES**

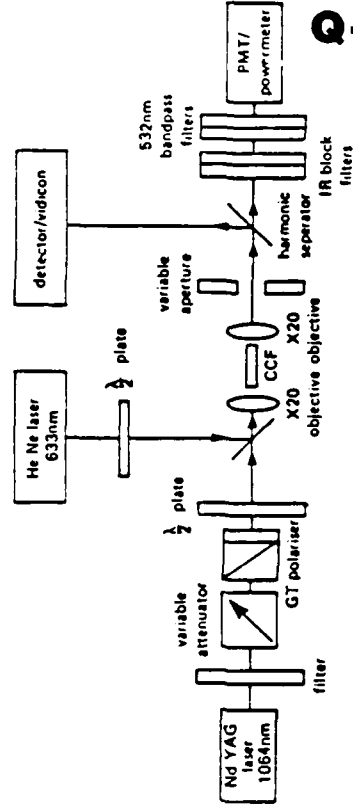
- Chemical stability
- Low melting point
- Optically transparent
- Refractive index < 2.0
- Non-centrosymmetric crystal
- Large transverse nonlinear coefficient

Q-15

ASSESSMENT OF CCF₈

- Polarising Microscope
 - Crossed Polars
 - * Uniformity of orientation, defects/voids
 - Parallel Polars
 - * Defects/Voids
- X-ray Diffraction
 - * Crystal Orientation
- Optical Transmission

EXPERIMENTAL SET-UP FOR OPTICAL CHARACTERISATION OF CCF₈

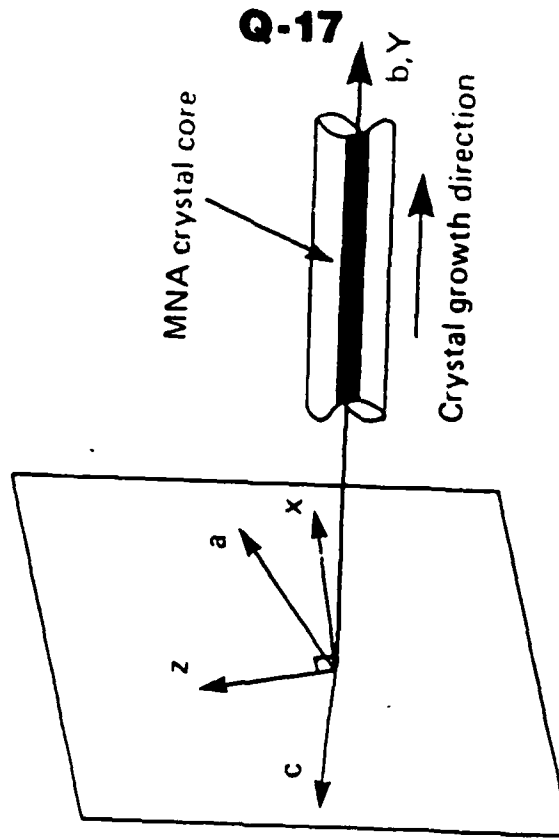


Q-16

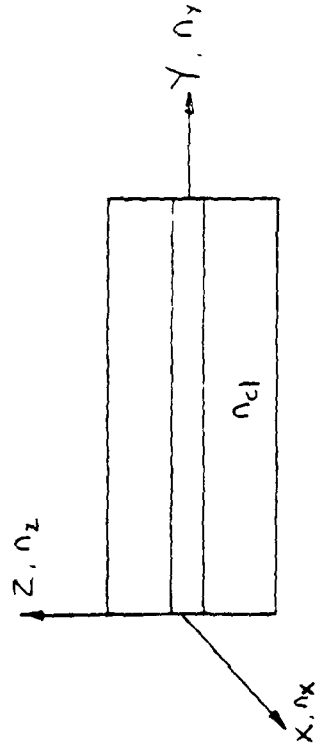
SUMMARY OF SHG EXPERIMENTS IN CCF₈

Reference	Core
Nayar (1982&1983)	benzil
Vidakovic et al (1984)	NPP
Umegaki et al (1985)	MNA
Umegaki et al (1986)	MNA
Tomaru et al (1986)	DAN
Holdcroft et al (1987)	MNA
Nayar et al (1987)	acetamide, MNA
Vidakovic et al (1987)	NPAN
Holdcroft et al (1988)	DAN
Kerkoc et al (1988)	DAN

MNA CRYSTAL ORIENTATION IN CCF₈



MNA CORED SILICA FIBRE POLARISER



- Refractive Indices of MNA:
 $n_x (633\text{nm}) = 1.8$ and $n_z (589\text{nm}) = 1.453$

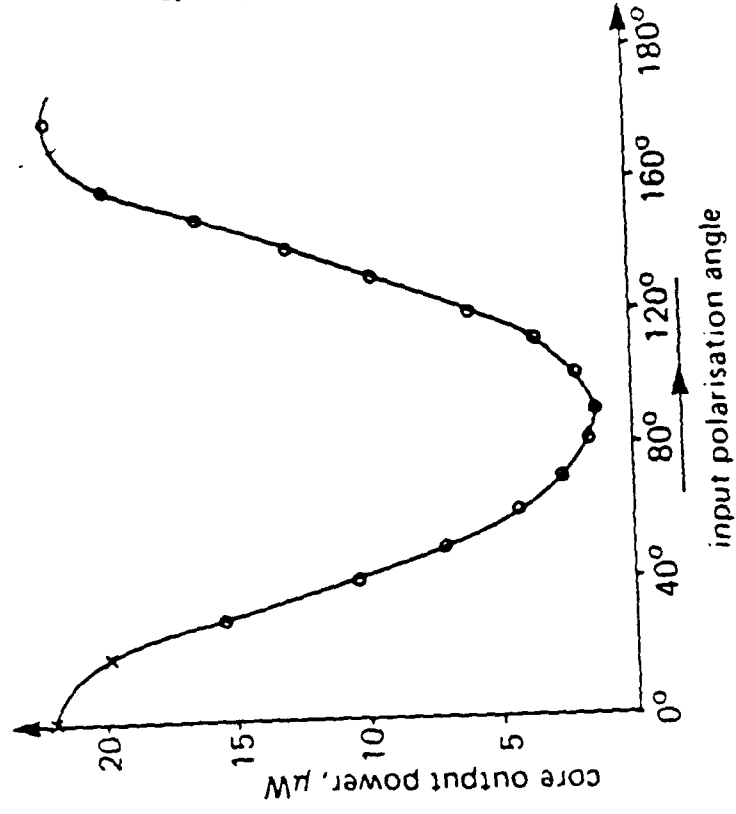
- Silica Cladding, $n_{cl} (589\text{nm}) = 1.458$

- Hence transmission of only x-polarised light

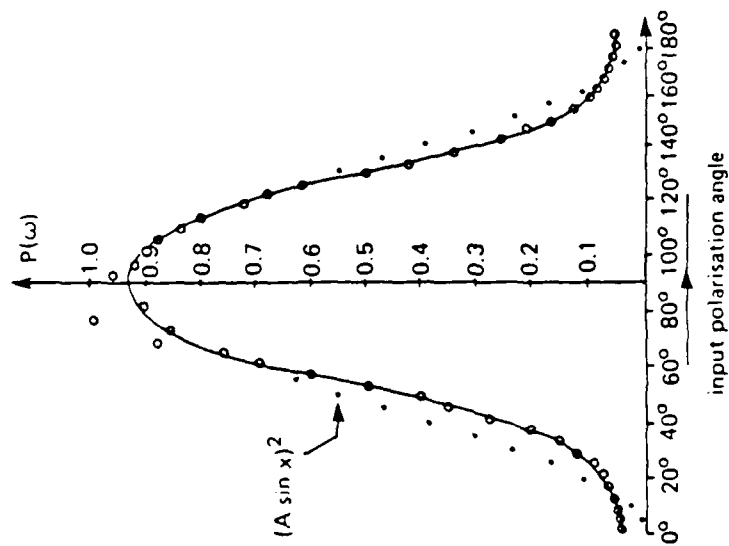


POLARISATION TRANSMISSION CHARACTERISTIC OF A MNA CORED SILICA FIBRE

Wavelength: 633nm; Extinction Ratio: 12.8dB



SH POWER CHARACTERISTIC OF A MNA CCF AS A FUNCTION OF INPUT POLARISATION



CCF INSERTION LOSSES

CRYSTAL CORE	LOSS, dB/cm
acetamide	1.1
benzil	<2.0
DAN	10
MNA	20
NPP	High

SUMMARY OF CCF SHG RESULTS

$\lambda_f = 1064\text{nm}$; Length = 10-15mm; Core dia. = 6-10 μm

Average $P_f = 10\text{mW}$; Peak $P_f = 50\text{W}$

Material	Transmission, %	Efficiency, %
Acetamide	5	$0.25\text{-}1 \times 10^{-6}$
DAN	0.5	2×10^{-3}
MNA	0.2-0.6	$0.2\text{-}4 \times 10^{-5}$

LATEST BTRL SHG RESULTS

FOR DAN IN SILICA CCFs

$\lambda_f = 1064\text{nm}$; P_f (avg) = 1mW; P_f (peak) = 10W

Pulse Width = 200ns; Rep Rate = 500Hz

Fibre length = 10-15mm; Core dia = 6 μm

Q-20

Publication	Throughput, %	Efficiency, %
CLEO'88	5-15	1-1.5

Ref: G E Holdcroft et al, paper WM55



PRESENT STATUS OF SHG IN CCFs

- Typical conversion efficiencies $< 0.1\%$

DUE TO

- Unsuitable crystal orientation

- Low transmission

— Poor crystal end quality

— Voids and defects

- Un-optimised waveguide design

— Lack of data on optical properties

DEVICE DESIGN REQUIREMENTS

- Bulk refractive indices
- Effective mode refractive indices
- Uniformity of guiding region dimensions and index difference

Q-21

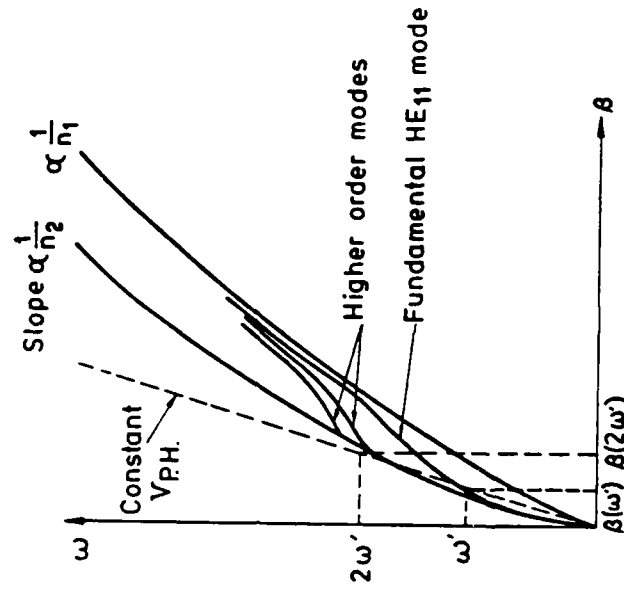
- Low waveguide attenuation

- Optical damage and intensity dependent index change

PHASE-MATCHING IN WAVEGUIDES

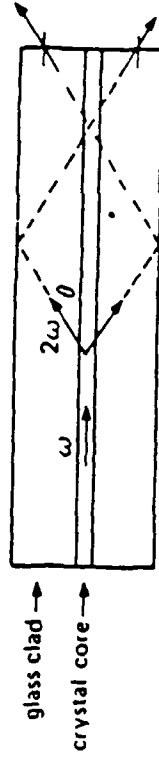
- Different mode orders
 - same or orthogonal polarisations
- Same order mode (orthogonal polarisations)
 - birefringent core material
 - elliptical core shape
- Hence require cladding glass of appropriate index and dispersion

PHASE-MATCHING FOR RADIATION SHIF



Q.22

RADIATION SHG IN CCFs

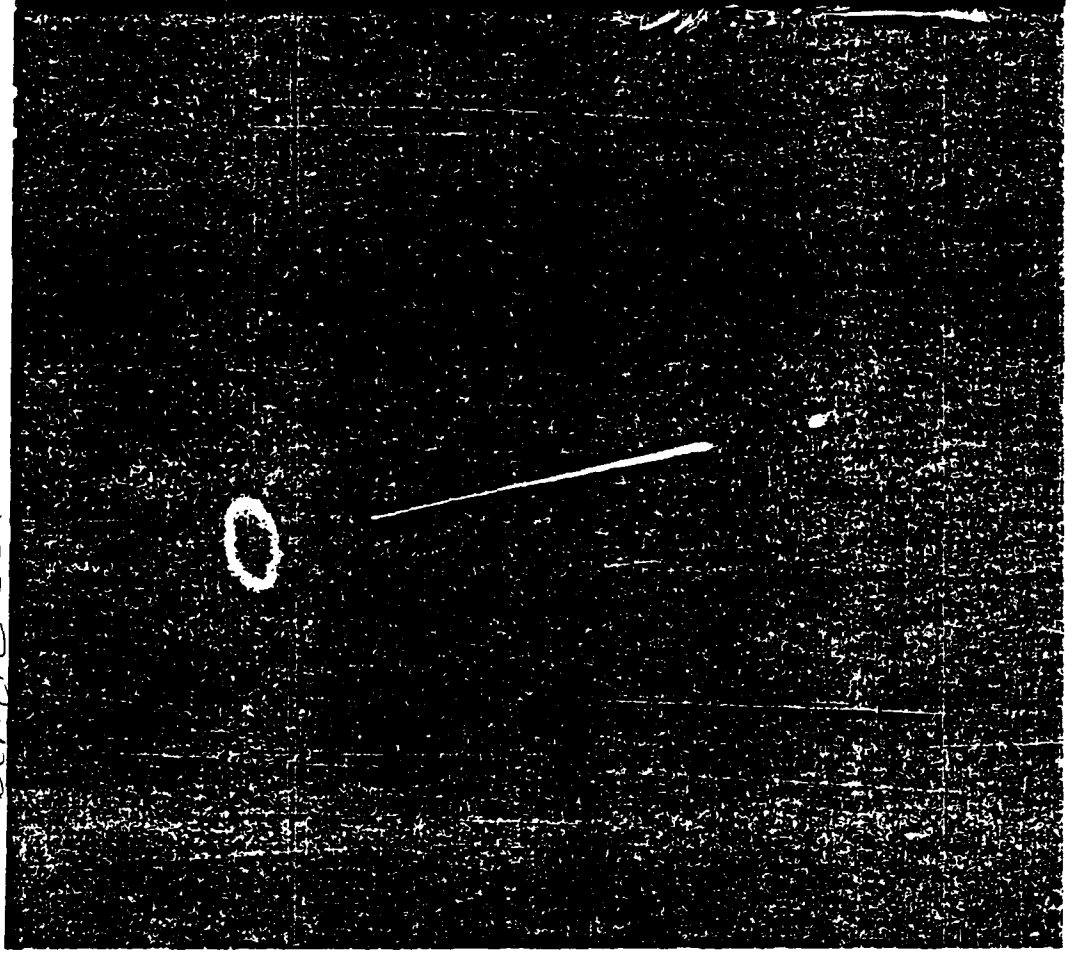


$$\cos\theta = \frac{n_e^{(\omega)}}{n_o^{(2\omega)}}$$

$$\delta n = n_o^{2\omega} - n_e^{2\omega} \geq [n_e^{\omega} - n_o^{\omega}]$$

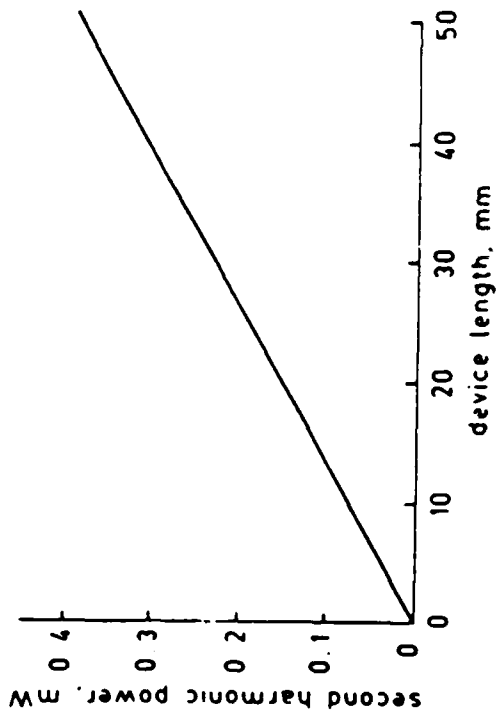
- Advantage: Relaxed phase-matching constraints on guide dimensions and dispersion
- Disadvantage: Efficiency \propto Fibre length

RADIATION FILED SHS IN A
BENZIL CCF



EFFICIENCY OF RADIATION SHG

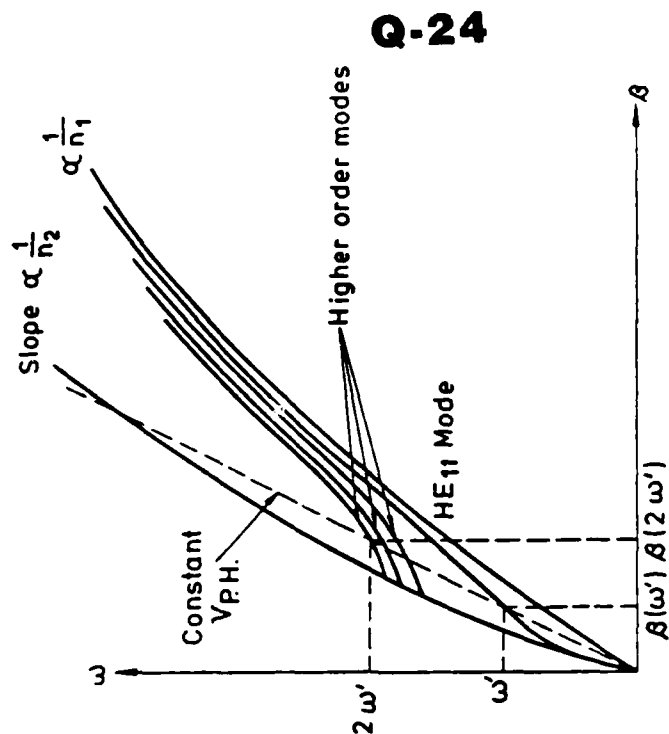
$P_f = 10\text{mW}$; $\lambda_f = 1.5\mu\text{m}$; $d = 250\text{pm/V}$; $n = 1.65$



© British Telecommunications plc



PHASE-MATCHING FOR GUIDED WAVE SHG



Q-24

© British Telecommunications plc



PHASE-MATCHED SHG IN WAVEGUIDES

• PUMP DEPLETION

$$\eta = \tanh^2 \left[\kappa \sqrt{P_m^{(\omega)} L} \right]$$

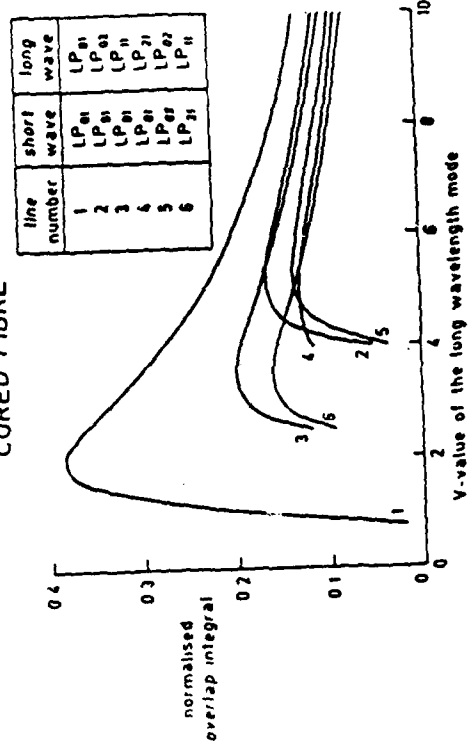
where

$$\kappa = \frac{\omega}{2} \epsilon_0 d_{im} \int_{-\infty}^{\infty} \int_{-\infty}^{\infty} E^{(\omega)} E^{(\omega)} \cdot E^{(2\omega)} dx dy$$

- For efficient SHG require optimisation of the "overlap integral".

- Hence waveguide design

NORMALISED FIELD OVERLAP INTEGRAL IN A CRYSTAL
CORED FIBRE

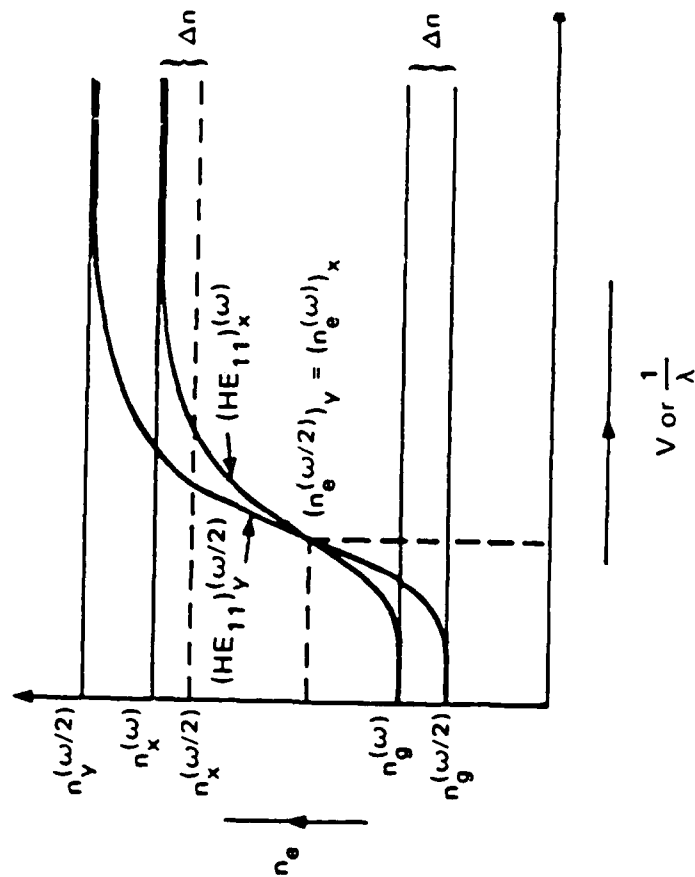


Q-25

© British Telecommunications plc

© British Telecommunications plc

SH PHASE-MATCHING BETWEEN THE LOWEST ORDER ORTHOGONAL MODES



SH POLARISATION

$$\begin{bmatrix} P_x \\ P_y \\ P_z \end{bmatrix} = \epsilon_0 \begin{bmatrix} d_{11} & d_{12} & d_{13} & d_{14} & d_{15} & d_{16} \\ d_{21} & d_{22} & d_{23} & d_{24} & d_{25} & d_{26} \\ d_{31} & d_{32} & d_{33} & d_{34} & d_{35} & d_{36} \end{bmatrix} \begin{bmatrix} E_x^2 \\ E_y^2 \\ E_z^2 \\ 2E_y E_z \\ 2E_z E_x \\ 2E_x E_y \end{bmatrix}$$

Q-26

USEFUL CRYSTAL CLASSES FOR PM-SHG
BETWEEN LOWEST ORDER ORTHOGONAL MODES

CRYSTAL SYSTEM	CLASS	COMMENTS
Triclinic	1	Any orientation
Monoclinic	m, 2	Specific orientation & index requirements
Orthorhombic	mm2	As above
Tetragonal	4, 4	z-axis transverse & -ve uniaxial
Trigonal	3, 3m	As above
Hexagonal	6, 6mm	As above

GUIDED WAVE SHG IN A SUITABLY
ORIENTATED mNA CCF

- Require: Y-axis parallel to the fibre axis

Wavelength, nm	Refractive Index
532	$n_z = 1.7006$
1064	$n_z = 1.6320$
1064	$n_x = 1.7196$

- PM between lowest order orthogonal modes with

$$n_g = 1.66 \text{ and } \Delta n_g = 0.0245$$

Calculated 10% SHG efficiency with

$$P_{in} = 1mW; L = 25mm; \text{Core dia} = 1.1\mu m$$

Q-27

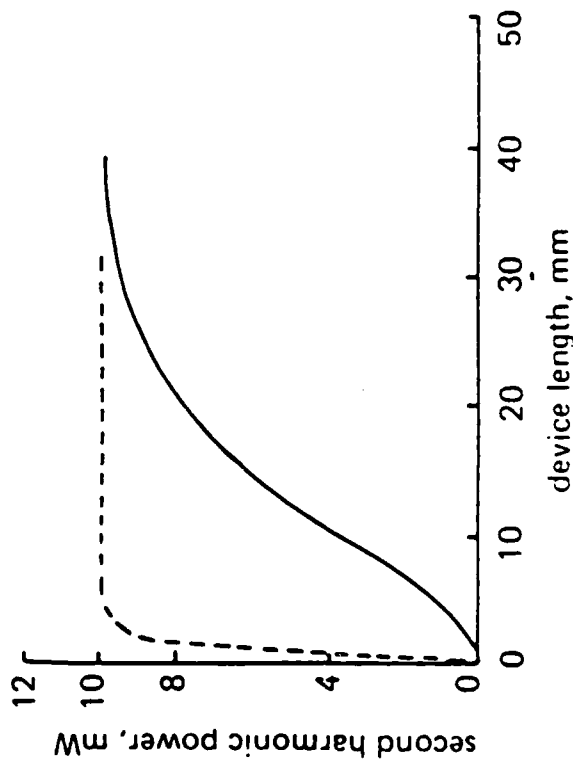


SHG OUTPUT FOR THE LP₀₁ MODE IN A CRYSTAL CORED FIBRE

Fundamental Power: 10mW

$V = 2.0$; $\lambda_f = 1500\text{nm}$; $\Delta = 0.1$; $n = 1.65$

$d(\text{-----}) = 250\text{pm/V}$; $d(\text{---}) = 20\text{pm/V}$



PHASE-MATCHING SCHEMES FOR GUIDED WAVE INTERACTIONS

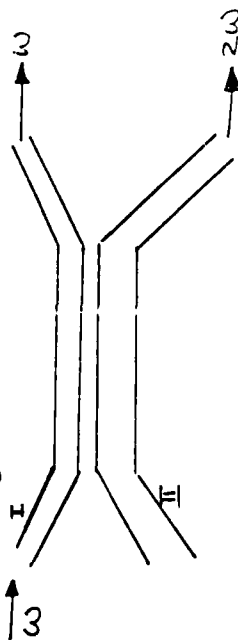
- Electro-optic/Temperature tuning

- Grating structures



$$\Delta\beta = \beta^{(2\omega)} - 2\beta^{(\omega)} = \frac{2\pi}{\Lambda}$$

- Coupled waveguides



ADVANTAGES OF CCF OPTICAL PARAMETRIC AMPLIFIER

- Independent of modulation format
- Independent of data bit rate
- Redundancy in pump lasers
- In-line device

A CCF ALL OPTICAL AMPLIFIER

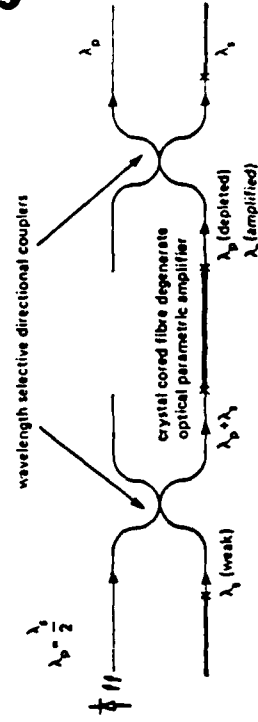
GAIN = 40dB

With

$$P_p = 10\text{mW}; d_{\text{eff}} = 250 \times 10^{-12} \text{ m/V}$$

$$V\text{-value} = 2.0; \Delta = 0.1; L = 10\text{mm}$$

Q-29



CONCLUSIONS

Semiconductor diode pumped nonlinear devices are
feasible

CCF DEVICE REQUIREMENTS

- Higher transmission
 - Defect/void free crystal growth
 - Better end preparation
- Efficient device designs
- New materials

R-1

M. Thakur

AT&T

TOWARDS NONLINEAR OPTICAL
APPLICATIONS OF POLYDIACETYLENES

TOWARD NONLINEAR OPTICAL APPLICATIONS OF POLYDIACETYLENES

M. THAKUR
AT&T BELL LABORATORIES

B. I. GREENE
J. ORENSTEIN
K. TAI
G. C. CHI
K. J. O'BRIEN
Y. SHANI

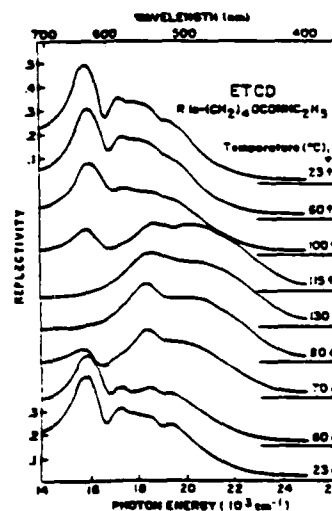
M. GOMEZ
H. TANAKA
A. TONELLI

TOPICS

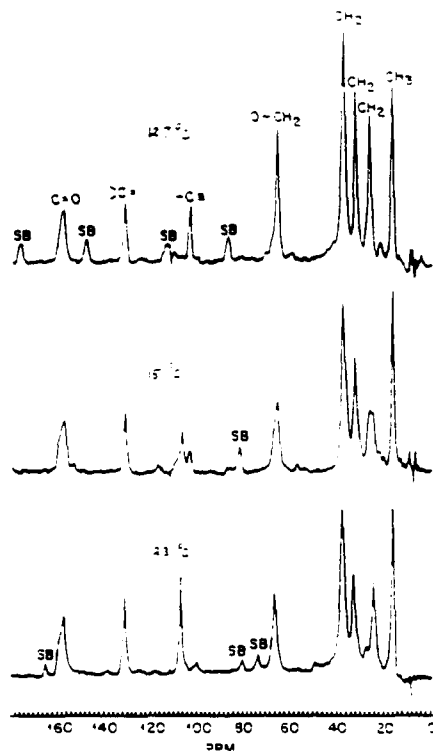
- MATERIALS ASSESSMENT
- GROWTH OF THIN SINGLE CRYSTAL FILMS
- FABRICATION OF DEVICE STRUCTURES
- DEMONSTRATION OF CHANNEL WAVEGUIDING
- INTENSITY DEPENDENT PHASE-MODULATION

IMPORTANT PARAMETERS FOR MATERIALS SELECTION

- EXTENT OF CONVERSION (MONOMER → POLYMER)
- EXTENT OF CONJUGATION (PLANARITY)
- THERMAL STABILITY (THERMOCHROMISM)
- SOLUBILITY
- EASE OF CRYSTALLIZATION



R-3



¹³C Chemical Shifts of Polydiacetylenes

¹³C, ppm vs. TMS

	C=O	C≡C	-C≡	α-CH ₂	β-CH ₂ , γ-CH ₂
ETCD (blue)	157.5	131.6	107.4	37.3	24.5
PTS-6 (blue)	—	131.3	107.1	—	—
PTS-12 (blue)	—	131.0	106	—	—
TCDU (blue)	—	—	107.3	—	—
ETCD (red)	158.3	132.0	103.6	37.8	26.4
TCDU (red)	155.8	131.5	102.9	37.9, 32.3	25.9, 21.8, 28.0, 30.8
ETCD (melt)	158.1	130.8	102.5	37.3	27.2

CONCLUSIONS FROM NMR STUDIES

- THE CONJUGATION LENGTH IS DETERMINED BY THE EXTENT OF PLANARITY OF THE CHAIN-BACKBONE.
- INCREASE OF CHAIN LENGTH DOES NOT GUARANTEE INCREASE OF CONJUGATION LENGTH.
- THE ACETYLENIC FORM IS PREDOMINANT IN POLYDIACETYLENES INDEPENDENT OF PHASES.

SINGLE

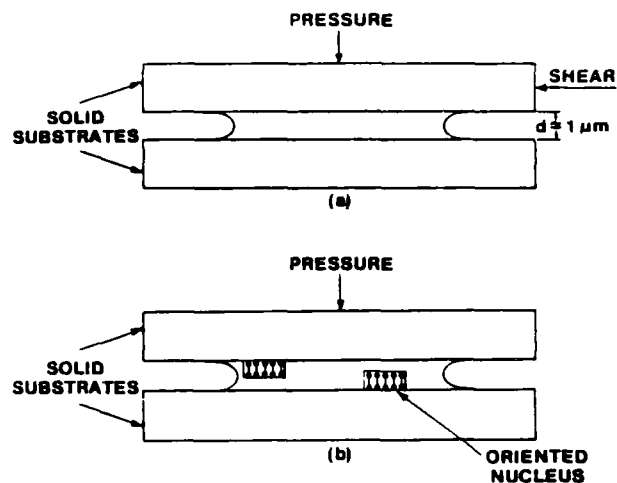
GROWTH OF THIN FILM CRYSTALS

• THE SHEAR METHOD

ORIENTATIONAL PRINCIPLES
 REQUIREMENTS ON MOLECULAR SHAPE
 GROWTH PARAMETERS
 CONTROL OF THICKNESS
 OPTICAL QUALITY OF FILMS

• COMPARISON WITH THE L-B METHOD

• ASSESSMENT OF APPLICABILITY

COMPARISON OF THE CALCULATED
MOLECULAR LENGTHS WITH THE OBSERVED
d-SPACINGS

MATERIALS	CALCULATED LENGTH L (Å)	COMPENSATED LENGTH $L \sin \phi$ (Å)	d-SPACINGS OF 1ST ORDER REFLECTIONS (Å)
$RC \equiv C - C \equiv CR$ WITH R			
1. $-CH_2OH$	~8.1	8.1	8.05
2. $-(CH_2)_4 OCONH C_2H_5$	~17.9	17.9	17.87
3. $-(CH_2)_4 OCO NH C_6H_5$	~19.5	19.5	18.94
4. $-CH_2 OSO_2 C_6H_4 CH_3$	~14.8	12.9	12.87
5. $-(CH_2) OCO NH CH_2COOC_4H_9$	~26.9	26.9	26.80
$NH_2 - \text{C}_6\text{H}_4 - C \equiv N$	~8.0	8.0	8.40
$HO - \text{C}_6\text{H}_4 - N - \text{C}_6\text{H}_4 - NO_2$	~10.5	10.5	10.05

SPREADING COEFFICIENT

$$S_{B/A} = \gamma_A - \gamma_B - \gamma_{AB}$$

$$= W_{AB} - W_{BB}$$

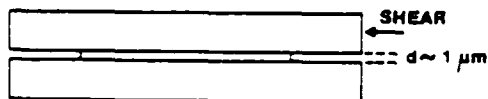
γ = SURFACE TENSION

W_{AB} = WORK OF ADHESION

W_{BB} = WORK OF COHESION

FOR SPONTANEOUS SPREADING

$$S_{B/A} > 0$$

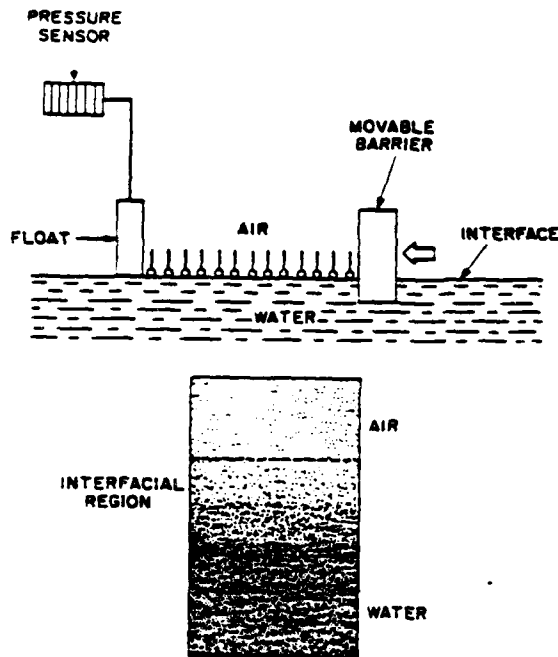


TOTAL SHEAR $T = T_{cap} + T_{ext}$

LATERAL PRESSURE $P \sim 10^7$ DYNES/cm²

EQUILIBRIUM SPREADING PRESSURE OF A MONOLAYER

$P_{mono} \sim 10^7$ DYNES/cm²



COMPARISON OF THE L-B AND THE SHEAR METHOD

- POLAR INTERACTIONS HAVE IMPORTANT ROLES IN BOTH THE METHODS.
- IN THE L-B TECHNIQUE A LIQUID IS USED AS THE SUBSTRATE. IN THE SHEAR METHOD SOLID SUBSTRATES ARE UTILIZED.
- THE L-B METHOD APPLIES TO AMPHIPHILIC MOLECULES ONLY. THE SHEAR METHOD IS APPLICABLE TO A BROADER RANGE OF MOLECULES.
- THE L-B METHOD PROVIDES ORDER ALONG ONE DIRECTION ONLY. THE SHEAR METHOD LEADS TO 3-D ORGANIZATION.
- THE L-B FILMS HAVE MICRO-DOMAIN MORPHOLOGY (POOR OPTICAL QUALITY). THE SHEAR-GROWN FILMS ARE UNIFORM SINGLE CRYSTALS (EXCELLENT OPTICAL QUALITY).

INTENSITY DEPENDENT PHASE MODULATION

$$n = n_0 + n_2 I$$

$$\Delta\phi = \frac{2\pi}{\lambda} n_2 I L, \quad L = \text{LENGTH OF PROPAGATION}$$

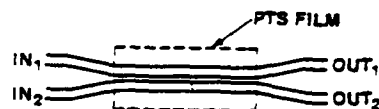
$\Delta\phi = \text{PHASE SHIFT}$

FOR $\lambda \sim 0.8 \text{ TO } 2.0 \mu$
 n_2 OF PTS $\sim 7 \times 10^{-6} \text{ cm}^2/\text{MW}$ (HERMANN AND SMITH, 1980)

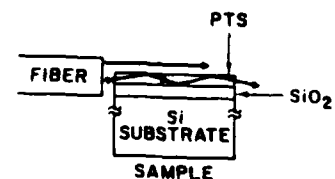
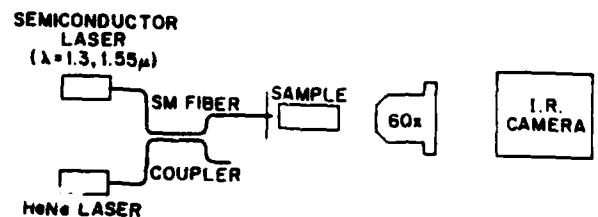
IF OPTICAL PULSES ($\lambda \sim 1 \mu$) OF PEAK POWER $\sim 500 \text{ mW}$
 ARE FOCUSED ON A CROSS-SECTION $\sim 1 \mu\text{m}^2$

$$\Delta\phi \rightarrow \pi$$

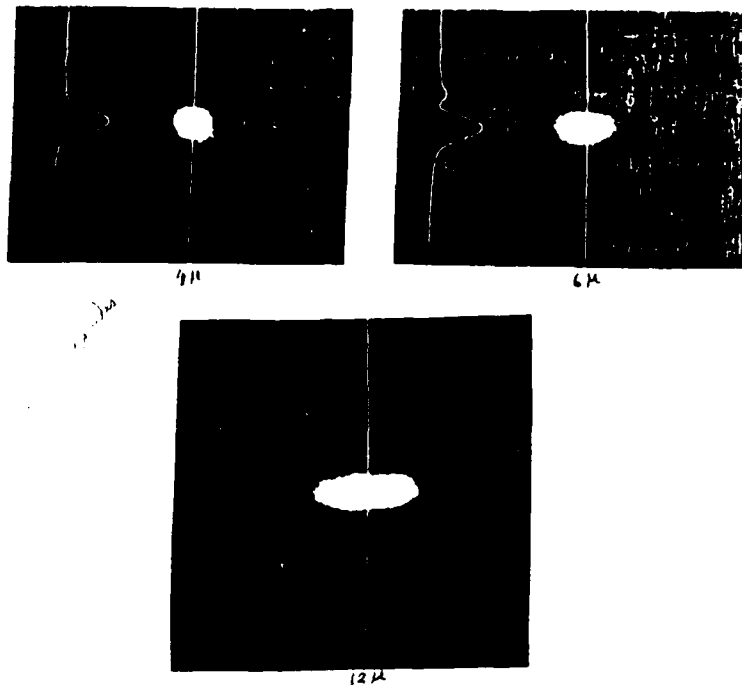
FOR $L \sim 1.4 \text{ mm}$.



WITH SUBPICOSECOND PULSES
 ENERGY REQUIREMENT $< 1 \text{ pJ/bit}$.
 THE DATA-RATE THAT THE DEVICE COULD HANDLE $\sim 1 \text{ THz}$
 NONABSORPTIVE \rightarrow NO THERMAL DAMAGE.



R-6



SUMMARY

- A COMPARATIVE EVALUATION IS MADE FOR DIFFERENT POLYDIACETYLENES IN RELATION TO NLO DEVICE APPLICATIONS.
- C^{13} - NMR RESULTS SHOW THAT THE CONJUGATION LENGTH IS DETERMINED BY THE EXTENT OF PLANARITY OF THE CHAIN BACKBONE AND NOT BY THE CHAIN LENGTH.
- THE ORIENTATIONAL PRINCIPLES OF THE SHEAR METHOD ARE DISCUSSED IN COMPARISON WITH THE L-B TECHNIQUE.

SUMMARY (Cont.)

- THE SUPERIORITY OF THE SHEAR METHOD IN PROVIDING GOOD OPTICAL QUALITY SINGLE CRYSTAL FILMS OF CONTROLLED THICKNESS AND ORIENTATION IS DEMONSTRATED WITH MANY EXAMPLES.
- CHANNEL WAVEGUIDING IS DEMONSTRATED (PROPAGATION > 5 mm) FOR SHEAR-GROWN PTS FILMS.
- PRELIMINARY RESULTS OF INTENSITY DEPENDENT PHASE CHANGE IN PTS WAVEGUIDES ARE DISCUSSED.

S-1

D. Haarer

Universitat Bayreuth, West Germany

**HIGH RESOLUTION
LASER SPECTROSCOPY IN POLYMERS**

Fig.3.1. Local saturation of an NMR line at the frequency ω_0 (a) before, (b) during, and (c) after irradiation at ω_0 [3.1]

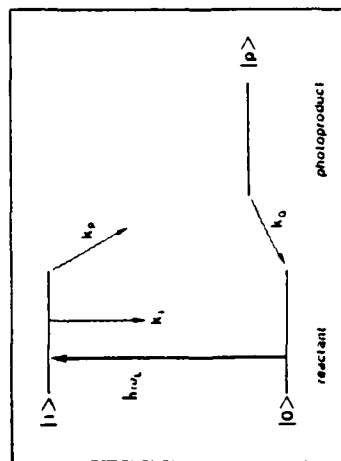
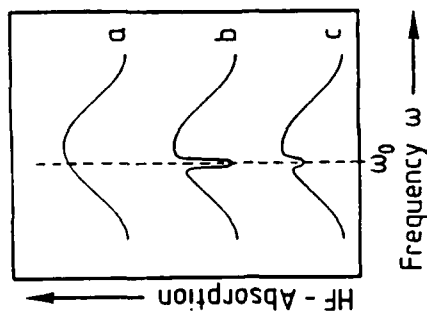


Fig.3.3. Three-level system with the reactant levels $|0\rangle$ and $|1\rangle$ and the photoproduct level $|p\rangle$. K_1 , K_p and K_0 are the decay rate constants of the various states. ω_1 is the hole-burning frequency

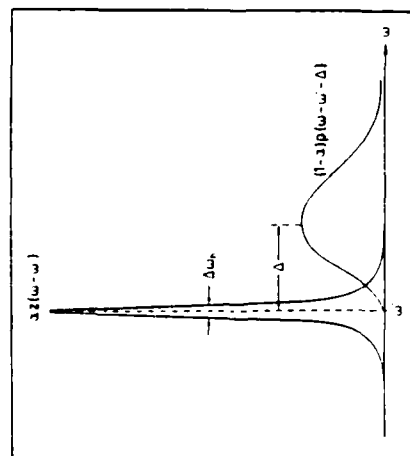


Fig.3.4. General lineshape function of an electronic excitation of a guest molecule in a solid host matrix. Schematic view of a zero-phonon line and its phonon sideband. The phonon sideband has an intensity of $(1-\alpha)$ and is displaced by the lineshift parameter Δ . The latter corresponds to half the "Stokes shift"

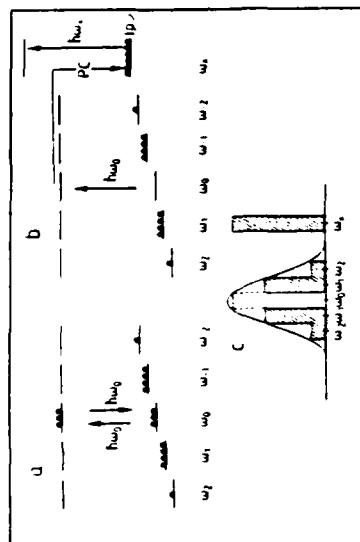


Fig.3.2. (a) Radiation saturation of an ensemble of five optical two-level systems at the center frequency ω_0 . (b) Photochemical bleaching of an ensemble of five two-level systems at the center frequency ω_0 . Creation of a photoproduct state absorbing at the frequency ω_a . (c) Absorption after photochemical bleaching as described in Fig.3.2b. The photoproduct shows up at the frequency ω_a .

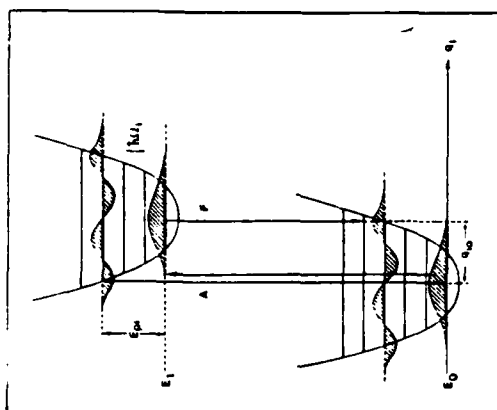


Fig. 3.5. Energy diagram for interpreting phonon side-band spectra in terms of the excited state displacement Q . The phonon frequency is $\hbar\omega$. The figure shows a zero-phonon and a three-phonon transition in absorption (A) and emission (F), respectively

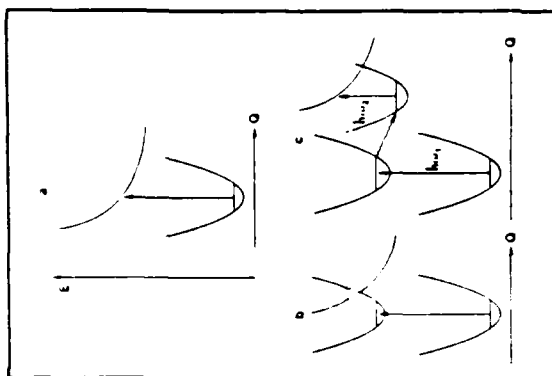


Fig. 3.6a-c. Photochemical reaction schemes plotted as a function of one configurational coordinate Q . (a) Repulsive exciplex-like state. (b) Level-crossing from a "quasi-stable" excited state. (c) Two-photon reaction with photon energies $h\nu_1$ and $h\nu_2$. The level which absorbs the photon $h\nu_2$ is a long-lived intermediate state

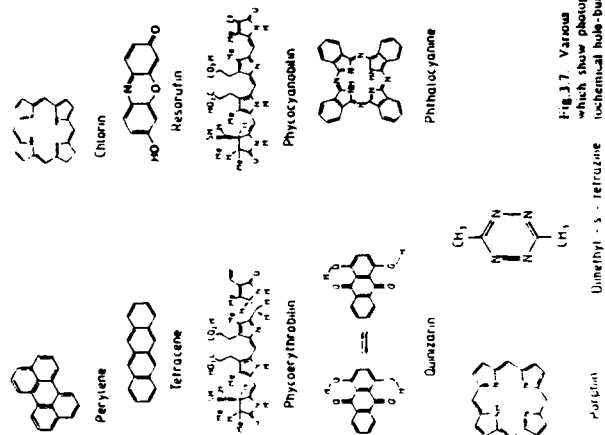


Fig. 3.7. Various dye molecules which show photochemical and photochemical hole-burning

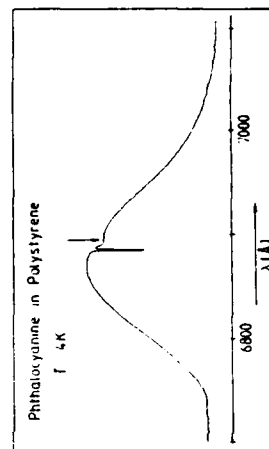


Fig. 3.8. Experimental hole spectrum of phthalocyanine in polystyrene at 4 K. The pseudo-phonon wing is marked by the wavy arrow

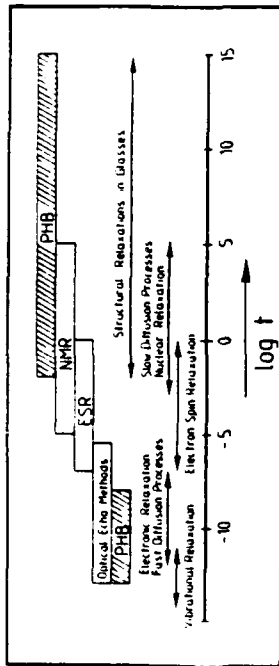


Fig. 3.9. Logarithmic scale of relaxation times and of methods of measuring characteristic time constants. Hole-burning is especially well suited for very short and very long relaxation times (see text)

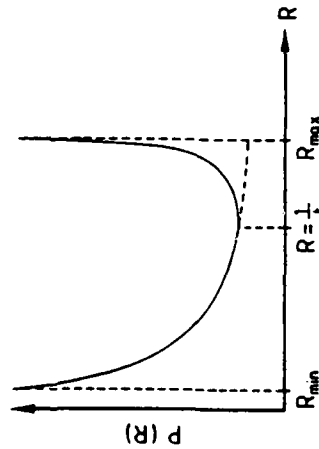


Fig. 3.11. Rate distribution as calculated by Jäcckle [3.98]. For the definition of the two limiting rates R_{\min} and R_{\max} see text

Fig. 3.10. (a) Periodic potential of a crystalline solid. (b) Potential along a fictitious coordinate q of a glass. Note the lack of periodicity. (c) Idealized two level scheme with the two parameters Δ and V_0 (see text). The oscillators in the two wells are separated by the distance d and have a zero-point frequency on the order of Ω

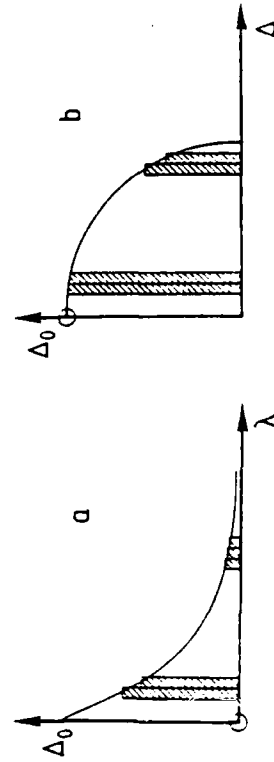
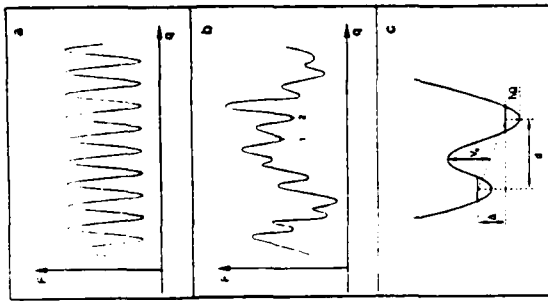


Fig. 3.12. Functional dependence of the tunnelling matrix element Δ_0 on the TLS-parameters λ (Fig. 3.12a) and Δ (Fig. 3.12b) (see text)

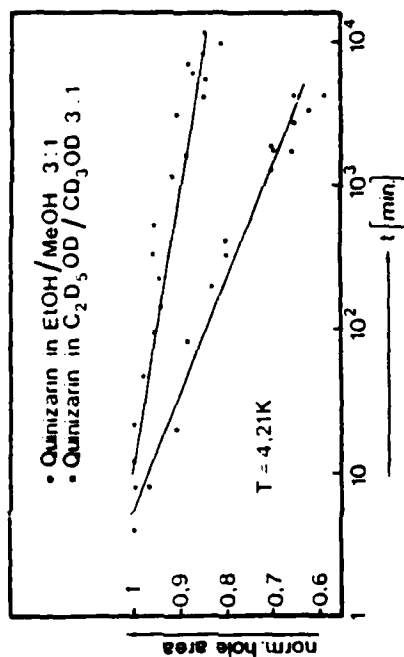


Fig. 3.13. The decay of the area of photochemical holes of quinizarin in alcohol glass for deuterated (squares) and protonated systems (dots)

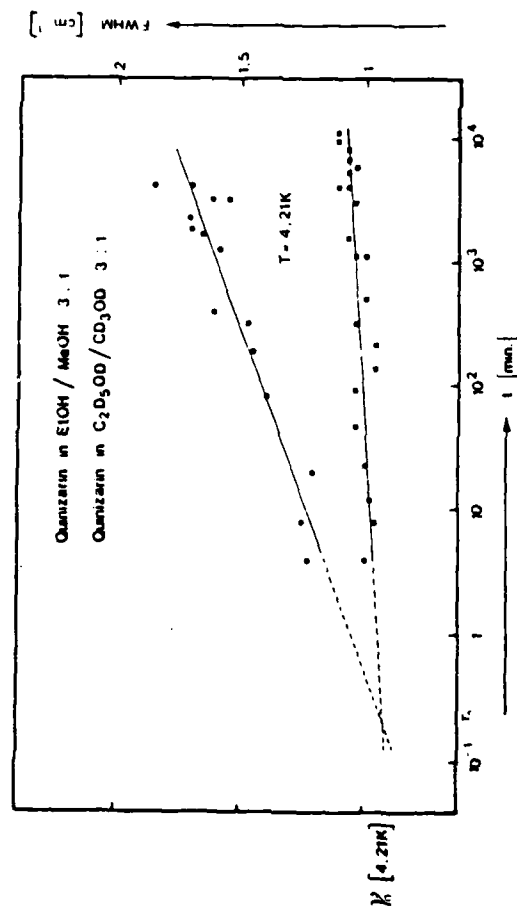


Fig. 3.14. Line broadening of the photochemical holes of quinizarin in alcohol glass for deuterated (squares) and protonated systems (dots)

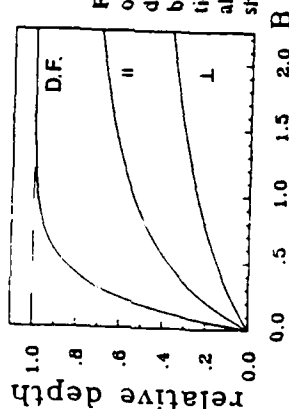


Fig. 3.15. Dependence of the relative depth of a photochemical hole on the irradiated light dose B. The upper curve shows the maximally bleached distribution function with a polarization factor of unity. The two curves with parallel and perpendicular polarization are also shown [3.40]

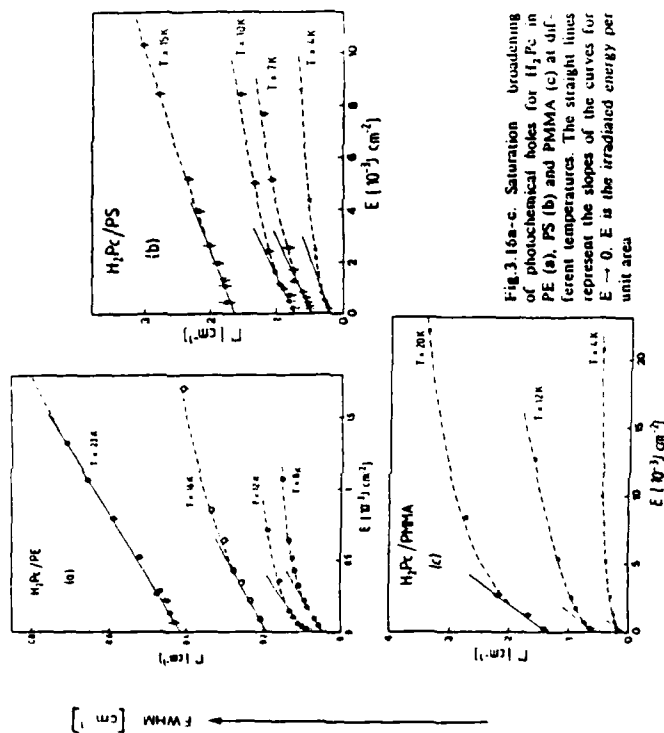
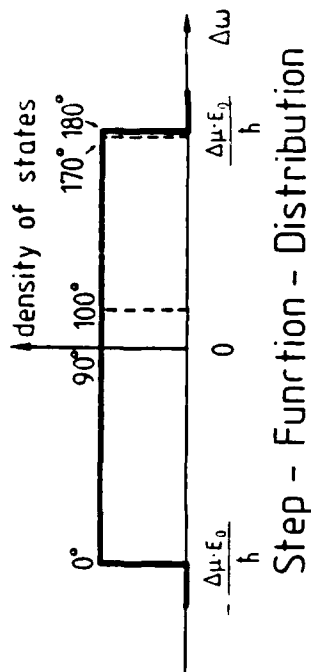


Fig. 3.16a-c. Saturation of photochemical holes for H₂PC in PE (a), PS (b) and PMMA (c) at different temperatures. The straight lines represent the slopes of the curves for E → 0. E is the irradiated energy per unit area



Step - Function - Distribution

Fig. 3.17. Distribution function of the absorption frequencies of guest molecules in an electric field E_0 . All molecules absorb at the 0-frequency for $E = 0$; they have identical dipole moment changes $\Delta\mu$ but are oriented randomly with respect to the external E -field. The numbers indicate the orientation angles for some representative frequency shifts

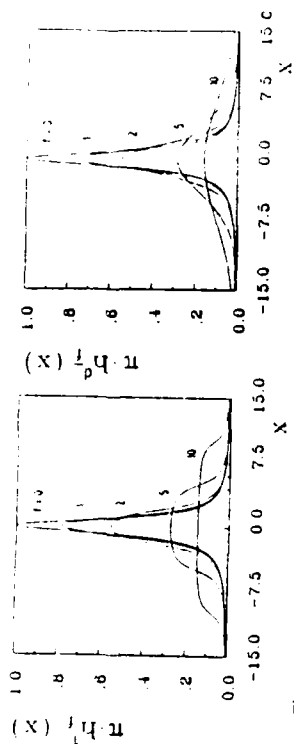


Fig. 3.18. (a) Theoretical lineshape of a spectral hole for different external field strengths f . All absorbers have the same $\Delta\mu$ value. For a field value of $f = 1$, the Stark broadening equals the linewidth. (b) The same calculations as a) with a Gaussian distribution of $\Delta\mu$ values

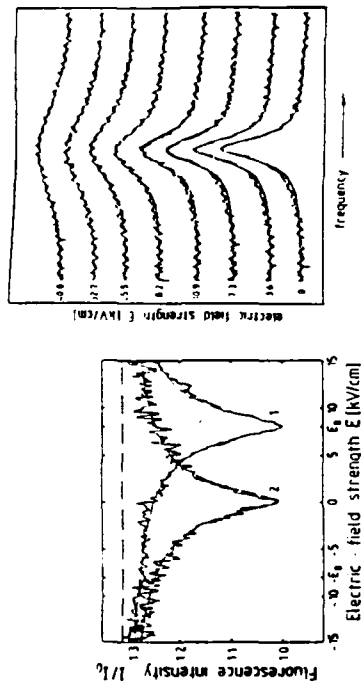


Fig. 3.19. Fluorescence excitation spectra of two holes. One spectrum was burned at $E = 0$ and one was burned at the field E_0 [3.123]

Fig. 3.20. Measured and calculated hole profiles for the system Zn-TBP ($C_{60}H_6Cl_{11}I_3$) in polyvinylbutyral (see [3.124]). Here the average change in dipole moment is $\Delta\mu = 0.174$ Debye units

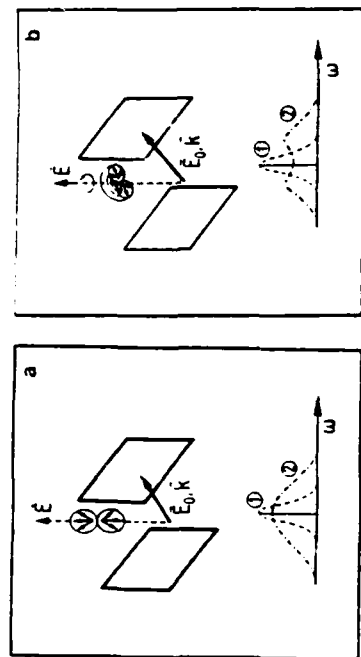


Fig. 3.21. Dipolar $\Delta\mu$ configurations for $\Delta\mu$ parallel (a) and perpendicular (b) to the transition dipole moment E_0 is the electric field strength and k is the wave vector of the incident light

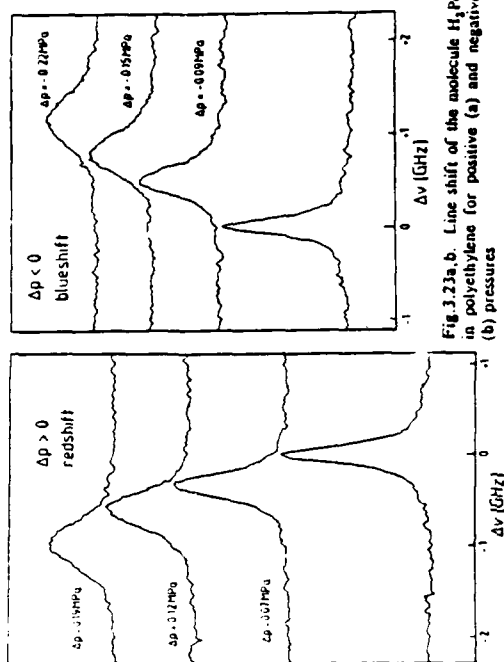


Fig. 3.23a, b. Line shift of the molecule H_2Pc in polyethylene for positive (a) and negative (b) pressures

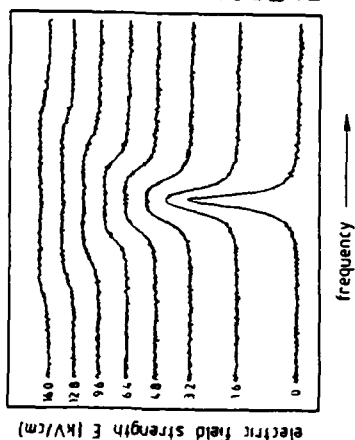


Fig. 3.22. Measured and calculated hole profiles for H_2C in polyvinylbutyral [3.124]. Here the calculated $\Delta\mu$ value is $\Delta\mu = 0.214$ Debye units

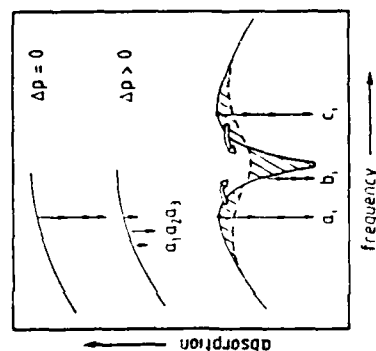


Fig. 3.24. Line shifts of H_2Pc in PS, PE and PMMA in the low pressure regime

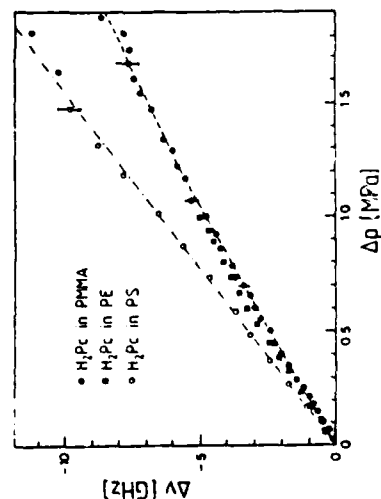


Fig. 3.25. Line broadening of sites which had been site-selected at $\Delta p = 0$ and which drift apart at higher pressures $\Delta p \neq 0$. At higher pressures the frequency range of the absorbers extends from a_1 to a_3 . The lower part of the figure shows the line broadening for various sets of molecules a_1 , b_1 and c_1

**POSTER SESSION
ABSTRACTS**

Optical Kerr Measurements on some Ferrocene Derivatives.

C.S.Winter, J.D.Rush and S.N.Oliver.

British Telecom Research Labs.,
Martlesham Heath,
Ipswich IP5 7RE,
England.

We report here preliminary results from a study of the third order non-linearities in a range of organo-metallic compounds. These initial measurements have been carried out using the optical power limiter technique developed by Soileau *et al*⁽¹⁾, where the critical power for self-focusing is measured and used to calculate n_2 . The materials measured were solutions of ferrocene in ethanol, varying from 10^{18} to 10^{19} molecules/cc and a liquid ferrocene derivative, bis(trimethylsilyl)ferrocene. A value of γ for ferrocene of 4.1×10^{-34} esu was found for the solution studies, in good agreement with that measured for the liquid derivative of 4.6×10^{-34} esu. The experiments were carried out at $1.06 \mu\text{m}$ with 10 ns pulses. We are currently repeating the measurements using other techniques and shorter pulses to distinguish the various possible contributions to the observed n_2 .

(1) M.J.Soileau, W.E.Williams and E.W.Van Stryland;IEEE J Quant Elect.,QE-19,(1983),731.

Theoretical models for the second hyperpolarizability of
novel conjugated polymers

*David N. Beratan
Jet Propulsion Laboratory
California Institute of Technology
Pasadena, CA 91109*

Theoretical models will be presented for the chain length dependence of the second electronic hyperpolarizability of simple polyenes, simple polyynes, and more complicated unsaturated organic materials. The hyperpolarizability of conjugated polymers which incorporate novel localized electronic states will be described as well. These materials present the possibility of achieving enhanced hyperpolarizabilities due to mixing of appropriate "gap states" with the delocalized states of the conjugated polymer. They also present the possibility of designing materials with "switchable" hyperpolarizabilities.

NONLINEAR OPTICAL PROPERTIES OF TRANSITION METAL POLY-YNES
E.A. Chauchard, M.P. Cockerham, P.L. Porter, S. Guha, C.C. Frazier
Martin Marietta Laboratories
1450 South Rolling Road
(301) 247-0700

Data from third harmonic generation (with a 1.06- μ m fundamental), power limiting and four-wave mixing measurements of solutions and films of transition metal poly-ynes were used to verify that these compounds have large third-order optical susceptibilities. The large third-order nonlinearities observed in four-wave mixing studies of metal poly-yne solutions may originate, in part, from contributions from the real and imaginary components of intense two-photon absorptions associated with the metal-organic compounds. We will discuss our latest four wave mixing experiments and the direct observation of two-photon absorption in metal poly-ynes.

We will also discuss the correlation of polymer chain length and structure with third-order hyperpolarizability per repeat unit for several metal polymers and oligomers.

REVERSE SATURABLE ABSORBERS: INDANTHRONE AND ITS DERIVATIVES

R. S. Potember, R. C. Hoffman, and K. A. Stetyick
Johns Hopkins University Applied Physics Laboratory
Johns Hopkins Road
Laurel, MD 20707-6099

Indanthrone has been shown to exhibit the phenomenon of reverse saturable absorption.¹ The wavelengths at which indanthrone behaves in this fashion can be changed by structural modification of the indanthrone chromophore. The derivatives which have been synthesized have been shown to be more efficient reverse saturable absorbers than the parent chromophore.

It is advantageous to extend the range of nonlinear behavior to any desired portion of the spectrum, and this is best accomplished by substitution on the aromatic portion of the indanthrone molecule. We have demonstrated that oxidized indanthrone, monochloroindanthrone and an oligomer of indanthrone are more efficient saturable absorbers than the parent. Oxidized and monochloroindanthrone exhibit reverse saturable absorption at both 1064 nm and 532 nm, whereas indanthrone itself exhibits the phenomenon at 532 nm only. The oligomer, which consists of three anthraquinone units, has proved to be an efficient reverse saturable absorber at 1064 nm as well as at 532 nm.

¹C. R. Giuliano and L. D. Hess, IEEE J. Quantum Elec. QE-3, 338 (1966).

This work was supported in part by the Dept. of the Navy under Contract No. N00039-87-C-5301.

THE PREPARATION AND CHARACTERIZATION OF POLYMERIC MATERIALS
WITH ENHANCED SECOND ORDER NONLINEARITIES. M.L. Schilling, H.E.
Katz, D.I. Cox, AT&T Bell Laboratories, Murray Hill, NJ 07920.

We have recently introduced a new class of organic materials for second order nonlinear optics, consisting of poled films of dye-containing polymers. In the past year, some uncommon functional groups (di- and tricyanovinyl) have been shown to enhance the molecular susceptibilities of the nonlinear moieties when used instead of their more usual counterparts. Dyes with enhanced nonlinearities by virtue of the cyanovinyl substituents have been exploited in the preparation of bulk materials with some of the highest second order susceptibilities yet reported.

The synthesis of conformationally defined dye aggregates, whose subunit dipoles are constrained to be additive, is in progress. These dyes can then be incorporated into polymeric materials, taking advantage of their enhanced effective dipole moments for increased orientation in poling experiments. We will report some of the new synthetic organic chemistry that has been utilized in preparing our latest electro-optical materials.

Second Harmonic Generation in Doped Glassy Polymer Films as a
Function of Physical Aging

Hilary L. Hampsch(a), Jian Yang(b), George K. Wong(b),
and John. M. Torkelson(a,c)*

(a) Department of Materials Science and Engineering

(b) Department of Physics and Astronomy

(c) Department of Chemical Engineering

and the Materials Research Center

Northwestern University

Evanston, Illinois

March 31, 1988

ABSTRACT

The temporal stability of second harmonic generation (SHG) intensity is measured in poly(methyl methacrylate) (PMMA) and bisphenol-A-polycarbonate (PC) doped with nonlinear optical dyes in electric field poled films. Doped PC films show slower SHG decay than doped PMMA films at times less than 8 hours. In PC+DANS films aged 10 hours at 25°C, there is no SHG decay over the first 8 hours, whereas in PMMA+DANS aged at 25°C and at 60°C the effect is much smaller. Two dopants show the effect of size on SHG decay, with the larger dopant showing increased temporal stability. Good agreement is obtained when decay curves are fit using a Williams-Watts stretched exponential.

* to whom correspondence should be addressed

ELECTRO-OPTIC, POLYMER CLAD, E-FIELD SENSOR

L. MICHAEL HAYDEN
GERALD F. SAUTER

UNISYS CORPORATION, CSD, St. Paul, MN, 55164

Abstract

There is a military need for sensor systems that combine high sensitivity, immunity to EMI/RFI, large bandwidth, and low power and cost. The hybridization of present day electronic components with optical components offers the promise of sensor systems that meet these requirements.

Unisys has been developing a PVDF-coated fiber optic, electric field sensor and now has expanded its program to include nonlinear organic polymers as cladding and waveguide material. This paper will report on progress using Guest/Host (GH) polymers as cladding material.

The concept of an all dielectric high frequency sensor is demonstrated. The sensor consists of a Ag⁺ exchange waveguide coated with a GH nonlinear polymer glass. The sensor is incorporated into one arm of a Mach-Zender interferometer and exhibits a figure of merit of 4 microradians/volt/meter/meter. The frequency response is flat from DC to our current instrumentation limit of 5 MHz.

This sensor design was chosen primarily as a vehicle that would allow an easy method to test and verify design parameters for fiber sensor systems. These parameters include index and depth of guide vs. index, thickness and E-O coefficients of the cladding. We will present a comparison of the results of this sensor with those from the PVDF sensor program.

MOLECULAR CONFORMATION AND THE STABILITY OF
TICT STATE IN P,P'-DISUBSTITUTE-1,6-DIPHENYL-
1,3,5-HEXATRIENES

C.T. Lin, H.W. Guan, R. K. McCoy and C. W. Spangler
Department of Chemistry
Northern Illinois University
DeKalb, IL 60115

ABSTRACT

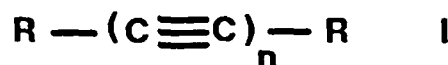
The p,p'-disubstituted linear diphenyl polyenes are expected to have a high optical nonlinear susceptibility because of its large permanent dipole moment induced by the substituents. The photophysical properties for a series of p,p'-disubstituted-1,6-diphenyl-1,3,5-hexatrienes (referred as D,A-DPH) are investigated, where D and A are the electron-donating and - accepting groups of -OCH₃, -N(CH₃)₂ and -NO₂. In all solvents used, a dual fluorescence is observed for D,A-DPH containing the internal rotation groups of -N(CH₃)₂ and/or -NO₂, suggesting that the "a*" fluorescence (the locally excited state gives the normal "b*" fluorescence) is originated from a twisted intramolecular charge transfer (TICT) state. The stability of TICT state is sensitive to the D and A substituents and their relative twisting angles. The observed results provide the evidence of the π -electron distortion and thus the enhancement of optical nonlinearity in this class of molecules.

Second and Third – Order Nonlinear Optical Properties of End – Capped Acetylenic Oligomers

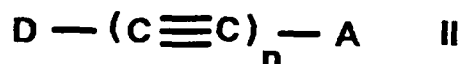
Joseph W. Perry, Albert E. Stiegman, Seth R. Marder and Daniel R. Coulter

*Jet Propulsion Laboratory, California Institute of Technology
4800 Oak Grove Drive, Pasadena, CA 91109*

We have been investigating the second and third – order nonlinear optical properties of a variety of acetylenic oligomers. A series of symmetric acetylenic oligomers of the form



have been investigated for third – order nonlinear susceptibility. A series of new compounds of the form



where D and A are electron donor and acceptor groups, respectively, have been synthesized and investigated for second – order nonlinearity. Third – order nonlinear susceptibilities of series I molecules in solution have been measured using third harmonic generation (THG). THG susceptibilities at 1064 nm have been determined for various oligomer lengths and end – capping groups. $\chi(3)$ increases with length and varies with the nature of the end – group. Series II compounds have been screened for second harmonic generation by using the Kurtz powder method. Several samples show SHG efficiencies comparable to urea. Characterization of molecular hyperpolarizabilities for the series is in progress.

Optical Field Induced Scattering in
Polymer Dispersed Liquid Crystal Films

P. Palffy-Muhoray, Michael A. Lee and J.L. West
Liquid Crystal Institute
Kent State University
Kent, OH 44242

ABSTRACT

We report observations of optical field induced scattering in polymer dispersed liquid crystal films due to reorientation of the liquid crystal molecules by the optical field of a CW argon ion laser. These composite materials consist of nearly spherical liquid crystal droplets dispersed in a polymer binder. As previously reported ^{1,2,3}, films of these materials may be switched from an opaque scattering state to a clear transparent state by application of a d.c. or low frequency a.c. electric field. An applied low frequency electric field is used to align the liquid crystal in an orientation such that the refractive index of the liquid crystal within the droplet is matched with that of the polymer binder. If a sufficiently intense optical field is applied to the transparent film, it will reorient the liquid crystal director, and give rise to a refractive index mismatch and hence scattering.

1. J.W. Doane, N.A. Vaz, B.-G. Wu and S. Zumer, App. Phys. Lett. 48, 269 (1986).
2. J.L West, Mol. Cryst. Liq. Cryst. (in press).
3. S. Zumer and J.W. Doane, Phys. Rev. A 34, 3373 (1986).

**FABRICATION OF WAVEGUIDE STRUCTURES FROM SOLUBLE
POLYDIACETYLENES. G.L. Baker, N.E. Schlotter, J.L. Jackel, P. Townsend,
S.Etemad, Bell Communications Research, Red Bank NJ 07701.**

Thin waveguide structures were fabricated from spun films of poly(3-BCMU) and poly(4-BCMU) by two separate processes. In the first, micron-sized features were patterned in polydiacetylene films using deep-UV lithography. This multilayer process utilizes a novel silicon-substituted polyacetylene as the resist layer, and can be used to generate sub-micron sized features in thick ($> 1\mu\text{m}$) polydiacetylene films.

In the second method, composite waveguides were fabricated from a patterned glass substrate and an overlayer of the polydiacetylene. These composite structures are relatively simple to prepare and are mechanically robust. Guides constructed as described above performed well with minimal losses and single-moded behavior at laser wavelengths of 1-1.5 μm .

AIR FORCE OFFICE OF SCIENTIFIC RESEARCH (AFSC)
NOTICE OF TRANSMITTAL TO DTIC
The technical report has been reviewed and is
being released to DTIC for release and is
unclassified.
MATTHEW J. KERPER
Chief, Technical Information Division